Analysis of transcriptional regulators involved in *Pseudomonas aeruginosa* antibiotic resistance and tolerance

Clayton Wallace Hall

A thesis submitted to the Faculty of Medicine in partial fulfillment of the requirements for the degree of Doctorate in Philosophy, Microbiology and Immunology

Department of Biochemistry, Microbiology, and Immunology

Faculty of Medicine

University of Ottawa

« Le rôle de l’infiniment petit est infiniment grand » – Louis Pasteur

Abstract

Cystic fibrosis (CF) is the most common fatal genetic disorder that afflicts young Canadians. The major cause of morbidity and mortality in patients with CF is chronic pulmonary infection with the opportunistic Gram-negative pathogen *Pseudomonas aeruginosa*. Once established, *P. aeruginosa* lung infections cannot be cleared despite sustained and aggressive antimicrobial therapy. Treatment failure of *P. aeruginosa* lung infections is caused by a combination of antibiotic resistance and tolerance mechanisms. Antibiotic resistance is mainly mediated by multidrug efflux pumps such as MexAB-OprM. Antibiotic tolerance has been attributed to biofilms and to nutrient starvation. In this thesis, I present an analysis of three transcriptional regulators (PA3225, RpoS, and RpoN) and their contributions to resistance and tolerance in *P. aeruginosa*. PA3225 is a transcriptional regulator that I initially identified as a candidate regulator of a type VI secretion system (T6SS) that had been previously implicated in biofilm tolerance. While a Δ*PA3225* deletion mutant did not, unfortunately, have dysregulated expression of the T6SS, I fortuitously discovered that the mutant displayed increased resistance to various antibiotics from different functional classes. I linked the increased antibiotic resistance of Δ*PA3225* to upregulation of MexAB-OprM and provided evidence that PA3225 may be a direct repressor of *mexAB-oprM*. Next, I sought to identify a transcriptional regulator of *ndvB*, which is another gene that plays a role in biofilm tolerance. I found that the stationary phase sigma factor, RpoS, was essential for expression of *ndvB* in stationary phase and biofilm cells. Moreover, RpoS was important for tolerance of stationary phase cells to tobramycin (TOB), an aminoglycoside antibiotic that is used to treat CF patients. In recent years, several groups have sought to identify novel treatments to combat antibiotic tolerance in *P. aeruginosa*. A popular strategy is metabolic

potentiation, which involves co-administration of an antibiotic with a metabolite to reverse tolerance due to nutrient starvation. For example, one group found that fumarate (FUM) combined with TOB (TOB+FUM) was highly effective at killing tolerant *P. aeruginosa*. FUM uptake depends on C_4-dicarboyxlate transporters, which are transcriptionally regulated by the alternative sigma factor, RpoN. Importantly, *rpoN* loss-of-function mutations are a recognised mechanism of pathoadaptation in CF clinical isolates. I demonstrated that TOB+FUM was unable to kill Δ*rpoN* stationary phase and biofilm cells due to loss of FUM uptake and that *rpoN* alleles from CF clinical isolates were unable to complement the Δ*rpoN* mutant. These findings could have important implications for TOB+FUM as a treatment modality in CF patients with a high burden of *rpoN* mutants. Overall, my work has provided interesting and, in the case of RpoN, clinically relevant insights into the regulatory networks that determine antibiotic susceptibility in *P. aeruginosa*.

Acknowledgments

I have been incredibly fortunate to be surrounded by exceptionally talented, generous, and caring people who have taught, challenged, encouraged, and loved me throughout my life. Mere words cannot begin to express how grateful I am to those who have given me the tools and opportunities to get to where I am today. For those who I have neglected to mention below, please know that this is due to an omission on my part – you are important to me and I wouldn't be who I am today without you.

Thank you Dr. Thien-Fah Mah for being the most supportive, caring, and committed PhD supervisor I could have ever asked for. I truly admire your enthusiasm for science, positive outlook in the face of adversity, and concern for the wellbeing of others. Thank you for valuing my ideas and allowing me to run with research questions that interested me. You are an amazing mentor, and I am very grateful that you kept me on track to finish my graduate studies on such a tight timeline.

A tremendous thank you to Li Zhang, who has made invaluable contributions to all of my research projects and who has made the lab an exceptionally enjoyable place to work. You are the heart of the Mah lab, and I could not have done my PhD in three years without your brilliant suggestions and vast technical expertise.

Thank you to all past and present members of the Mah lab, especially Dr. Aaron Hinz, Dr. Luke Gagnon, and J-P Nadeau for your friendship and for your significant help with the projects presented in this thesis.

Thank you to the members of my thesis advisory committee, Dr. Craig Lee, Dr. Chris Boddy, and Dr. Alex Blais, for supporting my research goals and for providing helpful advice during my graduate studies. Thank you also to the members of the Fullerton lab for helping me with Western blots and for allowing me to use your plate reader.

I would not have had the opportunity to pursue an MD/PhD degree had it not been for my early exposure to research with Dr. Andrew Makrigiannis. Thank you for taking a risk on a student fresh out of high school and for starting me off on the path to success. Thank you also to Dr.

Simon Bélanger, Dr. Mir Munir Rahim, and Dr. Megan Tu for your outstanding mentorship early on in my research journey.

I am deeply indebted to the most amazing friends anyone could ask for. Thank you especially to Laura Forrest, Becca Yaworski, Graham Gould Maule, Adam Pietrobon, Danny Jomaa, Melissa Phuong, Taylor Jamieson, Brendan Kelly, Dr. Ghadi Antoun, Tristan Delorme, Allison Welk, and Maria Maloney for always being there for me with your constant support, advice, and encouragement.

Thank you to my curling teammates over the years, especially Don Cain, Andy Girard, Jim Ford, Dr. Curtis McCloskey, Mathieu Gravel, Mark Frankish, Kurt West, and Jason Zelt for reminding me that life needs to be fun too.

Thank you to Uncle Exton and Aunt Melba for your eternal interest in what I've been up to and for your wisdom and advice over the years. I always learn life lessons from your stories.

Thank you to Mom and Dad for your unconditional love and unwavering support. From a very early age, you fostered my curiosity and always entertained my unending questions. When you didn't have an answer for me, you instilled in me the value of "looking things up". And when the books didn't hold an answer for me, you always encouraged me to voice my theories and how I might test them. I think that this open forum for ideas has been the most important influence in my development as a scientist and as a future clinician. You keep me grounded and remind me of the importance to always be kind, to care deeply for others, to be true to myself and my values, to be grateful for the gifts that I have received, to always strive for improvement, to learn from my errors, and to rejoice with those who do better.

Thank you to my sister Meaghan, who is the epitome of grace, kindness, and sincerity. Your hard work, witty sense of humour, and humility are just some of the many things that I admire about you. Know that you have always been a star who shines far too bright to be in anyone's shadow.

Merci à mon copain, Yves Lessard, pour ton amour, ton soutien, et ta patience au cours de mes études. Ta croyance que j'améliore le monde est ma source de motivation pour travailler fort chaque jour. J'ai hâte de commencer le prochain chapitre de ma vie main dans la main avec toi.

Table of contents

List of abbreviations

All abbreviations have been defined at first mention in the text. For quick reference, a non-comprehensive list of abbreviations is presented here:

5'RACE = 5' rapid amplification of cDNA ends

ABC = ATP-binding cassette

AMK = amikacin

AMP = ampicillin

ARG = L-arginine

CAR = carbenicillin

CCCP = carbonyl cyanide *m*-chlorophenyl hydrazone

CF = cystic fibrosis

CFU = colony forming units

CIP = ciprofloxacin

EMSA = electrophoretic mobility shift assay

ETC = electron transport chain

Ex/Em = excitation and emission wavelengths

GEN = gentamicin

GFP = green fluorescent protein

GLU = D-glucose

IPTG = isopropyl β-D-thiogalactopyranoside

MBC-P = minimum bactericidal concentration for planktonic cells

MBC-B = minimum bactericidal concentration for biofilm cells

MIC = minimum inhibitory concentration

NAL = nalidixic acid

OD_{600} = optical density at 600 nm

ONPG = *o*-nitrophenyl-β-galactoside

PA14 = strain UCBPP-PA14, the wildtype strain used in this work

PBS = phosphate buffered saline

PCR = polymerase chain reaction

PMF = proton motive force

qPCR = quantitative polymerase chain reaction

RNA-seq = transcriptome sequencing

RND = resistance-nodulation-division

SEM = standard error of the mean

SUC = succinate

T6SS = type VI secretion system

TCA = tricarboxylic acid cycle

TET = tetracycline

TOB = tobramycin

TOB+FUM = tobramycin and fumarate combination

TSS = transcriptional start site

WT = wildtype

X-gal = 5-bromo-4-chloro-3-indolyl-β-D-galactoside

Chapter 1: General introduction

1.1 Preface

Portions of sections 1.4 and 1.5 in this chapter have been previously published in the review article below (1) with modifications as necessary. The relevant sections taken from this review are clearly marked in the text.

> **Hall CW** and Mah T-F. 2017. Molecular mechanisms of biofilm-based antibiotic resistance and tolerance in pathogenic bacteria. *FEMS Microbiology Reviews* 41(3): 276-301.

Specific author contributions are as follows:

Clayton W. Hall – developed the review outline and wrote the manuscript.

Thien-Fah Mah – developed the review outline and edited the final manuscript.

1.2 *Pseudomonas aeruginosa*: an overview

Pseudomonas aeruginosa is a metabolically versatile, Gram-negative bacillus that is a member of the γ-proteobacteria class of Bacteria. *P. aeruginosa* is naturally present in the soil and in aquatic habitats, but it has also been isolated from surfaces in healthcare settings (2). *P. aeruginosa* does not normally colonise or infect humans with intact immune function (3). However, *P. aeruginosa* is commonly implicated in nosocomial infections and can cause serious opportunistic infections in patients who have conditions that impair one or more of the innate immune mechanisms that normally keep *P. aeruginosa* at bay (3). For instance, the genetic disease cystic fibrosis (CF) causes defects in the various bacterial clearance mechanisms of the lung, thereby predisposing patients with CF to chronic *P. aeruginosa* lung infections (4). An in-depth discussion of the pivotal role played by *P. aeruginosa* in CF is discussed later in this chapter.

P. aeruginosa infections are clinically very diverse and can range in severity from self-limiting (eg. hot tub folliculitis) to life threatening (eg. ventilator-associated pneumonia) as well as in acuity from acute (eg. keratitis) to chronic (eg. cystic fibrosis (CF) lung infections) (3). Failure of antimicrobial therapy is a major hurdle that clinicians face in treating many *P. aeruginosa* infections (5). For example, it is essentially impossible to clear chronic *P. aeruginosa* infections from the lungs of patients with CF using standard antimicrobial therapies that are currently in use clinically (6, 7). Recalcitrance to antibiotics has been attributed to both antibiotic resistance and antibiotic tolerance (1, 8). Antibiotic resistance is often associated with the expression of multidrug efflux pumps (9, 10) while antibiotic tolerance has been linked to the propensity of *P. aeruginosa* to form biofilms (1, 7, 11, 12). Biofilms are multicellular communities that exist as suspended aggregates or are attached to a biotic or abiotic surface (13). All of these concepts will also be explored in this chapter.

The ability of *P. aeruginosa* to exist in such diverse environments, from the soil to the lungs of a CF patient, can largely be attributed to the staggering amount of functional diversity encoded by the *P. aeruginosa* genome (14, 15). The next session explores some key concepts in transcriptional regulation that allow *P. aeruginosa* to adapt its transcriptome to its surroundings.

1.3 Transcriptional regulation of gene expression in *P. aeruginosa*

When the *P aeruginosa* genome sequence was published in 2000, it was the largest bacterial genome that had been sequenced at that time (14). With over 5,500 genes, of which approximately 7% are predicted to be part of the core essential genome, the *P. aeruginosa* genome provides the genetic complexity and functional diversity necessary for survival in diverse environments and hosts (14–16). Of course, coordination of the expression of such a large

complement of genes is essential. Expression of genes that are not important for survival under a given condition is a waste of precious resources while failure to express a gene important for fitness in a particular environment would be disadvantageous. Regulation of transcriptional initiation tends to be the major mechanism by which bacteria modulate gene expression (17). In support of an important role for transcriptional regulation in *P. aeruginosa* adaptation, approximately 10% of *P. aeruginosa* genes are annotated as being involved in transcriptional regulation (14). These regulatory genes include sigma factors, transcription factors, and two-component systems. These major classes of regulators as well as pertinent examples are presented below. It should be noted that, while not discussed here, small ligands, such as the alarmone (p)ppGpp, and local DNA conformation also affect transcriptional initiation. Moreover, gene expression in prokaryotes is not just regulated at the level of transcriptional initiation. Post-transcriptional, translational, and post-translational regulatory mechanisms also help ensure that genes are expressed when they are needed and silenced when they are not.

1.5.1 Sigma factors

In bacteria, the core RNA polymerase ($\alpha_2\beta\beta'\omega$) is able to elongate and terminate RNA transcripts; however, the core RNA polymerase is unable to initiate transcription on its own (17–20). RNA polymerase relies on dissociable sigma (σ) factor subunits for promoter recognition and transcriptional initiation (17–20). RNA polymerase in complex with a sigma factor is called the RNA polymerase holoenzyme. Each sigma factor has its own promoter specificity, allowing for the expression of discrete subsets of genes in a modular fashion (17–19, 21, 22). Most sigma factors belong to the σ^{70} family, which is made up of four groups based on structural and functional relatedness (23). The uniting features of all σ^{70} family factors are two highly conserved protein domains, regions 2 and 4, that bind, respectively, to the -10 and -35 DNA promoter elements (17–

19). Group 1 σ^{70} factors are essential and regulate the vast majority of genes in the genome (19). Due to their importance for the maintenance of basic cellular process, members of this group have also been called "housekeeping" sigma factors. In the case of *P. aeruginosa*, this role is satisfied by the RpoD sigma factor (24). σ^{70} factors in groups 2, 3, and 4 are alternative sigma factors. Group 2 σ^{70} factors are structurally very similar to group 1 σ^{70} factors (17–19). In contrast to group 1 σ^{70} factors, however, members of group 2 regulate responses, such as the general stress response, that are not necessarily essential to the cell under normal, exponential growth conditions (17–19). In *P. aeruginosa*, RpoS is the stationary phase sigma factor that regulates the general stress response (24). Group 3 σ^{70} factors are more divergent than groups 1 and 2 – members of this group regulate genes involved in specific functions, such as flagellar biosynthesis (17–19). For example, FliA is the sigma factor in *P. aeruginosa* that regulates expression of flagellar genes (24). Finally, group 4 σ^{70} factors are the most structurally and functionally divergent. Members of this group are also called extracytoplasmic function (ECF) sigma factors because they respond to signals from the environment, and most sigma factors in *P. aeruginosa* belong to this group (19, 24). For example, the envelope stress sigma factor AlgU, which is involved in expression of the alginate exopolysaccharide biosynthetic genes, is an ECF sigma factor (24). The expression and activity of σ^{70} factors can be regulated at various levels to ensure precise and tunable control over the cellular transcriptome. Sigma factor competition for RNA polymerase, transcriptional control over sigma factor-encoding genes, proteolytic degradation of the sigma factor, and sequestration of the sigma factor by an anti-sigma factor are all examples of how levels of a particular sigma factor can be modulated in the cell (25–28)

The other class of sigma factors, the σ^{54} family, is evolutionarily, structurally, and mechanistically distinct from σ^{70} factors (29). Bacteria normally only have one member of the σ^{54}

family – in the case of *P. aeruginosa*, RpoN is the σ^{54} factor (24). Unlike the σ^{70} factors, which recognize -10 and -35 promoter elements, σ^{54} factors recognize -12 and -24 promoter elements (29, 30). Another critical difference is that the RNA polymerase holoenzyme containing a σ^{54} factor cannot spontaneously form an open complex and initiate transcription due to the stability of closed complexes formed by this holoenzyme (29, 30). Transition from the closed to open state (isomerization) requires the activity of a bacterial enhancer binding protein (bEBP) (29–31). bEBPs have three core domains: a regulatory domain that responds to a given signal (often phosphorylation from a signal transduction pathway), an AAA+ ATPase domain that interacts directly with the σ^{54} factor and hydrolyses ATP, and a DNA binding domain that interacts with a DNA sequence (specific to a particular bEPB) (29–32). bEBPs activated by their cognate signal assemble into hexameric rings that bind enhancer DNA sequences relatively far upstream of the core σ^{54} promoter elements and interact with σ^{54} via a DNA looping mechanism (29–32). Coupling of ATP hydrolysis by the bEBP's AAA+ ATPase domain with holoenzyme conformational changes renders isomerization energetically favourable and allows for transcriptional initiation (29–32).

P. aeruginosa has more than twenty sigma factors, and the regulons and DNA binding specificities of many of these sigma factors have been elucidated (22). RpoS and RpoN are sigma factors that are relevant to the work discussed in this thesis and are, therefore, discussed in some detail below.

RpoS is the stationary phase sigma factor in *P. aeruginosa* (33), and its regulon has been elucidated by DNA microarray (34), RNA sequencing (RNA-seq) (22), and chromatin immunoprecipitation sequencing (ChIP-seq) (22). Levels of RpoS are high in stationary phase cells and in biofilms, which are stationary phase-like due to the high-density and starvation

conditions experienced by cells in these multicellular communities (35–38) RpoS has been implicated in quorum sensing regulation (34, 39, 40) as well as in the expression of virulence factors (41) and of the PSL exopolysaccharide (42). RpoS is involved in tolerance to a variety of stresses, including carbon source and oxygen limitation, acidic and hyperosmolar growth conditions, biocides such as ethanol and hydrogen peroxide, and antibiotics such as fluoroquinolones and carbapenems (41, 43–47). Several mechanisms that regulate RpoS levels in *P. aeruginosa* have been reported (48–57). The best characterized mechanism is direct transcriptional activation of the *rpoS* gene upon entry into stationary phase by PsrA, a transcription factor from the TetR family that responds to long-chain fatty acids (48–53).

As mentioned previously, RpoN is the only member of the σ^{54} family sigma factor present in the *P. aeruginosa* genome (24). RpoN regulates the expression of genes involved in a variety of processes, including nitrogen assimilation, carbon source utilization, motility, antibiotic tolerance, quorum sensing, biofilm formation, and virulence with the help of approximately 20 bEBPs (22, 24, 58–65). For instance, RpoN, along with the bEBP DctD, is important for the expression of the C4-dicarboxylate transporters in *P. aeruginosa* that allow growth on carbon sources such as fumarate, succinate, and malate (66).

While sigma factors give the cell the ability to grossly coordinate the expression of genes required for a specific response to an environmental condition (eg. starvation or heat), there are more signals that a bacterium needs to respond to than there are sigma factors. Fine tuning of gene expression in response to a very specific signal, such as the presence of a particular amino acid, can be achieved by transcription factors that sense the signal and modulate the affinity of the core transcriptional machinery for promoters of genes needed to respond to the signal.

1.5.2 Transcription factors

Trans-acting transcription factors bind to *cis* DNA sequences and modulate the ability of the RNA polymerase holoenzyme to initiate transcription at a promoter (17, 67, 68). Transcription factors generally consist of a DNA binding domain, which is often a helix-turn-helix, and a ligand binding domain (17, 67, 68). Binding of the transcription factor's ligand to its ligand binding domain may increase or decrease the affinity of the transcription factor for its DNA binding site, thereby coupling transcriptional regulation to a specific stimulus (17, 67, 68). Some transcription factors are part of extracellular signal transduction pathways called two-component systems (69). In these cases, the transcription factors are activated by covalent modification with a phosphoryl group (70). These are described in more detail in the next section.

Transcription factors act as activators or repressors of target gene transcription (17, 67, 68). Activators increase the affinity of the RNA polymerase holoenzyme for the promoter in question via one of three general mechanisms: 1) binding upstream of the core promoter elements and contacting the C-terminal domains of the α-subunits, 2) binding at a site that overlaps the -35 element and contacting the sigma factor, or 3) altering the conformation of DNA at promoters with suboptimal spacing between the -10 and -35 elements to allow for RNA polymerase holoenzyme binding (17, 67, 68). In contrast to activators, repressors tend to physically impair the interaction of the RNA polymerase holoenzyme with the promoter (17, 67, 68). For instance, repressors may bind to DNA binding sites that overlap the core promoter elements and sterically impede RNA polymerase holoenzyme binding (17, 67, 68). Alternatively, repressors may loop DNA around the promoter and render it inaccessible to the transcriptional machinery (17, 67, 68). Repressors may also act on activators and prevent their ability to recruit RNA polymerase holoenzymes to a promoter (17, 67, 68). Additionally, some repressors may not prevent RNA polymerase

holoenzyme binding (17, 67, 68). Instead, these repressors impair isomerization or prevent downstream movement of the transcriptional machinery (17, 67, 68).

Transcription factors can be grouped into families based on structural and functional similarities. For instance, the most abundant family of transcription factors is the LysR family (71). PA3225, which is the topic of **Chapter 2**, is a member of this family of transcription factors (71). LysR-type transcriptional regulators consist of a C-terminal ligand binding domain and an N-terminal winged helix-turn-helix DNA binding domain (71). Although prototypical members of this family act as activators and autorepressors (negative autoregulation), LysR-type repressors are also common and some members of this family have even been shown to act as autoactivators (positive autoregulation) (71). Classically, LysR-type transcription factors tend to bind DNA as dimers of dimers, which come together as a tetramer to create a topological bend in the DNA, and this bending impacts interactions of the regulator with the RNA polymerase holoenzyme (71).

Transcription factors have also been called one-component systems because the domain for direct sensing of the environmental stimulus (ie. the ligand binding domain) is on the same polypeptide as the response domain (which, in this case, is a DNA binding domain) (72). Next, we will consider two-component systems.

1.5.3 Two-component systems

Two-component systems allow transduction of an extracellular signal to an intracellular response and are so named because they generally consist of two players: 1) a sensor kinase and 2) its cognate response regulator (69). Generally speaking, sensor kinases are homodimeric, integral membrane proteins with a periplasmic sensor (or input) domain and a cytoplasmic kinase (or transmitter) domain (70). The sensor domain senses a particular stimulus (often a chemical ligand), which elicits a conformational change that ultimately leads to autophosphorylation of a

conserved histidine residue in the transmitter domain (70). This phosphoryl group is then transferred to a conserved aspartate residue in the receiver domain of the cognate response regulator, which is the second component of the signal transduction system (70). Prototypic response regulators are soluble cytoplasmic proteins with a receiver domain and an effector domain (70). Phosphorylation of the receiver domain results in a conformational change that activates the effector domain (70). Effector domains can carry out a range of functions, although the most common role of response regulators is DNA binding and transcriptional regulation (73). More complex signal transduction systems, called phosphorelays also exist (69). In this case, the sensor kinase phosphorylates a receiver with no effector domain (69). This atypical receiver then phosphorylates a histidine phosphotransfer (Hpt) module, and the Hpt proceeds to phosphorylate and activate the response regulator (69).

P. aeruginosa has a vast array of proteins that participate in two-component systems (14, 74). Many *P. aeruginosa* two-component systems have been implicated in virulence and antibiotic resistance (75, 76). Others are important for sensing the various nutrients that *P. aeruginosa* can use as carbon sources (77). An example of a *P. aeruginosa* two-component system that is involved in sensing a carbon source and that is relevant to **Chapter 4** of this thesis is the DctBD two-component system (66, 78). DctB is an integral cytoplasmic membrane sensor kinase that detects the presence of C_4-dicarboxylates, such as fumarate, malate, and succinate via its periplasmic sensor domain (79, 80). C_4-dicarboxylates are preferentially used as carbon sources by *P. aeruginosa* (81). In the presence of C_4-dicarboxylates, DctB autophosphorylates and transfers the phosphoryl group to a conserved aspartate residue in the REC receiver domain of its cognate response regulator, DctD (79). In addition to the N-terminal receiver domain, DctD has a σ^{54}-interaction region in an AAA+ ATPase domain and a Fis-type helix-turn-helix DNA binding

domain (79, 82, 83). Consistent with this domain architecture, phosphorylated DctD acts as a bEBP for RpoN-dependent transcriptional activation (see above commentary on RpoN) (79). DctD-activated, RpoN-dependent transcription of the C_4-dicarobxylate transporters, DctA and DctPQM, can then occur, thereby allowing uptake of the C_4-dicarboxylates into the cell where they are subsequently metabolized (66). Interestingly, DctA is thought to interact with DctB to prevent activation of DctBD signalling in the absence of C_4-dicarboxylate signals (79). It should also be appreciated that the DctBD two-component system is not the only mechanism that regulates expression of C_4-dicarboxylate transporters in *P. aeruginosa*, which further reinforces the importance of nuanced control over gene expression. The transcriptional repressor DctR and the RpoN-regulated carbon catabolite repression system (84) coordinate preferential expression of either *dctA* or *dctPQM* in the presence of high or low C_4-dicarboxylate concentrations, respectively (78, 85).

1.4 Antibiotic resistance in *P. aeruginosa*

1.4.1 Defining antibiotic resistance

This section is taken from (1) ***with modifications as necessary*****.**

Antibiotic resistance is a looming global health crisis (86) that is expected to cause more deaths than cancer in the world by 2050 according to the Review on Antimicrobial Resistance that was commissioned by the Government of the United Kingdom (https://amr-review.org/). Resistant microorganisms can grow in the presence of a bactericidal or bacteriostatic antimicrobial agent at a concentration that would normally be inhibitory to growth (87). Resistance is typically measured in planktonic cultures using the minimum inhibitory concentration (MIC), which is the lowest concentration of antimicrobial agent that will inhibit visible growth of the microorganism (87). It is common practice in the basic science literature to describe a strain with a higher MIC than the

reference strain (typically a wildtype strain) as "more resistant" while a strain with a lower MIC than the reference strain is deemed "less resistant". Clinically speaking, the usage of the term "resistance" is much more restrictive. A resistant isolate is an isolate with an MIC value that falls above the MIC breakpoint for resistance. MIC breakpoints are tied to pharmacokinetic parameters of the antibiotic as well as historical clinical experience, and they are intended to help predict the likelihood of a favourable treatment outcome. Resistance is most often thought of as being attributable to mutations or exchange of antibiotic resistance genetic elements (acquired resistance), although resistance may also be intrinsic and thus dependent on wild-type genes and innate properties of the cell (88–90). For instance, *P. aeruginosa* is intrinsically resistant to many antibiotics due to the relative impermeability of its outer membrane (9, 91). In general, antibiotic resistance is thought to be a property of planktonic, growing populations under nutrient replete conditions since growth is a requirement for resistance (87).

1.4.2 Antibiotic resistance mechanisms in P. aeruginosa: aminoglycosides as an example

Resistance mechanisms have been described as the means by which an antimicrobial agent is prevented from interacting with its intended target (92). Resistance mechanisms may be specific to a given antibiotic agent or class while other mechanisms may provide multidrug resistance. Generally, resistance mechanisms that prevent an antibiotic's interaction with its target can include 1) impaired uptake, 2) increased efflux, 3) target mutation or modification, and 4) antibiotic modification or degradation (90, 93).

For the purposes of discussion, let us consider in this section some of the resistance mechanisms employed by *P. aeruginosa* against aminoglycoside antibiotics (eg. tobramycin, gentamicin, amikacin) that are commonly used to treat *P. aeruginosa* CF lung infections (6, 94, 95). To understand resistance mechanisms of a given antibiotic, it is helpful to concurrently

understand how the antibiotic reaches and interacts with its target. Aminoglycosides target the ribosome and must therefore enter the cell to reach their intracellular target. Aminoglycosides, which are polycationic molecules, enter Gram-negative bacterial cells by first interacting with the negatively charged lipopolysaccharide (LPS) molecules that decorate the outer membrane (95–97). This interaction distorts the outer membrane and increases its permeability to the aminoglycoside in a process that has been called self-promoted uptake (95–97). Modifications to LPS that reduce its anionic charge have been implicated in aminoglycoside resistance because self-promoted uptake is presumably impaired (98). Once in the periplasm, the aminoglycoside must traverse the inner membrane via a poorly defined uptake mechanism that requires a threshold membrane potential. Thus, loss-of-function mutations in components of the electron transport chain have been show to confer aminoglycoside resistance due to loss of proton motive force and aminoglycoside uptake (99–101).

Once in the cell, the aminoglycoside antibiotic must contend with antibiotic efflux. In *P. aeruginosa* CF clinical isolates, overexpression of the chromosomally-encoded RND efflux pump MexXY-OprM is primarily responsible for aminoglycoside resistance (10). Loss-of-function mutations in *mexZ*, which encodes the transcriptional repressor of the *mexXY* operon, are the most common causes of MexXY overexpression (10). ArmZ, which encodes the anti-repressor of MexZ and is activated in response to ribosome stalling caused by aminoglycosides, can also promote MexXY expression (102–104). Gain-of-function mutations in the two-component system ParRS have also been shown to lead to upregulation of *mexXY* and aminoglycoside resistance, although the mechanism has not yet been elucidated (103, 105).

Aminoglycosides interact with the 30S ribosomal subunit at the A-site of the 16S rRNA, which accepts and proofreads new aminoacyl-tRNAs that are to be added to the elongating

polypeptide chain during translation (95–97). Interaction of aminoglycosides with the ribosome leads to protein mistranslation as well as protein synthesis arrest (95–97). While rare in CF isolates, aminoglycoside modifying enzymes encoded on mobile genetic elements can acetylate, phosphorylate, or adenylate aminoglycosides, thereby decreasing their affinity for the ribosome and impairing their ability to dysregulate translation (9, 106, 107). Moreover, target site modification of the 16S rRNA by 16S rRNA methylases has also been shown to reduce aminoglycoside binding and confer resistance (9, 106). While target site mutations are common in resistance to other antibiotics (eg. mutations in DNA gyrase conferring resistance to fluoroquinolones), 16S rRNA mutations do not seem to be a form of aminoglycoside resistance in *P. aeruginosa* (suggesting strong selective pressure against 16S rRNA mutations) (108). Interestingly, however, mutations in the translational elongation factor encoded by *fusA1* confer aminoglycoside resistance (109).

As mentioned briefly above, aminoglycosides cause protein mistranslation (95, 97). These mistranslated peptides fold improperly and can damage the inner membrane, leading to increased permeability of the inner membrane, increased influx of aminoglycosides and other molecules into the cytoplasm, and, ultimately, death of the cell (95, 97). It is this property that confers bactericidal activity to aminoglycosides, which is unusual among protein synthesis inhibitors as this functional class of antibiotics tends to be bacteriostatic (95, 97). Thus, mechanisms that improve the membrane stress response can increase aminoglycoside resistance. For instance, mutational activation of the AmgRS two-component system, which regulates membrane proteases that can degrade mistranslated peptides, promotes aminoglycoside resistance in *P. aeruginosa* while deletion of this signaling system promotes susceptibility (91, 110–112).

Overall, it is clear that *P. aeruginosa* has a number of innate and acquired resistance mechanisms to withstand aminoglycoside treatment. Bear in mind that *P. aeruginosa* has an arsenal of other mechanisms at its disposal that can confer resistance to other types of antibiotics such as β-lactams and fluoroquinolones (9). The MexAB-OprM multidrug efflux pump is one such mechanism and is discussed in more detail in **Chapter 2**.

1.5 *P. aeruginosa* biofilms and antibiotic tolerance

This entire section is taken from (1) ***with modifications as necessary*****.**

1.5.1 Defining antibiotic tolerance

Antibiotic tolerance is the ability of a bacterial population to survive transient exposure to a concentration of bactericidal antibiotic that would be otherwise lethal (87, 113, 114). Importantly, tolerance is not related to changes in the MIC, and there is no standardised method to assess clinical tolerance in spite of the clinical relevance of the tolerance phenomenon. In basic science, the gold standard method to measure tolerance is to assay survival (often via direct viability counting methods) as a function of antibiotic concentration or exposure time, although other metrics and methods to measure tolerance have also been described. (87) Tolerance can be genotypic (ie. inherited) or phenotypic (ie. dependent on the environmental conditions). Phenotypic tolerance is reversible once the environmental condition(s) that induced the tolerant phenotype have changed (113). Antibiotic persistence is a special case of tolerance (114). While tolerance refers to a population as a whole, persistence refers to a sub-population of tolerant bacteria, called persister cells, in a population that is otherwise readily killed by the antibiotic (114). In contrast to resistance in exponentially growing planktonic cells, tolerance is generally thought to be a property of non-growing, metabolically dormant, nutrient-restricted cells (113). Stationary phase planktonic cultures and biofilm cells are examples of bacterial populations that

are traditionally described as being antibiotic tolerant. Mechanisms of tolerance are thought to somehow prevent the bactericidal agent from exerting its downstream toxic effects even though the agent has bound to its target (92).

1.5.2 What are biofilms?

Biofilms are microbial communities that exist as suspended aggregates or that adhere to biotic or abiotic surfaces, and the cells within a biofilm are encased in self-produced matrix. Biofilms are medically important because they have been implicated in the pathogenesis of numerous bacterial infections that are difficult to successfully eradicate with antibiotics (115). For instance, *P. aeruginosa* biofilms cause chronic lung infections in cystic fibrosis (CF) patients (7, 116).

The phenotypic switch from a free-swimming, planktonic lifestyle to a surface-attached existence in a biofilm has been traditionally viewed as a highly regulated developmental process that depends on numerous environmental (eg. composition of the surface and growth conditions) and genetic factors (117–120). The classic developmental model of biofilm formation maintains that motile planktonic cells attach to a surface in response to a variety of environmental signals (121). For example, exposure to subinhibitory concentrations of aminoglycosides is one of the many signals that can trigger biofilm formation in *P. aeruginosa* (122). Attached cells produce a hydrated matrix composed of exopolysaccharides, extracellular DNA (eDNA), proteins, lipids, and phage particles (13). Over time, collections of sessile cells in microcolonies mature into macrocolonies. Cells can escape from mature biofilms to return to the planktonic lifestyle and subsequently colonize new surfaces (123).

There are several key characteristics that differentiate biofilm cells from planktonic cells. While planktonic cultures are exposed to relatively uniform environmental conditions, cells in a biofilm experience a gradient of nutrients and waste products (37). Subpopulations in biofilms are, as a result, physiologically heterogeneous, which makes the study of biofilms challenging since many experimental procedures such as susceptibility testing and transcriptomic profiling assess the biofilm as a whole instead of distinct biofilm subpopulations; however, recent technological advances have begun to allow for the study of subpopulations (124–128). Another important difference between the two lifestyles is that exponentially growing planktonic cells and biofilm cells do not share identical transcriptomes or proteomes, thereby giving rise to phenotypic differences between the two lifestyles (118, 119, 129–133).

Perhaps the most salient phenotypic difference between biofilms and planktonic cells is the fact that biofilm cells are much less susceptible to antimicrobial agents than their genetically identical planktonic counterparts (134, 135). For instance, *P. aeruginosa* biofilms growing on urinary catheters are approximately 1000-fold more recalcitrant to killing by tobramycin than planktonic cells (136). The decreased susceptibility of biofilms to antibiotics allows biofilm-based infections to persist chronically in spite of antibiotic therapy (115). It is generally accepted that the basis for biofilm-specific antibiotic resistance and tolerance is multifactorial (8, 137, 138), and mechanisms of resistance and tolerance vary depending on the particular antimicrobial agent, the bacterial strain and species, the age and developmental stage of the biofilm, and the biofilm growth conditions (139–143). Individually, no single mechanism can account for the heightened antibiotic recalcitrance that is characteristic of biofilms. In combination, however, these resistance and tolerance mechanisms severely limit our ability to effectively treat biofilm-based infections with the antimicrobial arsenal that is currently available (144). Understanding the mechanisms

underlying biofilm-specific antibiotic resistance and tolerance will help guide the development of treatments that would disrupt these mechanisms and render biofilms more responsive to antimicrobial therapy (73, 145, 146).

1.5.3 A sticking point: biofilm resistance or biofilm tolerance?

When in a biofilm, pathogenic bacteria likely employ both tolerance and resistance mechanisms to withstand antimicrobial challenges. In most cases, careful experimental work has made it possible to categorize, in a straightforward manner, a mechanism as being involved in resistance or tolerance. However, there appears to be some disagreement in the literature as to whether some mechanisms confer biofilm resistance or tolerance – while some authors might say a particular mechanism confers resistance, others might label it as a tolerance mechanism. One example of this is the *ndvB* gene product in *P. aeruginosa* biofilms that is studied by our group. We have historically described *ndvB* as an intrinsic biofilm antibiotic resistance gene (147); on the other hand, some authors writing about *ndvB* have described it as a gene involved in biofilm tolerance. As will be discussed later, killing of Δ*ndvB* biofilms by tobramycin and other antibiotics is increased compared to wildtype in the absence of a change in the planktonic MIC (147). We do not dispute that this satisfies the definition of tolerance, so *ndvB* can correctly be described as a gene involved in biofilm tolerance. However, the *ndvB* locus can also be thought of as a resistance determinant for two reasons. Firstly, cyclic glucans synthesized by the *ndvB* gene product sequester aminoglycoside antibiotics, thereby preventing them from interacting with the ribosome (147, 148). This mechanism falls in line with the definition of resistance mechanisms described by Kim Lewis (92). Secondly, induced expression of *ndvB* in wildtype exponential phase planktonic cells, which do not normally express *ndvB*, results in an increase in the MIC for tobramycin (147, 149). Somewhat confusingly, the *ndvB* gene can, therefore, be correctly thought

of as a determinant of both antibiotic tolerance and resistance in *P. aeruginosa* biofilms. This example illustrates that, while resistance and tolerance are well-defined terms, some mechanisms that mediate reduced biofilm susceptibility to antibiotics may not necessarily fit well within these definitions. Using the mechanistic definitions coined by Lewis (92), biofilm resistance mechanisms would include, among others, antibiotic efflux pumps, molecules (such as eDNA and NdvB-derived periplasmic glucans) that sequester antibiotics, and matrix β-lactamases, while tolerance mechanisms would include reduced growth rate, persister cells, and the mechanisms that handle antibiotic-induced oxidative stress.

Indeed, some authors go so far as to say that antibiotic recalcitrance of biofilms is only due to tolerance, which is problematic because it negates the contribution of resistance to chronic infections even though we know that resistant isolates arise in chronic infectious processes that involve biofilms (150). To acknowledge that biofilms employ a complex mixture of tolerance and resistance mechanisms, many authors have used the term "recalcitrance" to refer to the reduced susceptibility of biofilm cells to antibiotics while others have used the terms "tolerance" and "resistance" interchangeably (8, 92, 137, 138, 151). Another neutral approach would be to simply say that biofilms survive antimicrobial treatment via mechanisms that reduce antibiotic sensitivity or susceptibility. When discussing mechanisms in this thesis, I have made an attempt to use the terms "tolerance" and "resistance" in a manner that is consistent with how these mechanisms were described in the primary literature by the authors who have characterized them or when usage of one of the terms is clearly more accurate than the other term for a given mechanism.

A comprehensive discussion of many of the biofilm resistance and tolerance mechanisms employed by pathogenic bacteria in biofilms can be found in a review that I wrote in 2017 (1). An overview of some of these mechanisms is shown pictorially in a figure taken from that review (**Fig**

1-1). The sections that follow highlight, in detail, specific mechanisms of biofilm recalcitrance that are relevant to my thesis.

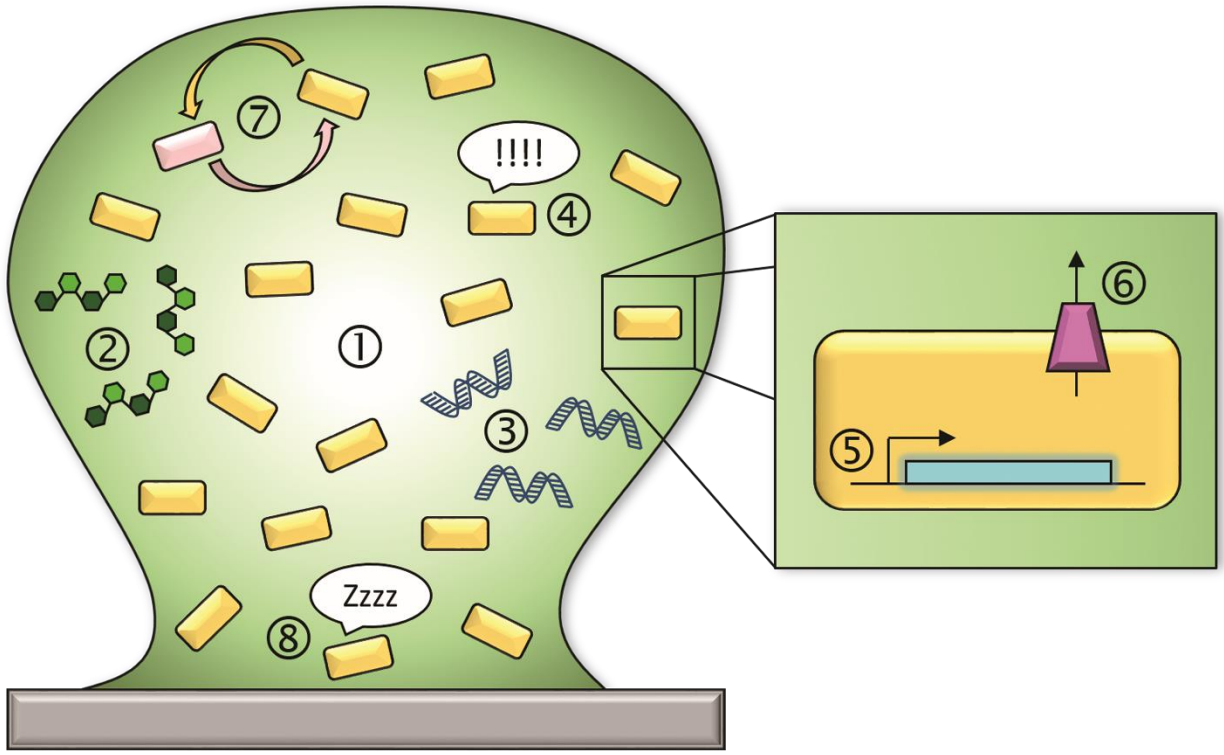

Figure 1-1. Schematic overview of the major antimicrobial resistance and tolerance mechanisms employed by bacterial biofilms.
Biofilm cells (yellow rectangles) are embedded in a mushroom-shaped matrix (shown in green). The biofilm is attached to a surface (grey rectangle), which can be biotic or abiotic. Pictorial representations of the resistance mechanisms are numbered as follows: (1) nutrient gradient (demonstrated here as a colour-intensity gradient) with less nutrient availability in the core of the biofilm, (2) matrix exopolysaccharides, (3) extracellular DNA, (4) stress responses (oxidative stress response, stringent response, etc.), (5) discrete genetic determinants that are specifically expressed in biofilms and whose gene products act to reduce biofilm susceptibility via diverse mechanisms (*ndvB*, *brlR*, etc.) (6) multidrug efflux pumps, (7) intercellular interactions (horizontal gene transfer, quorum sensing, multispecies communication etc.), and (8) persister cells. **Figure taken from reference (1).**

1.5.4 The role of ndvB in P. aeruginosa biofilm tolerance/resistance

This section is taken from (1) ***with modifications as necessary*****.**

The *ndvB* locus was first identified as a *P. aeruginosa* biofilm-specific antibiotic resistance gene in a screen for random transposon mutants that had decreased biofilm resistance to tobramycin in the absence of both a biofilm formation defect and an altered planktonic susceptibility (147). The screen also identified five other genetic determinants of biofilm-specific antibiotic resistance (*tssC1*, *PA0756-0757*, *PA1875-1877*, *PA2070*, and *PA5033*) (152–154). While the Δ*ndvB* mutant had the same minimal bactericidal concentration as PA14 wildtype for all antibiotics tested when growing planktonically, Δ*ndvB* biofilms were 16-fold more susceptible to tobramycin and eight-fold more susceptible to both gentamicin and ciprofloxacin than wildtype biofilms (147). It was determined that the Δ*ndvB* mutant had a biofilm-specific phenotype because, in wildtype, the *ndvB* transcript was 20-times more highly expressed in biofilm cells compared to exponential phase planktonic cells (147, 149). However, the mechanism underlying preferential expression of *ndvB* in biofilms was not known until my work in **Chapter 3**.

The membrane-bound NdvB glucosyltransferase is responsible for the production of cyclic β-(1→3)-glucans that are located in the periplasm and in the extracellular biofilm matrix (147, 148). The NdvB-derived cyclic glucans are composed of 12 to 15 glucose units, and nearly 50% of the glucose units are substituted at the *O*-6 position by 1-phosphoglycerol (148). Thanks to their anionic phosphoglycerol moieties, the cyclic glucans can physically interact with cationic aminoglycosides such as kanamycin and tobramycin in the periplasm, and this electrostatic interaction presumably prevents these antibiotics from breaching the inner membrane and accessing their intracellular targets (147, 148).

In some bacterial species that form symbiotic relationships with plants, cyclic glucans produced by NdvB homologs are important for intercellular signalling (155). It is not exactly known how this signalling function is achieved; however, cyclic glucans, like cyclodextrins, have large internal diameters that can host hydrophobic molecules, so one possibility is that cyclic glucans can act as chaperones for intercellular signalling molecules (155). Therefore, Beaudoin *et al* hypothesized that *P. aeruginosa* NdvB-derived cyclic glucans may play a role in signalling between cells in biofilms, and that this intercellular signalling may lead to a heightened state of antibiotic resistance through changes in gene transcription (149). Differential gene expression analysis between wildtype and Δ*ndvB* biofilms using DNA microarrays revealed that the transcription of several genes was affected by the absence of *ndvB* (149). Most notably, it was discovered that key genes involved in ethanol oxidation were transcriptionally downregulated in Δ*ndvB* biofilms (149). In fact, the ethanol oxidation genes were more highly expressed in wildtype biofilms compared to planktonic cells, and this lifestyle-dependent, preferential gene expression pattern required *ndvB* (149). Deletion of each of the ethanol oxidation genes resulted in mutants that had a minimal bactericidal concentration for tobramycin that was four-times lower than wild-type when growing as a biofilm, while planktonic susceptibility of the mutants to tobramycin was unaffected (149). The ethanol oxidation pathway therefore represents a novel mechanism of biofilm-specific antibiotic recalcitrance that is not yet understood, although it has been proposed that the enzymes involved may help reduce intracellular ROS which, as discussed above, is hypothesized to be involved in antibiotic-induced cell death (149). At this time, it is still not known how NdvB-derived cyclic glucans cause transcriptional changes in *P. aeruginosa* biofilms. A schematic showing the roles of NdvB-derived glucans in biofilm resistance through sequestration of antibiotics and through ethanol oxidation is shown in **Fig 1-2**.

Clinical reports have shown that NdvB-derived glucans are detectable in the blood of patients with *P. aeruginosa* bacteremia (156, 157), and it is known that cyclic glucans are important for biofilm persistence in the slow-killing *Caenorhabditis elegans* model of biofilm-based infection (Zhang *et al.* 2013). Moving forward, future investigations into how cyclic β-(1→3)-glucans contribute to pathogenesis and affect antibiotic treatment outcomes of biofilm-based infections *in vivo* will help us to understand the potential utility of therapeutically targeting NdvB in the clinical setting.

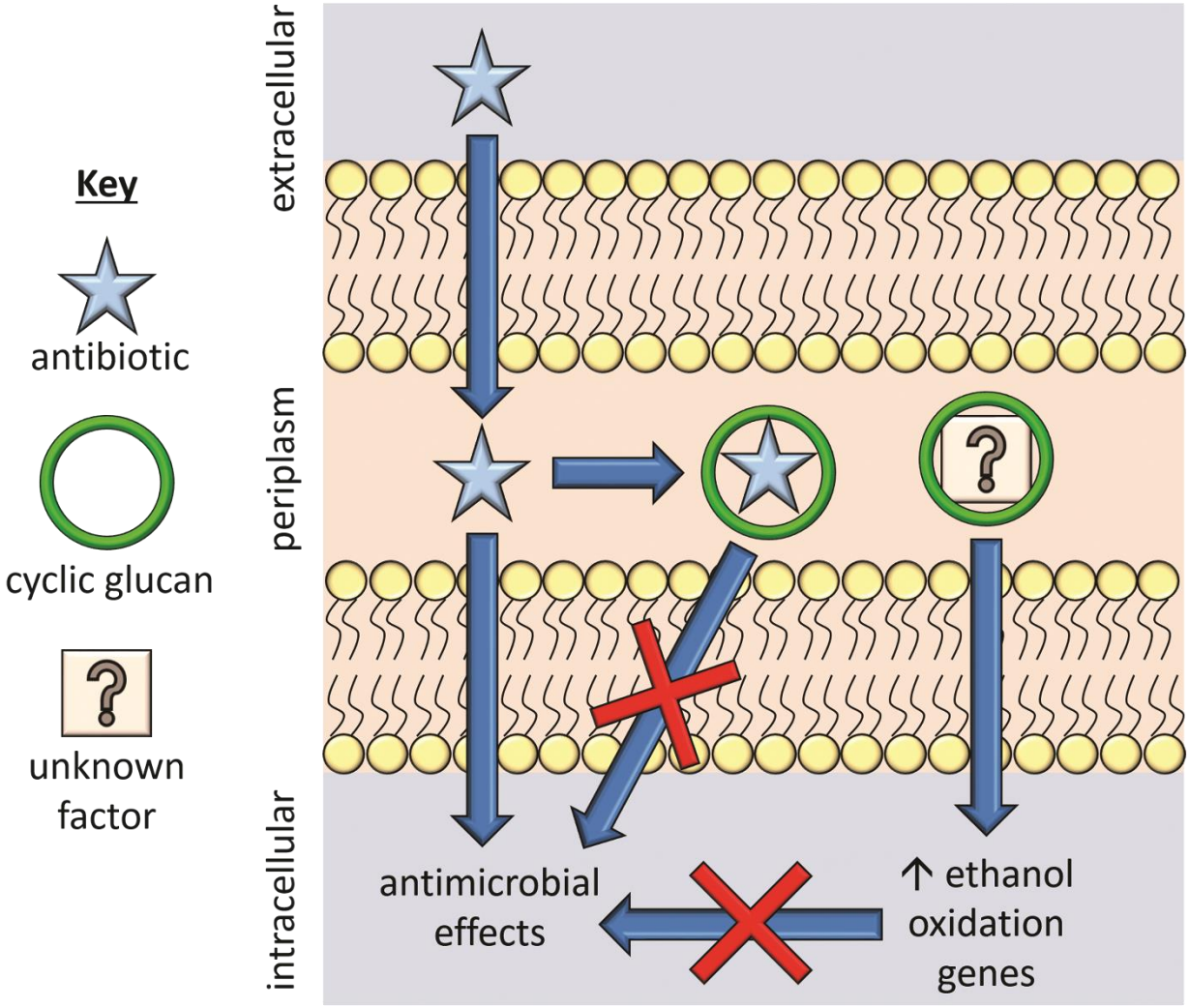

Figure 1-2. NdvB-derived cyclic glucans promote biofilm resistance to antibiotics through sequestration and signaling.

The NdvB glucosyltransferase produces periplasmic cyclic β-(1→3)-glucans in *P. aeruginosa* biofilm cells. The cyclic glucans can physically sequester aminoglycoside antibiotics in the periplasm, thereby preventing the antibiotics from reaching their intracellular targets and exerting their antimicrobial effects. NdvB-derived glucans also contribute to biofilm-specific antibiotic resistance via an uncharacterized signaling pathway that ultimately leads to upregulation of genes involved in ethanol oxidation. It is possible that the cyclic glucans may act as chaperones for an uncharacterized signal molecule or the cyclic glucans may act as signals themselves. The ethanol oxidation genes are also important for biofilm-specific antibiotic resistance via an unknown mechanism that may involve ROS detoxification.

1.5.5 Involvement of tssC1 in P. aeruginosa biofilm resistance

Type VI secretion systems (T6SS) were discovered relatively recently, and they serve as a novel secretory pathway in Gram-negative bacteria that enables delivery of many different effector proteins to prokaryotic and eukaryotic cells. Many excellent reviews have been published about the structure and functions of T6SS, and the reader is encouraged to consult these review articles for a more thorough discussion of T6SS than is presented here (158–161).

The *P. aeruginosa* genome contains three different T6SS, called Hcp secretion islands (HSI-I, -II, and -III) (158). Intriguingly, in the original transposon mutant screen for genetic determinants of biofilm-specific antibiotic resistance genes conducted by Mah *et al* (147), the *tssC1* (*hsiC1*) gene in the HSI-I locus was identified as a contributor to antibiotic resistance in *P. aeruginosa* biofilms (152). TssC1 is a core structural component of the HSI-I T6SS apparatus (162). The Δ*tssC1* deletion mutant formed biofilms that were indistinguishable from wild-type and the Δ*tssC1* mutant had no defect in planktonic resistance (152). However, when grown as a biofilm, the Δ*tssC1* strain was four-fold less resistant to tobramycin and ciprofloxacin, and two-fold less resistant to gentamicin compared to wild-type (152). Consistent with the biofilm-specific resistance phenotype of the Δ*tssC1* deletion mutant, the wild-type expression level of the *tssC1* gene was about 20-times higher in biofilms than in planktonic cells (152).

It is not currently known how *tssC1* is linked to biofilm-associated antibiotic resistance, although it is likely that the HSI-I T6SS apparatus as a whole is important for the resistance phenotype given that *hcp1*, which encodes another structural component of the HSI-I T6SS, was also important for biofilm resistance to antibiotics (152). It is possible that one of the effectors delivered via the T6SS apparatus acts on cells within the biofilm to increase antibiotic resistance. A comprehensive assessment of the impact of all known HSI-I T6SS effectors on biofilm-specific

antibiotic resistance could help to further elucidate the role of this secretion system in antibiotic resistance.

1.5.6 Nutrient starvation as a tolerance mechanism

Physiological heterogeneity in biofilms is characterized by differences in gene expression, metabolic activity, and phenotype, including antimicrobial tolerance, of cells located in different geographic areas of a biofilm (37, 124, 125, 163–166). Heterogeneity arises due to the gradient of oxygen and of other nutrients within the biofilm (35, 37). This gradient is created as the result of the fact that cells near the surface of the biofilm use up the available nutritional resources before the nutrients can penetrate deeper into the biofilm (37). For instance, several studies have demonstrated that a steep oxygen gradient exists within biofilms of various species such that deeper layers of the biofilm are oxygen-deprived (164, 165, 167–170). Cells within nutrient-poor or hypoxic zones have reduced metabolic activity and are in a stationary phase-like state (164, 165, 169–172) – it is believed that this slow growth rate confers tolerance since most antimicrobials target processes that are only essential for fast-growing cells (173–176). Further support for the majority of cells in biofilms being similar to stationary phase planktonic cells can be found in comparative transcriptomic studies (128, 130, 132, 177, 178). Due to their similarities, stationary phase cells have often been used in lieu of biofilm cells to study the effects of starvation on antibiotic tolerance. Stress responses to nutrient starvation, such as the RpoS-mediated general stress response, the stringent response, and the oxidative stress response have been linked to tolerance to some antibiotics in both stationary phase and biofilm cells (43, 44, 179–182). Starvation is also physiologically relevant in the human host, where nutrients and oxygen may be limiting at sites of chronic infection (12, 172).

Stationary phase and biofilm cells have reduced metabolism, leading to decreased electron transport chain activity, respiration, and proton motive force (172, 183–185). Recall that aminoglycoside uptake across the cytoplasmic membrane in Gram-negative bacteria is dependent on the proton motive force that is generated by electron transport chain activity and respiration (95, 97, 186). Thus, tolerance to aminoglycoside antibiotics in nutrient-restricted biofilm and stationary phase cells is thought to be primarily due to proton motive force dissipation and cellular membrane depolarization (45, 100, 185, 187). One logical way to re-sensitise nutrient-restricted, antibiotic tolerant cells to aminoglycosides would, therefore, be to supplement these cells with nutrients to restart metabolism, regenerate proton motive force, and promote both aminoglycoside uptake and downstream killing. This strategy is called metabolic potentiation of antibiotic lethality, and it has been used successfully in a variety of different bacteria with various antibiotics (188). For instance, Meylan and colleagues demonstrated that fumarate, a C_4-dicarboxylate, can potentiate tobramycin killing of antibiotic tolerant *P. aeruginosa* by restoring proton motive force and tobramycin uptake (185, 189).

Overall, it is clear that *P. aeruginosa* can be recalcitrant to antibiotic treatment through both resistance mechanisms and biofilm tolerance/resistance mechanisms. In CF, both of these factors are thought to play a major role in persistence of chronic *P. aeruginosa* lung infections in spite of antimicrobial therapy. CF will be explored in more detail in the next section.

1.6 Cystic fibrosis

1.4.1 Overview

CF is an incurable autosomal recessive genetic disorder, and it is the most common fatal genetic disease among Caucasian populations (6, 190). The disease affects multiple systems in

the body and is characterized by many clinical features including, but not limited to, chronic sinopulmonary infections, pancreatic insufficiency, nutrient malabsorption, and neonatal bowel obstruction (191, 192). In particular, chronic bacterial lung infections, such as those caused by *P. aeruginosa*, are the most important contributors to morbidity and mortality in CF patients because the chronic inflammatory response mounted against the bacteria promotes bronchiectasis and eventual respiratory failure (4, 6). Since early detection of CF has been shown to positively impact patient outcomes, newborn screening for CF has been implemented across all Canadian provinces and involves measurement of immunoreactive trypsinogen as well as genetic screening for common mutations (193). Positive screening tests are followed up with sweat tests and genetic testing as necessary to establish a CF diagnosis (193).

CF is caused by mutations in the *C*ystic *F*ibrosis *T*ransmembrane conductance *R*egulator (*CFTR*) gene on human chromosome 7 (194–198). CFTR is a chloride and bicarbonate channel that is unusual because it is the only known member of the ABC transporter superfamily that acts as an ATP-gated ion channel (194, 199, 200). As an ion channel, CFTR is an important modulator of electrolyte balance, luminal surface liquid pH, and fluid homeostasis in organs with CFTR-expressing epithelial cells (201). Loss of these critical physiological functions of CFTR lead to thick, sticky secretions in the lumens of epithelialised organs and ducts that contribute directly to the symptoms and pathophysiology of CF (6). Consistent with the widespread effects caused by loss of the anion channel, CFTR is found on the apical surface of epithelial cells in the airways, the pancreas, the sweat glands, the intestine, the kidneys, and the vas deferens (202).

1.4.2 Epidemiology

The most recent epidemiological data on CF in Canada can be found in the Canadian Cystic Fibrosis Registry (CCFR) 2017 Annual Data Report that is published by Cystic Fibrosis Canada.

In 2017, the incidence of CF in Canada was 1 in 3,600 live births, and there were over 4,300 Canadians (median age 22.8 years) living with CF (CCFR, 2017). The median age of survival was approximately 52 years (CCFR, 2017). Interestingly, it has been estimated that almost 1 in 25 Caucasians are heterozygous for disease-causing CFTR mutations, suggesting the possibility of a heterozygote advantage.

1.4.3 Genetics of CF

The most common *CFTR* mutation by far is deletion of a phenylalanine residue at position 508 (F508del), which leads to improper folding, aberrant processing, and destruction of the protein before it is trafficked to the membrane (203–205). While a very small fraction of F508del-CFTR may reach the cellular membrane, the mutant channel has a reduced probability of being in the open state (the state that allows for chloride conductance) compared to wildtype CFTR (205, 206). There are many other disease-causing *CFTR* mutations that are much less common and can disrupt transcription, normal transcript splicing, translation, membrane trafficking, channel gating, chloride conductance, and protein stability in the membrane (207, 208). Interestingly, several genes have also been identified that can modify symptoms and disease severity in patients with *CFTR* defects (209, 210).

1.4.4 Normal CFTR physiology and transepithelial fluid homeostasis

Epithelial cells, such as those found in the lungs, are polarized, which means that they have an apical membrane facing a lumen or external surface and a basolateral membrane that is in contact with the interstitium. In a tissue, the lateral surfaces of epithelial cells are tethered together by tight junctions, which limit the types of molecules that can diffuse paracellularly between the lumen and the bloodstream. Electrolyte and fluid homeostasis across epithelial tissues is a balancing act of absorption and secretion that is driven by the expression and regulated activity of

ion channels and pumps. Absorption refers to movement of water and ions in the basolateral direction to the bloodstream while secretion refers to movement of these molecules in the luminal direction.

Reabsorption of water and salt begin with active transport of sodium ions into the bloodstream through the activity of the sodium-potassium pump (Na^+/K^+-ATPase) found on the basolateral membrane of epithelial cells (201, 211). The activity of this pump creates an electrochemical gradient favouring sodium influx into the epithelial cell from the lumen via the epithelial sodium channel (ENaC) found on the apical surface of the cell (201, 211). As sodium is reabsorbed, chloride passively follows its electrochemical gradient via the paracellular route (201, 211). The movement of salt in the basolateral direction leads to water reabsorption through osmosis (201, 211).

The process of secreting salt and water into the lumen begins with the activity of the basolateral membrane Na^+-K^+-$2Cl^-$ co-transporter (NKCC1), which is a secondary active transporter that uses the inwardly directed sodium gradient generated by the Na^+/K^+-ATPase (see above) to actively accumulate chloride in epithelial cells against its electrochemical gradient (201, 211). As previously mentioned, CFTR is an apical membrane protein that serves as an ion channel for chloride. CFTR does not conduct chloride in its closed state (201, 211, 212). Therefore, when CFTR is in a closed state, chloride permeability of the apical membrane is low and reabsorption of salt and water predominates (201, 211). Phosphorylation of the regulatory domain of CFTR by cAMP-dependent protein kinase A and ATP binding to the nucleotide binding domains lead to opening of the gated channel, thereby increasing chloride conductance of the apical membrane such that chloride can passively follow its electrochemical gradient into the lumen (201, 211, 213, 214). The outward movement of chloride ions into the lumen creates an gradient that favours

passive secretion of sodium ions into the lumen via the paracellular route with water following by osmosis via aquaporins or via the paracellular route (201, 211). Importantly, CFTR also regulates the function of many other ion channels and pumps as well as aquaporins (201, 215). For instance, active CFTR inhibits the activity of ENaC, which further favours salt and water secretion (216–218).

Overall, CFTR activity plays a crucial role in regulating transepithelial fluid homeostasis and the volume of the luminal surface liquid. This basic understanding of CFTR function will help us understand how loss of CFTR causes disease in the section that follows.

1.4.5 CFTR dysfunction leads to impaired bacterial clearance in the lung

In the setting of CF, quantitative and/or qualitative defects in functional CFTR on the apical membrane lead to impaired chloride conductance across the apical membrane of epithelial cells (212). As a result, the balance of transepithelial fluid homeostasis is shifted towards water reabsorption, which leads to dehydration of the luminal surface liquid (201, 211). In the lung, the luminal surface liquid, which is called the airway surface liquid, has two main layers. The layer in proximity to the apical surface of the epithelial cells is called the periciliary layer and serves as a low-viscosity medium in which the cilia that form the mucociliary elevator can beat and remove debris and microorganisms (211). The mucociliary elevator is an important innate immune defense mechanism against bacteria (219). A sufficient volume of the periciliary layer is important to allow for proper movement of the cilia (211, 219). Overlying the periciliary layer is a viscoelastic mucous layer that traps particles (211, 219). In CF patients, dehydration of the periciliary layer results in compression of the cilia by the mucous layer, which becomes inspissated (211, 219, 220). Consequently, the ability of the mucociliary elevator to clear bacteria is significantly impaired.

Data from a porcine model of CF (221, 222), which has provided invaluable insights into CF airway disease (223)s, suggest that increased sodium reabsorption in the setting of impaired chloride secretion and the subsequent loss of airway surface liquid volume is not actually the primary defect in CF (224, 225). Instead, it is hypothesized that decreased pH of the airway surface liquid drives defective bacterial clearance (226–229). Although not discussed in detail above, CFTR also conducts bicarbonate and, as a result, is important for maintaining the alkaline pH of airway surface liquid (200, 230). It is believed that decreased airway surface liquid pH in CF can impair the activity of antimicrobial peptides that normally kill bacteria (228). Moreover, it has also been proposed that failure of mucins to detach from the hypoplastic submucosal glands in pigs with CF impairs mucociliary clearance, and this defect in mucous secretion may be related to bicarbonate abnormalities (231–235). Additionally, it has been postulated that innate immune cells in CF lungs either have an intrinsic functional deficiency and/or that the CF lung environment contributes to impaired immune cell activity (236). Overall, it is clear that CFTR function is critical to normal lung physiology and that multiple deficits in bacterial clearance increase the propensity of CF patients to develop chronic bacterial lung infections.

Whatever the true underlying defect may be in CF airway disease, it is clear that loss of CFTR has critical effects on the innate immune mechanisms that result in failure to clear and eradicate bacteria that enter the airways. Consequently, CF has been described by some as a primary innate immunodeficiency of the lung (237). As a result of innate immune failure, chronic bacterial infections are established in the CF lung (4, 237). These chronic lung infections cannot be cleared by the immune system or with antibiotics (4, 6, 237). The persistence of bacteria in the lung creates an exaggerated, but ineffective, immune response that causes substantial lung damage (237). Ultimately, declining lung function, bronchiectasis, and eventual respiratory failure will

result in death of the patient unless a lung transplant can be provided. While lung transplantation extends lifespan and improves quality of life, lung transplants do not cure extrapulmonary CF disease and transplantation itself is associated with many significant complications (238, 239).

While it is now appreciated that CF lung infections are polymicrobial (240), it has been well-established that the most clinically important cause of chronic CF lung infections is *P. aeruginosa* (4). The important role of *P. aeruginosa* in CF lung disease will be discussed next.

1.5 *P. aeruginosa* in the CF lung

1.5.1 Importance of P. aeruginosa to CF

P. aeruginosa causes chronic endobronchial lung infections in approximately 40% of Canadian adult CF patients (CCFR, 2017). Many clinical definitions for chronic *P. aeruginosa* infection exist (241). For instance, the Leeds criteria define chronic *P. aeruginosa* infection as isolation of the pathogen from more than half of sputum cultures collected from a patient over a 12 month period (242). Chronic *P. aeruginosa* pulmonary infection is a major predictor and cause of progressive degeneration in lung function, morbidity, and mortality (243–256).

1.5.2 Early acquisition and eradication of P. aeruginosa

In paediatric CF patients, *P. aeruginosa* is thought to be normally contracted from an environmental source (257–261); however, inter-patient transmission of clonal epidemic strains is also a recognised route of infection that can be limited with various infection prevention and control procedures (262–264). There is mounting evidence that the primary sites of initial *P. aeruginosa* infection are in the upper airway (eg. the paranasal sinuses), which are then thought to serve as persistent reservoirs for intermittent secondary infection of the lower airways (265–271).

Given the association of *P. aeruginosa* with morbidity and mortality in CF patients, prolonging the time before a *P. aeruginosa* chronic infection becomes established in the lung is an important cost-effective intervention with significant mortality benefits (241, 272). When *P. aeruginosa* is first detected in sputum cultures during periodic monitoring, eradication therapy with antibiotics such as oral ciprofloxacin, inhaled tobramycin, and/or inhaled colistin is initiated and is often highly successful at clearing *P. aeruginosa* from the lungs during the early years of life (241, 272, 273). Interestingly, there is still no clear evidence for which antibiotic regimens should be used as eradication therapy in spite of the clear benefit of eradication therapy to patient morbidity and mortality (241).

1.5.3 Establishment of a chronic infection

Although eradication therapy is often successful in early life, intermittent *P. aeruginosa* infections become increasingly frequent with advancing age, and a chronic infection is eventually established (4). Interestingly, it is still not clear what factors contribute to eradication therapy failure and establishment of a chronic infection, although prolonged cryptic infection, persistence of a reservoir in the upper airways, and early adaptation to the host environment have been proposed as potential players in this process (274, 275). Persistent infections cannot be eradicated in spite of prolonged antibiotic therapy with antimicrobial agents such as inhaled tobramycin, inhaled colistin, aztreonam, and azithromycin even if isolates display *in vitro* susceptibility to these antimicrobial agents (4, 6, 94, 273). As I described in previous sections, recalcitrance of *P. aeruginosa* to antibiotic treatment is a complex combination of antibiotic resistance and tolerance in the CF lung that mainly involves, in the case of aminoglycosides, MexXY upregulation and existence of the cells in biofilm communities. The goal of antibiotic therapy in the setting of chronic infection thus shifts from eradication to control of the chronic infection and treatment of

pulmonary exacerbations (273, 276). Pulmonary exacerbations are characterized by an acute worsening of pulmonary function that can be resolved with antibiotics and anti-inflammatory agents (277–279); however, the mechanisms underlying pulmonary exacerbations remain unclear.

1.5.4 The P. aeruginosa "biofilm" in CF

An important factor contributing to persistence of *P. aeruginosa* in the CF lung is biofilm formation (116). Unlike the surface attached biofilms that are frequently studied in the laboratory setting and that may be relevant to some infectious processes, *P. aeruginosa* biofilms in the CF lung are actually suspended cellular aggregates in the thickened mucous of the airways (7, 12, 280). Moreover, in contrast to surface-attached biofilms, where biofilm formation is postulated as an active, regulated developmental program, formation of aggregates is thought to be a passive process on the part of the microbe (281). It has been proposed that aggregation formation is instead driven by thermodynamic interactions between host polymers and bacterial cells to maximise system entropy (281).

Like surface-attached biofilms, suspended aggregates are tolerant to antibiotics (140, 281–284). While there is still much to learn about the mechanisms of tolerance in aggregates, heterogeneity in nutrient availability within the aggregate and stress responses seem to play important roles in mediating antibiotic recalcitrance (140, 172, 281). While biofilm models used in this thesis are surface attached, I acknowledge that mechanisms of biofilm tolerance in surface attached biofilms may not be applicable to CF unless they are also validated in aggregates in an environment that mimics the CF lung (eg. synthetic CF sputum medium (285)). The study of these aggregates *in vivo* is also challenging because the only two CF animal models that spontaneously develop lung infections like humans are the pig and ferret, which are expensive and cumbersome (286).

1.5.5 Pathoadaptation to the CF lung environment

The prolonged residence of *P. aeruginosa* within the CF lung provides ample opportunity for evolutionary adaptation to the host environment over time to ensure persistence (287). This phenomenon that has been called pathoadaptation (288). Pathoadaptive mutations that arise in CF-adapted *P. aeruginosa* isolates have been catalogued extensively and promote bacterial fitness in various ways (288–295). Generally, CF-adapted *P. aeruginosa* isolates display increased antibiotic resistance, improved immune evasion, and decreased virulence (288). Intriguingly, many mutations affect transcriptional regulators, further highlighting the importance of transcriptional regulation in *P. aeruginosa* that was emphasized above (288).

Many mutations increase antibiotic resistance through mutation of transcriptional repressors of multidrug efflux pumps. For instance, the MexZ repressor of the MexXY efflux pump is frequently mutated in CF clinical isolates, thereby leading to pan-aminoglycoside resistance (103, 288).

Other mutations decrease immune recognition. Of exceptional importance to **Chapter 4** of this thesis are the relatively common loss-of-function mutations in *rpoN*, which encodes the alternative sigma factor RpoN (σ^{54}) (288). One group found that approximately 20% of isolates in their study harboured putative RpoN loss-of-function mutations (296). RpoN is important for the expression of pili and flagella, which are pathogen associated molecular patterns that can be recognised by immune cells and that contribute to inflammasome activation (297). Therefore, loss of RpoN function is hypothesised to promote immune evasion and persistence in the CF lung. Unfortunately, the prevalence of RpoN loss-of-function mutants and the clinical impact of these mutants on CF lung disease are not known at this time.

Although not particularly relevant to the work presented in this thesis, it would be remiss to not briefly discuss the important role of alginate and mucoidy in pathoadaptation. Mucoid *P. aeruginosa* variants overproduce the exopolysaccharide alginate, and these mutants are associated with increased progression of lung disease and worsened patient outcomes (298, 299). Mucoidy promotes immune evasion and may reduce antibiotic effectiveness (300). Alginate overproduction is typically the result of loss-function-mutations in *mucA*, which encodes the anti-sigma factor of the envelope stress sigma factor, AlgU (301). In the absence of MucA repression, AlgU can promote transcription of the alginate biosynthetic genes, thereby leading to alginate overproduction and expression of the mucoid phenotype (302, 303).

Another common mutation is in the global transcriptional regulator, LasR. In *P. aeruginosa*, LasR is an important regulator of quorum sensing circuits and of the production of virulence factors, such as the elastase LasB (304, 305). Curiously, however, loss of LasR function is associated with lung disease progression (306). Various fitness benefits have been associated with *lasR* mutations, including improved utilization of nutrients available in the CF lung and antibiotic resistance (307–309). Interestingly, it has been recently postulated that *lasR* mutants are pro-inflammatory in the CF lung, which might explain the accelerated lung function decline in patients with these variants (310).

1.6 Rationales and hypotheses for this work

P. aeruginosa infections, such as those seen in CF patients, are difficult to treat due to a combination of antibiotic resistance and tolerance mechanisms (1). Our lab works on several antibiotic resistance genes in biofilms, such as *ndvB* and *tssC1*, that are important for biofilm recalcitrance to killing (147, 152). Importantly, these genes are upregulated in biofilms compared

to exponential phase cells, which explains their importance for resistance in biofilm cells but not in exponential phase cells (147, 152). Understanding the regulatory networks responsible for upregulation of these genes may give insight into how expression of these genes might be interrupted therapeutically to render biofilms more susceptible to standard antimicrobial therapies. Since transcriptional regulation is a major mechanism of control over gene expression in bacteria (17, 67), I hypothesized that one or more transcription factors might be important for expression of these biofilm resistance determinants. In **Chapter 2**, which was published in reference (311), I used a pulldown approach with the *tssABC1* promoter region and proteins from *P. aeruginosa* biofilms in an attempt to identify proteins that bound the *tssABC1* promoter region and that might be candidate regulators of the operon. While I found that the previously uncharacterised LysR-type transcriptional regulator PA3225 bound to the *tssABC1* promoter, PA3225 did not, unfortunately, appear to regulate expression of *tssABC1*. Interestingly, however, I did observe that deletion of PA3225 led to increased planktonic antibiotic resistance. This ultimately led to the demonstration that PA3225 likely acts as a repressor of the MexAB-OprM efflux pump and of the putative PA3228 efflux pump. In **Chapter 3**, my goal was to identify regulators of *ndvB* expression that explain why it is upregulated in biofilms compared to exponential phase cells. This time, instead of using a pulldown approach, my colleague, Dr. Aaron J. Hinz, used a transcriptional reporter to monitor *ndvB* expression over time. The reporter developed by Dr. Hinz led to the finding that *ndvB* is expressed in biofilms as well as in stationary phase cells. This observation led me to hypothesise that the RpoS stationary phase sigma factor was responsible for *ndvB* expression. Indeed, I discovered that expression of *ndvB* was, in fact, RpoS-dependent, and these findings are published in reference (312).

Chapter 4 is related to **Chapter 2** and **Chapter 3** in that it deals with transcriptional regulation and antibiotic resistance/tolerance. As previously mentioned, fumarate (a C_4-dicarboxylate) has been shown to potentiate killing of antibiotic tolerant *P. aeruginosa* stationary phase and biofilm cells by tobramycin, an aminoglycoside antibiotic (185, 189). I hypothesized that fumarate uptake was essential for this potentiation effect. I also mentioned during this chapter that expression of transporters required for fumarate uptake are regulated by the RpoN sigma factor in *P. aeruginosa* (66). Consistent with my hypothesis, I found that a Δ*rpoN* mutant was completely non-susceptible to combination treatment due to a lack of fumarate uptake. Also recall that RpoN loss-of-function mutations are relatively common in *P. aeruginosa* isolates from CF patients. Alleles with RpoN loss-of-function mutations from clinical isolates were unable to complement the Δ*rpoN* mutant for susceptibility to the tobramycin and fumarate combination treatment. This suggests that RpoN loss-of-function mutants might not be susceptible to the treatment, which is significant because the combination therapy has been proposed as a potential treatment option for CF patients with chronic *P. aeruginosa* lung infections. These findings, which are detailed in **Chapter 4**, have been submitted as a research article to *Antimicrobial Agents and Chemotherapy* and are currently undergoing minor revisions.

Overall, the three data chapters in my thesis provide three different examples of transcriptional regulators that play a role in mediating various mechansims of antibiotic resistance and tolerance in the opportunistic pathogen, *P. aeruginosa*. While reading these chapters, I hope that you, like me, are in awe of the number of tricks *P. aeruginosa* has up its metaphorical sleeves and that you appreciate why *P. aeruginosa* is an interesting, challenging, and important bacterium to study. Finally, it is my sincere hope that my data chapters, which are in chronological order, reflect the immense growth that I feel I have had as a scientist over the past three short years.

Chapter 2: PA3225 is a transcriptional repressor of antibiotic resistance mechanisms in *Pseudomonas aeruginosa*

2.1 Preface

This chapter has been previously published as a research article:

> **Hall CW**, Zhang L, and Mah T-F. 2017. PA3225 is a transcriptional repressor of antibiotic resistance mechanisms in *Pseudomonas aeruginosa*. *Antimicrobial Agents and Chemotherapy* 61(8): e02114-16.

Specific author contributions are as follows:

Clayton W. Hall – performed all pull-downs, gel shifts, Western blots, biofilm susceptibility assays, RNA preparations for RNA-seq, 5' RACE, and reverse transcriptase experiments as well as some of the qPCR experiments. Constructed some of the plasmids. Wrote original draft of the paper. Created all figures and tables.

Li Zhang – performed all planktonic susceptibility assays and most qPCR experiments. Constructed all deletion mutants and most plasmids. Revised the manuscript prior to submission for peer review.

Dr. Thien-Fah Mah – provided reagents and research materials, obtained funding, supervised research, conceptualized project, designed experiments, revised the manuscript prior to submission for peer review.

Mass spectrometry identification of PA3225 was done by Dr. Zhibin Ning at the Ottawa Institute for Systems Biology Proteomics Resource Centre. RNA-seq (RNA quality control, library construction, sequencing, and differential gene expression analysis) was performed by the McGill University and Génome Québec Innovation Centre.

2.2 Abstract

The *tssABC1* locus is part of the Hcp secretion island I (HSI-I) type VI secretion system (T6SS) in *Pseudomonas aeruginosa*. Previous work implicated the *tssC1* gene in *P. aeruginosa* biofilm-specific antibiotic resistance, and *tssC1* is preferentially expressed in biofilms compared to planktonic cells. Using a DNA-dependent protein pulldown approach, we discovered that PA3225, an uncharacterized LysR-type transcriptional regulator, specifically bound to the *tssABC1* upstream regulatory region. The deletion of PA3225 had minimal effects on *tssABC1* expression with a 2-fold decrease in *tssA1* expression levels in planktonic cells compared to the wildtype, and no significant change in *tssA1* expression observed in biofilms. Intriguingly, further investigations revealed that the Δ*PA3225* mutant was less susceptible to multiple, structurally unrelated antibiotics with various mechanisms of action when grown planktonically. The Δ*PA3225* mutant was additionally more resistant to ciprofloxacin when grown in a biofilm. The decreased antibiotic susceptibility of the Δ*PA3225* strain was linked to the transcriptional upregulation of the MexAB-OprM efflux pump. By using transcriptome sequencing (RNA-seq), other PA3225-regulated genes were identified, and the products of these genes, such as the putative ABC transporter PA3228, may also contribute to antibiotic resistance.

2.3 Introduction

In Gram-negative bacteria, type VI secretion systems (T6SSs) represent a novel class of secretion systems that are structurally and mechanistically similar to components of the T4 phage (reviewed in reference (313)). The opportunistic pathogen *Pseudomonas aeruginosa* possesses three characterized T6SSs, known as Hcp secretion island I (HSI-I), HSI-II, and HSI-III (314). The HSI-I T6SS secretes several toxins and is involved in interbacterial competition (reviewed in reference (315)). The HSI-T6SS locus is made up of several components, including the gene

products of the *tssABC1* operon (314). Intriguingly, via an unknown mechanism, the *tssC1* gene is required for biofilm-specific antibiotic resistance in *P. aeruginosa*: a Δ*tssC1* mutant is 4-fold more susceptible to tobramycin than the wildtype strain only when grown in a biofilm (152). The biofilm-specific antibiotic resistance phenotype of the Δ*tssC1* mutant is explained by the fact that *tssC1* is more highly expressed in wildtype biofilms than in wildtype planktonic cells (152).

The *tssABC1* locus is posttranscriptionally regulated by the actions of RetS (314), an orphan sensor kinase that mediates the switch between acute and chronic infections in *P. aeruginosa* (316, 317). RetS forms heterodimers with the GacS sensor kinase, thereby preventing the autophosphorylation of the latter kinase (318). GacS dimerized with RetS is therefore unable to activate its cognate response regulator, GacA. GacA is a positive regulator of the RsmY and RsmZ small RNAs, which sequester the global posttranscriptional regulator RsmA (319). RsmA prevents the translation of the HSI-I T6SS genes (320) and likely also affects the stability of the *tssABC1* cistron given that, in Δ*retS* planktonic cells, the expression of *tssC1* is upregulated compared to that in wildtype planktonic cultures (152). Another study also suggested that the expression of HSI-I T6SS genes is downregulated by the quorum-sensing regulators LasR and PqsR (MvfR), although this is likely an indirect regulatory effect because the binding sites for these two regulators have not been found in the HSI-I T6SS gene cluster (321). To date, a direct transcriptional regulator of *tssABC1* has not been identified.

Almost 10% of the *P. aeruginosa* genome is devoted to encoding transcription factors and two-component response systems (14), thus highlighting the importance of regulating gene expression at the transcriptional level in *P. aeruginosa*. Given the dependence of *P. aeruginosa* on transcriptional regulators to respond and adapt to the environment, we hypothesized that the

expression of the *tssABC1* operon may, in addition to the RetS- and quorum sensing-dependent regulatory networks, be directly regulated by one or more transcription factors.

In the present study, we report the identification of PA3225, a LysR-type transcriptional regulator, which interacted with the *tssABC1* upstream regulatory region but played a negligible role in activating *tssABC1* expression. Interestingly, over the course of our work with the Δ*PA3225* mutant, we observed that the deletion of *PA3225* led to decreased susceptibility to multiple antibiotics of different classes. PA3225 was subsequently found to promote antibiotic susceptibility by additionally acting as a transcriptional repressor of the MexAB-OprM efflux pump as well as of the putative antibiotic resistance determinants encoded by *PA1210*, *PA2864*, and *PA3228*.

2.4 Materials and methods

2.4.1 Bacterial strains, media, plasmids, and oligonucleotides

Bacterial strains and plasmids used in this study are listed in **Table 2-1**. The wildtype *P. aeruginosa* strain used in this work was UCBPP-PA14 (PA14). For simplicity, all PA14 genes in this paper are referred to by the gene names of their PAO1 orthologs (14, 322). The unmarked deletion mutants were constructed by two-step allelic exchange with pEX18Gm as previously described (323, 324). *Escherichia coli* strains were grown in LB broth at 37°C, and *P. aeruginosa* strains were grown at 37°C in LB broth or M63 minimal medium supplemented with 0.4% L-arginine and 1 mM $MgSO_4$. When antibiotic selection for plasmids was required, *E. coli* was grown in the presence of 25 μg/ml kanamycin, 20 μg/ml gentamicin, or 10 μg/ml tetracycline, and *P. aeruginosa* was cultured with 80 to 100 μg/ml gentamicin or 100 μg/ml tetracycline. Oligonucleotides are listed in **Table 2-2**. Most plasmids were constructed using standard molecular cloning techniques. The pMQ72::6×His-PA3225 plasmid, which expresses the

6×His-PA3225 allele under the control of the arabinose-inducible P_{BAD} promoter, was constructed by yeast homologous gap repair exactly as previously described (325).

Table 2-1. Microbial strains and plasmids used in this study

Strain or plasmid	Genotype or description	Source
Escherichia coli		
DH5α	F^- Φ80*lacZ*ΔM15 Δ(*lacZYA-argF*) *U169 recA1 endA1 hsdR17* (r_K^- m_K^+) *phoA supE44* λ^- *thi-1 gyrA96 relA1*	Invitrogen
BL21(DE3)	F^- *ompT hsdS*$_B$ (r_B^- m_B^-) *gal dcm* (DE3)	Invitrogen
S17-1	*recA pro hsdR* RP4-2-Tc::Mu-Km::Tn7	(326)
Pseudomonas aeruginosa		
TFM227	UCBPP-PA14 (wildtype)	(327)
TFM297	PA14 ΔPA3225	This study
TFM206	PA14 Δ*retS*	(152)
TFM301	PA14 Δ*retS* ΔPA3225	This study
TFM434	PA14 ΔPA1210	This study
TFM431	PA14 ΔPA1210 ΔPA3225	This study
TFM436	PA14 ΔPA2864	This study
TFM433	PA14 ΔPA2864 ΔPA3225	This study
TFM59	PA14 ΔPA3228	This study
TFM409	PA14 ΔPA3225 ΔPA3228	This study
TFM435	PA14 ΔPA3229	This study
TFM432	PA14 ΔPA3225 ΔPA3229	This study
TFM504	PA14 Δ*mexAB-oprM*	This study
TFM505	PA14 ΔPA3225 Δ*mexAB-oprM*	This study
Saccharomyces cerevisiae		
YPH500	*MATα ura3-52 lys2-801*^{amber} *ade2-101*^{ochre} *trp1-Δ63 his1-Δ200 leu2Δ1*	(328)

Plasmids		
pEX18Gm	Gene replacement vector, *sacB*, Gm^r	(323)
pEX18Gm::ΔPA3225	Deletion of PA3225, Gm^r	This study
pEX18Gm::ΔPA1210	Deletion of PA1210, Gm^r	This study
pEX18Gm::ΔPA2864	Deletion of PA2864, Gm^r	This study
pEX18Gm::ΔPA3228	Deletion of PA3228, Gm^r	This study
pEX18Gm::ΔPA3229	Deletion of PA3229, Gm^r	This study
pEX18Gm::Δ*mexAB-oprM*	Deletion of *mexAB-oprM*	This study
pET30a	His-tagged protein expression vector with IPTG inducible T7/*lacO* promoter, Kan^r	Novagen
pET30a-PA3225	Expression of 6xHis-PA3225, Kan^r	This study
pJB866	Expression vector with *m*-toluic acid inducible P_m promoter, Tc^r	(329)
pJB866-PA3225	Overexpression of PA3225, Tc^r	This study
pJB866-PA1210	Overexpression of PA1210, Tc^r	This study
pJB866-PA2864	Overexpression of PA2864, Tc^r	This study
pJB866-PA3228	Overexpression of PA3228, Tc^r	This study
pMQ72	Yeast-*Pseudomonas* shuttle vector with arabinose inducible P_{BAD} promoter, Gm^r	(325)
pMQ72::6xHis-PA3225	6xHis-PA3225 allele from pCH02 cloned into pMQ72, Gm^r	This study

Table 2-2. Oligonucleotides used in this study

Name	Sequence (5' to 3')	Purpose
Pulldown experiments		
CH3	Biotin-TCAGCTTGTGGTAGCTGGTG	*tssABC1* promoter bait
CH4	AAAACGGGTACATCCAGCAC	*tssABC1* promoter bait
CH7	Biotin-CAGAGCTCGATGCAACTCATC	*rpoD* promoter bait
CH8	TGTTGCGCTTTTCCGGACAT	*rpoD* promoter bait
Electrophoretic mobility shift assays (EMSA)		
CH16	TCAGCTTGTGGTAGCTGGTG	*tssABC1* EMSA probe
CH17	Cy5-AAAACGGGTACATCCAGCAC	*tssABC1* EMSA probe
CH20	CAGAGCTCGATGCAACTCATC	*rpoD* EMSA probe
CH21	Cy5-TGTTGCGCTTTTCCGGACAT	*rpoD* EMSA probe
CH26	AGGTTGGTGAGGAGGATGG	PA3225-PA3228 EMSA probe
CH27	Cy5-GTTACGCGTGGCGCTTTCAT	PA3225-PA3228 EMSA probe
CH29	AATCGAGCTCGCTCTGGATG	*mexAB-oprM* EMSA probe #1
CH30	Cy5-ATGGCTGGCGTTCGTTGCAT	*mexAB-oprM* EMSA probe #1
*mex*2F	Cy5-AATCGAGCTCGCTCTGGATG	*mexAB-oprM* EMSA probe #2
*mex*2R	TAGTTGACTGGATCAACCAC	*mexAB-oprM* EMSA probe #2
*mex*3F	Cy5-ATGTGGTTGATCCAGTCAAC	*mexAB-oprM* EMSA probe #3
*mex*3R	TGTAAACGTCCGAAAGCCTC	*mexAB-oprM* EMSA probe #3
*mex*4F	Cy5-GCTTTCGGACGTTTACAAAC	*mexAB-oprM* EMSA probe #4

*mex*4R	ATGGCTGGCGTTCGTTGCAT	*mexAB-oprM* EMSA probe #4
Cloning *(restriction sites underlined and bolded)*		
CH9	TTTT**GGATCC**ATGAAAGCGCCACGCGTAAC	Cloning of PA3225 into pET30a
CH10	TTTT**AAGCTT**TTATCACTCGGCGGCCGGTTCG	Cloning of PA3225 into pET30a and pJB866
CH37	TAAT**GGTACC**ATGAAAGCGCCACGCGTAAC	Cloning of PA3225 into pJB866
PA3225f1	AATT**GAGCTC**GGTCAGGCGATTGGAACG	Deletion of PA3225
PA3225r2	AATA**GGATCC**ATGAAGGCGGACAGCGAGC	Deletion of PA3225
PA3225f3	AATA**GGATCC**GAGCCGCTTCTACCTCTACA	Deletion of PA3225
PA3225r4	TAGG**AAGCTT**GTAGCCGCTGTCGACGTACT	Deletion of PA3225
PA3225f5	TCGCAATCGTCGATCAGCTA	Confirm ΔPA3225
PA3225r6	GCCAACTGGAAGCCGATCAT	Confirm ΔPA3225
PA1210f5	ACTA**GAATTC**GATGCTCGGCATGCTGCTCA	Deletion of PA1210
PA1210r6	ACAT**GGATCC**GGCGATCTCGTCATCGTTCC	Deletion of PA1210
PA1210f7	ACAT**GGATCC**GGCAGCATCGAGGTCAACG	Deletion of PA1210
PA1210r8	TATC**AAGCTT***C*GAGGACGGCTACCTGGTGT	Deletion of PA1210
PA1210f9	CCGTCGCTGCAACGTTCCTT	Confirm ΔPA1210
PA1210f10	ATAACGCCGCTGCGTCGAGA	Confirm ΔPA1210
PA2864f3	ATTA**GAATTC**GATGTGCCGCTGGTGCTGGT	Deletion of PA2864
PA2864r4	ACAT**GGATCC**GGTGACGATACGCAGGAT	Deletion of PA2864
PA2864f5	ATAA**GGATCC**ATCACCGACAACGGCTATG	Deletion of PA2864

PA2864r6	TATC**AAGCTT**AGAACGCCAGCCTGTAGGAC	Deletion of PA2864
PA2864f7	GTGGCTGCGGAAGAGATAGG	Confirm ΔPA2864
PA2864r8	AAGCCATCCGCCAGATGCGT	Confirm ΔPA2864
PA3228F2	GTCT**GAATTC**TACACCTGGTCGGCATCAGC	Deletion of PA3228
PA3228R2	ATCA**GGATCC**CGAACAGCGCCACCTCGAT	Deletion of PA3228
PA3228F3	ATCA**GGATCC**AGAAGATCGGCCTGGTCG	Deletion of PA3228
PA3228R3	GTGT**AAGCTT**GTGCAGCTCGCCGCTATG	Deletion of PA3228
PA3228F1	CTACTTCCTGCGCCAGGTCT	Confirm ΔPA3228
PA3228R1	CGAAGCGCGTGTTAGTCGAG	Confirm ΔPA3228
PA3229f1	ATCT**GAATTC**TGTCCGGCTGGATCATGTGG	Deletion of PA3229
PA3229r2	ACTA**GGATCC**ATGACGGCGGACACGACAGA	Deletion of PA3229
PA3229f3	ACAT**GGATCC**CGGCGAGCTGCACAAGATCC	Deletion of PA3229
PA3229r4	TATC**AAGCTT**CTTGCGTCTCGCGCCAGACT	Deletion of PA3229
PA3229f5	GCTTCGTCGGCGTCGACTGA	Confirm ΔPA3229
PA3229r6	CCTACCTGAGCCGCGAGTTC	Confirm ΔPA3229
*mexA*fSacI	GCAATC**GAGCTC**GCTCTGGATGC	Deletion of *mexAB-oprM*
*mexB*rBamHI	ACGT**GGATCC**TGCGCGTGAACGAACATGC	Deletion of *mexAB-oprM*
*oprM*fBamHI	ACGT**GGATCC**GACCGCCTACCTGACGCTG	Deletion of *mexAB-oprM*
*oprM*rHindIII	ACGT**AAGCTT**CGACCTGGTGCGCATGGAT	Deletion of *mexAB-oprM*
*mexA*fDiag1	GACAACGCTGCGAAGGTCTC	Confirm Δ*mexAB-oprM*
*oprM*rDiag2	CAGCAGGACCAGTGCATTCT	Confirm Δ*mexAB-oprM*

PA1210compF	TCGG**AAGCTT**ATGATCGAACGTCGTCCCTT	Cloning of PA1210 into pJB866
PA1210compR	ACTT**GAATTC**TCAGGCCACTTCCACCAGCA	Cloning of PA1210 into pJB866
PA2864compF	CCGG**AAGCTT**ATGAATCCACTGATCAAGAC	Cloning of PA2864 into pJB866
PA2864compR	AATT**GAATTC**TCAGCGGGACAGCTTGCCGT	Cloning of PA2864 into pJB866
PA3228compF	TCGG**AAGCTT**ATGCTTTATCGTCGTTTCGA	Cloning of PA3228 into pJB866
PA3228compR	AATT**GAATTC**TCAGTCGACGCCGACGAAGC	Cloning of PA3228 into pJB866
pMQ72::6xHis-PA3225 F	ACCCGTTTTTTTGGGCTAGCGAATTCGAGCTCGG TACCCGGGGAAGGAGATATACATATGCAC	Cloning of pMQ72::6xHis-PA3225
pMQ72::6xHis-PA3225 R	AATCTTCTCTCATCCGCCAAAACAGCCAAGCTT GCATGCCTGCAGAAGCTTTTATCACTCGGCGG	Cloning of pMQ72::6xHis-PA3225
qPCR		
*rpoD*F5	TCCTGGCCGACTACAATCGC	*rpoD* qPCR
*rpoD*R6	TTGACCGGCTCCACCTCTTC	*rpoD* qPCR
tssA1 F1	AACCTGCTGCTGCAGAGCAA	*tssA1* qPCR
tssA1 R1	ATACGGAAGGTGGGGTCGTT	*tssA1* qPCR
fha1 F1	AAGGTACTGGACCAGGGACA	*fha1* qPCR
fha1 R1	TGGTGTCGGTGAGGTAGTAC	*fha1* qPCR
PA3225f7	CGCGCATGCAGGAACAGCTC	PA3225 qPCR
PA3225r8	CCGGCCTGCTTGACCAGTTG	PA3225 qPCR
*mexA*f1	ACCTACGAGGCCGACTACCA	*mexA* qPCR
*mexA*r2	GCGTACTGCTGCTTGCTCAC	*mexA* qPCR

*mexB*f1	CCAGGTCCAGGTGCAGAACA	*mexB* qPCR
*mexB*r2	ACCACACCGACCACCATGAG	*mexB* qPCR
PA1210Qf1	CCTTCGCCGACTACTATGA	PA1210 qPCR
PA1210Qr2	CCTTCGCGGACATAGGTAAT	PA1210 qPCR
PA2864Qf1	TGGCCATCCTGCGTATCGTC	PA2864 qPCR
PA2864Qr2	CAGGCCGATGGATTCGAACC	PA2864 qPCR
PA3228Qf1	CCGAGCATGACCAACCTGAT	PA3228 qPCR
PA3228Qr2	GAGTTGCCGGTCTGCATGAT	PA3228 qPCR
5' RACE		
PA3225 gsp1	TGGATCAGCGCTTCCTCGAC	PA3225 5'RACE
PA3225 gsp2	CAGCCCTGTTCCATGTGGTG	PA3225 5'RACE
RT-PCR		
PA3225-6 RT F	CGCGCATGCAGGAACAGCTC	Operon confirmation
PA3225-6 RT R	ATGCTGATGCCGACCAGGTG	Operon confirmation
PA3226-7 RT F	TCGCTGAAGCAGGCCTATTG	Operon confirmation
PA3226-7 RT R	GGTCTTCTTCTCCTGCATGC	Operon confirmation
PA3227-8 RT F	CGACAACGACTTCCTCAACC	Operon confirmation
PA3227-8 RT R	ATCAGTTCGTTGGCGTGCAC	Operon confirmation
PA3228 RT F	TGCACGCCAACGAACTGATC	Operon confirmation
PA3228 RT R	GCTTCAGCGTGGTGATGTTG	Operon confirmation

2.4.2 Protein pulldown

The pulldown procedure was adopted from a protocol developed previously by Jutras *et al* (330).

Colony biofilms were grown as previously described (153). Briefly, wildtype PA14 cultures grown overnight were spotted onto M63 minimal medium plates supplemented with 0.4% L-arginine and 1 mM $MgSO_4$. Plates were incubated at 37°C for 24 h, followed by 24 h at room temperature. Biofilms were harvested and resuspended in BS/THES binding buffer (22 mM Tris-HCl [pH 7.4], 4.4 mM EDTA [pH 8.0], 8.9% [wt/vol] sucrose, 62 mM NaCl, 10 mM HEPES [pH 7.4], 5 mM $CaCl_2$, 50 mM KCl, 12% glycerol) supplemented with cOmplete EDTA-free protease inhibitor cocktail (Roche) and phosphatase inhibitor cocktail 2 (Sigma-Aldrich). The cell suspension was sonicated, and the cleared lysate was recovered by centrifugation at 20,000 × *g* for 30 min at 4°C. The concentration of protein in the colony biofilm lysate was determined by using the Bradford protein assay (Bio-Rad) with bovine serum albumin (BSA) as the standard.

Biotinylated promoter baits containing the upstream regions of *tssABC1* (positions −407 to +20 relative to the *tssA1* translational start site) and *rpoD* (positions −355 to +20 relative to the *rpoD* translational start site) were amplified from PA14 genomic DNA by PCR. To perform DNA affinity chromatography, 10 μg of the *tssABC1* or *rpoD* promoter bait was incubated with 50 μl of a 4% streptavidin agarose bead slurry (Invitrogen) in coupling buffer (10 mM HEPES [pH 7.4], 100 mM NaCl, 10% glycerol, 100 μM EDTA [pH 8.0]) for 1 h at 4°C. The beads were then washed three times in BS/THES binding buffer before incubation with 600 μg colony biofilm lysate and 50 μg/ml poly(dI-dC) (Sigma-Aldrich) for 3 h at 4°C. In order to limit nonspecific binding to the beads, the beads were then washed twice with BS/THES binding buffer containing 5 μg/ml poly(dI-dC) before being resuspended in 15 μl 2× SDS-PAGE sample buffer and heated

at 95°C for 5 min. Proteins bound to the promoter baits were resolved on a denaturing 10% polyacrylamide gel by SDS-PAGE, and the gel was visualized by silver staining. Protein bands were excised from the gel and were submitted to the Ottawa Institute for Systems Biology Proteomics Resource Centre for identification by high-performance chromatography–electrospray ionization tandem mass spectrometry (HPLC-ESI-MS/MS) followed by a Mascot database search (Matrix Science).

2.4.3 Purification of 6×His-PA3225

The *PA3225* open reading frame was PCR amplified from PA14 genomic DNA and subsequently cloned into the *Bam*HI/*Hind*III sites of pET30a by using standard methods so that the *PA3225* coding sequence would have a 6×His tag at its N terminus. The pET30a-PA3225 plasmid was sequenced at the Ottawa Hospital Research Institute's StemCore Laboratories to ensure that there were no PCR-induced errors in the *PA3225* open reading frame. A culture of *E. coli* BL21(DE3) cells carrying pET30a-PA3225 grown overnight was diluted 1:100 into LB broth, and the subculture was grown to the mid-logarithmic stage (optical density at 600 nm [OD_{600}] = 0.5). IPTG was then added to the culture at a final concentration of 1 mM, and the culture was grown for an additional 3 h at 37°C. The induced cells were resuspended in binding buffer (50 mM NaH_2PO_4, 300 mM NaCl, 10 mM imidazole [pH 8.0]) before being lysed by sonication. The soluble lysate was incubated with Ni-nitrilotriacetic acid (NTA) agarose beads (Qiagen) in batch with rotation for 1.5 h at 4°C. The beads were then washed twice in wash buffer (50 mM NaH_2PO_4, 300 mM NaCl, 20 mM imidazole [pH 8.0]). 6×His-PA3225 was eluted from the beads in elution buffer (50 mM NaH_2PO_4, 300 mM NaCl, 250 mM imidazole [pH 8.0]). The elution buffer was exchanged for BS/THES buffer by several rounds of centrifugation in an Amicon Ultra-15 centrifugal filter unit (EMD Millipore) with a 10-kDa-molecular-mass cutoff, according to the

manufacturer's instructions. The purity of 6×His-PA3225 was visually determined by SDS-PAGE (see **Fig S2-1** in the supplemental material), and the concentration of the purified protein was determined by using the Bradford protein assay (Bio-Rad) with BSA as the standard.

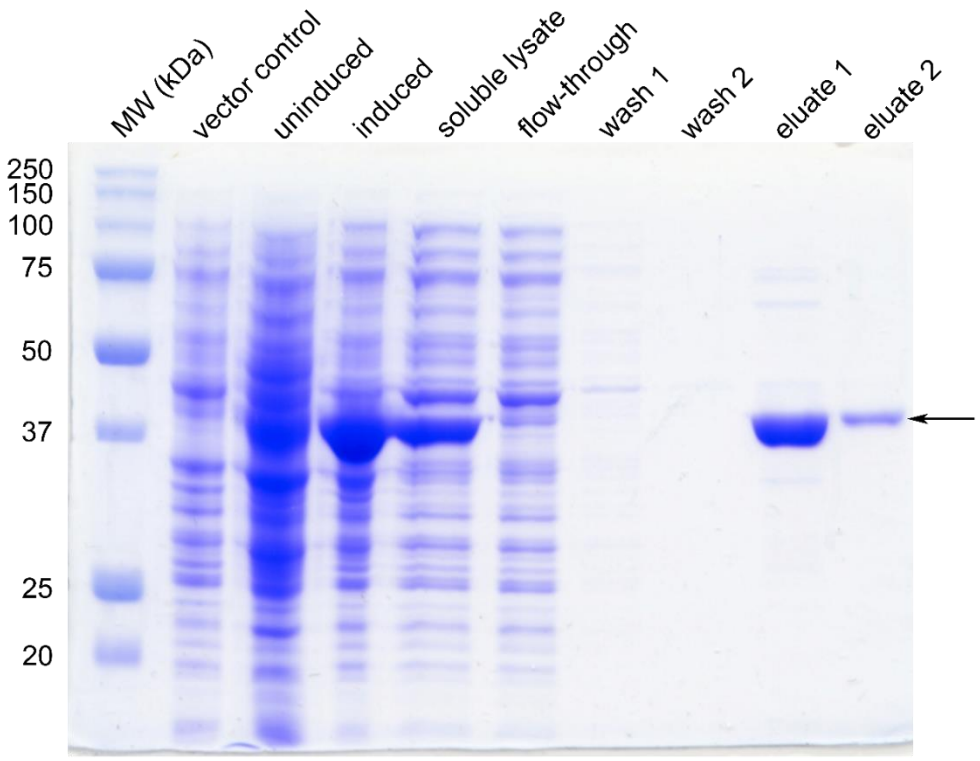

Figure S2-1. Purification of 6xHis-PA3225.
Aliquots from various stages of the 6xHis-PA3225 protein purification procedure (detailed in the Materials and Methods section of the main article text) were separated by SDS-PAGE and stained with Coomassie blue. The location of 6xHis-PA3225 is shown with an arrow. "Vector control" refers to whole cell proteins isolated from IPTG-induced *E. coli* BL21(DE3) carrying pET30a. The "uninduced" and "induced" lanes contain whole cell proteins from *E. coli* BL21(DE3) pET30a-PA3225 that was either uninduced or induced with IPTG, respectively. "Soluble lysate" refers to soluble proteins following sonication of IPTG-induced *E. coli* BL21(DE3) pET30a-PA3225 cells. Soluble lysate was incubated with Ni-NTA agarose beads, and a significant portion of 6xHis-PA3225 was captured by the beads given that the flow-through had much less 6xHis-PA3225 than the input lysate. Beads were washed twice followed by two elutions with imidazole-containing buffer. Protein from eluate 2 was used for all experiments requiring 6xHis-PA3225 due to the high purity of recombinant protein in this eluate.

2.4.4 EMSAs

Primers labeled with a 5′ Cy5 moiety (**Table 2-2**) were used to PCR amplify fluorescent probes from PA14 genomic DNA. The P*tssABC1* and P*rpoD* probes were identical in sequence to the promoter baits used in the DNA affinity chromatography experiment. Binding reactions were performed in BS/THES binding buffer with 5 nM the Cy5-labeled probe, 10 ng/μl poly(dI-dC), and various concentrations of purified 6×His-PA3225 (ranging from 0 to 1,000 nM). For the competition EMSA, an unlabeled probe (identical in sequence to the Cy5-labeled probe but lacking the 5′ Cy5 modification) was included in the binding reaction mixture. Reaction mixtures were incubated at 4°C in the dark for 1 h. Following incubation, reaction mixtures were electrophoresed for approximately 2 h at 4°C on a nondenaturing 5% polyacrylamide gel in 0.5× Tris-borate-EDTA (TBE) buffer at 135 V. Gels were visualized by using a Typhoon Trio scanner (GE Healthcare). EMSA figures are representative of data from at least two independent experiments performed with 6×His-PA3225 that was prepared on two different occasions.

2.4.5 qPCR analysis

For RNA derived from planktonic cells, cultures grown overnight in LB medium were diluted 1:100 in M63 medium and grown for 8 h at 37°C to an OD_{600} of approximately 0.650. Colony biofilms were grown as described above. RNA was isolated from planktonic and biofilm cultures by using TRIzol reagent and the Purelink RNA minikit (Invitrogen) according to the manufacturer's recommendations, and the RNA was treated with Purelink DNase I (Invitrogen) as necessary to remove contaminating DNA. Synthesis of cDNA was performed by using 2 μg of RNA and the iScript cDNA synthesis kit (Bio-Rad). Real-time qPCR was performed on a MyiQ single-color detection system (Bio-Rad) with 20-μl reaction mixtures containing 2 μl of cDNA, 2.5 μM each gene-specific primer (**Table 2-2**), and iQ SYBR green Supermix (Bio-Rad). All qPCR

experiments were performed with at least three biological replicates, each tested in triplicate. The expression level of *rpoD* was used as the internal reference standard. Fold changes were expressed as $2^{-\Delta\Delta Ct}$ values. Relative fold changes were graphed by using GraphPad Prism 7 software, and statistical significance was determined by using two-tailed Student's *t* tests.

2.4.6 Antibiotic susceptibility assays

MICs in LB and M63 media were determined by using the CLSI broth macrodilution method (CLSI, Wayne, PA). Visible growth inhibition was read after incubation overnight at 37°C. MIC determinations for the PA14 and Δ*PA3225* strains were performed five times.

To corroborate the MIC data, drug gradient plate assays were performed (331). Briefly, a layer of LB agar containing nalidixic acid (120 μg/ml), ciprofloxacin (0.1 μg/ml), norfloxacin (0.75 μg/ml), or tetracycline (16 μg/ml) was poured at an angle in square petri plates and allowed to solidify. The plate was placed horizontally, and the antibiotic-containing agar was then overlaid with antibiotic-free LB agar. An inoculation loop was used to streak cultures parallel to the linear antibiotic concentration gradient. Plates were incubated for 24 h at 37°C.

MBCs of tobramycin and ciprofloxacin for planktonic (MBC-P) and biofilm (MBC-B) cells were determined three times as previously described (332).

2.4.7 Western blotting

PA14, Δ*PA3225*, and Δ*mexAB-oprM* cell envelope proteins were isolated exactly as described previously (333). Protein concentrations were determined by using the Bradford protein assay (Bio-Rad) with BSA as the standard.

Envelope proteins (15 μg) were separated on 10% SDS-PAGE gels. For each experiment, two gels were run in parallel: one was Coomassie blue stained to visually ensure equal loading, while the other was used for Western blotting. Electrophoresed proteins were subsequently

transferred onto a polyvinylidene difluoride (PVDF) membrane by using the Bio-Rad Trans-Blot Turbo Transfer system according to the manufacturer's directions (transfer parameters of 25 V, 1.3 Å, and 10 min). Membranes were blocked for 1 h at room temperature with agitation in a solution containing 1× Tris-buffered saline with 0.1% Tween 20 (TBST) plus 5% BSA. The blocked membranes were incubated overnight at 4°C with a 1:4,000 dilution of anti-MexB rabbit polyclonal antiserum (333) in 1× TBST containing 5% BSA. Following incubation with the primary antibody, membranes were washed four times in 1× TBST. Membranes were then incubated with a 1:10,000 dilution of goat anti-rabbit IgG conjugated to horseradish peroxidase (Cell Signaling Technology) in 1× TBST containing 5% BSA. After incubation with the secondary antibody, membranes were washed four times in 1× TBST and then exposed to the Clarity ECL Western blotting substrate (Bio-Rad) as recommended by the manufacturer. Imaging was performed by using an ImageQuant LAS 4010 imaging system (GE Healthcare). The Western blotting experiment was performed four times.

2.4.8 5′ RACE

Identification of the *PA3225-PA3228* transcriptional start site was performed with a 5′ RACE kit (Invitrogen) according to the manufacturer's instructions, using the gene-specific primers listed in **Table 2-2**.

2.4.9 RNA-seq

RNA was isolated from planktonic and biofilm cultures of the PA14 and Δ*PA3225* strains as described above (three biological replicates under each condition for a total of 12 samples). RNA was submitted to the McGill University and Génome Québec Innovation Centre (MUGQIC) for library preparation, sequencing, and data analysis. Libraries were prepared by using the first-strand protocol, and paired-end sequencing of rRNA-depleted libraries was performed on an

Illumina HiSeq 2000 instrument. Reads were trimmed by using Trimmomatic (334) and subsequently aligned to the *P. aeruginosa* PA14 genome (GenBank accession number CP000438.1) by using TopHat (335) and Bowtie (336) software. Raw read counts from HTSeq (337) were input into DESeq (338) and edgeR (339) for differential gene expression analysis.

2.4.10 Accession number(s)

The raw and processed data from the RNA-seq experiment have been deposited in the NCBI Gene Expression Omnibus (GEO) (340, 341) under GEO series accession number GSE87213.

2.5 Results

2.5.1 A 34-kDa protein binds the tssABC1 promoter

A protein pulldown approach adapted from a method described previously by Jutras et al. (330) was used to discover potential transcriptional regulators of the *tssABC1* operon. A biotinylated *tssABC1* promoter bait was incubated with colony biofilm whole-cell extracts since the expression of *tssC1* is known to be upregulated in colony biofilms (152). An unbaited bead control was used to rule out proteins that interacted with the beads themselves, while beads coupled to the promoter of *rpoD* were used to control for nonspecific DNA-binding proteins and general transcriptional machinery. Due to their different expression profiles and unrelated activities, we expected that transcription factors regulating *rpoD* would be different from those regulating *tssABC1*.

Proteins from the colony biofilm whole-cell extract that bound to the *tssABC1* promoter bait were separated by SDS-PAGE, and the protein bands were visualized on the gel by silver staining (**Fig 2-1A**). Interestingly, one band at approximately 34 kDa was present in the eluate from the *tssABC1* promoter bait but not in the eluates from the *rpoD* or unbaited controls, suggesting that this protein interacted specifically with the *tssABC1* promoter bait. By using mass spectrometry, the band was shown to correspond to PA14_22470 (PA3225), a probable LysR-type transcriptional regulator that, to our knowledge, has not been previously characterized (322). Gel samples from the equivalent areas in the unbaited and *rpoD* controls were also submitted for analysis by mass spectrometry to account for background peptide hits, and no PA3225-derived peptides were identified in these controls.

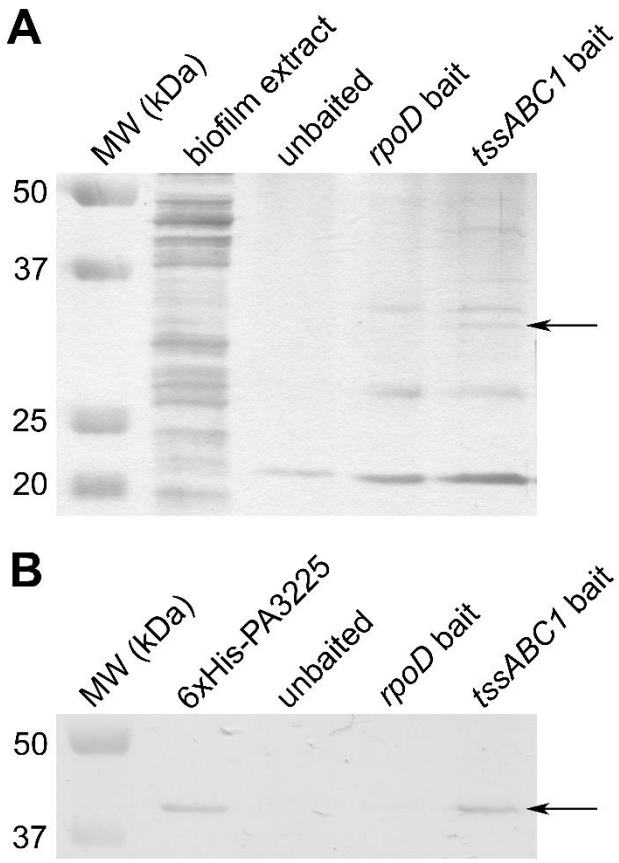

Figure 2-1. PA3225 binds to the *tssABC1* upstream regulatory region in pulldown assays. (A) The whole-cell extract from colony biofilms was incubated with streptavidin-agarose beads coupled to either no DNA or biotinylated DNA containing the upstream regulatory regions of *rpoD* or *tssABC1*. Bound proteins were visualized on a silver-stained SDS-PAGE gel, and the 34-kDa protein (shown with an arrow) that bound uniquely to the *tssABC1* DNA bait was identified as PA3225 by mass spectrometry. (B) Recombinant 6×His-tagged PA3225 was used as the sole protein input instead of the colony biofilm extract for the pulldown assay to further demonstrate that PA3225 interacts with the *tssABC1* upstream regulatory region. The protein band at 39 kDa, which corresponds to 6×His-PA3225, is shown with an arrow. MW, molecular weight (in thousands).

2.5.2 PA3225 directly interacts with the tssABC1 promoter

In order to confirm that PA3225 interacts specifically with the *tssABC1* promoter, recombinant PA3225 with an N-terminal 6×His tag (6×His-PA3225) was purified from an *Escherichia coli* BL21(DE3) strain carrying the isopropyl-β-D-thiogalactopyranoside (IPTG)-inducible pET30a-PA3225 plasmid (see **Fig S2-1** in the supplemental material). The pulldown experiment was repeated, this time using 2 μg of 6×His-PA3225 instead of the whole-cell colony biofilm extract as the input. As shown in (**Fig 2-1B**), recombinant PA3225 bound to the *tssABC1* promoter bait but not to the unbaited or *rpoD* negative controls.

To further demonstrate binding specificity for the *tssABC1* promoter, purified 6×His-PA3225 was used in electrophoretic mobility shift assays (EMSAs) with Cy5-labeled *tssABC1* and *rpoD* probes (Cy5-P*tssABC1* and Cy5-P*rpoD*, respectively) that were identical in sequence to the biotinylated promoter baits used in the pulldown experiment. A band with decreased electrophoretic mobility compared to that of the free Cy5-P*tssABC1* probe corresponding to the 6×His-Pa3225/Cy5-P*tssABC1* complex was observed at a 6×His-PA3225 concentration of 600 nM, and the intensity of the protein-DNA complex increased with increasing concentrations of 6×His-PA3225 (**Fig 2-2A**). No significant shift was observed with the Cy5-P*rpoD* negative-control probe even in the presence of 1 μM 6×His-PA3225 (**Fig 2-2B**).

In addition, a competition EMSA was performed, in which the unlabeled P*tssABC1* or P*rpoD* probe was added to binding reaction mixtures containing 5 nM the Cy5-labeled P*tssABC1* probe and 1 μM 6×His-PA3225 (**Fig 2-2B**). When in excess, the unlabeled P*tssABC1* probe successfully outcompeted the Cy5-P*tssABC1* probe for binding to 6×His-PA3225 given that the intensity of the protein-DNA complex decreased and the amount of the free Cy5-P*tssABC1*probe increased with increasing amounts of the unlabeled P*tssABC1* probe. On the other hand, the

addition of the unlabeled P*rpoD* probe did not affect the amount of free Cy5-*tssABC1* to an appreciable degree at any concentration of the P*rpoD* competitor that was tested, suggesting that the affinity of 6×His-PA3225 for the *tssABC1* promoter is much higher than that for the *rpoD* promoter. Taken together, these EMSA results suggest that 6×His-PA3225 interacts specifically with the *tssABC1* promoter region under the tested binding conditions.

2.5.3 Effect of PA3225 deletion on tssABC1 expression

Given that our pulldown assays and EMSAs demonstrated that 6×His-PA3225 physically interacts with the *tssABC1* promoter *in vitro*, we next wanted to establish whether PA3225 has a role in regulating *tssABC1* expression *in vivo*. Consequently, an unmarked Δ*PA3225* deletion mutant was constructed in the PA14 strain, and the expression level of *tssA1* in both planktonic and biofilm cultures of the PA14 and Δ*PA3225* strains was determined by quantitative PCR (qPCR) (**Fig 2-2C**). As was previously reported, the *tssABC1* transcript was upregulated in wildtype biofilms compared to wildtype planktonic cells (152). We observed an almost 2-fold decrease in the *tssA1* expression level in Δ*PA3225* planktonic cells. There was also a slight decrease in the *tssA1* expression level in Δ*PA3225* biofilms compared to that in wildtype biofilms; however, this difference was not statistically significant. We therefore concluded that PA3225 did not have a role in regulating *tssABC1* expression under our experimental conditions.

Previous studies have shown that the expression of the HSI-I T6SS locus is regulated posttranscriptionally by the RetS sensor kinase through a signaling cascade that converges on the posttranscriptional regulator RsmA (314). The deletion of *retS* results in a 12-fold upregulation of *tssC1* in planktonic cells (152). Since an intact RetS signaling cascade decreases *tssABC1* transcript levels, we wondered if the repressive effect of RetS on *tssABC1* expression could mask the regulatory role of PA3225. To test this hypothesis, a PA14 Δ*retS* ΔPA3225 double-deletion

mutant was constructed, and the planktonic expression level of *tssA1* in this mutant was compared to that in the PA14 Δ*retS* mutant by qPCR. The expression of *tssA1* was unaffected by the deletion of PA3225 in a Δ*retS* background (data not shown).

2.5.4 The T6SS gene fha1 is transcriptionally upregulated in biofilms, but fha1 expression does not depend on PA3225

Since the fragment upstream of the *tssABC1* operon that was used in the pulldown experiment also corresponds to the upstream regulatory region of the HSI-I T6SS *fha1-tssJKL1* operon, the expression level of *fha1* in wildtype PA14 was compared to that in the Δ*PA3225* strain by qPCR (**Fig 2-2D**). While we showed that *fha1* was preferentially expressed in biofilms compared to planktonic cells, there was no difference in *fha1* expression levels in the Δ*PA3225* strain compared to the wild type.

Overall, we have provided evidence that PA3225 binds to the *tssABC1* promoter and that this protein-DNA interaction is specific. While we were unable to demonstrate a change in the expression level of the *tssABC1* locus upon the deletion of *PA3225* in this study, we feel that characterization of PA3225 is important since it is likely that PA3225 plays some role in *tssABC1* transcription that will be elucidated as more information about the regulation of the HSI-I locus becomes available.

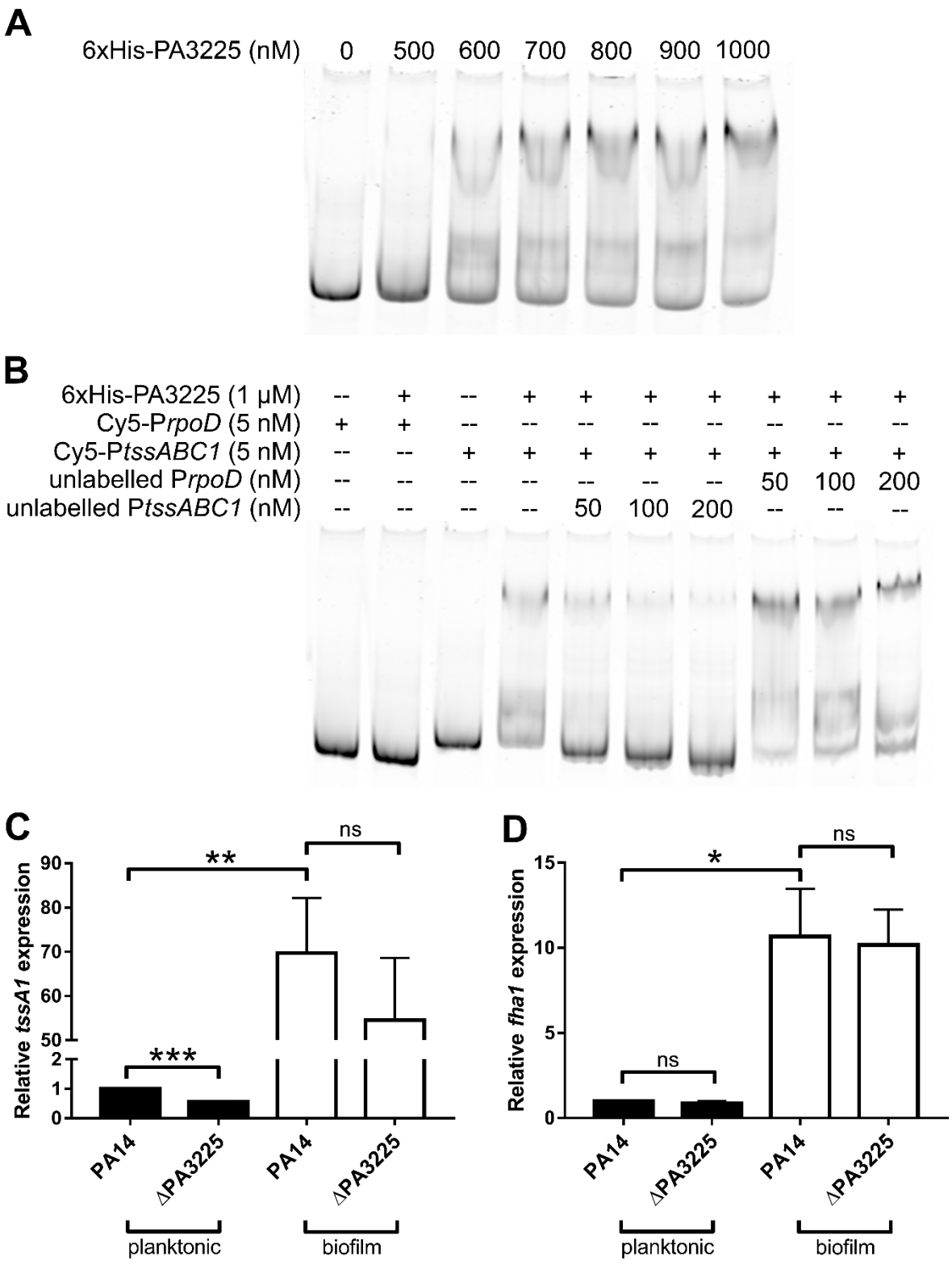
A
6xHis-PA3225 (nM) 0 500 600 700 800 900 1000
B
6xHis-PA3225 (1 µM) -- + -- + + + + + + +
Cy5-PrpoD (5 nM) + + -- -- -- -- -- -- -- --
Cy5-PtssABC1 (5 nM) -- -- + + + + + + + +
unlabelled PrpoD (nM) -- -- -- -- -- -- -- 50 100 200
unlabelled PtssABC1 (nM) -- -- -- -- 50 100 200 -- -- --
C
Relative tssA1 expression
90
80
70
60
50
2
1
0
**
ns
***
PA14
ΔPA3225
PA14
ΔPA3225
planktonic
biofilm
D
Relative fha1 expression
15
10
5
0
*
ns
ns
PA14
ΔPA3225
PA14
ΔPA3225
planktonic
biofilm

Figure 2-2. PA3225 directly binds the *tssABC1* upstream regulatory region but does not play a role in activating *tssA1* expression.

(A) EMSA showing that the *tssABC1* upstream regulatory region was bound by 6×His-PA3225. Increasing amounts of 6×His-PA3225 were incubated with 5 nM the fluorescent Cy5-P*tssABC1* probe containing the upstream regulatory region of the *tssABC1* operon, and the binding reaction mixtures were electrophoresed on a native polyacrylamide gel. (B) Competition EMSA demonstrating that 6×His-PA3225 does not bind the Cy5-P*rpoD* probe and that the unlabeled *rpoD* probe is not as effective as the unlabeled *tssABC1* probe at outcompeting the Cy5-P*tssABC1* probe for binding with 6×His-PA3225. (C) Planktonic expression of *tssA1* is decreased 2-fold in the absence of PA3225, but there is no significant decrease in *tssA1*expression in ΔPA3225 biofilms compared to wildtype biofilms as determined by qPCR. Data are shown as mean *tssA1*expression levels relative to those of wildtype planktonic cells and standard errors of the means. ***, $P \leq 0.001$; ns, not statistically significant (as determined by two-tailed Student's *t* tests). (D) qPCR analysis demonstrates that *fha1*, which is divergently transcribed from the *tssABC1* operon, is not regulated by PA3225. However, like the *tssABC1* operon, *fha1* is also upregulated in wildtype biofilms compared to wildtype planktonic cells. Mean *fha1* expression levels relative to those of wildtype planktonic cells and standard errors of the means are shown. *, $P \leq 0.05$; ns, not statistically significant (as determined by two-tailed Student's *t* tests).

2.5.5 PA3225 is a negative autoregulator of the PA3225-PA3228 operon and is preferentially expressed in biofilms

According to the *Pseudomonas* Genome Database annotation, PA3225 is a putative member of the LysR-type family of transcription regulators (322). *PA3225* is predicted to form an operon with three other genes (*PA3226*, *PA3227*, and *PA3228*) (322), and we confirmed that these genes are cotranscribed in an operon with *PA3225* by reverse transcription-PCR (RT-PCR) (see **Fig S2-2** in the supplemental material). Classically, a LysR-type transcriptional regulator binds directly to the promoter of the gene that encodes it, thereby repressing its own expression (71).

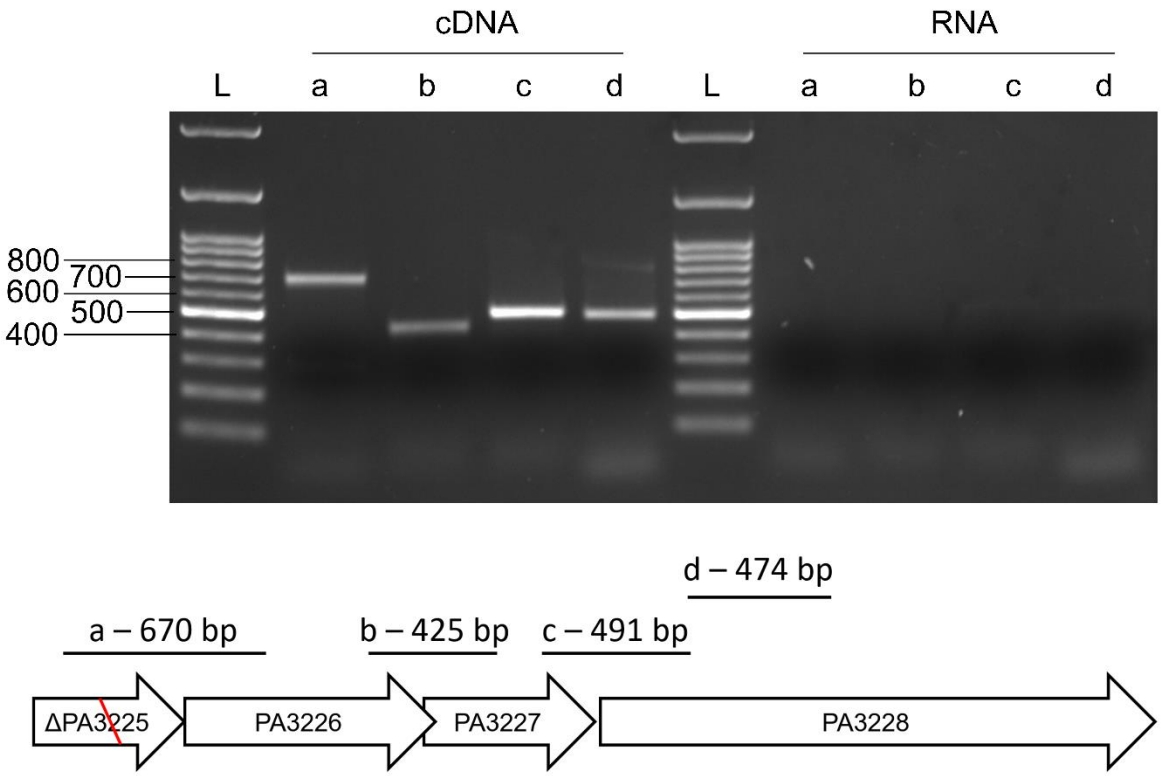

Figure S2-2. The *PA3225-PA3228* genes are co-transcribed.
RNA from planktonic ΔPA3225 cultures was reverse transcribed to cDNA, which was subsequently used as a template for PCR with primer sets (see Table 2-2) that amplified various regions of the predicted PA3225-PA3228 operon (regions "a" to "d" shown schematically in lower panel). PCR reactions performed with RNA in the absence of reverse transcriptase were included as controls to demonstrate the absence of contaminating genomic DNA.

In order to assess the regulatory effect of PA3225 on the activity of the *PA3225-PA3228* promoter as well as the expression pattern of *PA3225* in wildtype planktonic and biofilm cells, we performed qPCR with primers that amplified a portion of the PA3225 locus that had not been deleted in the construction of the Δ*PA3225* mutant (**Fig 2-3A**). The expression level of the *PA3225* transcript in planktonic cultures increased more than 20-fold in the Δ*PA3225* mutant relative to the wildtype, which suggested that PA3225 is a negative autoregulator of the *PA3225-PA3228* operon, as predicted. Since PA3225 was originally identified in biofilm whole-cell extracts, we next determined whether there was a difference in wildtype expression levels of PA3225 between planktonic and biofilm cells. The expression level of PA3225 was approximately five times higher in wildtype biofilms than in wildtype planktonic cells (**Fig S2-3**). The PA3225 transcript was upregulated around 10-fold in Δ*PA3225* biofilms compared to wildtype biofilms (**Fig S2-3**).

To determine if PA3225 binds to its own promoter and therefore acts as a direct negative autoregulator, we performed EMSAs with recombinant 6×His-PA3225 and a fluorescently labeled DNA probe containing the sequence between positions −351 and +20 relative to the *PA3225* translational start codon. The amount of shifted probe increased with increasing amounts of 6×His-PA3225 (**Fig 2-3B**), although the affinity of 6×His-PA3225 for the *PA3225-PA3228* upstream region was lower than that for *tssABC1* given that a higher concentration of 6×His-PA3225 was required to observe a visible shift in the Cy5-P*PA3225-PA3228* probe.

Overall, these qPCR and gel shift results are consistent with the conclusions that PA3225 is a transcriptional regulator that is preferentially expressed in biofilms and that PA3225 likely represses the expression of the *PA3225-PA3228* operon via direct binding to the *PA3225-PA3228* promoter.

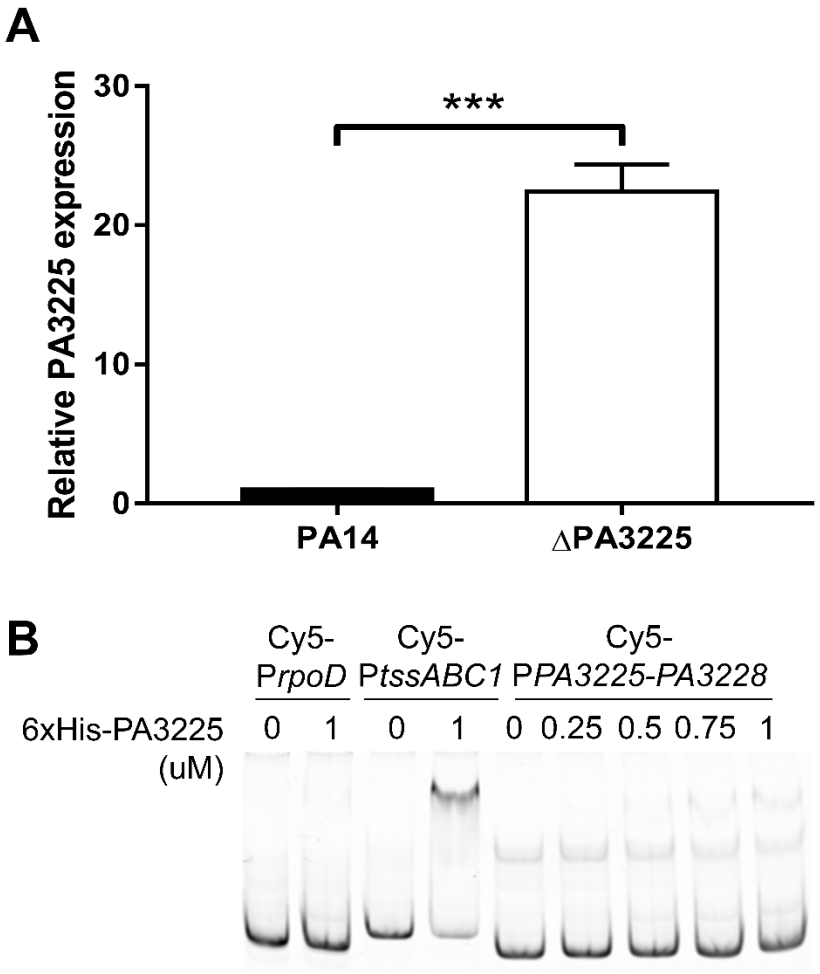

Figure 2-3. PA3225 is an autorepressor of the *PA3225-PA3228* operon.
(A) Deletion of PA3225 in planktonic cells results in increased expression levels of the PA3225-PA3228 locus as determined by qPCR using primers that amplify a portion of the PA3225 transcript that was not deleted during the generation of the ΔPA3225 mutant. Data are shown as mean PA3225 expression levels relative to those of wildtype planktonic cells and standard errors of the means. ***, $P \leq 0.001$ (as determined by two-tailed Student's *t* tests). (B) PA3225 directly binds the regulatory region upstream of the PA3225-PA3228 operon. An EMSA was performed by incubating increasing amounts of recombinant 6×His-PA3225 with a Cy5-labeled DNA probe (Cy5-P*PA3225-PA3228*) corresponding to the region spanning positions −351 to +20 (relative to the translational start site of PA3225) upstream of the PA3225-PA3228 operon. Binding of 6×His-PA3225 to the Cy5-*rpoD* and Cy5-*tssABC1* probes used in is included as negative and positive binding controls, respectively. Binding reaction mixtures were resolved on a native polyacrylamide gel, and the gel was visualized on a Typhoon Trio scanner.

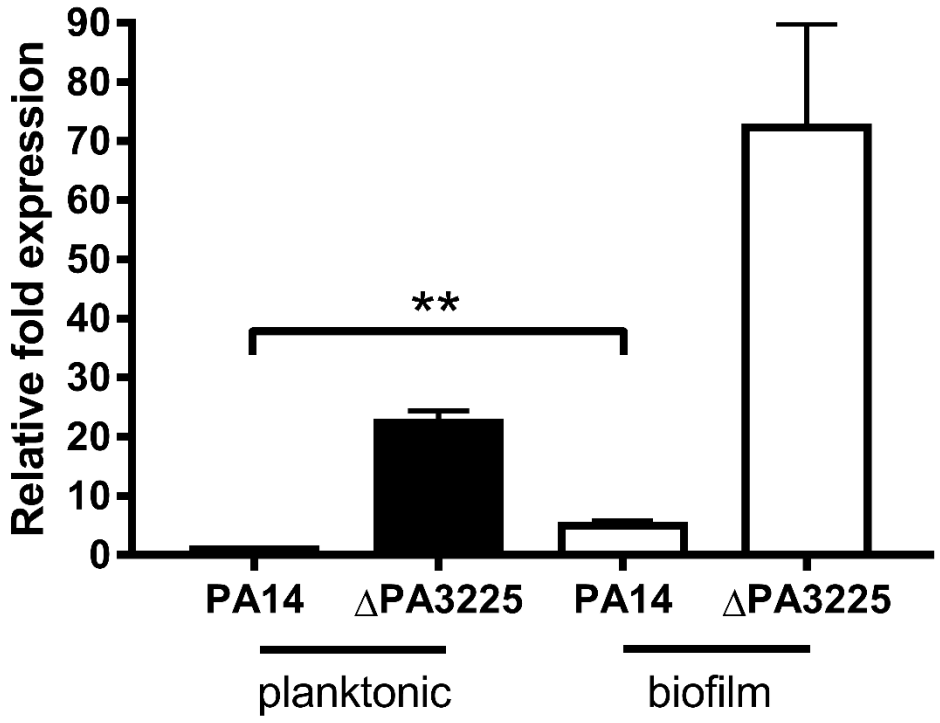

Figure S2-3. *PA3225* is upregulated in biofilms.
Deletion of PA3225 resulted in increased expression of the PA3225-PA3228 locus as determined by qPCR using primers that amplified a portion of the PA3225 transcript that was not deleted in the generation of the ΔPA3225 mutant. Additionally, in wild-type PA14, PA3225 expression in biofilms was 5-fold higher than that in planktonic cells. Data are shown as mean PA3225 expression relative to wild-type planktonic cells + SEM. ** $p \leq 0.01$ as determined by two-tailed Student's *t*-tests.

2.5.6 Deletion of PA3225 reduces susceptibility to multiple antibiotics in planktonic and biofilm cells

While attempting to introduce a pUCP19 derivative (which carries a selectable marker for carbenicillin resistance) (342) into the Δ*PA3225* mutant for other experiments, we noticed that the untransformed Δ*PA3225* mutant was, surprisingly, able to survive when plated onto LB agar containing high concentrations of carbenicillin. Although wildtype PA14 cells were effectively killed by 300 μg/ml carbenicillin, a carbenicillin concentration as high as 1,000 μg/ml was still not effective at eliminating the Δ*PA3225* mutant (D. Sparks and C. W. Hall, unpublished observations).

In order to obtain a more complete susceptibility profile of the Δ*PA3225* mutant, the MICs of a panel of antibiotics of different classes were determined in both LB medium and M63 minimal medium (**Table 2-3**). For each of the two types of media, the wildtype and mutant strains shared essentially identical growth curves (data not shown). Interestingly, the Δ*PA3225* mutant displayed increased planktonic resistance to several antibiotics with diverse mechanisms of action. Compared to wildtype PA14, the MIC values of the Δ*PA3225* strain in LB medium were increased 2-fold for ciprofloxacin, norfloxacin, and nalidixic acid and 4-fold for carbenicillin, cefotaxime, chloramphenicol, and tetracycline. In M63 minimal medium, the MIC values were higher for the Δ*PA3225* mutant than for the wildtype strain by 2-fold for tetracycline and 4-fold for ciprofloxacin, norfloxacin, nalidixic acid, carbenicillin, cefotaxime, and chloramphenicol. The MICs of gentamicin and tobramycin in both media were not affected by the absence of *PA3225*, suggesting that PA3225 was not important for susceptibility to these aminoglycoside antibiotics. To confirm that the phenotype of decreased multidrug susceptibility of the Δ*PA3225* mutant was truly due to the absence of *PA3225* and not due to polar effects of the deletion on adjacent genes,

we introduced the pJB866 vector carrying the *PA3225* open reading frame into the PA14 and Δ*PA3225* strains. Compared to the PA14 or Δ*PA3225* strain carrying the pJB866 plasmid, strains with pJB866::PA3225 generally had lower MICs for most antibiotics tested, indicating that *PA3225* overexpression restored antibiotic susceptibility (**Table 2-3**).

Table 2-3. Impact of *PA3225* deletion and overexpression on antibiotic susceptibility of *P. aeruginosa* in LB and M63[a]

Strain	MIC (μg/ml) of[b]								
	TOB	**GEN**	**CIP**	**NOR**	**NAL**	**CAR**	**CTX**	**CHL**	**TET**
PA14	4 (1)	8 (2)	1 (0.0625)	2 (0.5)	64 (32)	256 (128)	32 (32)	128 (16)	16 (4)
Δ*PA3225*	4 (1)	8 (2)	2 (0.25)	4 (2)	128 (128)	1024 (512)	128 (128)	512 (64)	64 (8)
PA14 pJB866	4 (1)	8 (2)	0.5 (0.5)	2 (2)	128 (128)	512 (128)	32 (32)	256 (16)	ND
PA14 pJB866::PA3225	4 (1)	8 (2)	0.25 (0.0625)	1 (0.25)	64 (16)	256 (64)	64 (8)	256 (16)	ND
Δ*PA3225* pJB866	4 (1)	8 (2)	1 (0.25)	4 (2)	256 (128)	512 (512)	128 (32)	512 (32)	ND
Δ*PA3225* pJB866::PA3225	4 (1)	8 (2)	1 (0.125)	2 (0.5)	64 (32)	512 (256)	128 (32)	256 (32)	ND

[a] MIC values in M63 are reported in parentheses.

[b] TOB, tobramycin; GEN, gentamicin; CIP, ciprofloxacin; NOR, norfloxacin; NAL, nalidixic acid; CAR, carbenicillin; CTX, cefotaxime; CHL, chloramphenicol; TET, tetracycline; ND, not determined

To confirm our findings that the Δ*PA3225* mutant was less susceptible to various antibiotics than the wildtype, we performed a drug gradient plate assay (331). In this assay, strains are streaked parallel to a linear antibiotic concentration gradient on an agar plate. Visible growth of PA14 was inhibited at lower concentrations of nalidixic acid (see **Fig S2-4A** in the supplemental material), ciprofloxacin (**Fig S2-4B**), norfloxacin (**Fig S2-4C**), and tetracycline (**Fig S2-4D**) than in the Δ*PA3225* mutant, confirming that the Δ*PA3225* strain was indeed less susceptible than the wild type to multiple antibiotics.

The minimal bactericidal concentration (MBC) is another metric of antibiotic susceptibility in planktonic and biofilm cells (147, 332). The MBC in planktonic cells (MBC-P) and the MBC in biofilm cells (MBC-B) of ciprofloxacin and tobramycin, two clinically important antibiotics that are used to treat *P. aeruginosa* infections, were determined for the wildtype and Δ*PA3225* strains (**Table S2-1**). In the case of ciprofloxacin, the MBC-P for the wildtype PA14 strain was 4 μg/ml, while the MBC-P for the Δ*PA3225* mutant was 8 μg/ml. Since *PA3225* was preferentially expressed in biofilms, we sought to determine if the lack of *PA3225* also rendered biofilms less susceptible to ciprofloxacin. The deletion of *PA3225* resulted in a 2-fold decrease in biofilm susceptibility to ciprofloxacin, as the MBC-B of ciprofloxacin for wildtype PA14 was 40 μg/ml, while that for the Δ*PA3225* mutant was 80 μg/ml. Consistent with the MIC results, the absence of *PA3225* did not affect either the MBC-P or the MBC-B of tobramycin. It is worthwhile to note that biofilm formation of the Δ*PA3225* mutant was essentially equivalent to that of the wildtype strain as determined by quantification of crystal violet staining of biofilms formed in 96-well microtiter plates (data not shown) (343).

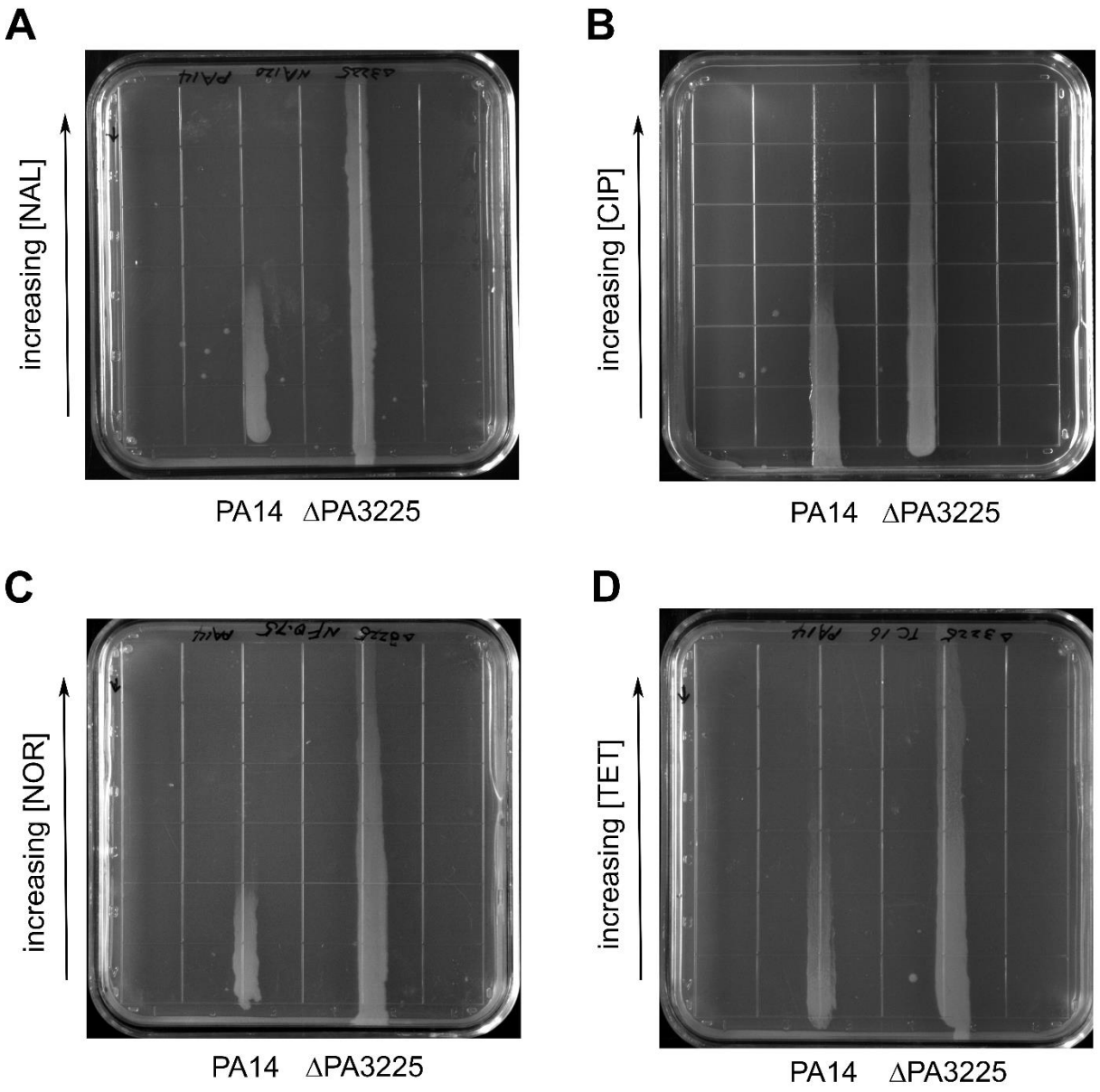

Figure S2-4. Drug gradient plate assays demonstrate that the Δ*PA3225* mutant has decreased antibiotic susceptibility compared to wildtype.
PA14 and Δ*PA3225* were struck on LB agar plates containing a concentration gradient of (**A)** nalidixic acid (0 to 120 μg/mL), (**B)** ciprofloxacin (0 to 0.1 μg/mL), (**C)** norfloxacin (0 to 0.75 μg/mL), and (**D)** tetracycline (0 to 16 μg/mL). In all cases, the Δ*PA3225* mutant had visible growth at a higher antibiotic concentration than the wildtype PA14 strain.

Table S2-1. Minimum bactericidal concentrations for planktonic (MBC-P) and biofilm (MBC-B) wildtype and Δ*PA3225* cells.

	Tobramycin (µg/ml)		Ciprofloxacin (µg/ml)	
Strain	**MBC-P**	**MBC-B**	**MBC-P**	**MBC-B**
PA14	32	100	4	40
Δ*PA3225*	32	100	8	80

Overall, the antibiotic susceptibility assays showed that the Δ*PA3225* mutant had reduced susceptibility to multiple antibiotics when grown planktonically and that biofilms formed by the Δ*PA3225* mutant had increased recalcitrance to ciprofloxacin compared to PA14 biofilms.

2.5.7 PA3225 is a novel transcriptional repressor of mexAB-oprM

Given that the Δ*PA3225* mutant was less susceptible to a variety of structurally and functionally unrelated antibiotics when grown planktonically, we next used qPCR to assess the expression levels of some of the *P. aeruginosa* RND multidrug efflux pump genes (*mexAB-oprM*, *mexCD-oprJ*, *mexEF-oprN*, and *mexXY*) in the Δ*PA3225* deletion mutant. We reasoned that the decreased susceptibility of the mutant could be potentially due to a loss of the PA3225-mediated transcriptional repression of multidrug efflux pumps. Interestingly, there was an almost 3-fold increase in the expression levels of *mexA* (**Figure 2-4A**) and *mexB* (**Figure 2-4B**) in Δ*PA3225* planktonic cells compared to the wildtype, suggesting that PA3225 may play a role in downregulating the expression of the MexAB-OprM efflux pump. The expression levels of the other RND multidrug efflux pumps were not affected by the deletion of PA3225 (data not shown).

Protein levels of MexB in the Δ*PA3225* strain were assessed by immunoblotting to determine if the transcriptional upregulation of *mexAB-oprM* translated to an increase in MexB production. Western blotting with anti-MexB antiserum revealed an increase in the MexB abundance in the Δ*PA3225* deletion mutant compared to the wildtype (**Figure 2-4C**). As expected, MexB was not detected in a Δ*mexAB-oprM* strain (**Figure 2-4C**).

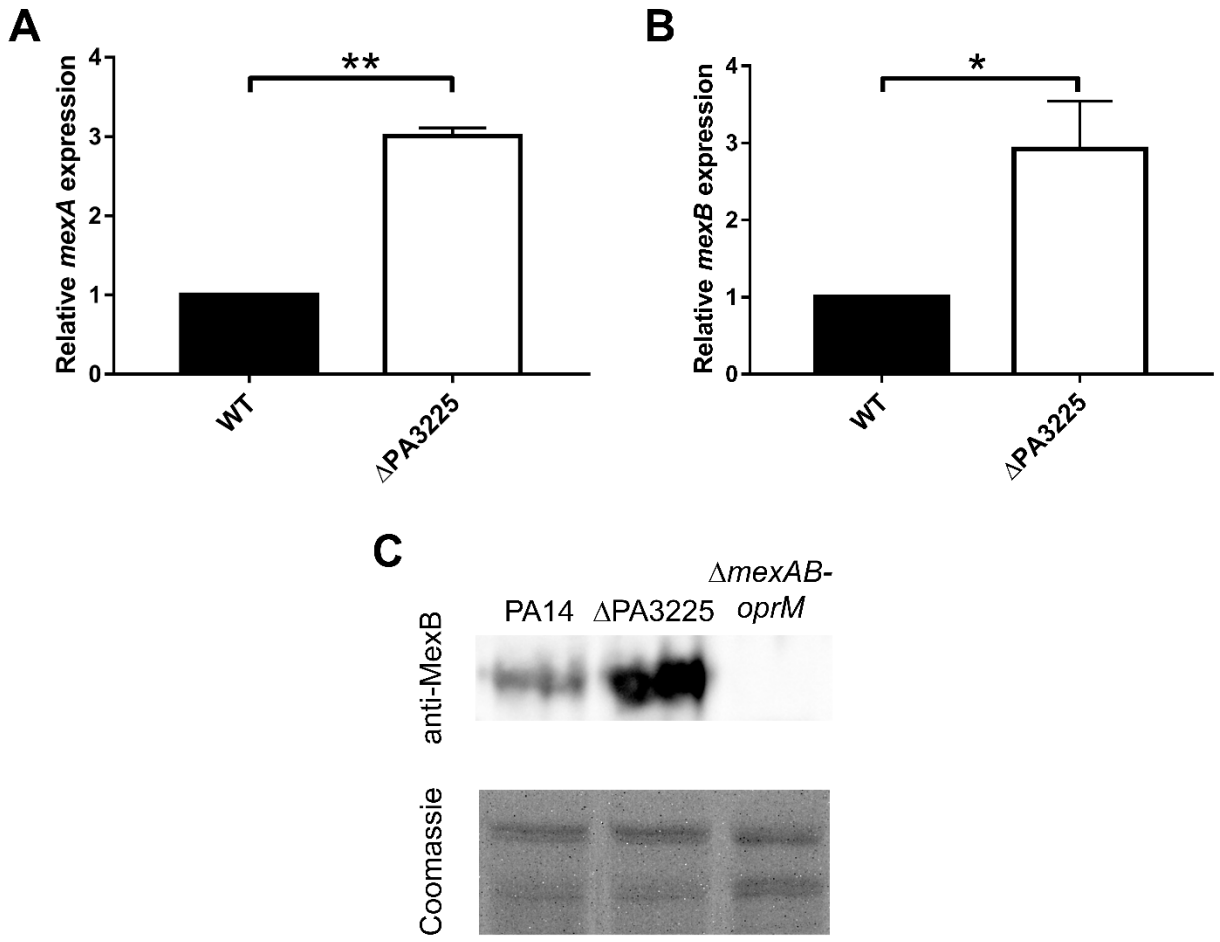

Figure 2-4. PA3225 is a novel transcriptional repressor of the MexAB-OprM multidrug efflux pump.

(A and B) Expression levels of *mexA* (A) and of *mexB* (B) are approximately three times higher in planktonic Δ*PA3225* cells than in planktonic wild-type cells as determined by qPCR. Data are presented as mean gene expression levels and standard errors of the means for Δ*PA3225* planktonic cells relative to wild-type planktonic cells. *, $P \leq 0.05$; **, $P \leq 0.01$ (as determined by two-tailed Student's *t* test). (C, top) Detection of the MexB protein in cell envelopes of the PA14, Δ*PA3225*, and Δ*mexAB-oprM* strains by Western blotting using anti-MexB antiserum. The blot is representative of data from four experiments. (Bottom) For each Western blot, another gel was run in parallel and Coomassie blue stained to demonstrate equal loading of the gel lanes.

To determine if PA3225 binds to the promoter of the *mexAB-oprM* operon, EMSAs were performed with the recombinant 6×His-PA3225 protein and fluorescently labeled DNA probes corresponding to various regions upstream of the *mexAB-oprM* locus (shown schematically in **Fig 2-5A**). There was decreased mobility of Cy5-P*mexAB-oprM* probe 1 with increasing concentrations of 6×His-PA3225 **Fig 2-5B**), indicating that the 6×His-PA3225 protein potentially interacted with the promoter region of the *mexAB-oprM* operon. To further define where 6×His-PA3225 bound to the *mexAB-oprM* promoter region, Cy5-P*mexAB-oprM* probe 1 was subdivided into three smaller, slightly overlapping Cy5-labeled probes (Cy5-P*mexAB-oprM* probes 2, 3, and 4). While Cy5-P*mexAB-oprM* probes 2 and 4 did not bind to 6×His-PA3225 under our conditions (**Fig 2-5C**), a shift was observed for Cy5-P*mexAB-oprM* probe 3 with increasing amounts of the recombinant 6×His-PA3225 protein (**Fig 2-5D**). This interaction could be competed with unlabeled P*mexAB-oprM* probe 3 but not with unlabeled P*mexAB-oprM* probe 2 or 4, suggesting that the interaction between 6×His-PA3225 and P*mexAB-oprM* probe 3 is specific (**Fig 2-5E**). Interestingly, Cy5-P*mexAB-oprM* probe 3 contains the −35 and −10 elements of the previously defined distal P_I promoter of the *mexAB-oprM* operon (344), suggesting that PA3225 might act at this site to repress *mexAB-oprM* expression. Future mutational studies of this promoter region will allow confirmation of this hypothesis.

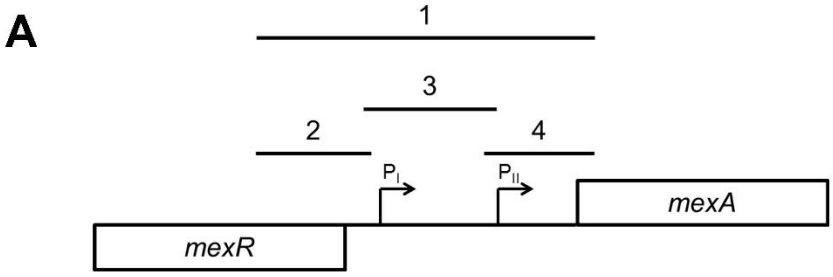
A
1
3
2
4
P I
P II
mexA
mexR

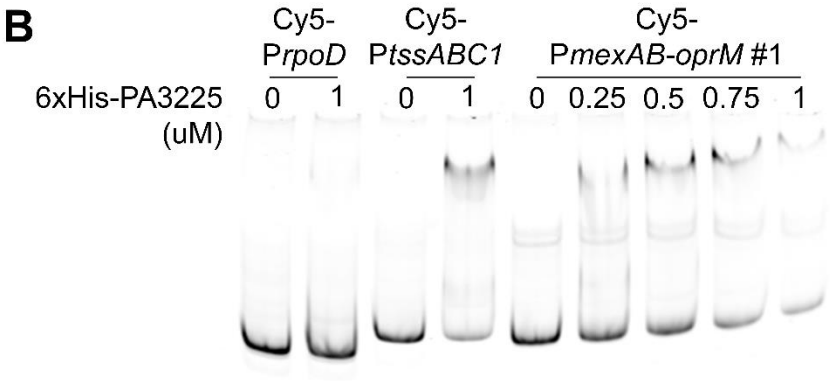
B
Cy5-
PrpoD
Cy5-
PtssABC1
Cy5-
PmexAB-oprM #1
6xHis-PA3225
(uM)
0 1 0 1 0 0.25 0.5 0.75 1

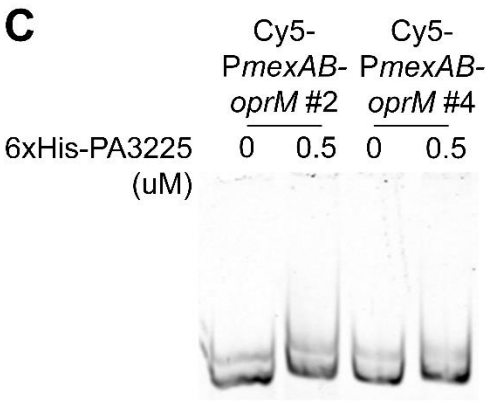
C
Cy5-
PmexAB-
oprM #2
Cy5-
PmexAB-
oprM #4
6xHis-PA3225
(uM)
0 0.5 0 0.5

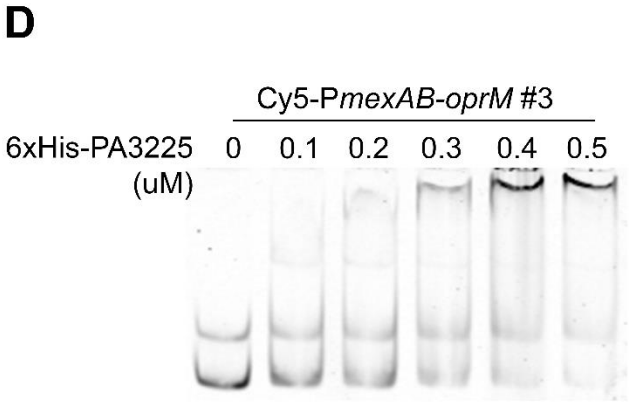
D
Cy5-PmexAB-oprM #3
6xHis-PA3225
(uM)
0 0.1 0.2 0.3 0.4 0.5

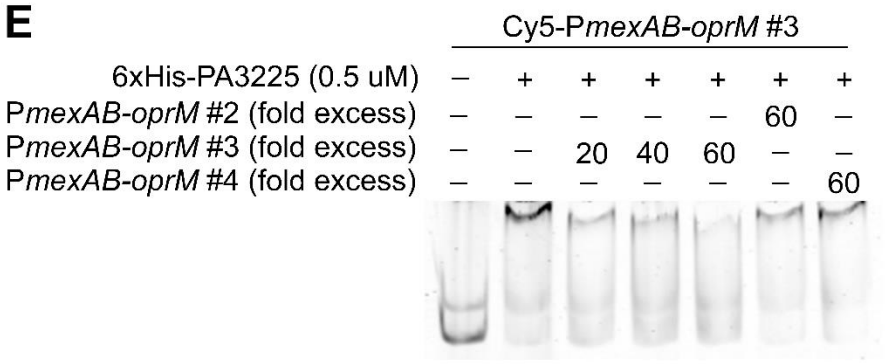
E
Cy5-PmexAB-oprM #3
6xHis-PA3225 (0.5 uM) – + + + + + +
PmexAB-oprM #2 (fold excess) – – – – – 60 –
PmexAB-oprM #3 (fold excess) – – 20 40 60 – –
PmexAB-oprM #4 (fold excess) – – – – – – 60

Figure 2-5. PA3225 binds to the promoter region of the *mexAB-oprM* operon.
(A) Schematic showing the region upstream of *mexAB-oprM* along with the approximate locations of the EMSA probes (labeled 1, 2, 3, and 4). The locations of two previously reported *mexAB-oprM* promoters (P_I and P_{II}) are shown with arrows. The P_I promoter is located on fragment 3. (B) EMSA of Cy5-P*mexAB-oprM* probe 1 with increasing amounts of 6×His-PA3225. Binding of 6×His-PA3225 to the Cy5-*rpoD* and Cy5-*tssABC1* probes used in is included as negative and positive binding controls, respectively. (C) EMSA of Cy5-P*mexAB-oprM* probes 2 and 4 demonstrating that these regions are not responsible for the observed binding of 6×His-PA3225 to the region upstream of *mexAB-oprM*. (D) EMSA showing that 6×His-PA3225 interacts with Cy5-P*mexAB-oprM* probe 3, which contains the P_I promoter of the *mexAB-oprM* operon. (E) The specificity of binding of 6×His-PA3225 to Cy5-P*mexAB-oprM* probe 3 was assessed by using a competition EMSA. Unlabeled P*mexAB-oprM* probe 3 (specific competitor) or unlabeled P*mexAB-oprM* probes 2 and 4 (nonspecific competitors) were incubated with reaction mixtures containing constant amounts of 6×His-PA3225 and Cy5-P*mexAB-oprM* probe 3.

To assess whether the decreased susceptibility of the Δ*PA3225* strain was dependent on MexAB-OprM, we deleted the *mexAB-oprM* locus in the PA14 and ΔPA3225 backgrounds and measured the susceptibility of these strains using MIC tests (**Table 2-4**). Consistent with data from previous reports, the Δ*mexAB-oprM* strain was significantly more susceptible than wildtype strain PA14 to quinolones, β-lactams, chloramphenicol, and tetracycline. The Δ*PA3225* Δ*mexAB-oprM* double-deletion mutant had essentially the same MICs as the Δ*mexAB-oprM* strain for most of the antibiotics tested. In other words, in the absence of the *mexAB-oprM* operon, the deletion of PA3225 did not reduce *P. aeruginosa* susceptibility, suggesting that the reduction in the antibiotic susceptibility of the Δ*PA3225* mutant involves the MexAB-OprM efflux pump.

Therefore, based upon the qPCR, immunoblot, gel shift, and drug susceptibility data, PA3225 is likely a novel transcriptional repressor of *mexAB-oprM*, and the upregulation of this efflux pump could be a factor contributing to the decreased antibiotic susceptibility of the Δ*PA3225* mutant.

Table 2-4. Contribution of *mexAB-oprM* to the decreased susceptibility of the Δ*PA3225* mutant

Strain	MIC (μg/mL) of[a]								
	TOB	**CIP**	**NOR**	**NAL**	**LVX**	**CAR**	**CTX**	**CHL**	**TET**
PA14	2	0.25	0.5	64	0.25	64	16	128	16
Δ*PA3225*	2	0.5	2	512	1	256	64	256	64
Δ*mexAB-oprM*	4	0.03	0.125	16	0.06	1	4	32	1
Δ*PA3225* Δ*mexAB-oprM*	2	0.03	0.25	16	0.06	1-2	4	32	1

[a] TOB, tobramycin; CIP, ciprofloxacin; NOR, norfloxacin; NAL, nalidixic acid; LVX, levofloxacin; CAR, carbenicillin; CTX, cefotaxime; CHL, chloramphenicol; TET, tetracycline

2.5.8 The regulon of PA3225 reveals that PA3225 typically acts as a transcriptional repressor

Since PA3225 is a predicted transcriptional regulator, the decrease in antibiotic susceptibility when *PA3225* is absent suggests that PA3225 is a repressor of one or more genes whose products may be involved in antibiotic resistance. While we already demonstrated that the regulatory targets of PA3225 include the *PA3225-PA3228* and *mexAB-oprM* operons, differential expression analysis of the Δ*PA3225* mutant compared to the wildtype was performed by using transcriptome sequencing (RNA-seq) in order to elucidate the other members of the PA3225 regulon in both planktonic and biofilm cells. Genes that were found to be significantly (log_2-fold change of >2 or <−2) up- or downregulated in planktonic or biofilm cells of the ΔPA3225 mutant compared to planktonic or biofilm cells of wildtype strain PA14 are presented in **Table 2-5** and **Table S2-2** in the supplemental material, respectively. The *PA3225*, *PA3226*, *PA3227*, and *PA3228* genes were significantly upregulated in both planktonic and biofilm cells of the Δ*PA3225* strain. This finding is in agreement with our qPCR and EMSA findings that PA3225 is an autorepressor of the putative *PA3225-PA3228* operon. According to the *Pseudomonas* Genome Database (322), *PA3226* encodes a probable hydrolase, *PA3227* (*ppiA*) is a peptidyl-prolyl *cis-trans* isomerase that is likely involved in the folding of periplasmic proteins (345, 346), and *PA3228* encodes a putative ATP-binding/permease fusion ATP-binding cassette (ABC) transporter that may function as a multidrug transporter based upon the NCBI Conserved Domain Database prediction (83). Three other genes (*PA1210*, *PA2864*, and *PA3229*) were also significantly upregulated in planktonic and biofilm cells of the Δ*PA3225* mutant compared to wildtype cells. *PA1210* encodes a putative pirin protein, while *PA2864* and *PA3229* are hypothetical proteins with unknown functions (322). The *PA1863* and *PA1864* loci, which encode the ModA ABC permease involved in molybdate uptake (347) and a TetR family transcriptional

regulator (322), respectively, were downregulated in Δ*PA3225* planktonic cells; however, the expression levels of PA1863 and PA1864 were not significantly different between PA14 biofilms and Δ*PA3225* biofilms.

To confirm the validity of the RNA-seq data, we performed qPCR to assess the expression levels of select PA3225-regulated loci in wildtype and Δ*PA3225* planktonic cultures. The expression level of *PA1210* was 38 times higher in Δ*PA3225* cultures than in wildtype cultures (**Fig 2-6A**). Similarly, *PA2864* and *PA3228* were 15- and 13-fold more highly expressed, respectively, in Δ*PA3225* planktonic cells than in wildtype cells (**Fig 2-6B** and **Fig 2-6C**). *PA1210*, *PA2864*, and *PA3228* are therefore transcriptionally repressed by PA3225. While it is likely that *PA3228* is directly repressed by PA3225 given that *PA3228* belongs to the same operon as *PA3225*, we did not test whether the PA3225-mediated regulation of *PA1210* and *PA2864* is direct or indirect.

Table 2-5. Differentially expressed genes in planktonic Δ*PA3225* compared to planktonic wildtype PA14

Gene name	PAO1 ortholog	Predicted function[a]	log_2 fold change in planktonic ΔPA3225[b]
PA14_48650	PA1210	Hypothetical protein	+ 4.158
PA14_22460	PA3226	Alpha/beta hydrolase	+ 4.044
PA14_22450	PA3227	Peptidyl-prolyl cis-trans isomerase A	+ 3.982
PA14_22470	PA3225	LysR-type transcriptional regulator	+3.617
PA14_22440	PA3228	ABC transporter ATP-binding protein/permease	+ 3.418
PA14_27070	PA2864	Hypothetical protein	+ 3.031
PA14_22420	PA3229	Hypothetical protein	+ 2.314
PA14_40380	PA1864	TetR family transcriptional regulator	- 4.116
PA14_40390	PA1863	Molybdate-binding periplasmic protein precursor	- 2.282

[a] Annotated gene functions as per the *Pseudomonas* Genome Database (322)

[b] Relative to planktonic wildtype PA14

Table S2-2. Differentially expressed genes in Δ*PA3225* compared to wildtype PA14

Gene name	PAO1 ortholog	Predicted function[a]	log_2 fold change in planktonic ΔPA3225[b]	log_2 fold change in ΔPA3225 biofilms[c]
PA14_48650	PA1210	Hypothetical protein	+ 4.158	+ 2.964
PA14_22460	PA3226	Alpha/beta hydrolase	+ 4.044	+ 4.345
PA14_22450	PA3227	Peptidyl-prolyl cis-trans isomerase A	+ 3.982	+ 4.151
PA14_22470	PA3225	LysR-type transcriptional regulator	+3.617	+ 3.929
PA14_22440	PA3228	ABC transporter ATP-binding protein/permease	+ 3.418	+ 3.773
PA14_27070	PA2864	Hypothetical protein	+ 3.031	+ 3.263
PA14_22420	PA3229	Hypothetical protein	+ 2.314	+ 2.388
PA14_40380	PA1864	TetR family transcriptional regulator	- 4.116	No significant difference
PA14_40390	PA1863	Molybdate-binding periplasmic protein precursor	- 2.282	No significant difference

[a] Annotated gene functions as per the *Pseudomonas* Genome Database (322)

[b] Relative to planktonic wildtype PA14

[c] Relative to wildtype PA14 biofilms

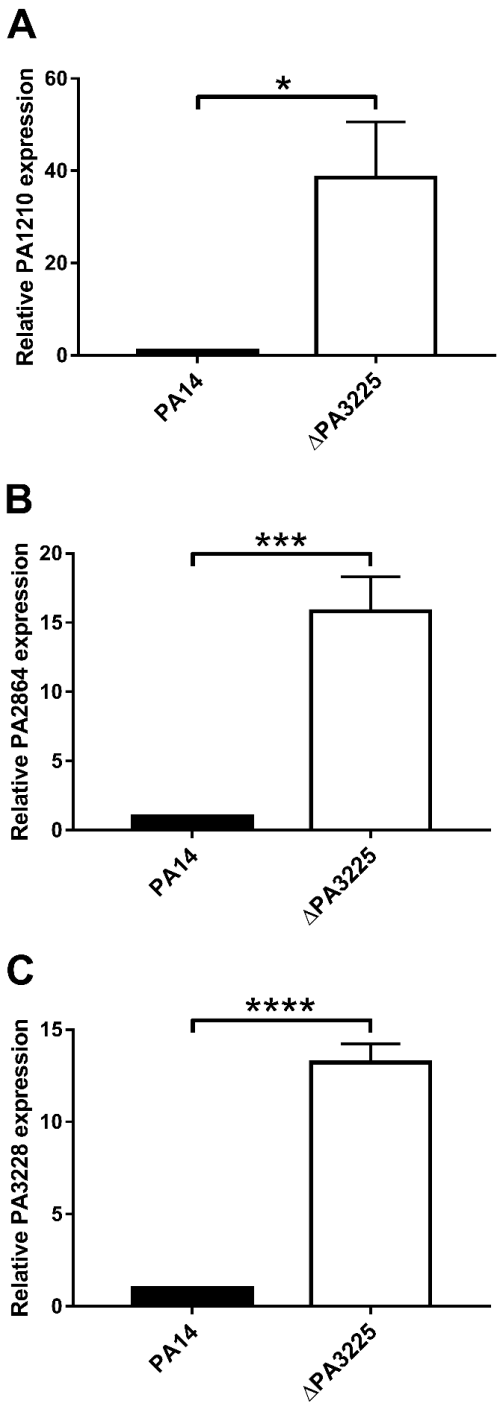

Figure 2.6 PA3225 is a transcriptional repressor of the *PA1210*, *PA2864*, and *PA3228* genes. Deletion of *PA3225* results in the upregulation of *PA1210* (A), *PA2864* (B), and *PA3228* (C) in planktonic *P. aeruginosa* cells. The expression levels of the PA3225-regulated genes in wildtype and Δ*PA3225* planktonic cultures were determined by qPCR. Mean fold changes in gene expression levels and standard errors of the means relative to the wildtype are shown. *, $P \leq 0.05$; ***, $P \leq 0.001$; ****, $P \leq 0.0001$ (as determined by two-tailed Student's *t* tests).

Since *PA3228* is located in an operon with *PA3225*, we were concerned that the change in the expression level of *PA3228* might be due to polar effects caused by the Δ*PA3225* mutation. In order to address this concern, the 6×His-PA3225 allele was cloned downstream of the arabinose-inducible P_{BAD} promoter in pMQ72 (325). The resulting plasmid, pMQ72::6×His-PA3225, was transformed into the Δ*PA3225* strain, and *PA3228* expression was measured by qPCR. The *PA3228* expression level in the Δ*PA3225* strain carrying pMQ72::6×His-PA3225 was significantly lower than that in the Δ*PA3225*/pMQ72 strain (see **Fig S2-5** in the supplemental material), suggesting that the increased expression level of *PA3228* in the Δ*PA3225* mutant is due to a loss of PA3225 repression and not due to a polar effect from the *PA3225* deletion. Moreover, this experiment confirmed that the 6×His-PA3225 protein is functional *in vivo*.

In a preliminary attempt to identify a candidate PA3225-binding site, the upstream intergenic regions of the *PA3225-PA3228*, *tssABC1*, *mexAB-oprM*, *PA1210*, and *PA2864* loci were submitted to the MEME suite program (348) for *de novo* motif identification. LysR-type transcriptional regulator boxes have the general sequence $TN_{11}A$ and typically display imperfect dyadic symmetry (71). While MEME identified several motifs in common that are found in the upstream regulatory regions of these genes (data not shown), none were especially obvious or compelling candidates for a putative PA3225-binding site. We also identified the location of the transcriptional start site of PA3225 by 5′ rapid amplification of cDNA ends (RACE) (**Fig S2-6**); however, visual inspection of the region upstream of the transcriptional start site and around a predicted PvdS sigma factor-binding site (22) also did not reveal an obviously plausible PA3225-binding site. An unbiased approach for the identification of the PA3225-binding site via chromatin immunoprecipitation sequencing (ChIP-seq) will therefore be pursued in a future study.

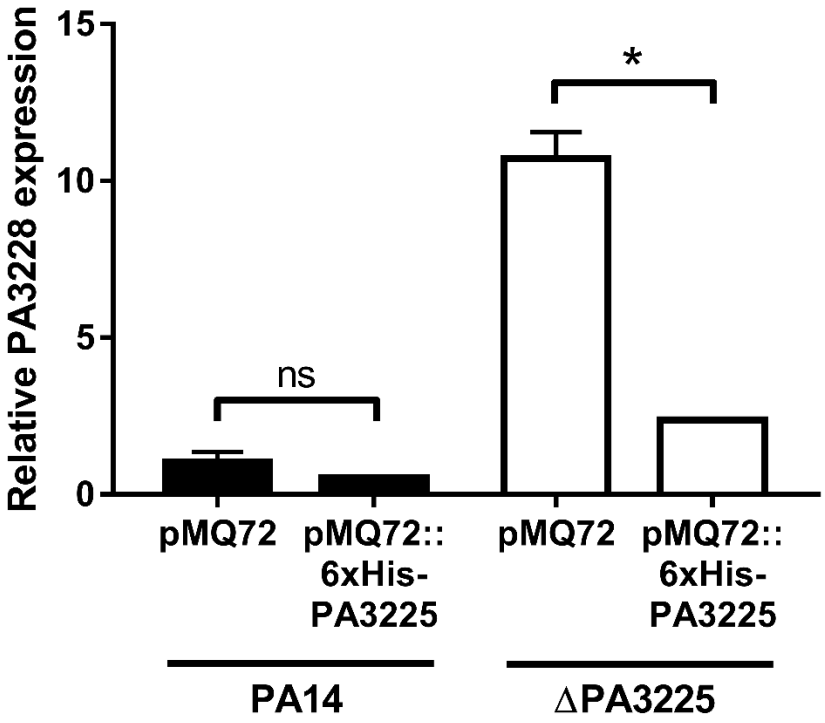

Figure S2-5. Overexpression of 6xHis-PA3225 reduces *PA3228* expression.
PA14 and Δ*PA3225* strains carrying pMQ72 and pMQ72::6xHis-PA3225 were grown to mid-exponential phase and then induced for two hours with 1% (w/v) arabinose. Expression of *PA3228* was measured by qPCR relative to PA14/pMQ72. Shown is the mean relative expression + SEM from two biological replicates, each tested in triplicate. * $p \leq 0.05$, ns = not statistically significant as determined by two-tailed Students *t*-tests.

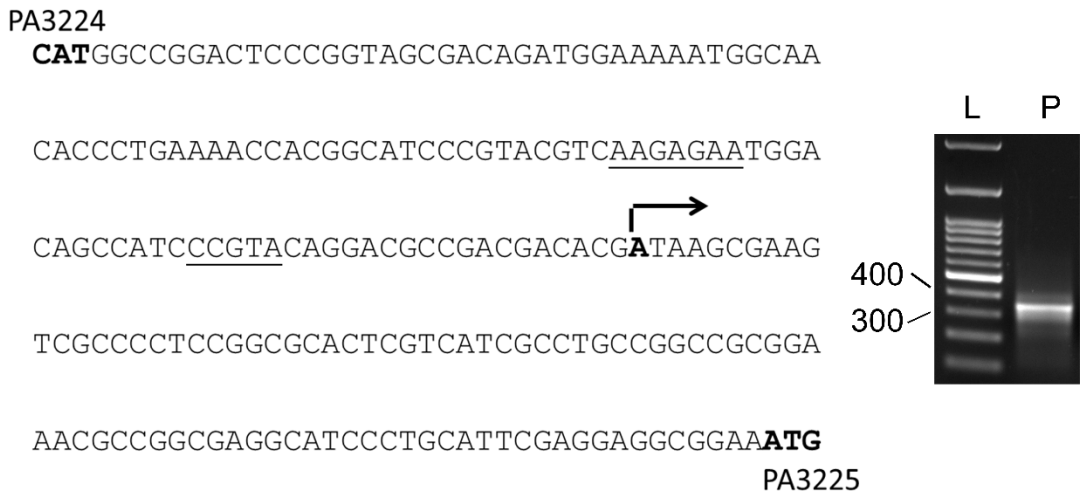

Figure S2-6. The *PA3224-PA3225* intergenic region.
5' RACE was used to identify the transcriptional start site of *PA3225* (shown bolded with a bent arrow in the sequence on the left). A putative bipartite PvdS sigma factor binding site is underlined in the sequence. Translational start codons of *PA3224* and *PA3225* are bolded. In the right panel, the 5' RACE product is shown in lane P and a size marker is shown in lane L.

2.5.9 PA1210, PA2864, and PA3228 are putative antibiotic resistance genes

While we had already established that the upregulation of *mexAB-oprM* underlies, at least in part, the decreased multidrug susceptibility of the Δ*PA3225* mutant, we wondered if the derepression of other members of the *PA3225* regulon may also affect the antibiotic susceptibility phenotype of the Δ*PA3225* strain. We therefore constructed deletion mutants of the *PA1210, PA2864*, *PA3228*, and *PA3229* loci in both the wildtype and Δ*PA3225* backgrounds, and we determined the MICs of several antibiotics for these mutants in LB medium (**Table 2-6**). The deletion of *PA1210* and *PA2864* in the wildtype PA14 background led to increased ciprofloxacin susceptibility. Additionally, the Δ*PA1210*, Δ*PA2864*, and Δ*PA3228* mutants were more susceptible to levofloxacin. The Δ*PA1210* and Δ*PA3228* strains were also less resistant to norfloxacin and carbenicillin than the wildtype. Although the deletion of *PA3229* led to increased susceptibility to norfloxacin, the Δ*PA3229* mutant had the same or, for some antibiotics, increased MIC values compared to those of wildtype strain PA14. MICs of strains complemented with *PA1210, PA2864*, and *PA3228* are presented in (**Table 2-7**). Complementation experiments showed that the expression of the cloned genes in the pJB866 vector could, for some antibiotics, increase the MIC.

Since *PA1210, PA2864*, and *PA3228* were upregulated in the Δ*PA3225* strain, we hypothesized that the deletion of these genes in a Δ*PA3225* background would further reveal any role that these genes might play as candidate antibiotic resistance determinants. As expected, the Δ*PA1210* Δ*PA3225*, Δ*PA2864* Δ*PA3225*, and Δ*PA3225* Δ*PA3228* double-deletion mutants were more susceptible than the parental Δ*PA3225* strain to most of the antibiotics that we tested (**Table 2-6**). The upregulation of *PA1210, PA2864*, and *PA3228* might therefore be partially responsible for the reduction in antibiotic susceptibility that we observed for the Δ*PA3225* mutant, and this

possibility will be explored further in future studies. *PA1210*, *PA2864*, and *PA3228* also appeared to affect susceptibilities to different subsets of antibiotics. *PA1210* and *PA2864* were mainly involved in fluoroquinolone resistance. In contrast, *PA3228* was important for resistance to a broader range of antibiotics, including β-lactams, fluoroquinolones, chloramphenicol, and tetracycline. Therefore, *PA1210*, *PA2864*, and *PA3228* potentially represent novel, PA3225-regulated antibiotic resistance genes in *P. aeruginosa*.

Table 2-6. Contribution of PA3225-regulated genes to susceptibility of *P. aeruginosa*[a].

Strain	MIC (μg/ml) of[b]								
	TOB	**CIP**	**LVX**	**NOR**	**NAL**	**CAR**	**CTX**	**CHL**	**TET**
PA14	4	0.25	1	2	64	256	32	128	16
Δ*PA1210*	4	0.125	0.25	0.5	64	128	32	128	16
Δ*PA2864*	4	0.125	0.5	2	64	256	64	128	16
Δ*PA3228*	4	0.25	0.25	1	64	128	32	128	16
Δ*PA3229*	4	0.5	1	1	128	512	64	256	32
Δ*PA3225*	4	0.5	2	4	256	512	128	256	64
Δ*PA1210* Δ*PA3225*	4	0.25	1	2	256	256	128	512	64
Δ*PA2864* Δ*PA3225*	2	0.25	1	1	256	256	128	512	64
Δ*PA3225* Δ*PA3228*	4	0.25	0.25	1	64	128	64	128	16
Δ*PA3225* Δ*PA3229*	4	0.5	2	4	256	512	128	512	64

[a] MIC values were determined in LB

[b] TOB, tobramycin; CIP, ciprofloxacin; LVX, levofloxacin; NOR, norfloxacin; NAL, nalidixic acid; CAR, carbenicillin; CTX, cefotaxime; CHL, chloramphenicol; TET, tetracycline

Table 2-7. Antibiotic susceptibilities of *P. aeruginosa* strains complemented with PA3225-regulated genes[a].

Strain	MIC (µg/ml) of[b]					
	CIP	**LVX**	**NOR**	**NAL**	**CAR**	**CTX**
PA14 pJB866	0.25	1	1	128	64	32
PA14 pJB866::PA1210	0.25	1	2	128	256	64
PA14 pJB866::PA2864	0.25	1	1	128	256	128
PA14 pJB866::PA3228	0.25	1	1	64	256	64
Δ*PA1210* pJB866	0.25	1	1	64	128	16
Δ*PA1210* pJB866::PA1210	0.25	2	1	64	256	32
Δ*PA2864* pJB866	0.25	1	1	64	128	64
Δ*PA2864* pJB866::PA2864	0.5	1	2	256	256	64
Δ*PA3228* pJB866	0.25	0.5	0.5	64	128	32
Δ*PA3228* pJB866::PA3228	0.5	1	1	128	128	64

[a] MIC values were determined in LB

[b] CIP, ciprofloxacin; LVX, levofloxacin; NOR, norfloxacin; NAL, nalidixic acid; CAR, carbenicillin; CTX, cefotaxime.

2.6 Discussion

The major findings of this study are presented schematically in **Fig 2-7**. This study initially sought to identify a novel transcription regulator of the *tssABC1* operon, which was previously shown to be involved in *P. aeruginosa* biofilm recalcitrance (152). Using a pulldown approach, we identified an uncharacterized LysR-type transcription factor, PA3225, which interacted with the promoter region of *tssABC1*. While PA3225 appeared to bind specifically to the region upstream of the *tssABC1* locus, the deletion of *PA3225* resulted in only a minor decrease in the *tssA1* expression level in planktonic cells. The regulation of HSI-I T6SS expression is controlled by multiple regulatory mechanisms, such as the RetS signaling cascade (152, 314, 317) and the LasR and PqsR (MvfR) quorum-sensing systems (321). It is possible, therefore, that we did not observe a large change in the *tssA1* gene expression level in the Δ*PA3225* mutant due to potential redundancy in the regulatory networks controlling the expression of the *tssABC1* operon. Further work will be required in order to better dissect the role of PA3225 in regulating *tssABC1* transcription in the context of other known regulators of the HSI-I T6SS locus.

During our characterization of PA3225, we observed that, compared to the wildtype strain, the Δ*PA3225* mutant had reduced susceptibility to multiple antibiotics, including β-lactams, quinolones, chloramphenicol, and tetracycline. Δ*PA3225* biofilms were additionally more resistant to ciprofloxacin than were wildtype biofilms. We found that the decreased multidrug susceptibility of the Δ*PA3225* mutant could be explained, at least partially, by the transcriptional derepression of the genes encoding the MexAB-OprM multidrug efflux pump. The typical substrates extruded by the MexAB-OprM efflux pump include β-lactams, quinolones, chloramphenicol, and tetracycline but not aminoglycosides such as gentamicin (349, 350). In fact, the substrate specificities of the MexAB-OprM efflux pump mirror the susceptibility profile of the Δ*PA3225*

mutant. Our results from both gene and protein expression experiments strongly support a role for PA3225 in regulating the transcription of *mexAB-oprM*. Hence, PA3225 is a new addition to a group of several transcription factors that have been shown to regulate the expression of the *mexAB-oprM* locus. The transcription of the *mexAB-oprM* operon is directly repressed by MexR, and the *mexR* gene is divergently transcribed from the *mexAB-oprM* operon (344, 351–353). Interestingly, the *mexAB-oprM* operon is also directly repressed by NalD, which belongs to the TetR family of transcriptional regulators (354, 355). Additional regulators such as AmpR, BrlR, MexT (reviewed in reference (10)), and CpxR (356) also affect the expression of *mexAB-oprM*. The large number of regulators that impact *mexAB-oprM* expression is a testament to the complexity of *mexAB-oprM* transcriptional regulation in *P. aeruginosa*. While we showed that the binding of PA3225 to the region upstream of *mexAB-oprM* and of *mexR* leads to the downregulation of *mexAB-oprM* expression, it is important to realize that we did neglected to determine whether PA3225 represses *mexAB-oprM* directly or if PA3225 represses *mexAB-oprM* by upregulating *mexR* expression. The interplay between previously characterized *mexAB-oprM* regulators and PA3225 in regulating *mexAB-oprM* will be the topic of future investigations.

Transcriptomics analysis of the Δ*PA3225* mutant via RNA-seq revealed that PA3225 also acts as a transcriptional repressor of several genes, including *PA1210*, *PA2864*, and *PA3228*. Unmarked deletion mutants of these three genes were more susceptible to several antibiotics, indicating that *PA1210*, *PA2864*, and *PA3228* potentially encode novel determinants of low-level antibiotic resistance. Intriguingly, a mutant carrying a transposon insertion in the *PA2864* open reading frame was previously shown to be less susceptible to ciprofloxacin than the wild type (357). In contrast, our susceptibility data suggested that the Δ*PA2864* strain is more susceptible to

ciprofloxacin than wildtype strain PA14. The reasoning behind this discrepancy is not yet clear to us.

PA3228 was previously suggested to be important for the possible development of planktonic ciprofloxacin resistance (358). Here, we demonstrated that the Δ*PA3228* deletion mutants (especially in the Δ*PA3225* background) were more susceptible than the parental wildtype and Δ*PA3225* strains to a broad range of antibiotics, thereby suggesting a role for PA3228 in intrinsic drug resistance. *PA3228* is predicted to encode a 610-amino-acid ABC transporter with both ATPase and permease domains (83, 322). Based upon our susceptibility data and bioinformatics predictions, we hypothesize that PA3228 is an ABC multidrug efflux pump. ABC transporter-type antibiotic efflux pumps are relatively rare in Gram-negative bacteria (10). However, the contribution of ABC transporters to antibiotic resistance in Gram-negative bacteria may have been underestimated. Recently, the *PA4456-PA4452* operon, which encodes components of an ABC transporter and is regulated by the PhoPQ two-component system, has been implicated in *P. aeruginosa* resistance to tetracycline, ciprofloxacin, chloramphenicol, and trimethoprim (359). Unlike PA3228, which encodes both the ATP-binding and permease domains, PA4456 contributes the ATP-binding domain, while PA4455 possesses the permease domain (322, 359). Characterization of the putative ABC multidrug efflux pump encoded by PA3228 is under way in our laboratory.

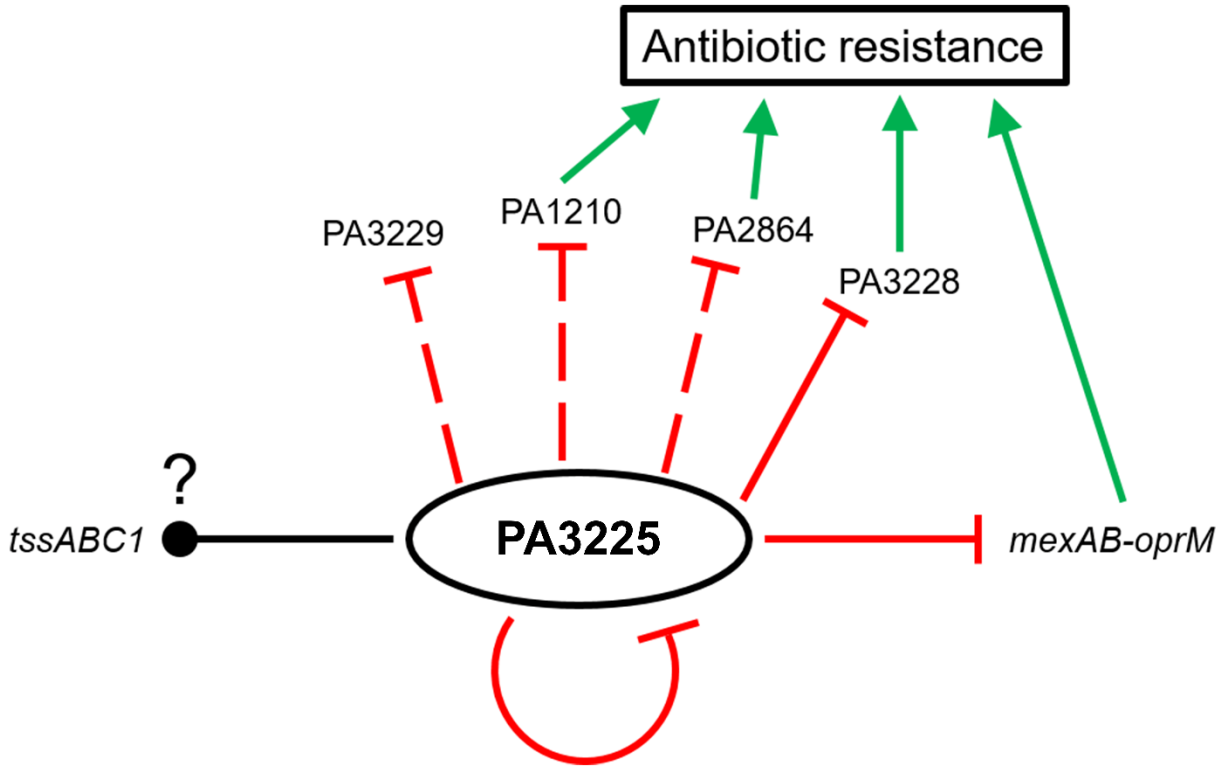

Figure 2-7. Summary schematic of the proposed mechanisms involved in the decreased susceptibility of *P. aeruginosa* upon deletion of the *PA3225* gene.
Solid red lines indicate that our EMSA results suggested that PA3225 acts as a direct transcriptional repressor of the gene, while dashed red lines indicate that we did not use an EMSA to assess whether PA3225 is a direct or indirect transcriptional repressor of the indicated locus. The solid black line with a question mark indicates that PA3225 binds directly to the promoter of *tssABC1*, but the role of PA3225 in regulating *tssABC1* expression is not entirely clear given that the *tssA1* expression level is only slightly decreased in ΔPA3225 planktonic cells and is not significantly different in ΔPA3225 biofilms compared to the wild type. Green arrows pointing toward the box indicating "Antibiotic resistance" indicate that the genes in question potentially contribute to antibiotic resistance in *P. aeruginosa*. Based on our data, the derepression of some or all of these genes in the Δ*PA3225* mutant leads to a decrease in antibiotic susceptibility.

2.7 Acknowledgments

We thank Xian-Zhi Li for helpful review of the manuscript prior to submission. Keith Poole (Queen's University, Kingston, Canada) kindly provided the anti-MexB antiserum for the Western blots. We are grateful to Rebecca Yaworski and the Fullerton laboratory (University of Ottawa) for assistance with the Western blots and to the Baetz laboratory (University of Ottawa) for providing materials for yeast cloning.

This work was supported by grants from Cystic Fibrosis Canada and from the Natural Sciences and Engineering Research Council of Canada to T.-F.M. C.W.H. is a Vanier Scholar (Canadian Institutes of Health Research) and was previously supported by a Cystic Fibrosis Canada summer studentship during the completion of this work.

We have no conflicts of interest to report. The funders had no role in study design, data collection and interpretation, or the decision to submit this work for publication.

Chapter 3: *Pseudomonas aeruginosa* biofilm antibiotic resistance gene expression requires the RpoS stationary-phase sigma factor

3.1 Preface

This chapter has been previously published as a research article:

> **Hall CW**, Hinz AJ, Gagnon LB, Zhang L, Nadeau JP, Copeland S, Saha B, and Mah T-F. 2018. *Pseudomonas aeruginosa* biofilm antibiotic resistance gene *ndvB* expression requires the RpoS stationary phase sigma factor. *Applied and Environmental Microbiology* 84(7): e02762-17.

Specific contributions of each author are listed below:

Clayton W. Hall: Designed and performed all experiments for the data presented in **Figures 3-5**, **3-6**, **3-7**, **3-8**, **3-9**, and **3-10**. Constructed all strains and plasmids for aforementioned figures. Wrote the original draft of the paper with AJH. Responded to reviewer comments.

Aaron J. Hinz: Designed and performed all experiments for the data presented in **Figures 3-1**, **3-2**, **3-3**, and **3-4**. Constructed all strains and plasmids for aforementioned figures. Wrote the original draft of the paper with CWH.

Luke B.P. Gagnon: Assisted AJH with experiments for the data presented in **Figures 3-1**, **3-2**, **3-3**, and **3-4**.

Li Zhang: Cloning of pSC01 and pBS01 (pAH06)..

Jean-Paul Nadeau: Cloning of pBS01 (pAH06).

Sarah Copeland: Cloning of pSC01.

Bratati Saha: Cloning of pBS01 (pAH06).

Thien-Fah Mah: Provided reagents and research materials, obtained funding, supervised research, conceptualized project, designed experiments, reviewed final draft of manuscript.

3.2 Abstract

Chronic, biofilm-based bacterial infections are exceptionally difficult to eradicate due to the high degree of antibiotic recalcitrance exhibited by cells in biofilm communities. In the opportunistic pathogen *Pseudomonas aeruginosa*, biofilm recalcitrance is multifactorial and arises in part from the preferential expression of resistance genes in biofilms compared to exponential-phase planktonic cells. One such mechanism involves *ndvB*, which we have previously shown to be expressed specifically in biofilms. In this study, we investigated the regulatory basis of this lifestyle-specific expression by developing an unstable green fluorescent protein (GFP) transcriptional reporter to observe the expression pattern of *ndvB*. We found that in addition to its expression in biofilms, *ndvB* was upregulated in planktonic cells as they enter stationary phase. The transcription of *ndvB* in both growth phases was shown to be dependent on the stationary-phase sigma factor RpoS, and mutation of a putative RpoS binding site in the *ndvB* promoter abolished the activity of the promoter in stationary-phase cells. Overall, we have expanded our understanding of the temporal expression of *ndvB* in *P. aeruginosa* and have uncovered a regulatory basis for its growth phase-dependent expression.

3.3 Importance

Bacterial biofilms are more resistant to antibiotics than free-living planktonic cells, and understanding the mechanistic basis of this resistance can inform treatments of biofilm-based infections. In addition to chemical and structural barriers that can inhibit antibiotic entry, the

upregulation of specific genes in biofilms contributes to the resistance. We investigated this biofilm-specific gene induction by examining expression patterns of *ndvB,* a gene involved in biofilm resistance of the opportunistic pathogen *Pseudomonas aeruginosa*. We characterized *ndvB* expression in planktonic and biofilm growth conditions with an unstable green fluorescent protein (GFP) reporter and found that the expression of *ndvB* in biofilms is dependent on the stationary-phase sigma factor RpoS. Overall, our results support the physiological similarity between biofilms and stationary-phase cells and suggest that the induction of some stationary-phase genes in biofilms may contribute to their increased antibiotic resistance.

3.4 Introduction

Antibiotic resistance in bacterial pathogens is a continuing public health concern that severely impacts the ability to treat infections (89, 90). Increased resistance in bacterial populations is caused by the acquisition of resistance genes through horizontal gene transfer and by selection of resistance mutations (360, 361). In addition, numerous structural and functional traits contribute to the underlying intrinsic resistance of microbes, which can reduce the spectrum and efficiency of antibiotics used in treatments (88, 89). Identifying the genetic and physiological mechanisms of intrinsic resistance in microbes can potentially inform the therapeutic use of already proven antibiotics.

Antibiotic resistance is especially problematic for cystic fibrosis patients harboring chronic biofilm-based *Pseudomonas aeruginosa* lung infections. *P. aeruginosa* has high intrinsic resistance to multiple antibiotics that, combined with its ability to readily acquire elevated resistance by *de novo* mutation, can make infections impossible to eliminate (362). The intrinsic resistance is mediated by drug efflux pumps, stress responses, low outer membrane permeability, and other poorly understood genetic functions (9, 110, 363). Resistance is additionally increased

in biofilms, the predominant lifestyle of *P. aeruginosa* in cystic fibrosis airway infections (116). Bacterial biofilms are a physiological state characterized by bacterial adhesion to a substrate and the production of an extracellular matrix composed of polysaccharides, protein, and DNA (13, 115). Multiple physical and physiological factors contribute to the increased antibiotic resistance of *P. aeruginosa* biofilms compared to free-living planktonic cultures, including reduced penetration of the antibiotic through the extracellular matrix and the presence of persister cells, which exist in a metabolically inactive state that protects against antibiotic action (137, 169, 364, 365).

Biofilm resistance is also mediated by several genetic mechanisms that are specifically expressed in biofilms but not in exponential-phase planktonic cells (1, 147, 153, 154, 366, 367). One of these mechanisms requires the gene *ndvB*, which encodes a glucosyltransferase enzyme that catalyzes the synthesis of periplasmic β-(1→3)-cyclic glucans (147). The glucans are thought to promote aminoglycoside resistance by sequestering antibiotics in the periplasm away from their cellular target (147, 148). In addition, *ndvB* is required, via an uncharacterized mechanism, for the biofilm-specific expression of genes that are involved in ethanol oxidation, and these *ndvB*-regulated genes may also play a role in biofilm resistance (149). The expression of *ndvB* is elevated in biofilms in comparison to that in exponentially growing planktonic cultures (147); however, the regulatory mechanism(s) responsible for this upregulation is unknown. Investigation of the genetic and physiological requirements of *ndvB* transcription may uncover the basis of its biofilm-specific expression and potentially identify conditions that diminish *ndvB* expression and reduce antibiotic resistance of biofilms.

In the present study, we examined transcriptional activity of *ndvB* and investigated the environmental and genetic factors governing its regulation. We used an unstable green fluorescent

protein (GFP) variant as a reporter of *ndvB* promoter activity to examine the gene's temporal expression in live cells (368, 369). Importantly, GFP is functional in bacterial biofilms and has been extensively used to visualize *P. aeruginosa* cells in biofilms (163, 370–372). The resulting observations motivated genetic tests that demonstrated the requirement of the stationary-phase sigma factor RpoS for *ndvB* induction in biofilms.

3.5 Materials and Methods

3.5.1 Bacterial strains and growth conditions

The bacterial strains, plasmids, and primers used in this study are listed in **Table 3-1** and **Table 3-2**. All *P. aeruginosa* strains were derived from the burn wound isolate UCBPP-PA14 (PA14) (327). The unmarked *P. aeruginosa* Δ*rpoS* deletion mutant was generated by two-step allelic exchange with the pEX18Gm suicide vector as previously described (323, 324). Bacteria were grown aerobically at 37°C with LB medium or M63 medium supplemented with 0.4% arginine and 1 mM $MgSO_4$ (149). *Pseudomonas* isolation agar (PIA; Difco) or LB with 0.1 μg/ml of ciprofloxacin or 20 μg/ml of nalidixic acid was used for counterselection of *Escherichia coli* following *E. coli-Pseudomonas* conjugation. *Saccharomyces cerevisiae* was grown aerobically at 30°C in yeast extract-peptone-dextrose medium (1% Bacto yeast extract, 2% Bacto peptone, and 2% glucose). Yeast selections were plated on synthetic, defined uracil drop-out medium, which contained (per liter) 6.7 g of yeast nitrogen base without amino acids (Wisent), 2 g of uracil drop-out supplement, and 20 g of glucose. Plasmids were transformed into *E. coli* by the calcium chloride or Inoue method and into *P. aeruginosa* by electroporation (373), conjugation with *E. coli* S17-1, or triparental mating with the pRK2013 helper plasmid (374). Antibiotics were used at the following concentrations: 100 μg/ml for ampicillin (Ap), 25 μg/ml for kanamycin (Km), and

15 μg/ml for gentamicin (Gm) with *E. coli*; 250 μg/ml for carbenicillin (Cb) and 50 to 100 μg/ml for gentamicin (plasmids); or 20 μg/ml for gentamicin (chromosomal insertions) with *P. aeruginosa*.

Table 3-1. Strains and plasmids used in this study.

Name	Genotype or description	Source
Strains		
PA14	*P. aeruginosa* burn wound isolate	(327)
TFM15	PA14 Δ*ndvB*; unmarked deletion of *ndvB* (codons 273 to 727 deleted)	(147)
TFM425	PA14 Δ*rpoS*; unmarked deletion of *rpoS* (codons 15 to 272 deleted)	This study
TFM423	PA14 *attTn7*::mini-Tn7T-Gm-*lacZ*; promoterless *lacZ*; Gm^R	This study
TFM427	PA14 *attTn7*::mini-Tn7T-Gm-P_{ndvB}-*lacZ*; P_{ndvB}-*lacZ* fusion; Gm^R	This study
TFM456	PA14 *attTn7*::mini-Tn7T-Gm-$P_{ndvB\text{-}mut}$-*lacZ*; P_{ndvB}-*lacZ* fusion with mutated RpoS binding site; Gm^R	This study
DH5α	*E. coli* strain; *supE44*, Δ*lacU169*(φ80 *lacZ*ΔM15), *recA1*, *hsdR17*, *thi-1*, *relA1*	(375)
S17-1	*E. coli* strain; *recA pro hsdR* RP42Tc::MuKm::Tn7	(326)
YPH500	*S. cerevisiae* uracil auxotroph; MATα, *ura3-52*, *lys2-801^{amber}*, *ade2-101^{ochre}*, *trp1-Δ63*, *his3-Δ200*, *leu2-Δ1*	(328)
Plasmids		
pMQ80	*araC*-P_{BAD}-*gfpmut3* reporter on *E. coli-S. cerevisiae-Pseudomonas* shuttle vector; Gm^R	(325)
pSC01	P_{ndvB}-*gfp* stable *gfp* reporter; pMQ80 with *ndvB* promoter upstream of *gfpmut3*; Gm^R	This study
pAH04	*araC*-P_{BAD}-*gfp*(ASV) reporter; pMQ80 with *gfp* protease tag from pJBA113; Gm^R	This study
pAH05	P_{ndvB}-*gfp*(LAA) reporter; pSC01 with *gfp* protease tag from pJBA110; Gm^R	This study
pAH06	P_{ndvB}-*gfp*(LVA) reporter; pSC01 with *gfp* protease tag from pJBA111; Gm^R	This study
pAH07	P_{ndvB}-*gfp*(AAV) reporter; pSC01 with *gfp* protease tag from pJBA112; Gm^R	This study

pAH08	P_{ndvB}-*gfp*(ASV) reporter; pSC01 with *gfp* protease tag from pJBA113; Gm^R	This study
pJBA110	pUC18Not-$P_{A1/04/03}$-RBSII-*gfp*(LAA)-T_0-T_1; Source of LAA protease tag; Ap^R	(376)
pJBA111	pUC18Not-$P_{A1/04/03}$-RBSII-*gfp*(LVA)-T_0-T_1; Source of LVA protease tag; Ap^R	(376)
pJBA112	pUC18Not-$P_{A1/04/03}$-RBSII-*gfp*(AAV)-T_0-T_1; Source of AAV protease tag; Ap^R	(376)
pJBA113	pUC18Not-$P_{A1/04/03}$-RBSII-*gfp*(ASV)-T_0-T_1; Source of ASV protease tag; Ap^R	(376)
pEX18Gm	Allelic exchange suicide vector; *sacB*, Gm^R	(323)
pEX18Gm::Δ*rpoS*	pEX18Gm derivative for unmarked deletion of *rpoS*; Gm^R	This study
pUC18-mini-Tn7T-Gm-*lacZ*	Mini-Tn7T transcriptional *lacZ* fusion vector; Ap^R, Gm^R	(377)
pUC18-mini-Tn7T-Gm-P_{ndvB}-*lacZ*	pUC18-mini-Tn7T-Gm-lacZ carrying the sequence from -112 to -1 relative to the translational start site of *ndvB*; Ap^R, Gm^R	This study
pUC18-mini-Tn7T-Gm-$P_{ndvB\text{-mut}}$-*lacZ*	Same as pUC18-mini-Tn7T-Gm-P_{ndvB}-*lacZ* except that the sequence CTAGACT was mutated to AGAGACT; Ap^R, Gm^R	This study
pTNS2	Transposase helper plasmid for mini-Tn7 integration; Ap^R	(377)
pRK2013	Helper plasmid for triparental matings; Km^R	(374)
pUC18	High-copy *E. coli* cloning/sequencing plasmid; Ap^R	(378)
pUCP19	Broad host range cloning and expression vector; Cb^R	(342)
pUCP19::$rpoS^+$	pUCP19 with *rpoS* under the control of its native promoter and terminator; Cb^R	This study

Table 3-2. Oligonucleotides used in this study

Name	Sequence (5' to 3') [a]	Function
*ndvB*p-F-2 [b]	cttctcctttactcatatgtatatctccttcAGAGATGAAACCAGGTTCCGG	P_{ndvB}-*gfp* fusion
*ndvB*p-R-2 [b]	caaaaacgcgtaacaaaagtgtctataatcaACCCGGCAGGCCGGGTTG	P_{ndvB}-*gfp* fusion
AH-GFP-Tag-F [b]	tcatccgccaaaacagccaagcttgcatgcctgcagactagtGGAGTCCAAGCTCAGCTAATTAAGC	GFP stability tag
AH-GFP-Tag-R [b]	acagctgctgggattacacatggcatggatgaactatacaaaAGGCCTGCAGCAAACGACGAA	GFP stability tag
*rpoS*del1	ATCCAT**GGATCC**TAGTCTGATCGGCCGTTTTG	*rpoS* deletion
*rpoS*del2	ATCATCGTGGTCAAACTCCG	*rpoS* deletion
*rpoS*del3	CGGAGTTTGACCACGATGATGACAAGCAGCGTGAGGTGGT	*rpoS* deletion
*rpoS*del4	ATCCAT**CTGCAG**TGCCAGAAAACCCAGCGAAG	*rpoS* deletion
*rpoS*compF	AATAAT**GGTACC**CTGCGAGCGGTAGTCTGATC	*rpoS* complementation
*rpoS*compR	CATCAT**AAGCTT**ATCTACTTAGGCTCACACGC	*rpoS* complementation
*ndvB*p-*lacZ* for	ATCCAT**CTGCAG**GGACTAGACTTGCAACAGAC	P_{ndvB}-*lacZ* fusion
*ndvB*p-mut-*lacZ* for [c]	ATCCAT**CTGCAG**GGAAGAGACTTGCAACAGAC	Mutant P_{ndvB}-*lacZ* fusion
*ndvB*p-*lacZ* rev	ATCCAT**AAGCTT**AGAGATGAAACCAGGTTCCG	P_{ndvB}-*lacZ* fusion
Tn7R	CACAGCATAACTGGACTGATTTC	Tn7 insertion verification
glmS-down	GCACATCGGCGACGTGCTCTC	Tn7 insertion verification
ndvB-F	ACAAGGGCTTCTTCCACATC	*ndvB* qPCR
ndvB-R	TCTTCGGTGATGCACCATTC	*ndvB* qPCR
rpoD-F	TCCATCGCCAAGAAGTACAC	*rpoD* qPCR
rpoD-R	TTGTAGCCACGACGGTATTC	*rpoD* qPCR
rpoS-F	CGAACCTTCACCCGAAGAAA	*rpoS* qPCR

rpoS-R	AAGAGAGACGTCTACCGAAGT	*rpoS* qPCR
gfp-gsp1	AGCACGTGTCTTGTAGTTCC	5’ RACE
gfp-gsp2	ATCTGGGTATCTCGCAAAGC	5’ RACE
gfp-gsp3	CTACA**GGATCC**GAAAGTAGTGACAAGTGTTGG	5’ RACE
3’ RACE adapter primer	GGCCACGC**GTCGAC**TAGTAC$(T)_{17}$	5’ RACE
AUAP	GGCCACGC**GTCGAC**TAGTAC	5’ RACE
M13R	TCACACAGGAAACAGCTATGAC	Sequencing

[a] Restriction sites are indicated in bold.

[b] Primer used for yeast-recombination cloning. Upper-case indicates sequences targeted for PCR amplification. Lower-case indicates sequences homologous to the vector used for recombination.

[c] Primer contains two changes (underlined) to the predicted *ndvB* promoter element.

3.5.2 Construction of gfp reporter vectors by yeast recombination

A yeast recombination gap repair method was used to generate the *gfp* reporter vectors as described by Shanks et al. (325). In brief, a yeast-bacterium shuttle vector was digested with a restriction enzyme, creating a gap. A PCR amplicon with ends homologous to vector sequences on both sides of the gap was cotransformed with the linearized vector into yeast cells. Recombination between the vector and amplicon by endogenous yeast functions generated recircularized vectors containing the inserted sequences. Yeast cells carrying circularized vectors were selected using a vector-encoded marker.

The base vector of the *gfp* reporters was the yeast-*E. coli*-*Pseudomonas* shuttle vector pMQ80 (325), which carries the bright *gfp* variant (*gfpmut3*) downstream of the arabinose-inducible promoter system (*araC*-P*BAD*). Selectable markers on the vector backbone include the *aacC1*gentamicin resistance gene (bacteria) and the *URA3* gene, which complements uracil auxotrophy (yeast) (325). To generate the P*ndvB*-*gfp* reporter (pSC01), the 500-bp region upstream of the *ndvB* start codon was PCR amplified from PA14 chromosomal DNA with primers *ndvB*p-F-2 and *ndvB*p-R-2 (**Table 3-2**). The primers included 31-bp tails homologous to pMQ80 vector sequences, which targeted the amplicon for recombination upstream of the Shine-Dalgarno sequence of *gfpmut3*, effectively replacing the *araC*-P_{BAD} sequences with the *ndvB* promoter. The purified PCR product was cotransformed with *Bam*HI-digested pMQ80 into yeast cells auxotrophic for uracil, using the "Lazy Bones" protocol (379). Transformants were selected on uracil drop-out medium and streaked for isolation. Plasmids were isolated from yeast cultures (380) and PCR screened for presence of the insert.

The reporters with unstable *gfp* variants were similarly generated using pSC01 as the base vector. The variants were amplified from four vectors (pJBA110 to pJBA113 (**Table 3-1**)) that carry *gfp* with 11-amino-acid C-terminal protease tags (AANDENYALAA), with each vector encoding a different final triplet (underlined) (376). The primers AH-GFP-Tag-F and AH-GFP-Tag-R (**Table 3-2**) were used to amplify 150-bp fragments that included the final 81 nucleotides of the tagged *gfp* genes. The inserts were recombined in yeast with pSC01 digested with SpeI, which cleaved close to the *gfp* stop codon. The resulting P*ndvB-gfp* reporters differed in the final three amino acids of the protease tag as follows: pAH05, LAA; pAH06, LVA; pAH07, AAV; and pAH08, ASV. An arabinose-inducible *gfp* reporter encoding the ASV tag (pAH04) was constructed in the same manner using the pMQ80 base vector. The yeast-derived vectors were transformed into *E. coli* DH5α, verified by Sanger sequencing (StemCore Laboratories, Ottawa Hospital Research Institute), and mobilized into *P. aeruginosa* by triparental mating with selection on PIA containing 100 μg/ml of gentamicin.

3.5.3 Biofilm and planktonic growth assays and microscopy

Biofilms were grown in M63-arginine by two methods: the air-liquid interface coverslip assay and the colony biofilm assay (381). For the air-liquid interface coverslip assay, exponential-phase LB cultures of PA14 carrying the reporter plasmids were diluted 1:100 in 4 ml of M63-arginine with 30 μg/ml of gentamicin in flat-bottom six-well plates. A flame-sterilized glass coverslip was half-submerged in each well, and plates were incubated for 19 h at 37°C to allow biofilms to form on the coverslip. The coverslips were gently rinsed with saline to remove nonadherent cells, and the biofilms that formed at the air-liquid interface of the coverslip were observed by phase-contrast and fluorescence microscopy. The colony biofilms were prepared by diluting exponential-phase LB cultures to an optical density at 600 nm (OD_{600}) of 0.05 in M63-

arginine and spotting 5 µl on semipermeable membranes (0.22-µm pore size) on M63-arginine agar plates containing 30 µg/ml of gentamicin. Following 20 h of incubation at 37°C, the membranes were removed, and the cells were gently stamped on glass slides and examined by fluorescence microscopy.

Planktonic growth curves were inoculated by washing 19-h LB cultures in M63-arginine and diluting them in 500 ml M63-arginine containing 30 µg/ml of gentamicin. For LB growth curves, 19-h LB cultures were diluted (1:100) in 50 ml of LB containing 30 µg/ml of gentamicin. Cultures were incubated at 37°C in Erlenmeyer flasks with agitation at 250 rpm, and samples were removed periodically for OD_{600} measurements, RNA isolation, and microscopy.

Images of planktonic and biofilm cultures were taken at a magnification of ×630 using a Leica AF6000 microscope with a Leica DFC350 FX camera. Fluorescence images were obtained using the BrightLine GFP-3035B filter set (Semrock) and Leica application suite advanced fluorescence software. Exposure times for phase-contrast and fluorescence images were 1.5 s and 8 s, respectively.

3.5.4 Quantification of GFP stability

Green fluorescence was quantified in PA14 cells expressing arabinose-inducible stable and ASV-tagged GFP from vectors pMQ80 and pAH04 (**Table 3-1**). Exponential cultures were grown in LB broth supplemented with gentamicin, and GFP expression was induced by adding arabinose at 10 mM (pMQ80) or 100 mM (pAH04). After 4 h of induction, the cells were pelleted, washed, and resuspended in M63-arginine lacking arabinose to stop GFP induction. The cultures were transferred to a black 96-well clear-bottom plate (Corning) and incubated at 37°C in a plate reader (Tecan Infinite F200 PRO) that measured cell density (OD_{595}) and green fluorescence (excitation wavelength, 500 nm; emission wavelength, 535 nm) at 15-min intervals. The fluorescent signal

specific to GFP was determined by subtracting the background signal of PA14 cells not expressing GFP from the total signal. The GFP-specific fluorescence measured immediately after the shift was set at 100%, and fluorescence measured over time was plotted as the percentage of this initial measurement. The data were fitted with exponential regression lines to estimate the decay constants (λ) of the equation $N(t) = N(i)e^{\lambda}t$, where $N(i)$ is the initial percent fluorescence and $N(t)$ is the percent fluorescence at time t. The GFP half-lives ($t_{1/2}$) were then determined by the equation $t_{1/2} = -\ln(2)/\lambda$.

3.5.5 RNA extraction and qPCR

Overnight cultures of wildtype PA14 and the Δ*rpoS* mutant were diluted 1:1,000 into LB and grown on a culture roller at 37°C to exponential phase (OD_{600} = 0.5) or stationary phase (OD_{600} = 2). Biofilms were grown as colony biofilms as described above. Cultures were pelleted, and RNA was extracted from the cells using TRIzol reagent and the PureLink RNA minikit (Ambion). RNA was digested with DNase as necessary, and complete removal of genomic DNA from the samples was confirmed by PCR using the *rpoD*-F and *rpoD*-R primers. The iScript cDNA synthesis kit (Bio-Rad) was used for first-strand cDNA synthesis from 2 μg of RNA in a volume of 40 μl as recommended by the manufacturer.

qPCR experiments were performed using a MyiQ single-color detection system (Bio-Rad) with 20-μl reaction mixtures containing SYBR green Supermix (Bio-Rad), 500 nM (each) forward and reverse gene-specific primers, and 2 μl of cDNA. The thermocycler program was 95°C for 90 s followed by 45 cycles of 60 s at 95°C, 30 s at 56°C, and 30 s at 72°C. Melt curve analysis was performed to ensure that amplification yielded single, specific products. Relative gene expression was calculated using the $2^{-\Delta\Delta}CT$ method, and fold changes were expressed as $2^{-\Delta\Delta}CT$. Expression

of the housekeeping gene *rpoD* was used for normalization. For each condition, qPCR experiments were performed in triplicate for at least three biological replicate samples.

3.5.6 Construction of pUCP19::rpoS^{+}

To enable complementation of the Δ*rpoS* mutant, a 1.57-kb fragment containing the *rpoS* promoter, coding, and terminator sequences (38, 52) was amplified by PCR using PA14 genomic DNA as the template and primers *rpoS*compF and *rpoS*compR. The fragment was ligated into the *Kpn*I/*Hind*III sites of pUCP19 to create pUCP19::*rpoS*$^{+}$. The pUCP19 and pUCP19::*rpoS*$^{+}$ plasmids were mobilized into *P. aeruginosa* strains by electroporation.

3.5.7 Construction of PndvB-lacZ reporters and Miller assays

A fragment encompassing part of the region immediately upstream of *ndvB* (−112 to −1 relative to the *ndvB* translational start site) was PCR amplified from PA14 genomic DNA using primers *ndvB*p-*lacZ*-for/*ndvB*p-*lacZ*-rev and subsequently cloned into the *Pst*I/*Hind*III sites of the pUC18-mini-Tn7T-Gm-*lacZ* vector (377). Sequence-verified plasmids (StemCore Laboratories, Ottawa Hospital Research Institute) were introduced into PA14 by electroporation with the pTNS2 helper plasmid, as previously described (382). Transformants were selected on LB plates with 20 μg/ml of gentamicin and screened for successful chromosomal insertion of the mini-Tn*7* reporter construct by PCR using the *glmS*-down/Tn7R primer pair. To generate an *ndvB*p-*lacZ* fusion with a mutated RpoS binding site, the *ndvB* promoter was amplified using the primer pair *ndvB*p-mut-*lacZ* for/*ndvB*p-*lacZ* rev, and the insert was cloned into the *Pst*I/*Hind*III restriction sites of pUC18-mini-Tn7T-Gm-*lacZ* as described above. This promoter fusion mutated the putative −10 RpoS binding site in the *ndvB* promoter from CTAGACT to AGAGACT (mutated nucleotides are

underlined). Miller assays were performed with stationary-phase cells carrying the *lacZ* reporters as described previously (383).

3.5.8 TSS mapping

The 5′ RACE system for rapid amplification of cDNA ends (version 2.0; Invitrogen) was used per the manufacturer's recommendations for templates with high GC content. Briefly, RNA was isolated from PA14 or PA14/pSC01 stationary-phase cells as described above. Reverse transcription was performed using the *gfp*-gsp1 primer at 50°C for 50 min. Column-purified first-strand cDNA was incubated with dATP in the presence or absence of TdT (+TdT or −TdT, respectively). The resulting dA-tailed cDNA was subjected to PCR with *gfp*-gsp2 and the 3′ RACE adapter primer followed by nested PCR with *gfp*-gsp3 and AUAP. 5′ RACE products were run on a 1% agarose gel and visualized with ethidium bromide staining. The major and minor 5′ RACE products from PA14/pSC01 +TdT were gel purified and ligated into the *Sal*I/*Bam*HI sites of pUC18. Plasmids were sequenced, and the *ndvB* transcriptional start site (TSS) was localized by alignment of the plasmid sequencing results with the *ndvB*promoter region.

3.5.9 Stationary-phase susceptibility assays

The stationary-phase assay was adapted from previous studies, with some modifications (43, 61, 384). Overnight (18-h) stationary-phase cultures of each strain were grown in LB at 37°C. For strains carrying pUCP19 or pUCP19::*rpoS*$^{+}$, the overnight cultures were grown in the presence of 250 μg/ml of carbenicillin to maintain plasmid selection. The stationary-phase cultures were washed twice in fresh LB, after which the washed cells were resuspended at the original concentration in LB medium. One-milliliter aliquots of the washed stationary-phase cells were dispensed into 1.5-ml Eppendorf tubes, and various concentrations of tobramycin in water were

added in a fixed volume of 50 µl to obtain final tobramycin concentrations of 0, 50, 100, 200, 300, 400, and 500 µg/ml. Cells were incubated for 8 h at 37°C with rotation on a tube revolver/rotator (Thermo Scientific; speed, 40 rpm). Following antibiotic treatment, 200-µl aliquots of treated cells were washed twice in phosphate-buffered saline (PBS, pH 7.4) and resuspended at the original concentration in PBS. Washed cells were 10-fold serially diluted in PBS, and survival was assessed by colony counting using the drop plate method. Survival was expressed as $\log_{10}$CFU per milliliter. Log_{10} reductions were calculated as the difference between survival at 0 µg/ml of tobramycin and the survival at 200 µg/ml.

3.5.10 Statistical analyses

Statistical analyses were performed using GraphPad Prism 7 software. The statistical tests that were used are specified in the figure legends when appropriate. Statistical significance is indicated as follows: ns, not significant ($P > 0.05$); *, $P \leq 0.05$; **, $P \leq 0.01$; ***, $P \leq 0.001$; and ****, $P \leq 0.0001$.

3.6 Results

3.6.1 ndvB transcriptional fusions to unstable gfp variants

We constructed a *gfp* transcriptional reporter to visualize the expression of *ndvB* in *P. aeruginosa* cells. The 500-bp sequence located immediately upstream of the *ndvB* translational start site was inserted upstream of the *gfp* gene in the shuttle vector pMQ80 using a yeast recombination-based cloning method (see Materials and Methods) (325, 385). The transcriptional fusion was constructed such that the *gfp* reporter retained its own Shine-Dalgarno sequence that was present in pMQ80. The resulting vector (pSC01) was transformed into *P. aeruginosa* (PA14), and GFP expression in cell cultures was examined by fluorescence microscopy. Reverse transcriptase PCR experiments have shown that *ndvB* transcription is preferentially expressed in PA14 biofilms compared to exponential-phase planktonic cultures, which exhibit negligible *ndvB* expression (147). However, we observed constitutive fluorescence in exponential-phase planktonic cells carrying the pSC01 reporter (**Fig 3-1**). Thus, while the P*ndvB-gfp* reporter was clearly functional (i.e., GFP was actively expressed), its fluorescence poorly corresponded to established *ndvB* expression patterns.

We suspected that the constitutive fluorescence of the pSC01 reporter was due to the long half-life of GFP, which has been estimated to be greater than 24 h in *E. coli* and *Pseudomonas fluorescens* (376). High GFP stability in the *ndvB* reporter could cause steady-state fluorescence even in the absence of *ndvB* transcription. To address this possibility, we utilized unstable GFP variants which contain 11-amino-acid tags fused to the C terminus of GFP. These tags target proteins for degradation by tail-specific proteases (376, 386), and the rate of proteolysis is dependent on the sequences of the final three amino acids. Thus, by altering these sequences, GFP variants with a range of stabilities can be generated (376).

We fused four variants of the protease tag to the C terminus of GFP in the *ndvB* reporter vector (pSC01) by yeast recombination cloning (pAH05 to pAH08 (**Table 3-1**)). We transformed the four unstable GFP reporter plasmids (which differed only in the final three amino acids of the protease tag) into PA14 and examined fluorescence during planktonic growth. For each of the reporters, fluorescence was absent in exponential cultures, suggesting that the tags effectively reduced the half-life of GFP (**Fig 3-1** and data not shown). However, three of the variants (pAH05 to pAH07) failed to fluoresce under any growth conditions tested, including biofilms (a known inducing condition for *ndvB* expression), indicating that they were too unstable to visualize *ndvB* transcription. The fluorescence of the ASV-tagged GFP variant (pAH08) was not completely abolished, as evidenced by faint, but reproducible, fluorescence observed in stationary-phase cultures (**Fig 3-1**). Although *ndvB* expression was not expected in this growth phase, the ASV-tagged variant was a more promising *ndvB* reporter candidate and was characterized further.

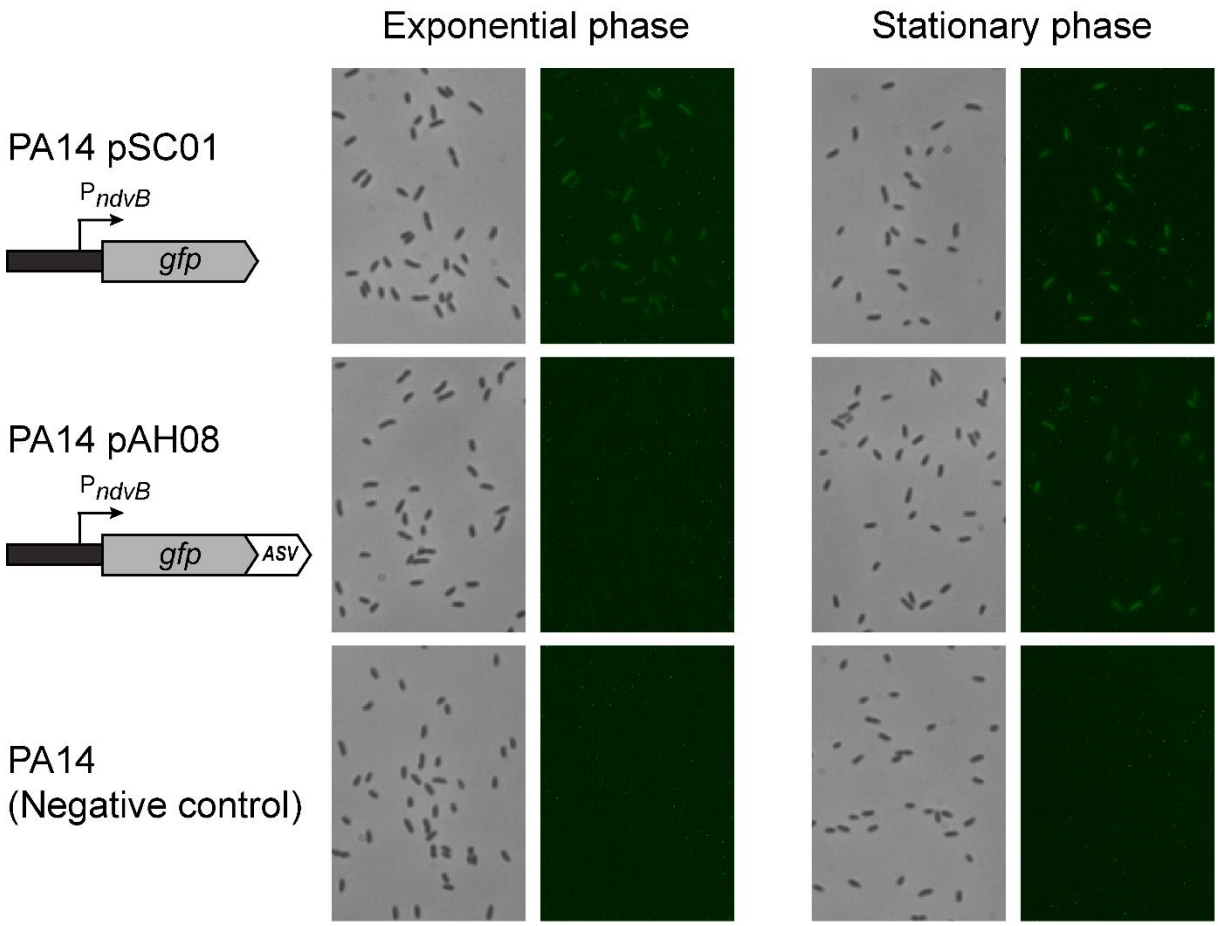

Figure 3-1. Expression of P*ndvB-gfp* reporters in planktonic cultures.
Cultures of the stable *ndvB-gfp* reporter (PA14/pSC01), the ASV-tagged reporter (PA14/pAH08), and a negative control (PA14) were diluted (OD_{600} = 0.05) in M63-arginine medium and incubated at 37°C with shaking. Samples were removed after 6 h (exponential phase) and 12 h (stationary phase) for phase-contrast (left panels) and fluorescence (right panels) microscopy at a magnification of ×630. The brightness was increased in each of the fluorescent panels for image clarity. The images are representative of at least three replicate cultures.

3.6.2 Stability of ASV-tagged GFP in PA14

To directly measure the impact of the ASV tag on GFP stability, we examined the kinetics of GFP decay in PA14 using arabinose-inducible GFP constructs (pMQ80 and pAH04 (**Table 3-1**)). Exponential-phase planktonic cultures were grown in arabinose-containing rich medium to induce GFP expression and then shifted to arabinose-free minimal medium to block further expression. GFP stabilities were determined by quantifying the reduction in fluorescence over time with a plate reader. As shown in **Fig 3-2**, cultures expressing the ASV-tagged GFP construct (pAH04) exhibited a pronounced decline in fluorescence in comparison to cultures with the untagged construct (pMQ80). We calculated the GFP half-lives from decay constants (λ) estimated during intervals in which the decline in fluorescence was exponential. The half-life of ASV-tagged GFP was approximately 1.9 h for the first 5 h after the downshift ($\lambda = -0.386$; $R^2 = 0.99$) and increased to approximately 6.5 h for the next 5 h (time [T] = 5 h to 10 h; $\lambda = -0.107$; $R^2 = 0.96$). In contrast, following a small reduction immediately after the downshift, untagged GFP was extremely stable over the course of the experiment, with an estimated half-life of 53 h (T = 1 h to 10 h; $\lambda = -0.013$; $R^2 = 0.97$). These results confirmed that the introduction of the ASV tag substantially reduces the fluorescent half-life of GFP in PA14 planktonic cultures. Notably, the decay slowed at the later time points, suggesting that the nutrient availability and/or physiological state of the cultures can influence the proteolysis rate.

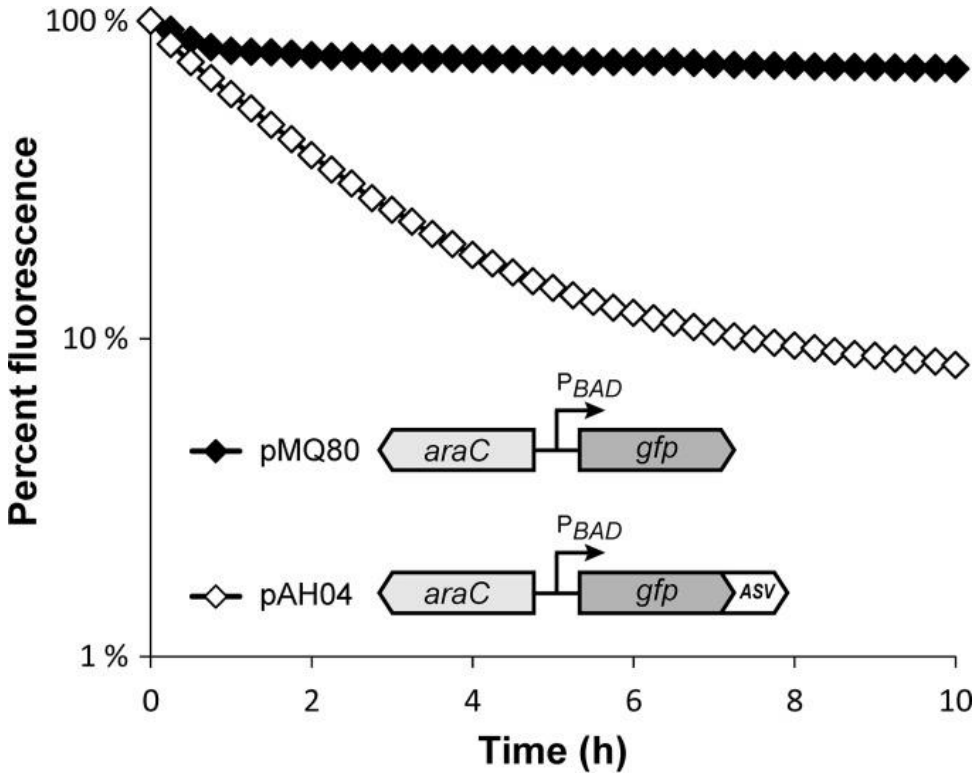

Figure 3-2. Stability of unmodified and ASV-tagged GFP in *P. aeruginosa*.
Exponential cultures of PA14 harboring arabinose-inducible unmodified GFP (pMQ80) and ASV-tagged GFP (pAH04) were treated with arabinose for 4 h to induce GFP expression. The cultures were washed to inhibit further induction, and GFP fluorescence was measured at intervals for 10 h. The fluorescence is given as percentage of initial fluorescence of eight replicate cultures (mean ± SEM; the error bars are smaller than the symbols).

3.6.3 Expression of the ASV-tagged ndvB-gfp reporter in biofilms

The reduced GFP half-life caused by the ASV protease tag enabled the visualization of *ndvB* transcriptional downregulation in planktonic exponential-phase cultures (**Fig 3-1**). We next characterized the fluorescence of the *ndvB* reporters in biofilms, in which upregulation of *ndvB* transcription has been well documented (147, 149). Biofilms were grown on the air-liquid interface of glass coverslips submerged in growth medium or as colony biofilms on agar plates (381) (see Materials and Methods). Biofilms of the reporter strains were visually indistinguishable from wildtype biofilms, indicating that the vectors did not influence biofilm formation (**Fig 3-3**; phase panels). Biofilm cells carrying the stable GFP reporter (pSC01) showed robust fluorescence (**Fig 3-3**). Importantly, fluorescence was also evident for the unstable reporter (pAH08) but to a lesser degree, which was consistent with the reduced stability of ASV-tagged GFP (**Fig 3-3**). Thus, based on the increased fluorescence of biofilms compared to exponential-phase planktonic cultures (**Fig 3-1**), we concluded that the fluorescence of the ASV-tagged reporter conformed to previously established *ndvB* expression patterns.

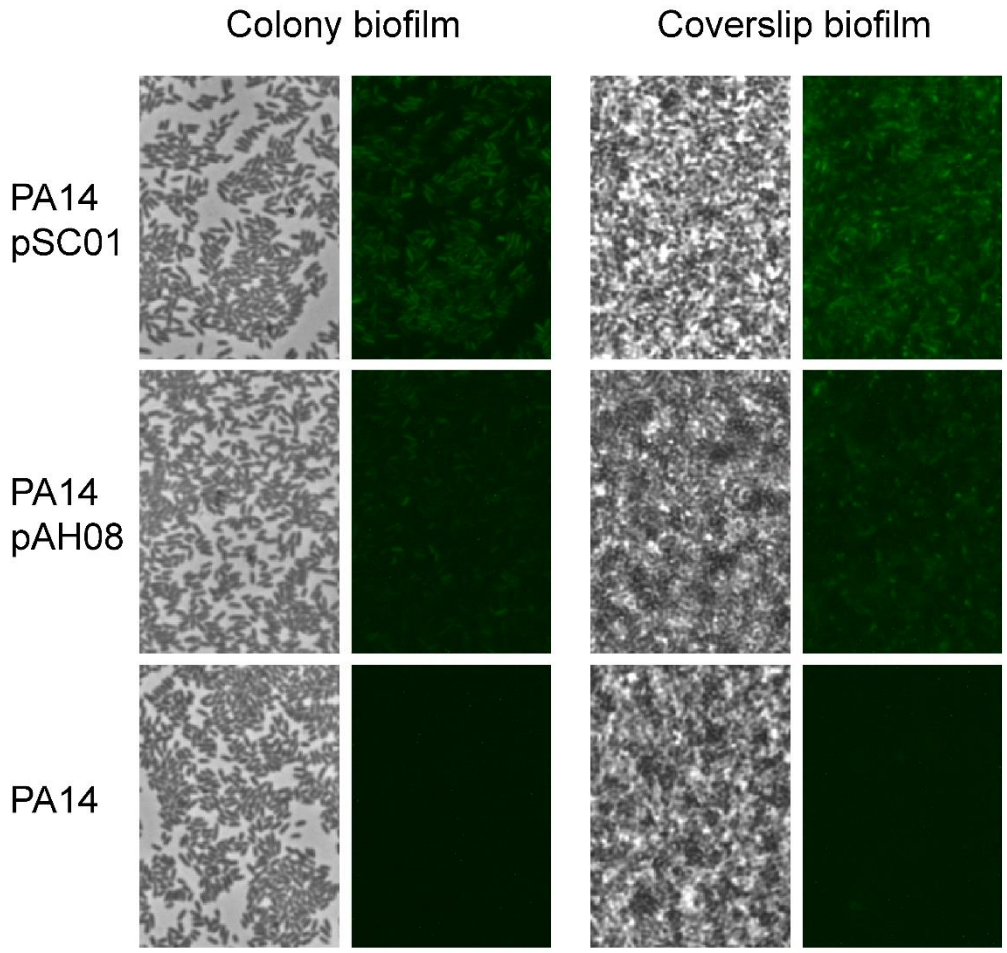

Figure 3-3. Expression of P*ndvB-gfp* reporters in biofilms.
Biofilms were grown at the air-liquid interface of coverslips partially submerged in M63-arginine medium (coverslip biofilms) and on semipermeable membranes on M63-arginine agar plates (colony biofilms). The coverslip biofilms were rinsed and the coverslips placed on a slide for phase-contrast (left panels) and fluorescence (right panels) microscopy at a magnification of ×630. The colony biofilms were stamped onto a slide for imaging. The images are representative of those from at least three replicate biofilm cultures.

3.6.4 ndvB transcription is induced in stationary-phase planktonic cultures

We next used the *ndvB* transcriptional reporter to explore the temporal regulation of *ndvB* expression. In particular, we were interested in identifying specific conditions that induce *ndvB* transcription, which might hint at the mechanism(s) underlying its regulation. As described for the planktonic expression experiments, we observed fluorescence in overnight cultures of PA14 carrying the ASV-tagged P*ndvB-gfp* reporter (pAH08), suggesting that *ndvB* might be expressed in stationary-phase planktonic cultures in addition to biofilms (**Fig 3-1**). We examined planktonic expression of the P*ndvB-gfp* reporters in more detail by observing the fluorescence of planktonic cells throughout a growth curve (**Fig 3-4A**). Subcultures of PA14 carrying the unstable GFP reporter (pAH08) showed little or no fluorescence during the lag and exponential phases of growth in both LB and minimal M63 media. However, at early stationary phase, fluorescence was detected in both media, indicating that *ndvB* promoter activity is induced at the onset of stationary phase (**Fig 3-4**). This pattern was also observed with the stable GFP reporter (pSC01) as a transient reduction of fluorescence intensity in exponential-phase cells, which we interpret as dilution of existing GFP by cell division, followed by induction and increased fluorescence intensity at stationary phase (data not shown). The GFP induction was observed at the same phase of the growth curve in both LB and M63 growth media.

Although the fluorescence profile of the pAH08 reporter agreed with *ndvB* transcriptional patterns in exponential-phase and biofilm cultures, it was possible that the stationary-phase fluorescence might be an artifact of the reporter system. For example, GFP proteolysis might be compromised during stationary phase and allow accumulation of GFP in the absence of significant transcriptional upregulation. Therefore, we used qPCR to validate the microscopic observation by comparing relative *ndvB* mRNA levels at time points corresponding to different planktonic growth

phases. The results corroborated those observed with the *gfp* reporter. The early stationary-phase cells contained greater *ndvB* transcript levels than exponential-phase cells in both LB and M63 cultures, and this induction corresponded to the phase of growth at which the pAH08 *gfp* reporter fluoresced (**Fig 3-4**). Thus, *ndvB* expression was confirmed to be upregulated in stationary-phase planktonic cells as well as in biofilms.

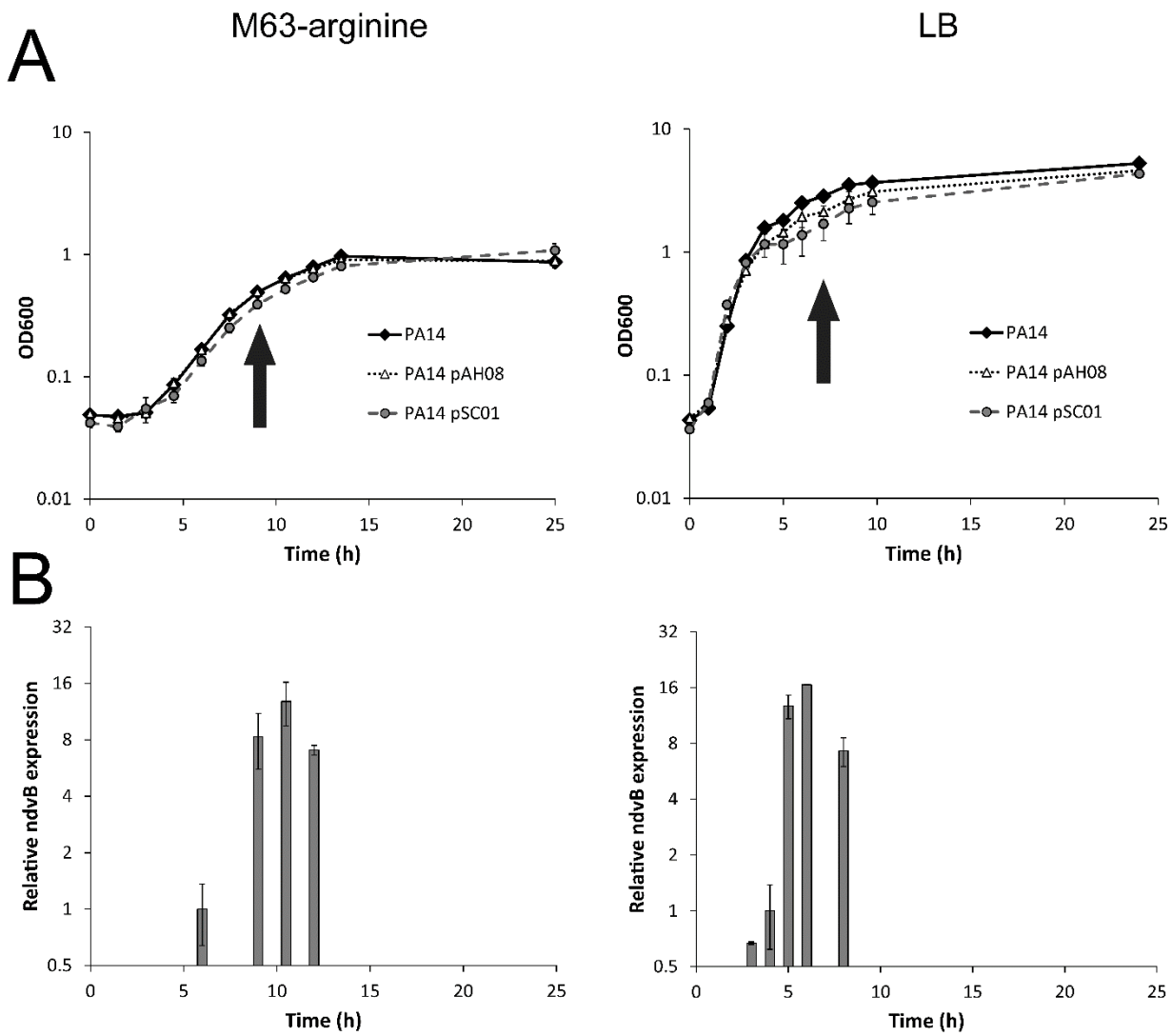

Figure 3-4. *ndvB* is upregulated in stationary-phase planktonic cultures.
(A) Growth curves of planktonic cultures of PA14 carrying the stable (pSC01) and ASV-tagged (pAH08) *ndvB-gfp* reporters grown in M63-arginine (left) or LB (right) medium. At each time point, samples were removed for optical density measurements and microscopy. Arrows indicate the earliest observation of fluorescence for the unstable reporter (pAH08), which coincides with the entry to stationary phase. (B) Expression of *ndvB* was measured by qPCR in PA14 planktonic cultures corresponding to the time points of the growth curves in panel A. Expression was quantified at four time points for the M63 cultures (6 h, 9 h, 10.5 h, and 12 h) and five time points for the LB cultures (3 h, 4 h, 5 h, 6 h, and 8 h). *ndvB* expression is given relative to the 6-h time point for M63 or the 4-h time point for LB. The mean and SEM are presented for the data from three replicate cultures assayed in triplicate qPCRs.

3.6.5 ndvB expression is RpoS dependent

Given that *ndvB* expression coincided with entry into stationary phase, we considered the possibility that the stationary-phase sigma factor RpoS might regulate *ndvB* transcription. RpoS levels rise at the onset of stationary phase (33), and RpoS is known to regulate the expression of a number of *P. aeruginosa* genes in stationary phase. The RpoS sigma factor regulon, or "sigmulome," has been documented by two independent groups using microarray (34) and transcriptome sequencing (RNA-seq) (22) comparisons of wildtype and *rpoS* mutant strains. Data mining of the aforementioned transcriptomic studies revealed that while *ndvB* was listed as a member of the RpoS sigmulome in the study by Schulz et al. (22), *ndvB* expression was not affected by deletion of *rpoS* in the work done by Schuster et al. (34).

To clarify the role of RpoS in *ndvB* expression, we constructed an unmarked Δ*rpoS* deletion mutant and assayed *ndvB* expression of this mutant at different growth stages by quantitative PCR (qPCR). Consistent with our findings in **Fig 3-4**, *ndvB* was significantly upregulated in wildtype stationary-phase and biofilm cells compared to wildtype exponential-phase cells (**Fig 3-5**). Interestingly, however, induction of *ndvB* expression was not observed in Δ*rpoS* stationary-phase cells or in Δ*rpoS* biofilms (**Fig 3-5**).

Introduction of an *rpoS* complementation plasmid (pUCP19::*rpoS*$^{+}$) into the Δ*rpoS* mutant restored stationary-phase *rpoS* expression to wildtype levels (**Fig 3-6A**). Importantly, stationary-phase expression of *ndvB* was also restored to wildtype levels in the Δ*rpoS* mutant carrying pUCP19::*rpoS*$^{+}$ as determined by qPCR (**Fig 3-6B**). Furthermore, overexpression of *rpoS* in wildtype cells led to overexpression of *ndvB* (**Fig 3-6B**). Overall, these results indicate that the *rpoS* gene is essential for the upregulation of *ndvB* in both stationary-phase and biofilm cells.

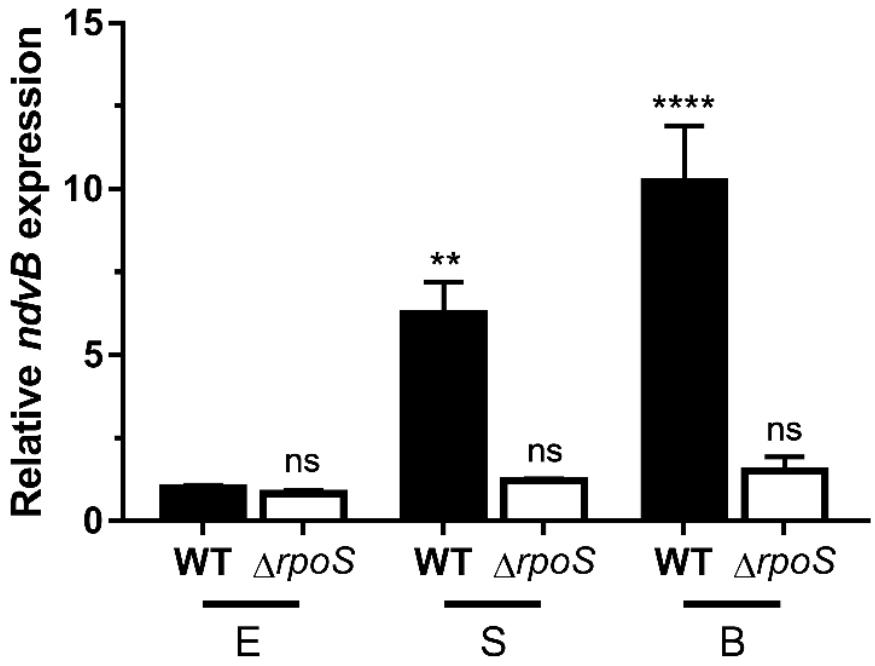

Figure 3-5. RpoS is required for the upregulation of *ndvB* expression observed in stationary-phase and biofilm cells.

The expression of *ndvB* (relative to that in exponential-phase wildtype cultures) was assessed by qPCR in wildtype (WT) PA14 and Δ*rpoS* strains grown planktonically to exponential (E) or stationary (S) phase or as biofilms (B). Data are expressed as means + SEMs for three biological replicates assayed in three technical replicates. Statistical significance was determined using one-way analysis of variance (ANOVA) with Dunnett's test (the exponential-phase wild type was used as the comparison control).

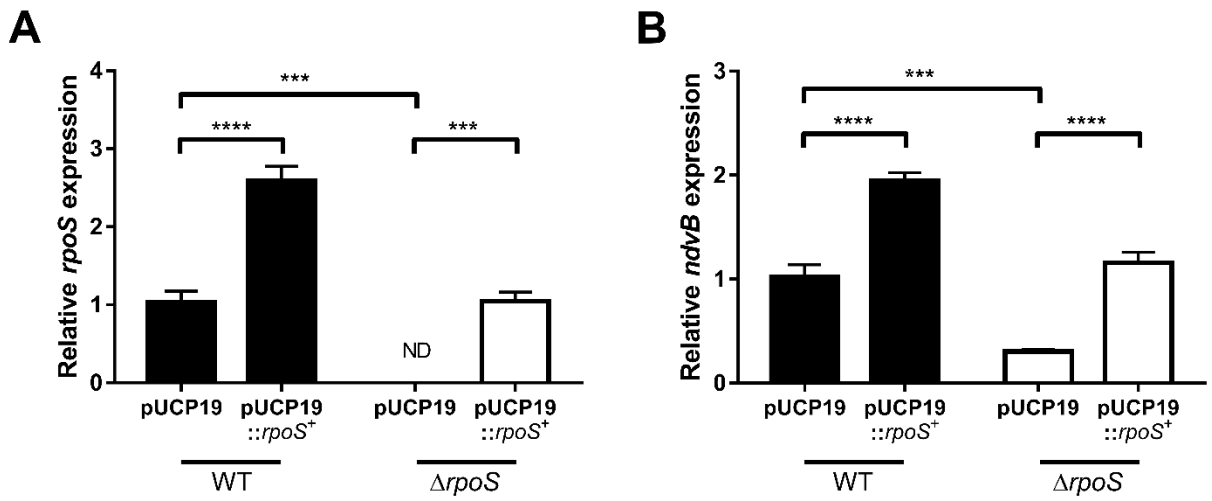

Figure 3-6. Complementation of the Δ*rpoS* strain restores *rpoS* and *ndvB* expression in stationary phase.

Stationary-phase expression of *rpoS* (A) or *ndvB* (B) (relative to PA14 pUCP19) was assessed by qPCR in PA14 wildtype and Δ*rpoS*strains carrying pUCP19 or pUCP19::*rpoS*$^{+}$. Data are presented as mean relative gene expression + SEMs for four biological replicates assayed in triplicate. Statistical significance was determined using one-way ANOVA with Tukey's multiple-comparison test. ND, not detected (the relative expression value was set to zero for statistical analyses).

3.6.6 RpoS regulates ndvB directly

To determine whether the RpoS-dependent regulation of *ndvB*is direct, we searched for a sequence upstream of *ndvB* that matched the consensus −10 RpoS binding site. The consensus −10 RpoS binding site was previously defined as CTATACT by Schuster et al. (34), and this consensus motif was recently corroborated by Schulz et al. (22). To our knowledge, a consensus −35 RpoS binding motif has not been described for *P. aeruginosa*. Interestingly, we found that the *ndvB* promoter region contains the sequence CTAGACT (−109 to −103 relative to the translational start site; the underlined fourth position deviates from the consensus motif described by Schuster et al.), which closely matches the −10 consensus motifs (**Fig 3-7A**). To investigate the importance of this motif for *ndvB* expression, a transcriptional reporter construct was generated in which part of the regulatory region upstream of the *ndvB* gene (from −112 to −1 relative to the *ndvB* translational start site) was cloned upstream of the *lacZ* reporter gene. Another reporter construct identical to the first but with engineered mutations in the putative −10 RpoS binding site (agAGACT; lowercase letters indicate the mutated positions) was also produced (**Fig 3-7B**). The first and second positions were chosen for mutation because these positions are highly conserved in the consensus motifs and are, therefore, likely essential for RpoS binding to the *ndvB* promoter. These reporter constructs were chromosomally integrated into wildtype PA14, and β-galactosidase activity was measured in stationary-phase cultures. As shown in **Fig 3-7C**, the activity of the mutated reporter (P*ndvB*$_{\text{-mut}}$-*lacZ*) was significantly decreased compared to that of the wildtype reporter (P*ndvB*-*lacZ*). The activity of the P*ndvB*$_{\text{-mut}}$-*lacZ* reporter did not differ significantly from that of the promoterless *lacZ* control (**Fig 3-7C**).

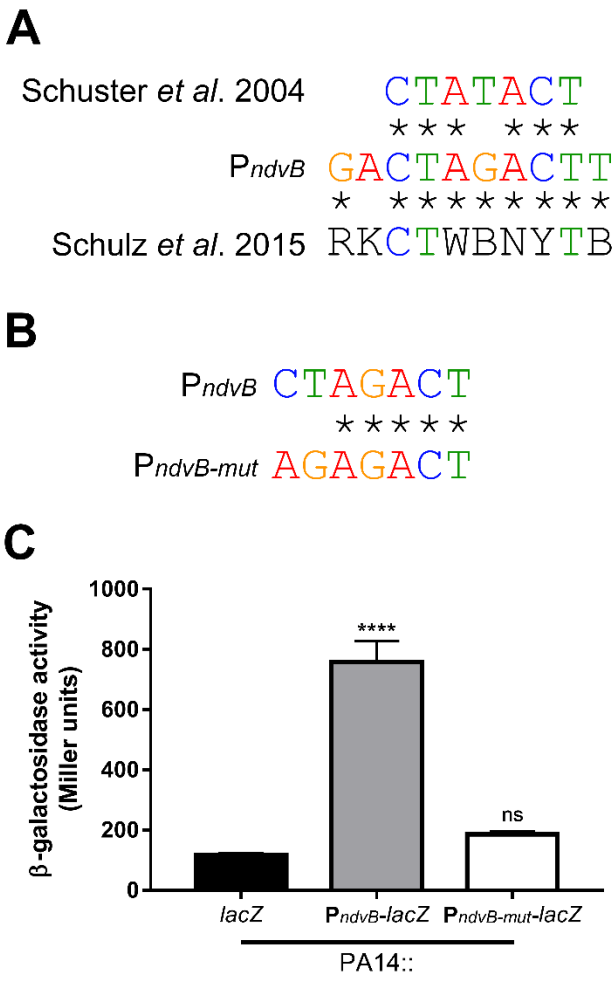

Figure 3-7. The *ndvB* promoter contains a sequence that matches the RpoS consensus binding site.

(A) Comparison of the proposed −10 RpoS binding site in the *ndvB* promoter to the consensus −10 RpoS elements independently determined by Schuster et al. () and by Schulz et al. (). Sequence identity is shown using asterisks. (B) Comparison of the proposed −10 RpoS binding site in the *ndvB* promoter with the mutated site in the $P_{ndvB\text{-}mut}$-*lacZ* reporter. (C) β-Galactosidase activity of promoterless *lacZ* negative control (*lacZ*), P_{ndvB}-*lacZ*, and $P_{ndvB\text{-}mut}$-*lacZ* reporter constructs that were chromosomally integrated into wildtype PA14 at the *att*Tn*7* site. Data are expressed as mean + SEMs for three biological replicates. Statistical significance was determined using one-way ANOVA with Dunnett's test (promoterless *lacZ* was used as the comparison control).

If the CTAGACT sequence in the *ndvB* promoter serves as the −10 element for RpoS binding, then transcription of *ndvB* should be initiated approximately 10 bp downstream of this sequence. Wurtzel et al. (387) mapped the transcriptional start sites (TSS) for about half of all protein-coding genes in *P. aeruginosa* using RNA-seq. Unfortunately, however, their work did not identify the *ndvB* TSS in spite of the fact that RNA from early stationary-phase cells was used for the analysis. In order to map the TSS of *ndvB*, 5′ rapid amplification of cDNA ends (RACE) was performed with RNA from PA14/pSC01 and *gfp*-specific primers (**Fig 3-8A**). Sequencing of the major 5′ RACE product revealed a TSS located 8 bp downstream of the CTAGACT sequence, which is consistent with this motif serving as the −10 element for RpoS binding in the *ndvB* promoter (**Fig 3-8B**). A smaller, minor 5′ RACE product was also obtained, and sequencing revealed a second potential TSS that would be located 7 bp upstream of the annotated translational start site of *ndvB* (**Fig 3-8C**). However, we reasoned that the promoter of this second TSS is not likely to play a significant role in *ndvB* expression under our conditions because activity of the *ndvB* promoter was insignificant when the major, RpoS-directed promoter was mutated (**Fig 3-7C**).

Together, the presence of a putative −10 RpoS binding site in the *ndvB* promoter, the necessity of this motif for *ndvB* promoter activity, and the presence of a TSS 8 bp downstream of this sequence support the hypothesis that RpoS directly regulates transcription of *ndvB*. The sequences of the RpoS regulatory motif and the transcriptional start site of *ndvB* within the upstream regulatory region of *ndvB* are shown in their genomic context in **Fig 3-9**.

A

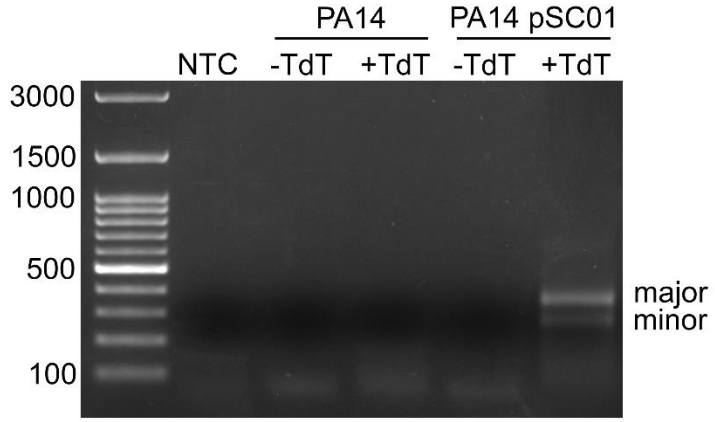

B major

```
                                    RpoS          +1
pSC01       TCGTCGCGCAGGCCGGACTAGACTTGCAACAGACCCGCCGGCCCGGCGCCTGTACACCCC
RACE1       GTCGACTAGTACT--TTTTTTTTTTTTTTTTGACCCGCCGGCCCGGCGCCTGTACACCCC
RACE2       GTCGACTAGTACTTTTTTTTTTTTTTTTTAGACCCGCCGGCCCGGCGCCTGTACACCCC
RACE3       GTCGACTAGTACTTTTTTTTTTTTTTTTTGACCCGCCGGCCCGGCGCCTGTACACCCC
                          *    **      ****************************

pSC01       GGGGGGTGCGGGGTAGCATCCGCCGCCCCGTGTTCAGCGAAACATCCGGAACCTGGTTTC
RACE1       GGGGGGTGCGGGGTAGCATCCGCCGCCCCGTGTTCAGCGAAACATCCGGAACCTGGTTTC
RACE2       GGGGGGTGCGGGGTAGCATCCGCCGCCCCGTGTTCAGCGAAACATCCGGAACCTGGTTTC
RACE3       GGGGGGTGCAGGGTAGCATCCGCCGCCCCGTGTTCAGCGAAACATCCGGAACCTGGTTTC
            ********* **************************************************

                                                        gfp
pSC01       ATCTCTGAAGGAGATATACATATGAGTAAAGGAGAAGAACTTTTCACTGGAGTTGTCCCA
RACE1       ATCTCTGAAGGAGATATACATATGAGTAAAGGAGAAGAACTTTTCACTGGAGTTGTCCCA
RACE2       ATCTCTGAAGGAGATATACATATGAGTAAAGGAGAAGAACTTTTCACTGGAGTTGTCCCA
RACE3       ATCTCTGAAGGAGATATACATATGAGTAAAGGAGAAGAACTTTTCACTGGAGTTGTCCCA
            ************************************************************
```

C minor

```
                                    RpoS
pSC01       TCGTCGCGCAGGCCGGACTAGACTTGCAACAGACCCGCCGGCCCGGCGCCTGTACACCCC
RACE4       ------------------------------------------------------------
RACE5       ------------------------------------------------------------

                                                                      +1
pSC01       GGGGGGTGCGGGGTAGCATCCGCCGCCCCGTGTTCAGCGAAACATCCGGAACCTGGTTTC
RACE4       ----------------------------GTCGACTAGTACTTTTTTTTTTTTTTTTTC
RACE5       ----------------------------GTCGACTAGTACTTTTTTTTTTTTTTTTTC
                                          * *   *        *  ****

                                                    gfp
pSC01       ATCTCTGAAGGAGATATACATATGAGTAAAGGAGAAGAACTTTTCACTGGAGTTGTCCCA
RACE4       ATCTCTGAAGGAGATATACATATGAGTAAAGGAGAAGAACTTTTCACTGGAGTTGTCCCA
RACE5       ATCTCTGAAGGAGATATACATATGAGTAAAGGAGAAGAACTTTTCACTGGAGTTGTCCCA
            ************************************************************
```

Figure 3-8. Identification of the transcriptional start of *ndvB* by 5′ RACE.
(A) RNA was extracted from PA14 or PA14/pSC01, and first-strand cDNA synthesis was performed with a *gfp*-specific primer. First-strand cDNA was incubated with dATP without or with TdT (−TdT and +TdT, respectively). The dA-tailed cDNA was subsequently amplified by two rounds of PCR as described in Materials and Methods. The 5′ RACE products were analyzed by electrophoresis on a 1.2% agarose gel. Two 5′ RACE products (major and minor) were obtained. Note that 5′ RACE products were observed only for the reaction that used RNA from PA14/pSC01 and that had been incubated with TdT, demonstrating the specificity of the *gfp* gene-specific primers and the dependence of the obtained the products on the poly(dA) tail added by TdT. NTC, no-template control. (B) Three pUC18 plasmids carrying the major 5′ RACE product (RACE1, -2, and -3) were sequenced using the M13R primer (StemCore Laboratories, Ottawa Hospital Research Institute), and the obtained sequences were aligned to that of pSC01 using Clustal Omega (). Sequence identity is shown by asterisks. The GTCGACTAGTAC$(T)_{17}$ sequence is derived from the 3′ RACE adapter primer. The −10 RpoS element is shown in blue, the TSS is shown in yellow with a +1, and the *gfp*coding sequence is in green. (C) Two pUC18 plasmids carrying the minor 5′ RACE product (RACE4 and -5) were analyzed as described for the major product.

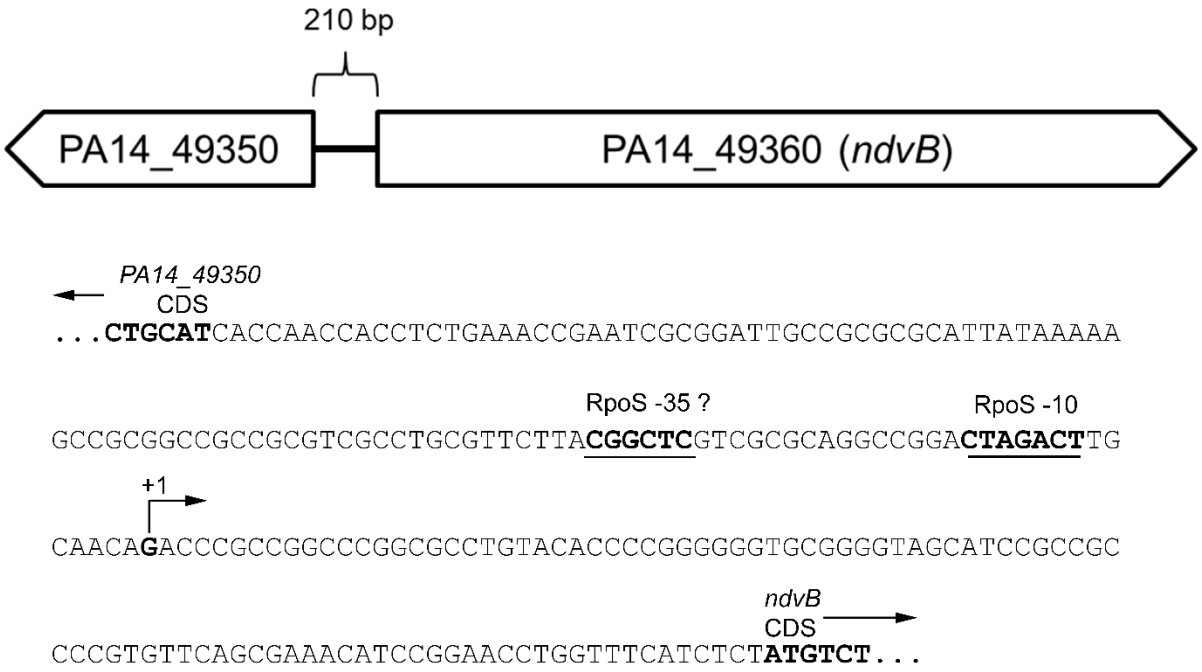

Figure 3-9. The *ndvB* promoter region.
The divergently transcribed PA14_49350 and *ndvB* genes are shown schematically. The sequence of the 210-bp intergenic region between PA14_49350 and *ndvB* is presented below the schematic. Relevant features are annotated on the sequence.

3.6.7 ndvB does not appear to contribute to stationary-phase tolerance to tobramycin

Previous data from our group and others have implicated *ndvB* in biofilm resistance to tobramycin (147–149). Since we discovered in the current study that *ndvB* is additionally expressed in stationary-phase cells, we hypothesized that the Δ*ndvB* mutant would be more susceptible to tobramycin than wildtype PA14 in stationary phase. To address this hypothesis, overnight stationary-phase cultures of the wild type and the Δ*ndvB* mutant were washed and subsequently exposed to various concentrations of tobramycin for 8 h at 37°C (see Materials and Methods). Survival posttreatment was assessed by colony counts. To our surprise, the susceptibility of the Δ*ndvB* mutant did not differ from that of wildtype PA14 for any concentration of tobramycin tested (**Fig 3-10A**).

While NdvB-derived cyclic glucans have traditionally been thought to be located in the periplasm (147), it has been demonstrated that the cyclic glucans produced by NdvB can be released into the growth medium and are a major carbohydrate component of the extracellular matrix in PA14 biofilms (148, 388). The relative contributions of periplasmic and extracellular glucan to tobramycin resistance have not been determined. We hypothesized that a phenotype for the Δ*ndvB* mutant was not observed in our stationary-phase susceptibility assay because extracellular glucan that can interact with tobramycin was being removed during washing of the stationary-phase cells. To address this methodological concern, unwashed overnight, stationary-phase cells were used for the tobramycin susceptibility assay instead of washed cells. Since cyclic glucans can sequester aminoglycosides (147, 148), it was expected that unwashed PA14 would be less susceptible to tobramycin than the unwashed Δ*ndvB* strain. However, no statistically significant difference in susceptibility was observed between wildtype PA14 and the Δ*ndvB* strain under these conditions (data not shown).

3.6.8 RpoS contributes to stationary-phase tolerance to tobramycin

P. aeruginosa rpoS contributes to stationary-phase tolerance to carbapenems and fluoroquinolones (43). To our knowledge, *rpoS* has not been previously implicated in stationary-phase tobramycin tolerance. In fact, work by another group suggests that deletion of *rpoS* in the wildtype PAO1 background does not impact stationary-phase tobramycin tolerance in *P. aeruginosa* (61). To address the role of RpoS in stationary-phase tobramycin tolerance under our conditions, washed overnight cultures of the Δ*rpoS* mutant were exposed to increasing concentrations of tobramycin as described above. Surprisingly, the Δ*rpoS* mutant was found to be more susceptible to tobramycin than the wildtype PA14 strain during stationary-phase (**Fig 3-10A**). For instance, when treated with 200 μg/ml of tobramycin for 8 h, survival of the Δ*rpoS* mutant was approximately 2 $\log_{10}$ units lower than that of the wildtype strain (**Fig 3-10B**). Complementation of the Δ*rpoS* mutant with the pUCP19::*rpoS*$^{+}$ plasmid restored survival of the mutant to wildtype levels when treated with 200 μg/ml of tobramycin (**Fig 3-10C** and **Fig 3-10D**).

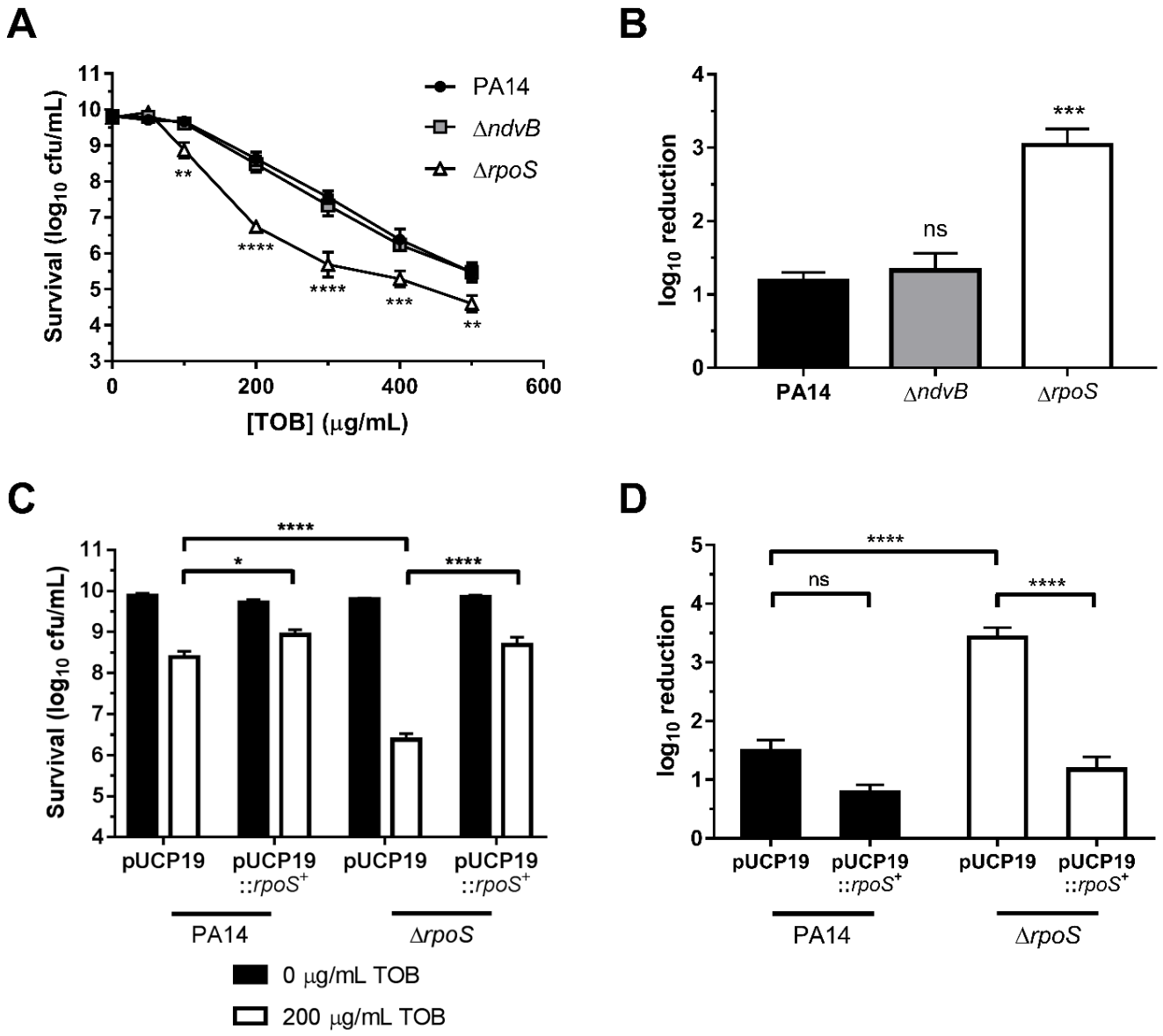
A
Survival (log10 cfu/mL)
[TOB] (μg/mL)
PA14
ΔndvB
ΔrpoS
B
log10 reduction
ns
***
PA14
ΔndvB
ΔrpoS
C
Survival (log10 cfu/mL)
pUCP19
pUCP19 ::rpoS+
PA14
ΔrpoS
0 μg/mL TOB
200 μg/mL TOB
D
log10 reduction
ns
****

Figure 3-10. Concentration-dependent tobramycin killing of washed stationary-phase cells. (A) Washed stationary-phase cultures of wildtype PA14 and Δ*ndvB* and Δ*rpoS* strains were exposed to various tobramycin (TOB) concentrations (0 to 500 μg/ml) for 8 h at 37°C. Cell survival following antibiotic treatment was assessed by colony counts using the drop plate method. Data are presented as means ± SEMs for three independent experiments. In some cases, error bars are smaller than the symbols. Statistical significance was determined by two-way ANOVA with Dunnett's *post hoc* multiple-comparison test for each concentration of tobramycin (PA14 was used as the comparison control). (B) Log_{10} reduction of PA14, Δ*ndvB*, and Δ*rpoS* stationary-phase cells exposed to 200 μg/ml of tobramycin (calculated as the difference between survival at 0 μg/ml and survival at 200 μg/ml from panel A). Data are means + SEMs for three experiments. Statistical significance was determined by one-way ANOVA with Dunnett's multiple-comparison test (PA14 was used as the comparison control). (C) Washed stationary-phase PA14 or Δ*rpoS* cells carrying pUCP19 or pUCP19::$rpoS^+$ were exposed to 0 or 200 μg/ml of tobramycin. Data are means + SEMs for four independent experiments. Statistical significance was determined by two-way ANOVA with Tukey's multiple-comparison test. (D) Log_{10} reduction of PA14 and Δ*rpoS* strains carrying pUCP19 or pUCP19::$rpoS^+$ when exposed to 200 μg/ml of tobramycin (calculated as the difference between survival at 0 μg/ml and survival at 200 μg/ml from panel C). Data are means + SEMs for four experiments. Statistical significance was determined by one-way ANOVA with Tukey's multiple-comparison test.

3.7 Discussion

The ability of bacteria to survive antibiotic exposure depends, to a large extent, on their intrinsic resistance functions. Thus, understanding the requirements for expression of intrinsic resistance functions can provide insights for the development of therapies aimed at weakening bacterial defenses. In this study, we investigate the environmental and genetic regulation of *ndvB*, a gene that contributes to antibiotic tolerance in *P. aeruginosa* biofilms. We developed a fluorescent transcriptional reporter to examine the expression of *ndvB* in cells at different growth phases. The use of an unstable variant of GFP was necessary to accurately represent the downregulation of *ndvB* transcription that occurs during planktonic growth and upregulation in biofilms, described previously by our group (147, 149).

A novel finding of this study was that *ndvB* is also upregulated in stationary-phase cells. We subsequently demonstrated that induction of *ndvB* in stationary-phase planktonic cells and in biofilms depends on the stationary-phase sigma factor RpoS. This report provides indirect, but compelling, evidence that RpoS binds directly to the *ndvB* promoter to induce *ndvB* transcription. Mature biofilms and stationary-phase planktonic cultures are thought to exhibit similar physiological states, characterized by high cell density, nutrient depletion, and buildup of waste products (389). Likewise, protein levels of RpoS have been shown to be similar between stationary-phase and biofilm cells (35), although the distribution of *rpoS* transcripts is heterogeneous among different biofilm subpopulations (36, 124, 128). This similarity is supported by global transcriptome comparisons between planktonic and biofilm cultures of *P. aeruginosa*, which indicate that gene expression profiles of stationary-phase planktonic cultures are more similar to those of mature biofilms than exponential-phase planktonic cultures (130–132, 178). It has been traditionally thought that biofilm cells existing in a stationary-phase-like state are slow

growing (169, 171, 174) and that the reduction in growth rate is, at least partially, responsible for the reduced antibiotic susceptibility of biofilm cells relative to that of rapidly growing, exponential-phase cells. Our data suggest that a stationary-phase-like state also contributes to biofilm recalcitrance through the RpoS-mediated expression of *ndvB* and, potentially, of other resistance and/or tolerance determinants. Interestingly, the *psl* locus, which encodes the biosynthetic enzymes necessary for Psl polysaccharide synthesis, has also been shown to be regulated by RpoS (42). Psl plays an important structural role in the biofilm matrix of some *P. aeruginosa* strains, and it has a proposed role in biofilm antibiotic resistance (390).

The contribution of *ndvB* to biofilm resistance to tobramycin has been well documented (147–149). It was, therefore, surprising that *ndvB* did not contribute to tobramycin tolerance in stationary-phase cells given that we have demonstrated in this report that *ndvB* is also expressed in stationary phase. Differing levels of cyclic glucan in stationary-phase and biofilm cells could account for this result. For instance, Sadovskaya et al. (148) compared relative cyclic glucan contents of planktonic and biofilm PA14 cells. The biofilms were grown in M63 (with Casamino Acids) statically at 30°C for 64 h, while the planktonic cultures were grown under the exact same conditions except with shaking. Given the extended incubation time, the planktonic cultures were presumably in stationary phase. The glucan content per gram of cells was 50% higher in biofilms than in the planktonic cells. Therefore, absolute differences in cyclic glucan content between biofilms and stationary-phase cells may explain the importance of these molecules for biofilm, but not stationary-phase, resistance to tobramycin. Indeed, the enzymatic activity of some NdvB homologues is regulated posttranslationally in other bacterial species (155, 391), but whether or how NdvB protein activity is regulated in *P. aeruginosa* and if this regulation is different in stationary-phase and biofilm cells constitute an open area for investigation. Furthermore, it is

relevant to note that while biofilm communities are grossly stationary-phase-like, biofilms consist of heterogeneous subpopulations of cells that experience different environments (37, 392). In contrast, stationary-phase cells experience a relatively homogenous environment due to mixing of the liquid culture. It is possible that cyclic glucans protect a specific biofilm subpopulation that is not represented in stationary-phase cultures. Further work will be required to better pinpoint where cyclic glucans are present within biofilms and what cells are protected from antibiotic treatment by the glucans.

In *P. aeruginosa*, RpoS has been implicated in protection against a variety of stressors, including hyperosmolar or acidic growth conditions, exposure to hydrogen peroxide or ethanol, carbon starvation when grown in minimal media with glucose, and heat shock (41, 46). Interestingly, a role for RpoS in mediating antibiotic tolerance of stationary-phase cells to ofloxacin, biapenem, and imipenem has been demonstrated using time- and concentration-dependent killing assays (43). While a recent report indicated that deletion of *rpoS* in the wildtype PAO1 background does not impact stationary-phase tobramycin tolerance (61), our results suggest that *rpoS* does play a role in stationary-phase tolerance of PA14 to tobramycin. The discrepancy in results may be due to strain differences or variations in the experimental methods. Highlighting the potential impact of differences in experimental approach, Viducic et al. (61) observed significant killing of PAO1 after 8 h of incubation with 32 μg/ml of tobramycin, while we observed no killing of PA14 after 8 h of incubation with 50 μg/ml of tobramycin. Our stationary-phase cultures were also at a higher density (approximately 5×10^9 CFU/ml) than in the study by Viducic et al. (1×10^8 CFU/ml), which might contribute to the differences in results since stationary-phase cell density is known to affect antibiotic susceptibility (384). Overall, the contribution of RpoS to

stationary-phase tobramycin tolerance appears to be highly dependent on the experimental conditions.

While not addressed in this paper due to the focus on stationary-phase cells, the contribution of RpoS to antimicrobial resistance or tolerance in *P. aeruginosa* biofilms has been somewhat controversial. While biofilms formed by an *rpoS* mutant have been described as thicker and more resistant to tobramycin than wildtype biofilms (129, 393), Stewart et al. (45) demonstrated that RpoS did not play a role in biofilm tolerance to tobramycin. RpoS did, however, contribute to ciprofloxacin tolerance in *P. aeruginosa* biofilms (45). Somewhat paradoxically, we have demonstrated that RpoS regulates the expression of a known mechanism of aminoglycoside resistance in biofilms (147). These findings can be reconciled by the fact that RpoS is a pleiotropic regulator with many target genes that may have opposing effects on antimicrobial susceptibility.

ndvB was initially described as a biofilm-specific antibiotic resistance gene due to its *in vitro* phenotype when comparing exponential-phase planktonic cells and biofilms (147). By more precisely mapping the activity of the *ndvB* promoter, we have refined our understanding of the expression pattern of this gene. Determining that *ndvB* expression is induced in both stationary-phase planktonic cultures and biofilm cells allowed us to identify RpoS as the sigma factor responsible for *ndvB* promoter activity. Thus, *ndvB* can be situated within a broader response to stresses encountered by stationary-phase and biofilm cells.

3.8 Acknowledgments

We thank Robert Shanks (University of Pittsburgh) for providing the yeast shuttle vector and for assistance in the design of the reporter fusion. We also thank Alexandre Poulain (University of Ottawa) for the use of the plate reader and members of Kristin Baetz's laboratory (University of Ottawa) for the yeast strain, reagents, and technical assistance. We thank Antonius T. M. Van Kessel for assistance with the Miller assays.

This research was supported by grants to T.-F.M. from Natural Sciences and Engineering Research Council of Canada and Cystic Fibrosis Canada. C.W.H. was supported by a Vanier Canada Graduate Scholarship.

T.-F.M., A.J.H., C.W.H., and L.Z. designed the experiments, A.J.H., C.W.H., L.G., L.Z., J.-P.N., S.C., and B.S. performed the experiments, and T.-F.M., A.J.H., and C.W.H. wrote the manuscript.

Chapter 4: Potentiation of aminoglycoside lethality by C_4-dicarboxylates requires RpoN in antibiotic tolerant *Pseudomonas aeruginosa*

4.1 Preface

This chapter has been submitted as a research article to *Antimicrobial Agents and Chemotherapy*:

> **Hall CW**, Farkas E, Zhang L, and Mah T-F. 2019. Potentiation of aminoglycoside lethality by C_4-dicarboxylates requires RpoN in antibiotic tolerant *Pseudomonas aeruginosa*. *Antimicrobial Agents and Chemotherapy* AAC01313-19, minor revisions.

Specific contributions of each author are listed below:

Clayton W. Hall – conceptualized project, designed all experiments, performed all experiments for data presented in **Figures 4-1**, **4-2**, **4-3**, **4-4**, **4-5**, **S4-2**, **S4-3**, **S4-4**, **S4-5**, **S4-6**, constructed **Figure 4-6**, wrote original draft of manuscript, wrote Ontario Lung Association Grant-in-Aid for funding (awarded).

Eszter Farkas – performed experiments for **Figure S4-1** and some replicates for **Figure 4-1d**, reviewed manuscript.

Li Zhang – performed experiments for **Table S4-3** and worked with CWH to obtain data for **Figure 4-1h** and **Figure S4-6**, reviewed manuscript.

Thien-Fah Mah – provided equipment and research materials, provided funding, supervised research, edited and reviewed manuscript, reviewed Ontario Lung Associate Grant-in-Aid (awarded)

4.2 Abstract

Antibiotic tolerance contributes to the inability of standard antimicrobial therapies to clear the chronic *Pseudomonas aeruginosa* lung infections that often afflict patients with cystic fibrosis (CF). Metabolic potentiation of bactericidal antibiotics with carbon sources has emerged as a promising strategy to re-sensitise tolerant bacteria to antibiotic killing. Fumarate (FUM), a C_4-dicarboxylate, has been recently shown to re-sensitise tolerant *P. aeruginosa* to killing by tobramycin (TOB), an aminoglycoside antibiotic, when used in combination (TOB+FUM). Fumarate and other C_4-dicarboxylates are taken up intracellularly by transporters regulated by the alternative sigma factor, RpoN. Once in the cell, FUM is metabolised, leading to enhanced electron transport chain activity, regeneration of the proton motive force, and increased TOB uptake. In this work, we demonstrate that a Δ*rpoN* mutant displays impaired FUM uptake and, consequently, non-susceptibility to TOB+FUM treatment. RpoN was also found to be essential for susceptibility to other aminoglycoside and C_4-dicarboxylate combinations. Importantly, RpoN loss-of-function mutations have been documented to evolve in the CF lung, and these loss-of-function alleles can also result in TOB+FUM non-susceptibility. Our findings raise the question of whether TOB+FUM will be a suitable treatment option in the future for CF patients infected with *P. aeruginosa* isolates that lack RpoN function.

4.3 Introduction

Pseudomonas aeruginosa is an important pathogen in patients with cystic fibrosis (CF), and chronic *P. aeruginosa* lung infection is a significant contributor to morbidity and mortality (252, 394). Treatment with antibiotics such as the aminoglycoside tobramycin (TOB) can control, but not eradicate, chronic *P. aeruginosa* infections (94, 276). There is, therefore, an urgent need

to identify novel treatment strategies that would improve antibiotic efficacy in treating chronic *P. aeruginosa* lung infections.

The failure of antibiotics like TOB to clear *P. aeruginosa* can be attributed to a combination of genetic determinants and environmental factors (1, 9, 92). Environmental conditions, such as nutrient limitation, can trigger changes in bacterial physiology that confer phenotypic antibiotic tolerance, which is defined as the survival of bacteria in the presence of a concentration of bactericidal antibiotic that would be otherwise lethal (87). Antibiotic tolerance is reversible once the environmental conditions that promoted the tolerant phenotype have changed. For instance, growth arrest and metabolic dormancy triggered by high bacterial density and low nutrient availability (conditions experienced by cells in stationary phase cultures, biofilms, and the multicellular aggregates observed in the CF lung) contribute to tolerance to TOB and many other antibiotics (45, 140, 164, 169, 175, 176, 179, 180, 395).

Nutrient limitation and the ensuing starvation response can promote tolerance to TOB by reducing TOB entry into the cell. Aminoglycoside uptake into bacteria is energy-dependent and requires a threshold membrane potential (95, 186, 396). Cells that are metabolically quiescent have a decreased proton motive force (PMF) compared to actively growing cells and, therefore, TOB entry is significantly reduced in cells that are starved (185). Thus, nutrient supplementation combined with TOB is a logical strategy to regenerate PMF, promote TOB uptake, and re-sensitise the cells to TOB. Indeed, the addition of various metabolites to starved, tolerant cells in order to promote aminoglycoside uptake and killing has been successfully employed by other groups (185, 188, 189, 397–402). For instance, Meylan *et al* showed that fumarate (FUM), a C_4-dicarboxylate, can sensitise starved, phenotypically tolerant *P. aeruginosa* cells to TOB killing (185).

P. aeruginosa uses two transporters, DctA and DctPQM, to take up C_4-dicarboxylates into the cell (66). Control over *dctA* and *dctPQM* transcription involves multiple players, including the alternative sigma factor RpoN (66, 78). Consequently, RpoN is required for growth on C_4-dicarboxylates (66). Although RpoN is an important regulator of genes involved in metabolism and virulence (22, 24), several studies have reported the that loss of RpoN function is, somewhat paradoxically, a relatively common mechanism of pathoadaptation to the CF lung (288, 289, 296, 403). Smith *et al* found that almost 20% of patients in their study had isolates with non-synonymous or frameshift mutations in *rpoN* (296).

Given the critical role of RpoN in promoting expression of FUM transporters, we hypothesised that *P. aeruginosa* lacking RpoN function would be non-susceptible to TOB and FUM combination treatment (TOB+FUM). We found that loss of RpoN function, either through gene deletion or clinically-observed loss-of-function point mutations, renders *P. aeruginosa* non-susceptible to TOB+FUM due to a lack of FUM uptake. This finding raises concerns about whether TOB+FUM will be effective as a future treatment modality for CF patients infected with *P. aeruginosa* RpoN loss-of-function mutants.

4.4 Materials and methods

4.4.1 Bacterial strains and growth conditions

Bacterial strains and plasmids are listed in **Table S4-1**. Primers used in this study are listed in **Table S4-2**. Our laboratory's wildtype UCBPP-PA14 (PA14) strain and the isogenic Δ*rpoN* mutant were routinely cultured aerobically in LB broth Miller (Bio Basic) supplemented with 2 mM L-glutamine (Bio Basic). M9 medium was prepared as a 5x stock (33.9 g/L Na_2HPO_4, 15 g/L KH_2PO_4, 2.5 g/L NaCl, 5 g/L NH_4Cl). 1x M9 was sterilised by autoclaving and supplemented with 2 mM $MgSO_4$ and 0.1 mM $CaCl_2$. When needed, media were solidified with 1.5% agar (Bio

Basic). Plasmids were constructed using standard molecular cloning techniques and mobilised into *Escherichia coli* DH5α or S17-1 by $CaCl_2$ chemical transformation. Plasmids were introduced into *P. aeruginosa* strains by conjugation with *E. coli* S17-1. When required for selection or plasmid maintenance, antibiotics were used at the following concentrations: 100 µg/mL ampicillin (AMP), 20 µg/mL gentamicin (GEN), and 20 µg/mL nalidixic acid (NAL) for *E. coli*; 200 µg/mL carbenicillin (CAR), 50 µg/mL GEN, and 100 µg/mL tetracycline (TET) for *P. aeruginosa*.

Table S4-1. Bacterial strains and plasmids

Name	Genotype or description	Reference
Strains		
PA14	Wildtype *P. aeruginosa*; burn wound isolate	(327)
Δ*rpoN*	Unmarked deletion of *rpoN* in PA14	This study
PA14-*lacZ*	PA14 with chromosomal *lacZ* and TET^R markers	(404)
DH5α	*E. coli* strain; *supE44* Δ*lacU169*(φ80 *lacZ*ΔM15) *recA1 hsdR17 thi-1 relA1*	Invitrogen
S17-1	*E. coli* strain; *recA pro hsdR* RP42Tc::Mu-Km::Tn7	(326)
Plasmids		
pEX18Gm	Allelic exchange suicide vector; *sacB*, GEN^R	(323)
pEX18Gm::Δ*rpoN*	pEX18Gm derivative for unmarked deletion of *rpoN*; GEN^R	This study
pMQ70	Expression plasmid with arabinose-inducible P_{BAD} promoter; CAR^R	(325)
pMQ70::*rpoN*	pMQ70 carrying *rpoN* from wildtype PA14; CAR^R	This study
pMQ70::$rpoN^{L343S}$	pMQ70 carrying PA14 *rpoN* with engineered L343S mutation; CAR^R	This study
pMQ70::$rpoN^{L419P}$	pMQ70 carrying PA14 *rpoN* with engineered L419P mutation; CAR^R	This study
pMQ70::$rpoN^{A449V}$	pMQ70 carrying PA14 *rpoN* with engineered A449V mutation; CAR^R	This study
pMQ70::*dctA*	pMQ70 carrying *dctA* from wildtype PA14; CAR^R	This study

Table S4-2. Oligonucleotides

Name	Sequence (5'→3')[a]	Purpose
*rpoN*delUF	TCAG**aagctt**GCCGAAATTCATCCTCCTCGA	pEX18Gm::Δ*rpoN* construction
*rpoN*delUR	TCAG**ctgcag**GGCTGAGGGCTTAGTACCTTATTCG	pEX18Gm::Δ*rpoN* construction
*rpoN*delDF	TCAG**ctgcag**TGACTGACTGACGTTGATCCACGCCAAGGT	pEX18Gm::Δ*rpoN* construction
*rpoN*delDR	TCAG**ggatcc**TTGTTCGAGTACGCGTTTCTTGCT	pEX18Gm::Δ*rpoN* construction
*rpoN*DxF	GAATTCCACATCCACCAC	Δ*rpoN* confirmation
*rpoN*DxR	GGCGATGCCATTGCCGAA	Δ*rpoN* confirmation
pMQ*rpoN*F	CATCAT**gagctc**gaaggagatatacatATGAAACCATCGCTAGTC	pMQ70::*rpoN* construction
pMQ*rpoN*R	CATCAT**aagctt**TCACACCAGTCGCTTGCGCTC	pMQ70::*rpoN* construction
L343S_F	CAACCAGT**C**GCAGGAAGC	pMQ70::*rpoN*^{L343S} construction
L343S_R	GCTTCCTGC**G**ACTGGTTG	pMQ70::*rpoN*^{L343S} construction
L419P_F	GGCATTTTCGAGC**C**GAAATATTTC	pMQ70::*rpoN*^{L419P} construction
L419P_R	GAAATATTTC**G**GCTCGAAAATGCC	pMQ70::*rpoN*^{L419P} construction
A449V_F	CTGGTGG**T**CGCGGAAAATGC	pMQ70::*rpoN*^{A449V} construction
A449V_R	GCATTTTCCGCG**A**CCACCAG	pMQ70::*rpoN*^{A449V} construction
pMQ*dctA*F	CATCAT**gagctc**gaaggagatatacatATGACCAAACAACCCTTC	pMQ70::*dctA* construction

pMQ*dctA*R	CATCAT**aagctt**CGAACAGGTTTGAGCTTAGAC	pMQ70::*dctA* construction
pMQseqF	GGACCAAAGCCATGACAAAA	pMQ70 derivative sequencing
pMQseqR	TTAATCTGTATCAGGCTG	pMQ70 derivative sequencing

[a] Restriction sites are bolded and in lowercase. Engineered ribosomal binding sites are underlined and in lowercase. Engineered point mutations are bolded and underlined.

4.4.2 Construction of the ΔrpoN mutant

Deletion of *rpoN* in PA14 was achieved using two-step allelic exchange (324). Briefly, regions upstream and downstream of the *rpoN* coding region were amplified by PCR using the *rpoN*delUF/*rpoN*delUR and *rpoN*delDF/*rpoN*delDR primer pairs. Fragments were cloned into pEX18Gm using standard molecular cloning techniques to create pEX18Gm::Δ*rpoN*. pEX18Gm::Δ*rpoN* was mobilised into *P. aeruginosa* by conjugation with *E. coli* S17-1 and plating onto LB agar supplemented with 2 mM L-glutamine, 50 µg/mL GEN, and 20 µg/mL NAL. GEN-resistant colonies were counter-selected on no salt LB agar plates supplemented with 10% sucrose (Wisent) and 2 mM L-glutamine. Sucrose-resistant, GEN-susceptible colonies were screened by PCR for the Δ*rpoN* allele with the *rpoN*DxF/*rpoN*DxR primer pair. We further confirmed that our Δ*rpoN* mutant had decreased pyocyanin production compared to wildtype PA14 and was unable to swim and to twitch (data not shown) since loss of *rpoN* has been previously reported to lead to these phenotypes (64, 65).

4.4.3 Construction of pMQ70 derivatives

The coding regions of *rpoN* and *dctA* were amplified by PCR from PA14 genomic DNA using primers pMQ*rpoN*F/pMQ*rpoN*R and pMQ*dctA*F/pMQ*dctA*R respectively. An engineered ribosomal binding site was included in the forward primers upstream of the start codon. Point mutations were introduced into *rpoN* by splicing-by-overlap-extension PCR with complementary primers carrying the desired mutation. Briefly, upstream fragments were amplified using pMQ*rpoN*F with L343S_R, L419P_R, or A449V_R and downstream fragments were amplified using pMQ*rpoN*R with L343S_F, L419P_F, or A449V_F. Upstream and downstream fragments were then used as templates for a second PCR reaction with the pMQ*rpoN*F/pMQ*rpoN*R primer set in order to splice the fragments. Amplified genes were cloned downstream of the arabinose-

inducible P_{BAD} promoter in *Sac*I/*Hind*III-digested pMQ70. Plasmids were sequenced using pMQseqF and pMQseqR (StemCore Laboratories, Ottawa Hospital Research Institute). Sequence-verified plasmids were mobilised into *P. aeruginosa* strains by conjugation with *E. coli* S17-1, and transconjugants were selected on LB agar supplemented with 2 mM L-glutamine, 200 µg/mL CAR, and 20 µg/mL NAL.

4.4.4 Minimum inhibitory concentration (MIC) assays

MIC assays were performed in LB with 2 mM L-glutamine using the macrobroth or the microbroth dilution methods as outlined in guideline M07-A10 from the Clinical and Laboratory Standards Institute (CLSI, Wayne, PA, USA). Assays were incubated statically at 37°C for 16-18 h. The MIC was interpreted as the lowest concentration of antibiotic that prevented visible growth.

4.4.5 Stationary phase killing assay

The killing assay for stationary phase cells was adapted from previously published protocols (185, 189). Briefly, 50 mL of LB supplemented with 2 mM L-glutamine in a 250 mL Erlenmeyer flask was inoculated 1:10,000 with overnight stationary phase cultures. 150 µg/mL CAR was added as necessary for maintenance of pMQ70 derivatives. Cultures were grown aerobically to stationary phase at 37°C and 225 rpm for 16-18 h. If bacteria carried pMQ70 derivatives, P_{BAD} activity was induced in the stationary phase cultures by adding L-(+)-arabinose (Sigma) to a final concentration of 0.2% and incubating at 37°C and 225 rpm for an additional 2 h. Stationary phase cells were harvested by centrifugation, washed in 10 mL phosphate buffered saline (PBS) (pH 7.4), and then resuspended in one volume of M9 medium. Cells were aliquoted into separate glass culture tubes. When indicated, 50 µM carbonyl cyanide *m*-chlorophenyl hydrazone (CCCP) (Sigma) was added to the cells 15 mins prior to addition of antibiotics and carbon sources. CCCP was prepared as a 10 mM stock in DMSO. Aminoglycoside antibiotics

and carbon sources (concentration normalised to 60 mM total carbon unless indicated otherwise) were added to the cells, and the cells were incubated at 37°C and 225 rpm. Tobramycin sulfate (Research Products International), gentamicin sulfate salt (Sigma), and amikacin hydrate (Sigma) were prepared as 10 mg/mL stocks in sterile water. Sodium fumarate dibasic (Sigma), sodium succinate dibasic (Sigma), L-arginine monohydrochloride (Sigma), and D-glucose (Fisher Scientific) were prepared as sterile 1 M stocks in water and used at the indicated concentrations. Following treatment (4 h unless otherwise indicated), aliquots of cells were washed in PBS. Cell survival was assessed by serial microdilution in PBS and drop-plating onto LB agar plates supplemented with 2 mM L-glutamine. 100 µg/mL TET and/or 40 µg/mL 5-bromo-4-chloro-3-indolyl-β-D-galactoside (X-gal) were added to plates when necessary to differentiate PA14-*lacZ* and Δ*rpoN* colonies. Plates were incubated for 18 h at 37°C prior to colony counting, and survival for each strain under the different treatment conditions was expressed as $\log_{10}$ cfu/mL.

4.4.6 Colony biofilm killing assay

The colony biofilm assay was performed as described previously (185, 189). Briefly, UV-sterilised 0.2 µm polycarbonate membrane discs (GVS Life Sciences) were placed on LB agar plates supplemented with 2 mM L-glutamine and inoculated with $5x10^5$ cfu from overnight PA14 or Δ*rpoN* cultures. Biofilms were incubated at 37°C for 4 h prior to being transferred to M9 plates with or without 16 µg/mL TOB and/or 15 mM FUM for an additional 20 h. Biofilms were homogenised in PBS by vortexing. Survival was assessed by serial microdilution and drop plating of the dilutions onto LB agar plates supplemented with 2 mM L-glutamine. Plates were incubated for 18 h at 37°C prior to colony counting, and survival for each strain under the different treatment conditions was expressed as $\log_{10}$ cfu/biofilm.

4.4.7 Extracellular FUM quantification

Stationary phase cells were prepared in M9 medium as for the killing assay. Cells were treated with 15 mM FUM for 0 h or 4 h, after which supernatants were collected and filter-sterilised. The concentration of FUM in the supernatants was determined using the colorimetric Fumarate Assay Kit (Sigma) exactly as described by the manufacturer.

4.4.8 Respiration assay

Stationary phase cells were prepared in M9 medium as for the killing assay. Resazurin sodium salt (Sigma) was prepared as a sterile 1 mg/mL stock in water and was added to a final concentration of 0.1 mg/mL followed by 0 or 15 mM FUM. When indicated, 0.1% sodium azide (NaN_3) was also added. Cells were aliquoted into a 96-well plate, and the plate was incubated with shaking at 37°C in a Synergy HT multi-mode plate reader (Biotek). Resazurin reduction to resorufin was measured by fluorescence (Ex/Em: 550/590 nm, gain 55).

4.4.9 TOB accumulation assay

Intracellular TOB accumulation was indirectly assayed using a modified version of a previously described qualitative microbiological assay (153). Stationary phase cells were prepared as for the TOB+FUM killing assay in M9 medium and subsequently treated for 1 h with 64 µg/mL TOB or 64 µg/mL TOB and 15 mM FUM. After treatment, 1 mL of cells was washed once in PBS to remove extracellular antibiotic and cells were subsequently lysed for 1 h at room temperature in 100 µL of 0.1 M glycine (pH 3.0). The lysate was dried using a nitrogen evaporator (Organomation). The dried lysate was resuspended in 50 µL of sterile water. LB agar plates were freshly inoculated with a lawn of *E. coli* DH5α, and wells were punched into the agar. The lysate was added to wells. The plates were incubated at 37°C for 16 hours after which the diameter of the zone of *E. coli* DH5α growth inhibition was measured. A larger zone of growth inhibition was

interpreted as being due to an increased amount of tobramycin present in the *P. aeruginosa* cell lysate.

4.4.10 Statistical analysis

All graphs and statistical analyses were performed using GraphPad Prism 7 software. Unless otherwise stated, two-way ANOVA was performed with either Tukey's or Sidak's multiple comparisons test. The level of statistical significance is presented for relevant comparisons using the following symbols: ns (not significant), $p>0.05$; *, $p\leq0.05$; **, $p\leq0.01$; ***, $p\leq0.001$; ****, $p\leq0.0001$.

4.5 Results

4.5.1 FUM-mediated potentiation of TOB lethality is RpoN-dependent

Survival of PA14 wildtype and Δ*rpoN* stationary phase cells was determined following incubation for 4 h with or without various concentrations of TOB and/or 15 mM FUM (**Fig 4-1a**), for 4 h with or without 64 µg/mL TOB and various concentrations of FUM (**Fig 4-1b**) and for various amounts of time with or without 64 µg/mL TOB and/or 15 mM FUM (**Fig 4-1c**). In the TOB concentration ([TOB])-dependent, FUM concentration ([FUM])-dependent, and time-dependent killing assays, both wildtype and Δ*rpoN* were tolerant to TOB in the absence of FUM. Moreover, FUM alone did not cause cell death or significant growth. Wildtype cells were significantly more susceptible to TOB+FUM than TOB alone as previously described (185, 189); however, Δ*rpoN* cells remained tolerant to TOB even in the presence of FUM under all [TOB], [FUM], and incubation times tested. Introduction of the complementation vector pMQ70::*rpoN* restored susceptibility of Δ*rpoN* stationary phase cells to TOB+FUM (64 µg/mL TOB, 15 mM FUM, 4 h) (**Fig 4-1d**). RpoN was also required for stationary phase susceptibility to TOB with succinate (SUC) (**Fig S4-1a**), another C_4-dicarboxylate, and to FUM combined with the aminoglycoside antibiotics gentamicin (GEN) (**Fig S4-1b**) or amikacin (AMK) (**Fig S4-1c**). Therefore, the results suggest that RpoN is generally important for potentiation of aminoglycoside lethality by C_4-dicarboxylates in antibiotic tolerant *P. aeruginosa* stationary phase cells. To ensure that RpoN was important for TOB+FUM susceptibility in another model of antibiotic tolerance, we assessed TOB+FUM susceptibility of wildtype and Δ*rpoN* colony biofilms. While TOB+FUM killed wildtype biofilms to a much greater extent than TOB alone, there was no significant difference in survival of Δ*rpoN* biofilms following TOB monotherapy or TOB+FUM combination treatment (**Fig S4-2**).

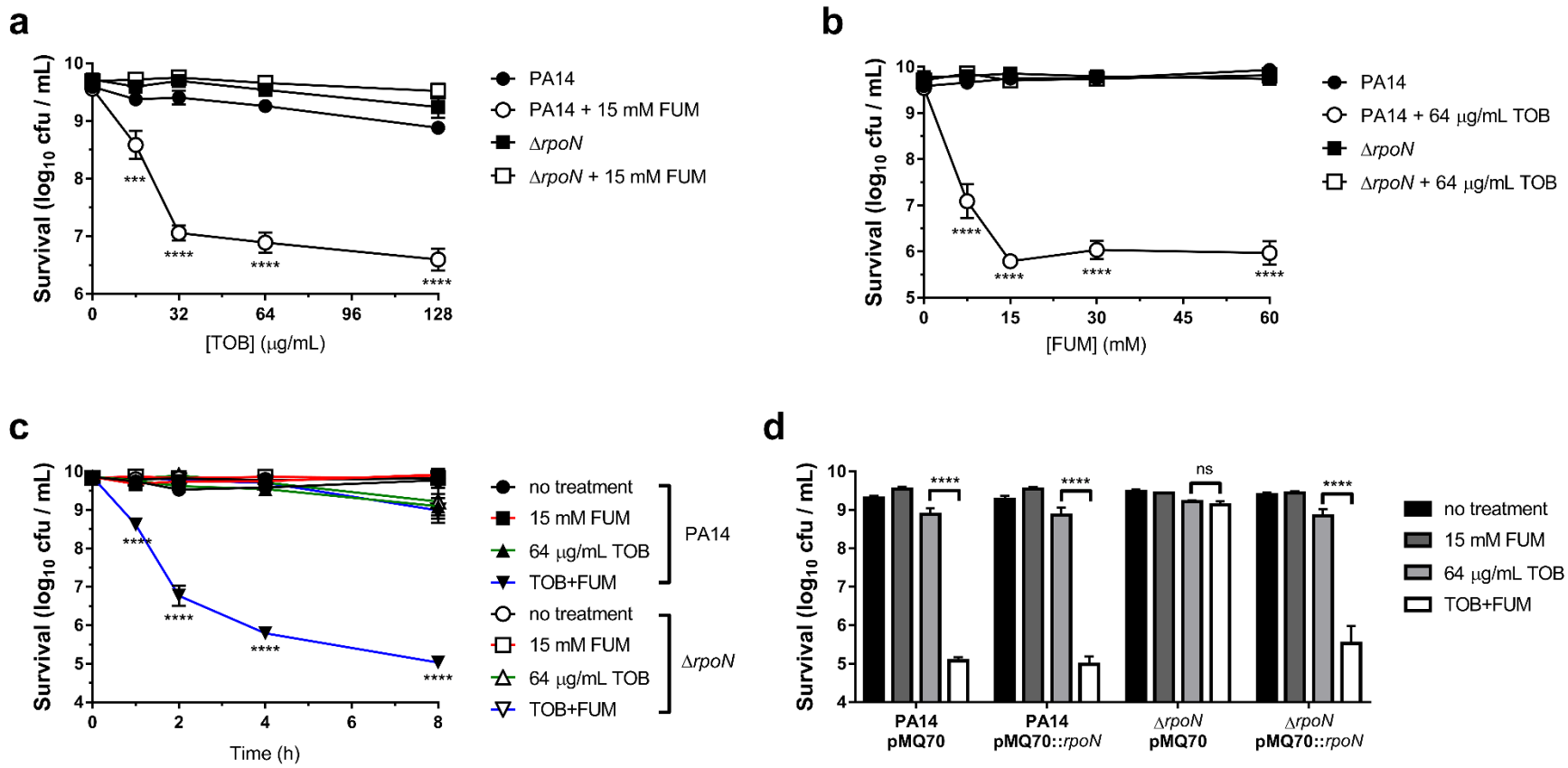
a
Survival (log10 cfu / mL)
[TOB] (μg/mL)
PA14
PA14 + 15 mM FUM
ΔrpoN
ΔrpoN + 15 mM FUM
b
Survival (log10 cfu / mL)
[FUM] (mM)
PA14
PA14 + 64 μg/mL TOB
ΔrpoN
ΔrpoN + 64 μg/mL TOB
c
Survival (log10 cfu / mL)
Time (h)
no treatment
15 mM FUM
64 μg/mL TOB
TOB+FUM
PA14
ΔrpoN
d
Survival (log10 cfu / mL)
ns
PA14 pMQ70
PA14 pMQ70::rpoN
ΔrpoN pMQ70
ΔrpoN pMQ70::rpoN
no treatment
15 mM FUM
64 μg/mL TOB
TOB+FUM

Figure 4-1. Stationary phase Δ*rpoN* cells are not susceptible to TOB+FUM treatment.
(a) Survival of PA14 wildtype and Δ*rpoN* stationary phase cells that were incubated for 4 h with or without various concentrations of TOB and/or 15 mM FUM. (b) Survival of PA14 wildtype and Δ*rpoN* stationary phase cells that were incubated for 4 h with or without 64 µg/mL TOB and/or various concentrations of FUM. (c) Survival of PA14 wildtype and Δ*rpoN* stationary phase cells that were incubated for various periods of time with or without 64 µg/mL TOB and/or 15 mM FUM. (d) Survival of PA14 wildtype and Δ*rpoN* stationary phase cells carrying pMQ70 or pMQ70::*rpoN* following incubation for 4 h with or without 64 µg/mL TOB and/or 15 mM FUM. Data in (a-d) are presented as mean log10 cfu/mL ± SEM for at least three biological replicates.

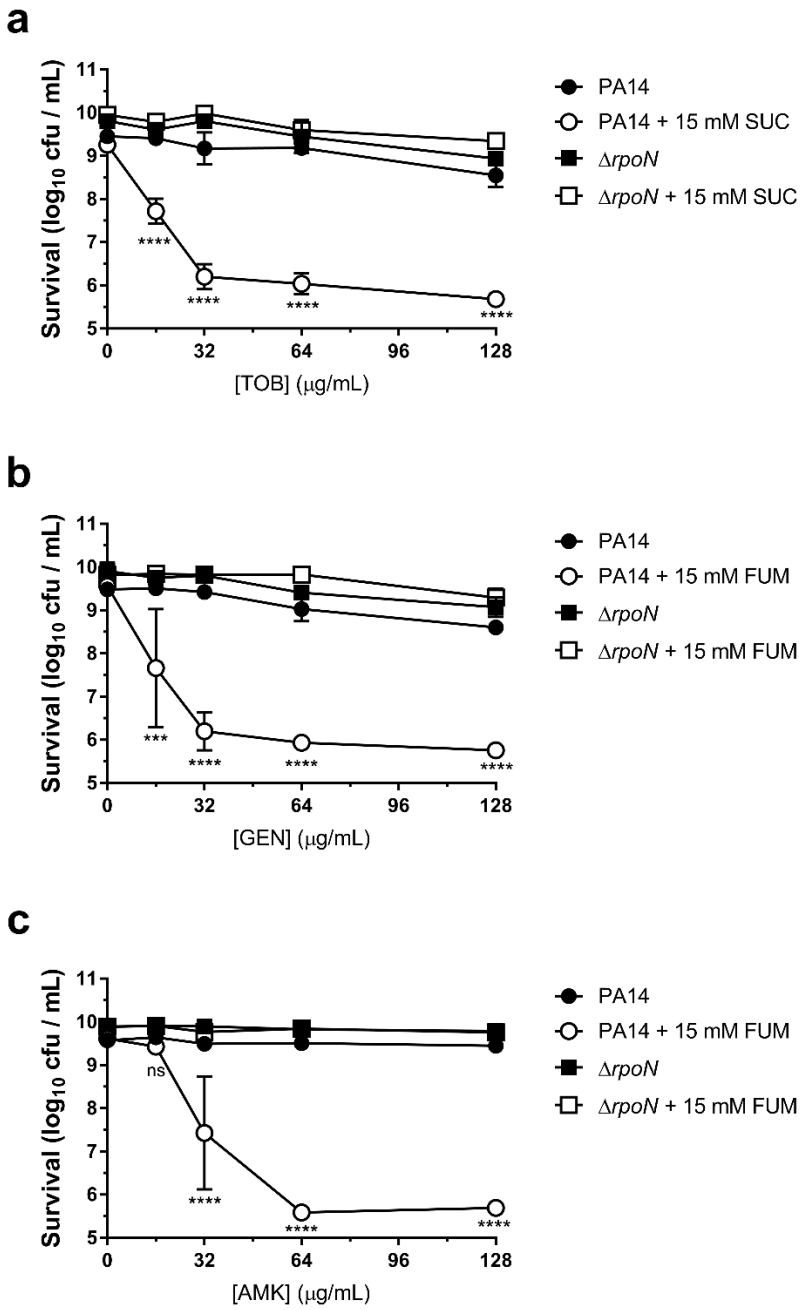

Figure S4-1. RpoN is required for stationary phase susceptibility to aminoglycosides combined with C_4-dicarboxylates.

Survival of PA14 wildtype and Δ*rpoN* stationary phase cells that were incubated for 4 h with no treatment, various concentrations of aminoglycoside (tobramycin, TOB; gentamicin, GEN; amikacin, AMK), 15 mM C_4-dicarboxylate (fumarate, FUM; succinate, SUC), or aminoglycoside with C_4-dicarboxylate. The tested aminoglycoside and C_4-dicarboxylate combinations were (a) TOB+SUC, (b) GEN+FUM, and (c) AMK+FUM. Data are presented as mean log10 cfu/mL ± SEM for three biological replicates.

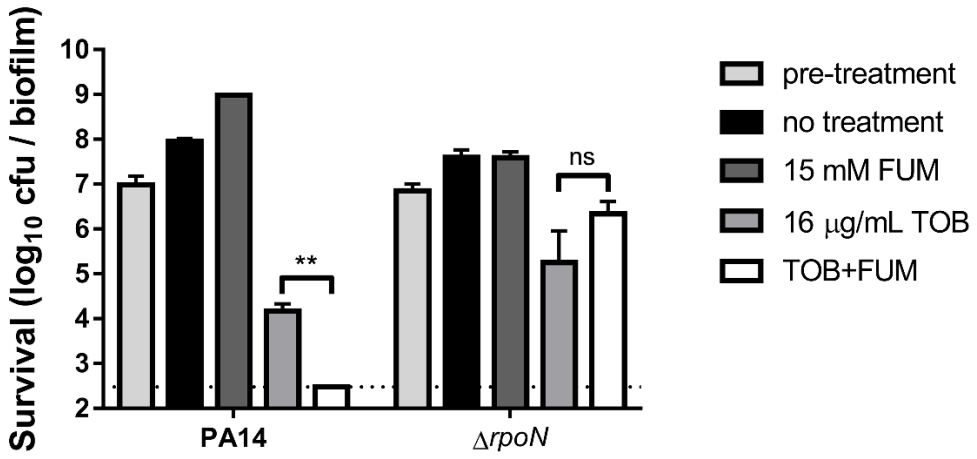

Figure S4-2. RpoN is required for colony biofilm susceptibility to TOB+FUM.
Survival of 4 h-old PA14 wildtype and Δ*rpoN* colony biofilms (pre-treatment) that were treated for 20 h on M9 plates containing no supplements (no treatment), 15 mM FUM, 16 μg/mL TOB, or TOB+FUM. Data are presented as mean $\log_{10}$ cfu/biofilm ± SEM for three biological replicates. The dashed line indicates the limit of detection of the assay (all replicates for PA14 with TOB+FUM were below the limit of detection).

Koeva *et al* reported that TOB-resistant strains are not susceptible to TOB+FUM treatment (189). We confirmed that the aminoglycoside minimum inhibitory concentrations (MIC) for the Δ*rpoN* mutant were identical to those for the wildtype (**Table S4-3**), indicating that increased resistance could not explain the non-susceptibility of the Δ*rpoN* mutant to TOB+FUM. Addition of 2 mM L-glutamine during the killing assay with TOB+FUM also did not render the Δ*rpoN* mutant susceptible to TOB+FUM (**Fig S4-3**), demonstrating that the dependence of PA14 Δ*rpoN* on exogenous L-glutamine as a nitrogen source (59) did not influence the lack of Δ*rpoN* TOB+FUM susceptibility.

Overall, the data presented above support our hypothesis that RpoN plays an important role in mediating TOB+FUM susceptibility in the PA14 laboratory strain.

Table S4-3. Antibiotic MICs (μg/mL) determined in LB with 2 mM L-glutamine for strains used in this study

Strain	TOB	TOB+FUM[a]	GEN	GEN+FUM[a]	AMK	AMK+FUM[a]
PA14	2	2	2	2	2	2
PA14-*lacZ*	2	2	ND[b]	ND[b]	ND[b]	ND[b]
Δ*rpoN*	2	2	2	2	2	2
PA14/pMQ70	4	4	4	4	4	4
PA14/pMQ70::*rpoN*	4	4	4	4	4	4
PA14/pMQ70::*dctA*	4	4	4	4	4	4
Δ*rpoN*/pMQ70	2	2	4	4	4	4
Δ*rpoN*/pMQ70::*rpoN*	4	4	4	4	4	4
Δ*rpoN*/pMQ70::*dctA*	4	4	4	4	4	4

[a]FUM added at a final concentration of 15 mM
[b]ND = not determined

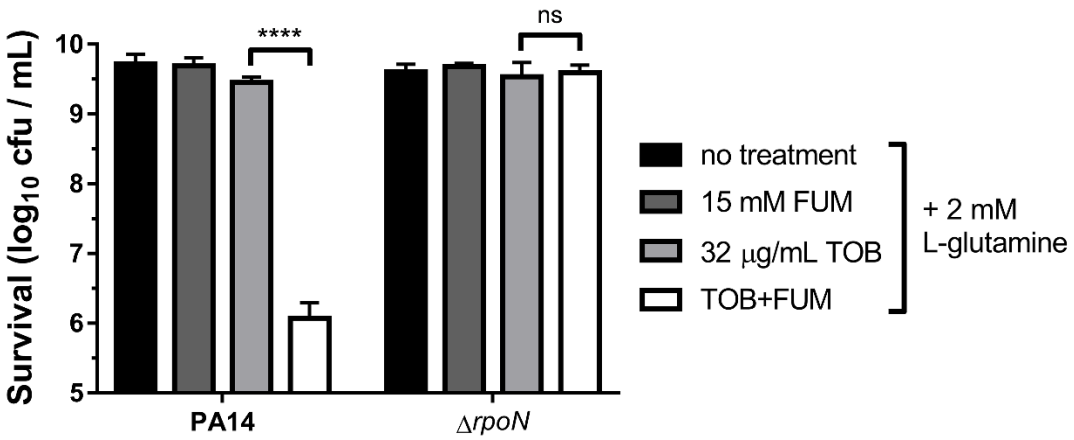

Figure S4-3. L-glutamine supplementation does not reverse non-susceptibility of Δ*rpoN* to TOB+FUM.

Survival of PA14 wildtype and Δ*rpoN* stationary phase cells that were incubated for 4 h in the presence of 2 mM L-glutamine with no additional treatment, 15 mM FUM, 32 μg/mL TOB, or TOB+FUM. Data are presented as mean $\log_{10}$ cfu/mL ± SEM for three biological replicates.

4.5.2 FUM is not taken up intracellularly and does not promote respiration or TOB uptake in the ΔrpoN mutant.

Meylan *et al* found that the extracellular FUM concentration decreases when stationary phase cells are treated with FUM (185), suggesting that FUM is taken up into the cell where it is subsequently metabolised. Koeva *et al* made the interesting observation that strains that do not grow with FUM as the sole carbon source are not susceptible to TOB+FUM treatment (189). FUM uptake through the DctA and DctPQM transporters is transcriptionally regulated by RpoN (66). Thus, Δ*rpoN* mutants, including our PA14 Δ*rpoN* strain (**Fig S4-4**), fail to grow in minimal media with FUM as the sole carbon source(66). We therefore hypothesised that regulation of FUM uptake by RpoN is an essential step in FUM-mediated potentiation of TOB lethality.

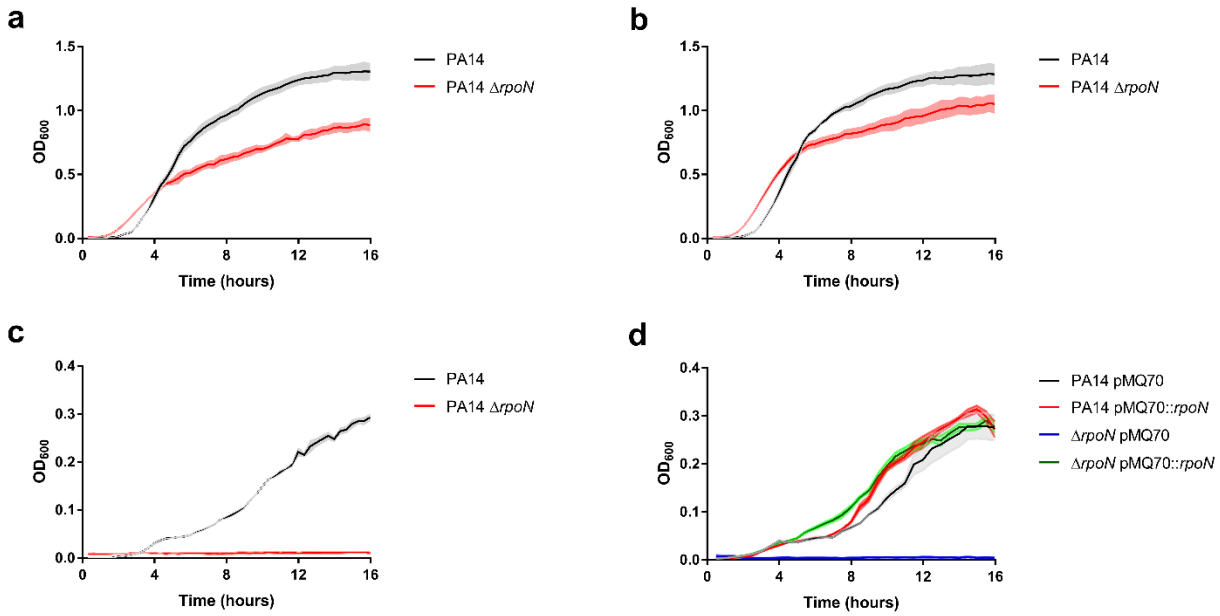

Figure S4-4. RpoN is required for growth with FUM as the sole carbon source.
Growth curves of indicated strains in (a) LB, (b) LB with 2 mM L-glutamine, (c and d) M9 with 30 mM FUM and 2 mM L-glutamine. Lines represent the mean OD_{600} of two biological replicates, each with six technical repeats. Lighter shading represents the SEM.

To assess the extent of FUM uptake by PA14 and Δ*rpoN*, we measured the concentration of extracellular FUM immediately after addition of FUM to the cultures (0 h) and following a 4 h incubation (**Fig 4-1e**). In contrast to PA14/pMQ70, the extracellular [FUM] did not appreciably decrease after 4 h in FUM-treated Δ*rpoN*/pMQ70 cells, which is consistent with the inability of Δ*rpoN* to take up FUM. Complementation of the Δ*rpoN* mutant with pMQ70::*rpoN* led to a significant reduction in extracellular [FUM] after 4 h.

FUM potentiates TOB killing by promoting electron transport chain (ETC) activity, which regenerates the PMF of stationary phase cells and enables subsequent TOB uptake across the cytoplasmic membrane (185). We assessed the ability of FUM to promote respiration using a resazurin assay (**Fig 4-1f**). Resazurin can be reduced to fluorescent resorufin by components of the ETC. A low, basal increase in fluorescence over time was observed for all strains in the absence of FUM. When PA14/pMQ70, PA14/pMQ70::*rpoN*, and Δ*rpoN*/pMQ70::*rpoN* were treated with FUM, there was a rapid increase in resazurin reduction to resorufin (**Fig 4-1f**), which is suggestive of increased ETC activity and metabolic reduction. In contrast, the addition of FUM to Δ*rpoN*/pMQ70 did not lead to an increase in fluorescence relative to the basal fluorescence in the absence of FUM (**Fig 4-1f**), suggesting that FUM does not promote respiration in the Δ*rpoN* mutant. To confirm that the FUM-dependent increase in resazurin reduction was due to ETC activity, we treated cells with the cytochrome *c* oxidase inhibitor NaN_3 in the presence or absence of FUM. NaN_3 impaired FUM-dependent resazurin reduction (**Fig S4-5**).

To probe the role of the PMF generated by the ETC in TOB+FUM killing, we treated cells with TOB+FUM in the presence of CCCP, a proton ionophore that dissipates the PMF. CCCP completely abolished the ability of pMQ70::*rpoN* to restore Δ*rpoN* TOB+FUM susceptibility (**Fig 4-1g**), which is consistent with a role for the PMF in TOB+FUM killing.

Given that FUM was unable to promote increased ETC activity in Δ*rpoN* (**Fig 4-1f**), we anticipated that FUM treatment would also not lead to increased TOB uptake in the Δ*rpoN* mutant. TOB accumulation was determined using a modified version of a previously described microbiological assay (153). Stationary phase cells treated with TOB or TOB+FUM were lysed, and the lysate was added to plates that had been inoculated with a lawn of TOB-sensitive *Escherichia coli*. Following incubation, the diameters of the zones of growth inhibition were measured. Larger zones of inhibition were interpreted as being due to the presence of a relatively higher concentration of TOB in the lysate and, thus, a higher amount of intracellular TOB in the *P. aeruginosa* cells. We observed a larger zone of growth inhibition with lysates from PA14 cells treated with TOB+FUM than from PA14 treated with TOB alone, suggesting that wildtype cells accumulated more TOB in the presence of FUM (**Fig 4-1h**). As predicted, no difference in zone of inhibition diameter and, therefore, in TOB accumulation was observed in TOB versus TOB+FUM treated Δ*rpoN* (**Fig 4-1h**). A picture of a representative experiment is shown in **Fig S4-6**. Importantly, lysates from untreated cells or cells treated with FUM alone did not produce zones of growth inhibition on the lawn of *E. coli* (data not shown).

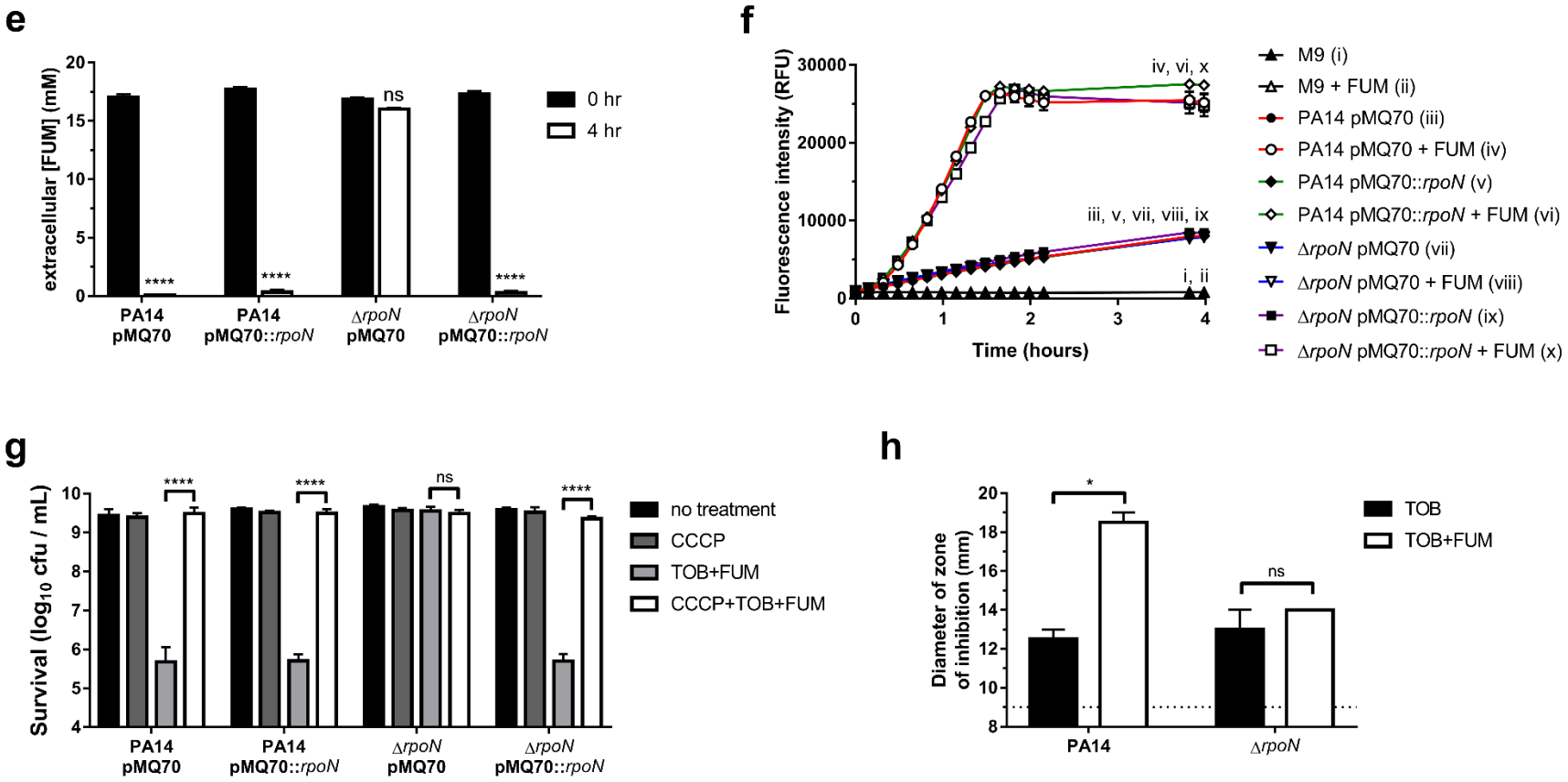
e
extracellular [FUM] (mM)
20
15
10
5
0
****
ns
****
****
0 hr
4 hr
PA14 pMQ70
PA14 pMQ70::rpoN
ΔrpoN pMQ70
ΔrpoN pMQ70::rpoN
f
Fluorescence intensity (RFU)
30000
20000
10000
0
iv, vi, x
iii, v, vii, viii, ix
i, ii
0
1
2
3
4
Time (hours)
M9 (i)
M9 + FUM (ii)
PA14 pMQ70 (iii)
PA14 pMQ70 + FUM (iv)
PA14 pMQ70::rpoN (v)
PA14 pMQ70::rpoN + FUM (vi)
ΔrpoN pMQ70 (vii)
ΔrpoN pMQ70 + FUM (viii)
ΔrpoN pMQ70::rpoN (ix)
ΔrpoN pMQ70::rpoN + FUM (x)
g
Survival (log10 cfu / mL)
10
9
8
7
6
5
4
****
****
ns
****
no treatment
CCCP
TOB+FUM
CCCP+TOB+FUM
PA14 pMQ70
PA14 pMQ70::rpoN
ΔrpoN pMQ70
ΔrpoN pMQ70::rpoN
h
Diameter of zone of inhibition (mm)
20
18
16
14
12
10
8
*
ns
TOB
TOB+FUM
PA14
ΔrpoN

Figure 4-1. Stationary phase Δ*rpoN* cells are not susceptible to TOB+FUM treatment.
(e) Loss of *rpoN* impairs FUM uptake. Extracellular [FUM] in cultures of PA14 or Δ*rpoN* stationary phase cells carrying pMQ70 or pMQ70::*rpoN* was measured after 0 or 4 h. Data are presented as mean extracellular [FUM] + SEM for three biological replicates. (f) FUM promotes respiration in wildtype but not Δ*rpoN* stationary phase cells. Reduction of resazurin to resorufin was measured over time in PA14 or Δ*rpoN* stationary phase cells carrying pMQ70 or pMQ70::*rpoN* exposed to 0 or 15 mM FUM. Data are shown as mean fluorescence intensity ± SEM for two independent experiments with 3 technical replicates per experiment. Since some data sets were obscured by others on the graph, Roman numerals were used to show the locations of the data sets. (g) The PMF is required for TOB+FUM killing. Survival of stationary phase cells following 4 h treatment with or without CCCP and/or TOB+FUM. Data are presented as mean $\log_{10}$ cfu/mL ± SEM for three biological replicates. (h) FUM increases intracellular TOB accumulation in wildtype but not Δ*rpoN* stationary phase cells. Zones of *E. coli* DH5α growth inhibition caused by lysates of PA14 or Δ*rpoN TOB* or TOB+FUM were used to approximate relative amounts of intracellular TOB. Data are shown as the mean diameter + SEM of the growth inhibition zones for two independent experiments. The dashed line indicates the limit of detection (the diameter of the wells).

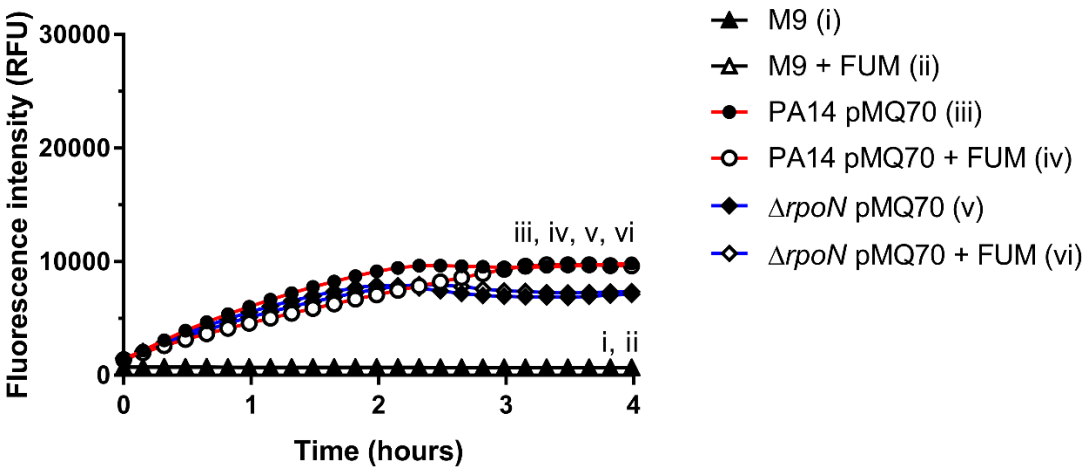

Figure S4-5. FUM-dependent increase in resazurin reduction is dependent on the ETC. Reduction of resazurin to resorufin was measured over time in NaN_3-treated stationary phase cells of the indicated strains in the presence or absence of 15 mM FUM. Data are shown as mean fluorescence intensity ± SEM for two independent experiments with three technical replicates per experiment. Since some data sets were obscured by others on the graph, Roman numerals were used to indicate the locations of the data sets.

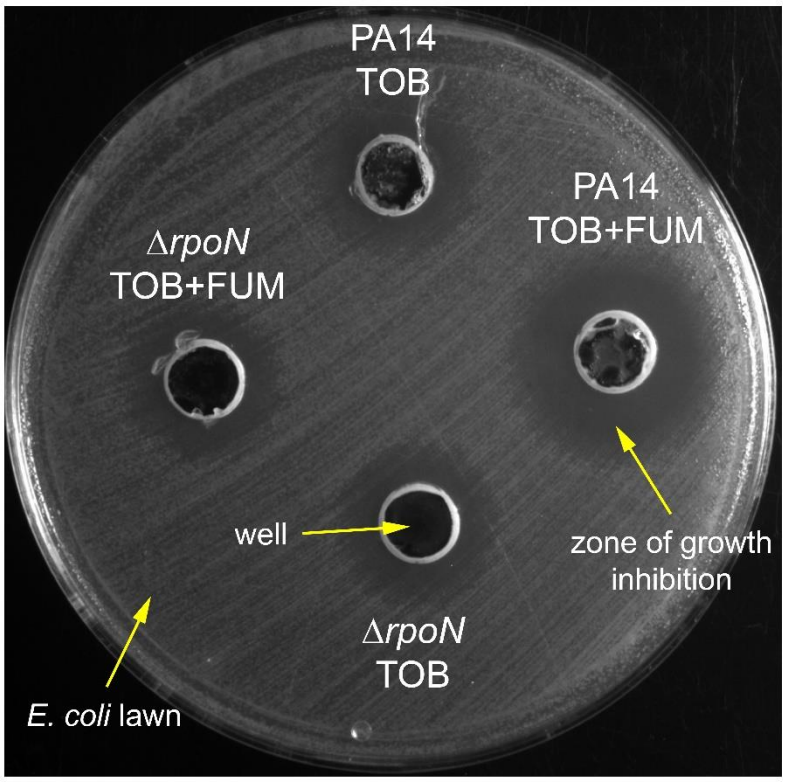

Figure S4-6. FUM increases TOB accumulation in wildtype but not Δ*rpoN* stationary phase cells.
Image of a representative experiment showing zones of *E. coli* DH5α growth inhibition caused by lysates from PA14 and Δ*rpoN* cells treated with TOB or TOB+FUM.

*4.5.3 RpoN-independent expression of the DctA transporter is sufficient to promote Δ*rpoN *TOB+FUM susceptibility.*

Given that RpoN is required for expression of the *dctA* and *dctPQM* FUM transporter genes (66), we hypothesised that the Δ*rpoN* strain was not susceptible to TOB+FUM because FUM transporters were not expressed and FUM was not being taken up by the cell. Thus, restoring FUM uptake by overexpression of a FUM transporter should restore TOB+FUM susceptibility in the Δ*rpoN* mutant. We constructed pMQ70::*dctA*, which carries the *dctA* C_4-dicarboxylate transporter gene under the control of P_{BAD}, and introduced this plasmid into the wildtype and Δ*rpoN* strains. DctA is a more efficient transporter than DctPQM at the millimolar FUM concentrations used in the assay (66). The pMQ70::*dctA* plasmid restored FUM uptake (indirectly measured as extracellular FUM depletion) in the Δ*rpoN* strain (**Fig 4-2a**). Consistent with this finding, pMQ70::*dctA* also promoted FUM-dependent respiration (**Fig 4-2b**). The pMQ70::*dctA* plasmid restored susceptibility of Δ*rpoN* stationary phase cells to TOB+FUM (**Fig 4-2c**), suggesting that lack of FUM uptake can explain the non-susceptibility of Δ*rpoN* to TOB+FUM. CCCP treatment abolished the ability of the pMQ70::*dctA* plasmid to promote TOB+FUM susceptibility in the Δ*rpoN* mutant (**Fig 4-2d**), indicating that TOB+FUM susceptibility of the Δ*rpoN*/pMQ70::*dctA* strain was PMF-dependent.

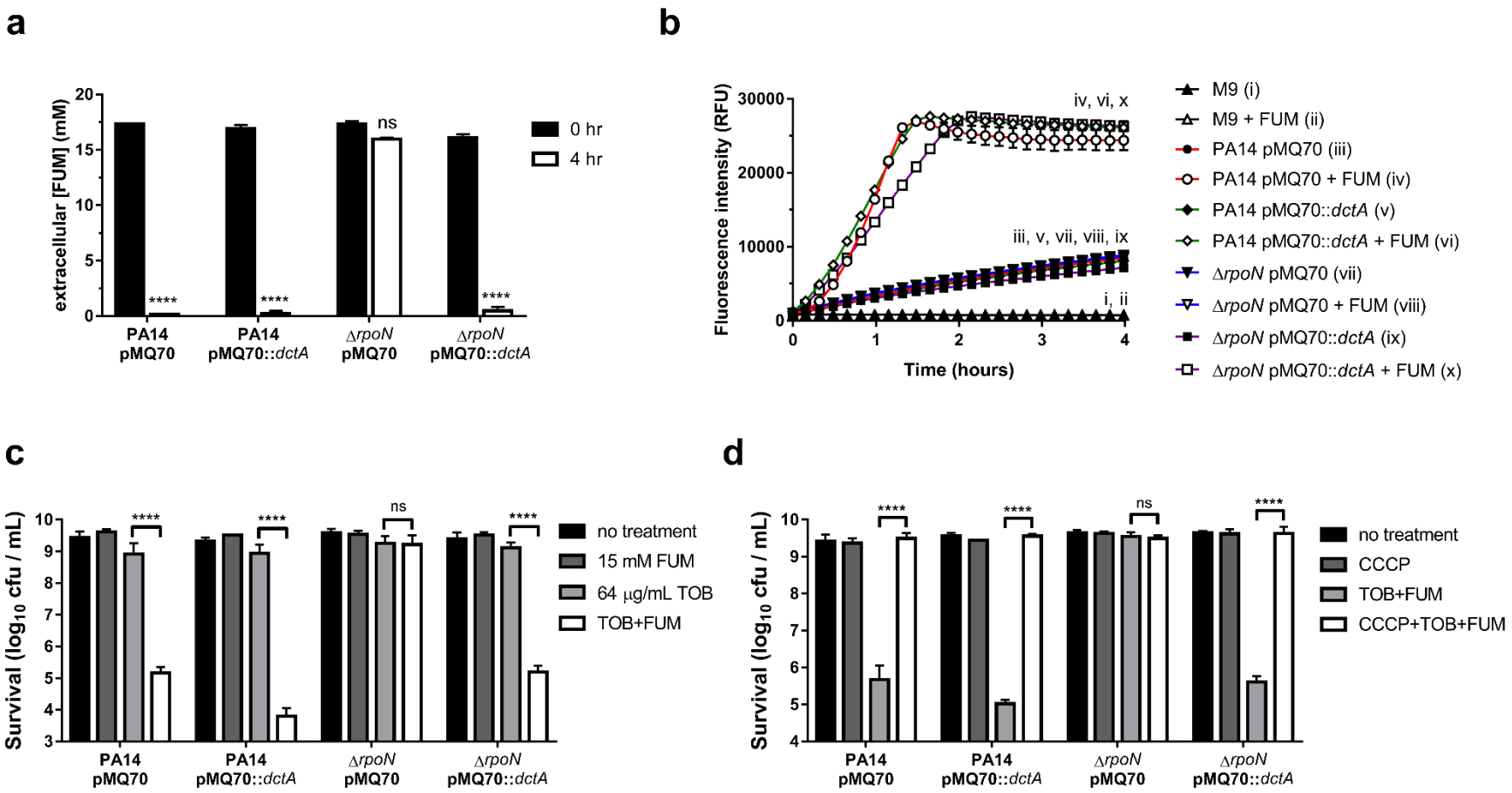
a
extracellular [FUM] (mM)
20
15
10
5
0
0 hr
4 hr
ns
****
PA14 pMQ70
PA14 pMQ70::dctA
ΔrpoN pMQ70
ΔrpoN pMQ70::dctA
b
Fluorescence intensity (RFU)
30000
20000
10000
0
iv, vi, x
iii, v, vii, viii, ix
i, ii
Time (hours)
M9 (i)
M9 + FUM (ii)
PA14 pMQ70 (iii)
PA14 pMQ70 + FUM (iv)
PA14 pMQ70::dctA (v)
PA14 pMQ70::dctA + FUM (vi)
ΔrpoN pMQ70 (vii)
ΔrpoN pMQ70 + FUM (viii)
ΔrpoN pMQ70::dctA (ix)
ΔrpoN pMQ70::dctA + FUM (x)
c
Survival (log10 cfu / mL)
no treatment
15 mM FUM
64 μg/mL TOB
TOB+FUM
d
CCCP
TOB+FUM
CCCP+TOB+FUM

Figure 4-2. RpoN-independent DctA expression restores TOB+FUM susceptibility in Δ*rpoN* stationary phase cells.

(a) Extracellular [FUM] in cultures of PA14 or Δ*rpoN* stationary phase cells carrying pMQ70 or pMQ70::*dctA* was measured after 0 or 4 h. Data are presented as mean extracellular [FUM] + SEM for three biological replicates. (b) Reduction of resazurin to resorufin was measured over time in PA14 or Δ*rpoN* stationary phase cells carrying pMQ70 or pMQ70::*dctA* exposed to 0 or 15 mM FUM. Data are shown as mean fluorescence intensity ± SEM for two independent experiments with 3 technical replicates per experiment. Since some data sets were obscured by others on the graph, Roman numerals were used to indicate the locations of the data sets. (c) Survival of PA14 wildtype and Δ*rpoN* stationary phase cells carrying pMQ70 or pMQ70::*dctA* following incubation for 4 h with or without 64 µg/mL TOB and/or 15 mM FUM. Data are presented as mean $\log_{10}$ cfu/mL ± SEM for three biological replicates.

4.5.4 RpoN alleles from clinical isolates with predicted loss-of-function mutations cannot rescue TOB+FUM susceptibility in the PA14 ΔrpoN mutant

Loss of RpoN function is a recognised means of *P. aeruginosa* pathoadaptation to the CF lung; however, only some reports have documented specific *rpoN* mutations that are observed clinically in CF isolates. The AAJ010 isolates used by Huus *et al* (297) carried the *rpoN* non-synonymous amino acid change L343S arising from a T1028C mutation (Alex Wong, personal communication). The Danish transmissible DK2 lineage carried a T1256C missense, loss-of-function mutation leading to a L419P amino acid change (289, 294). Smith *et al* found *rpoN* missense, nonsense, and frameshift mutations in isolates from several CF patients, including a C1346T mutation leading to A449V that was predicted to negatively impact RpoN function (296). The L343S, L419P, and A449V mutations all map to the RpoN DNA binding domain (**Fig 4-3a**).

We constructed pMQ70::*rpoN*^{L343S}, pMQ70::*rpoN*^{L419P}, and pMQ70::*rpoN*^{A449V} and assessed the ability of these plasmids to complement the Δ*rpoN* mutant in TOB+FUM killing assays (**Fig 4-3b**). The plasmids carrying the L343S and the L419P *rpoN* alleles were unable to restore TOB+FUM susceptibility to an appreciable extent in Δ*rpoN* stationary phase cells, indicating that these were loss-of-function mutations. The A449V mutation did not lead to a loss of RpoN function in the killing assay given that pMQ70::*rpoN*^{A449V} was able to restore TOB+FUM killing of the Δ*rpoN* strain to wildtype levels (**Fig 4-3b**). This result was not entirely unexpected given the conservative nature of the A449V amino acid change. Overall, these data suggest that some *rpoN* missense mutations observed in *P. aeruginosa* CF clinical isolates can lead to TOB+FUM non-susceptibility.

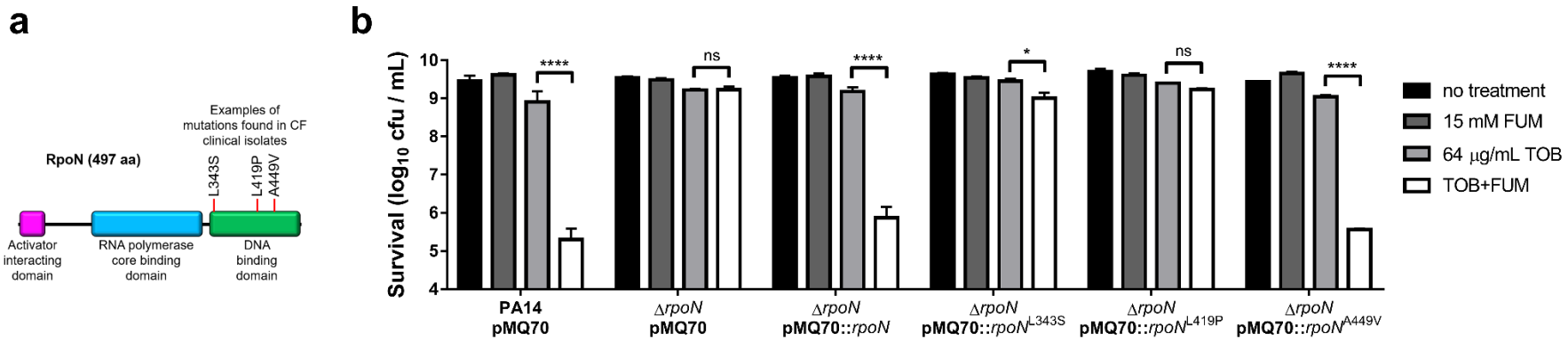

Figure 4.3 Loss-of-function RpoN alleles from CF clinical isolates impair TOB+FUM killing.
(a) Schematic representation of RpoN showing some mutations in the DNA binding domain that have been previously observed in CF clinical isolates. (b) Survival of PA14 wildtype and Δ*rpoN* stationary phase cells carrying pMQ70, pMQ70::*rpoN*, or pMQ70::*rpoN* with clinically relevant point mutations following incubation for 4 h with or without 64 μg/mL TOB and/or 15 mM FUM. Data are presented as mean $\log_{10}$ cfu/mL ± SEM for three biological replicates.

4.5.5 TOB+FUM kills wildtype cells and spares ΔrpoN cells in mixed genotype cultures

P. aeruginosa within the CF lung is genetically and phenotypically heterogeneous. It is likely, therefore, that bacteria retaining RpoN function ($RpoN^+$) and bacteria with pathoadaptive loss of RpoN function ($RpoN^-$) co-exist in the lungs of a given patient. To model a heterogeneous population, we mixed stationary phase PA14-*lacZ* ($RpoN^+$) and Δ*rpoN* ($RpoN^-$) cells at various PA14-*lacZ*:Δ*rpoN* starting ratios (1:100, 1:10, 1:1, 10:1, and 100:1) and incubated the populations for 4 h without treatment or with TOB+FUM treatment (64 µg/mL TOB and 15 mM FUM). Survival of each genotype was assessed by colony counting on plates supplemented with 40 µg/mL X-gal or both X-gal and 100 µg/mL tetracycline (TET). PA14-*lacZ* cells were selectively killed while Δ*rpoN* cells were spared upon treatment of the mixed genotype populations with TOB+FUM (**Fig 4-4a-e**). The colony counts of the PA14-*lacZ* and Δ*rpoN* strains were also used to calculate $\log_{10}$ PA14-*lacZ*:Δ*rpoN* ratios for each condition (**Fig 4-4f**). The PA14-*lacZ*:Δ*rpoN* ratios of the inocula were similar to the PA14-*lacZ*:Δ*rpoN* ratios of the untreated bacteria, indicating that the relative genotype proportions in the population remained stable over 4 h in the absence of TOB+FUM. In the presence of TOB+FUM, however, the PA14-*lacZ*:Δ*rpoN* ratios decreased. Overall, these data support the conclusion that, in mixed genotype stationary phase populations, cells with intact RpoN function are killed by TOB+FUM while cells lacking RpoN function survive treatment with TOB+FUM. The consequence is enrichment of $RpoN^-$ cells within the population. While the experimental system is simplistic, these data suggest that TOB+FUM treatment may select for $RpoN^-$ cell survival in more complex settings, such as in the CF lung where RpoN loss-of-function is known to evolve. The clinical consequences of a high proportion of $RpoN^-$ isolates in the CF lung are not known and require further study if TOB+FUM is to be used as a future treatment option for chronic *P. aeruginosa* lung infections.

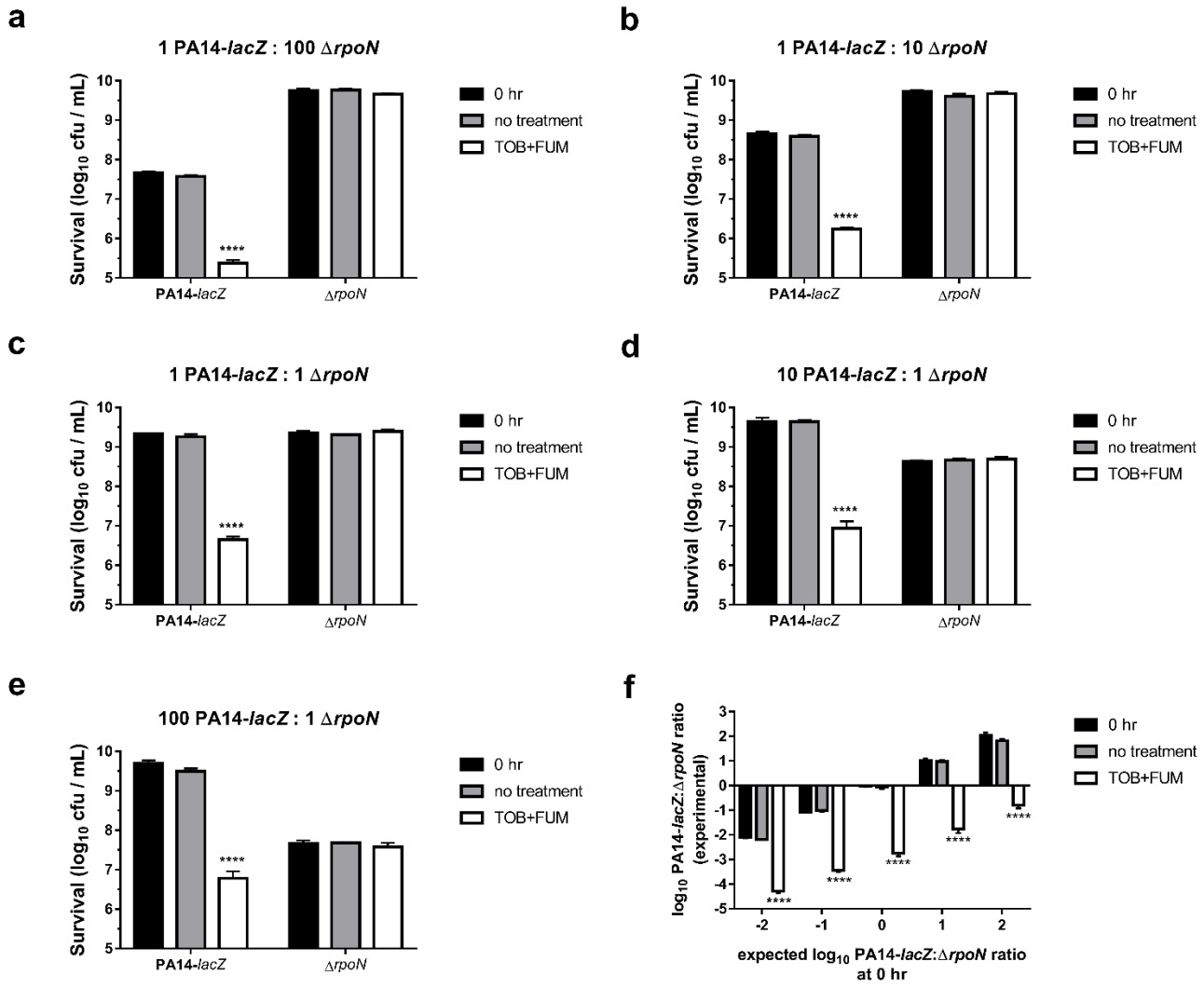

Figure 4-4. TOB+FUM specifically kills cells with RpoN function in mixed genotype populations.

PA14-*lacZ* and Δ*rpoN* stationary phase cells were mixed at (a) 1:100, (b) 1:10, (c) 1:1, (d) 10:1, and (e) 100:1 ratios, and survival of individual genotypes was determined prior to treatment (0 h) or following 4 h incubation with either no treatment or with TOB+FUM (64 µg/mL TOB and 15 mM FUM). Data are presented as mean $\log_{10}$ cfu/mL ± SEM for three biological replicates. Data in (a-e) were used to calculate $\log_{10}$ PA14-*lacZ*:Δ*rpoN* ratios. TOB+FUM treatment consistently reduced the $\log_{10}$ PA14-*lacZ*:Δ*rpoN* ratios, indicating a decrease in PA14-*lacZ* cells relative to Δ*rpoN* in the population.

4.5.6 L-arginine or D-glucose can promote TOB killing of ΔrpoN stationary phase cells.

Faced with the unsuitability of TOB+FUM and of other aminoglycoside with C_4-dicarboxylate combinations for killing Δ*rpoN* cells, we wondered if metabolites other than C_4-dicarboxylates would be able to potentiate TOB killing of the Δ*rpoN* mutant. Unbuffered L-arginine (ARG) has been previously shown to promote TOB killing of wildtype *P. aeruginosa* cells (397, 401). We found that TOB+ARG treatment (64 μg/mL TOB and 10 mM ARG) was also effective at killing Δ*rpoN* cells (**Fig 4-5**).

Other than FUM and SUC, Meylan *et al* found other carbon sources, such as acetate, gluconate, and D-glucose (GLU), that potentiated TOB lethality (185). We did not observe significant killing with 30 mM acetate and 64 μg/mL TOB in either PA14 or Δ*rpoN* (data not shown). Moreover, we did not test the ability of gluconate to potentiate TOB killing of Δ*rpoN* because Δ*rpoN* mutants have been shown to accumulate gluconate, suggesting a defect in gluconate utilization (63). Intriguingly, GLU was able to potentiate TOB killing in PA14 and, to a slightly lesser extent, in Δ*rpoN* (**Fig 4-5**). Determining whether ARG and GLU also promote TOB killing by enhancing respiration and TOB uptake will be the topic of future study. TOB combined with either ARG or GLU may prove to be a more attractive combination therapy than TOB+FUM in the setting of a high burden of RpoN loss-of-function mutants.

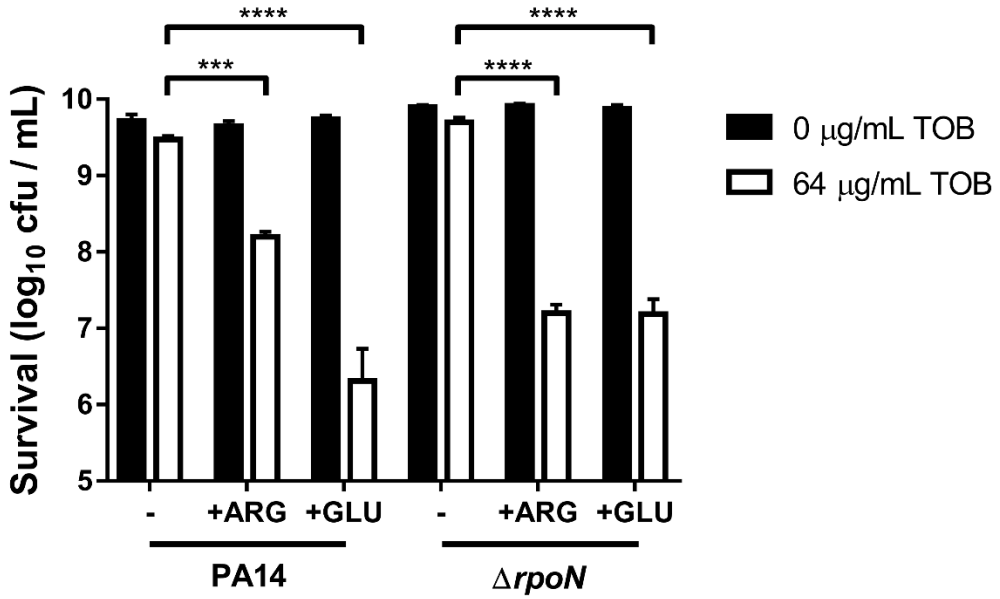

Figure 4-5. L-arginine or D-glucose can potentiate TOB killing of Δ*rpoN* cells.
Survival of PA14 wildtype and Δ*rpoN* stationary phase cells following incubation for 4 h with or without 64 μg/mL TOB in the presence or absence of 10 mM L-arginine (ARG) or 10 mM D-glucose (GLU). Data are presented as mean log_{10} cfu/mL ± SEM for three biological replicates.

4.6 Discussion

Chronic bacterial infections that are recalcitrant to standard antimicrobial treatment regimens contribute to patient morbidity and mortality, promote the emergence of antibiotic resistance, and pose a significant cost to the healthcare system. It is important to acknowledge that chronic infections involve a complex combination of antibiotic tolerance, antibiotic resistance, and host factors. Therefore, different treatment strategies, likely used in combination, will be needed in order to address these mechanistically different phenomena. Novel therapeutic strategies, such as metabolic potentiation of existing antibiotics, have been proposed in order to specifically combat antibiotic tolerance (188). TOB+FUM has been recently identified as a combination treatment that can kill antibiotic tolerant *P. aeruginosa* (185, 189), which contributes to the chronic lung infections that afflict patients with CF. Genetic requirements for TOB+FUM susceptibility have not been previously explored.

In this work, we have shown that the sigma factor RpoN is required for susceptibility of *P. aeruginosa* stationary phase and biofilm cells to TOB+FUM as well as to other aminoglycoside and C_4-dicarboxylate combinations. RpoN is an activator of C_4-dicarboxylate transporter gene expression (66), and we have shown that the non-susceptibility of Δ*rpoN* cells to TOB+FUM is due to a loss of FUM uptake. The proposed mechanism is presented schematically in **Fig 4-6**. Importantly, RpoN loss-of-function mutations are often seen in *P. aeruginosa* strains isolated from the CF lung, and we observed that clinical RpoN loss-of-function mutations result in TOB+FUM non-susceptibility. Moreover, TOB+FUM selectively kills cells retaining RpoN function and spares cells with loss of RpoN function in a heterogenous population, effectively leading to selection for RpoN mutant survival. Overall, these data suggest that TOB+FUM might not be an effective strategy to eradicate *P. aeruginosa* from the lungs of CF patients with a high burden of

RpoN loss-of-function mutants. However, further *in vitro* experiments with clinical isolates, *in vivo* experiments with animal models, and clinical data from human trials will be needed to further validate this concern. In light of our work, we suggest that clinical trials assessing TOB+FUM effectiveness should consider stratifying patients based on the relative frequency of isolates with *rpoN* mutations to determine if this parameter influences treatment response.

Recently, exciting strategies have been proposed to prevent the expression of RpoN-regulated virulence factors such as flagella in an effort to impair *P. aeruginosa* pathogenicity (58, 405, 406). While these strategies are likely to be relevant in the context of acute infectious processes that rely on RpoN-dependent virulence factors, they are unlikely to be helpful in the context of chronic *P. aeruginosa* CF lung infections where RpoN loss-of-function seems to provide a fitness benefit. Several theories have been proposed to explain why *rpoN* mutants evolve in the CF lung. These include immune evasion (403) and improved anaerobic survival (407). Perhaps *rpoN* mutation is also beneficial because it renders bacteria relatively insensitive to antibiotic potentiation by certain metabolites, like C_4-dicarboxylates. Some support for this conjecture can be found in the recent observation that, unlike for $RpoN^+$ strains, TOB susceptibility of the $RpoN^-$ DK2 strain is not increased by host-derived metabolites (402). Indeed, nutritional conditions in the CF lung have been previously shown to select for antibiotic tolerant *lasR* mutants (307). Whatever the underlying reason(s) may be for pathoadaptive loss of RpoN function in the context of the CF lung, what this means for patient outcomes has not been investigated and would be an interesting avenue for future study.

While our data suggest that aminoglycosides combined with C_4-dicarboxylates might not be effective in killing *P. aeruginosa* isolates with RpoN loss-of-function, we have shown that two other carbon sources, ARG and GLU, can potentiate TOB killing of both wildtype and Δ*rpoN*

antibiotic tolerant cells. Mechanisms of non-susceptibility to these treatments and whether these treatment combinations can lower bacterial burden more effectively than TOB alone in patients with *rpoN* mutants are questions that have yet to be answered.

Metabolic potentiation of antibiotic activity has tremendous potential to help patients who are battling chronic bacterial infections that are tolerant to antibiotics. Taking the case of TOB+FUM and *P. aeruginosa* as an example, we propose that, when developing antibiotic and metabolite combinations for a given infection, it will be important to consider whether genetic mutations impairing sensing, uptake and/or metabolism of the metabolite can evolve or are already present in the bacterial population. Ultimately, we hope that the work presented here will help guide efforts to personalise TOB+FUM treatment to CF patients who will benefit most from this combination therapy.

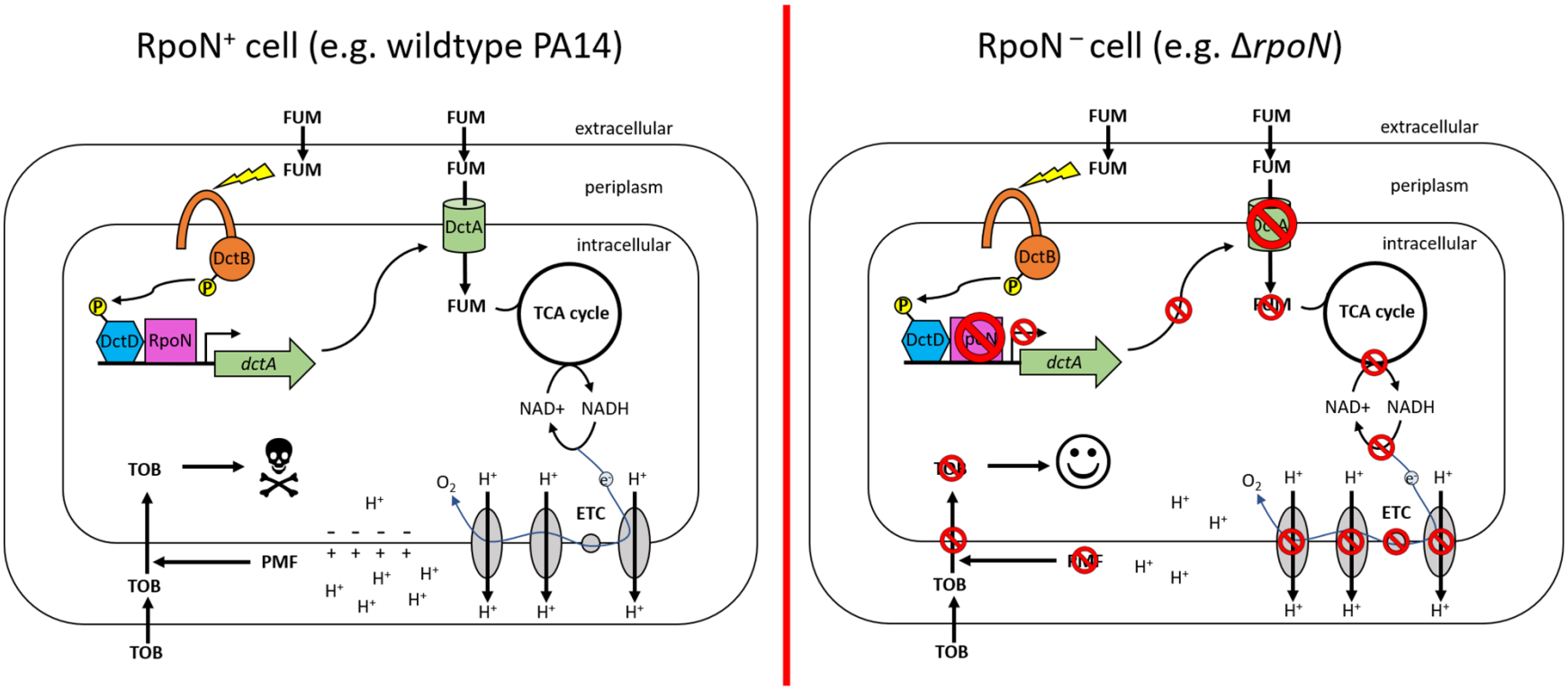

Figure 4-6. Proposed model for RpoN-dependent susceptibility to TOB+FUM.
In the wildtype RpoN+ strain (left panel), FUM enters the cell through C_4-dicarboxylate transporters (eg. DctA), that are transcriptionally regulated by RpoN. Once in the cell, FUM is metabolised in the tricarboxylic acid (TCA) cycle to produce reducing equivalents that promote ETC activity. Increased respiration leads to regeneration of the membrane potential, TOB uptake, and subsequent TOB-dependent cell death. On the other hand, in the Δ*rpoN* RpoN$^-$ strain, the lack of functional RpoN means that C_4-dicarboxylate transporters are not expressed, and FUM cannot enter the cell. As a consequence, TOB uptake is not increased and the cell remains tolerant to TOB.

4.7 Acknowledgments

We thank Dr. Rees Kassen (University of Ottawa) and Dr. Aaron Hinz (University of Ottawa and Carleton University) for providing the PA14-*lacZ* strain, Dr. Morgan Fullerton's laboratory (University of Ottawa) for use of their plate reader, and Conor O'Dwyer (University of Ottawa) for technical assistance with the nitrogen evaporator. Thank you to Dr. Xian-Zhi Li (Health Canada) for critical review of the manuscript prior to submission for peer review. CWH was supported by a Vanier Canada Graduate Scholarship (Canadian Institutes of Health Research) and an Audrey J. Boyce MD/PhD Fellowship (University of Ottawa). A portion of this work was presented by CWH at the 2019 AMMI Canada-CACMID Annual Conference (Ottawa, ON). Research in the Mah laboratory is funded by the Natural Sciences and Engineering Research Council of Canada.

4.8 Author contributions

Project conceptualisation and experimental design: CWH

Performed experiments: CWH, EF, LZ, and CT

Data analysis: CWH

Writing – original draft: CWH

Writing – review and editing: CWH and TFM. All authors reviewed and approved the final manuscript prior to submission.

Obtained funding and provided reagents/materials/equipment: TFM

Chapter 5: General discussion

In this thesis, I have presented an analysis of three different transcriptional regulators that contribute to antibiotic resistance and tolerance in the opportunistic bacterial pathogen, *P. aeruginosa*.

In **Chapter 2**, I attempted to identify a transcriptional regulator of the type VI secretion *tssABC1* operon, which contributes to biofilm antibiotic resistance in *P. aeruginosa*. While I found that PA3225 bound to the promoter region of this operon, deletion of *PA3225* did not affect *tssABC1* expression. Since publishing the research article that forms **Chapter 2**, a transcriptional regulator of the *tssABC1* operon (and of other type VI secretion system genes) was identified by another group (408). Allsopp and colleagues found that AmrZ, which is a global regulator of genes involved in virulence (409), bound directly to the *tssABC1* promoter region (408). Interestingly, overexpression of AmrZ only led to a 1.5-fold increase in *tssA1* expression; however, the impact of *amrZ* deletion was not assessed (408). Clearly, transcriptional regulation of *tssABC1* does not appear to be as pivotal as the post-transcriptional control exerted by RsmA (317, 320, 408).

The fortuitous discovery that deletion of *PA3225* resulted in increased resistance to a variety of MexAB-OprM antibiotic substrates ultimately led to the finding that PA3225 represses *mexAB-oprM* expression. *mexAB-oprM* has a number of regulators (10), suggesting that regulation of its expression across a variety of different conditions is important for the cell. Interestingly, *PA3228*, which encodes an ABC transporter and is in the same operon as *PA3225*, also seemed to play a role in the reduced susceptibility of the Δ*PA3225* mutant to fluoroquinolones. Characterisation of this putative efflux pump is underway in our lab.

In **Chapter 3**, I described the discovery that *ndvB*, which is involved in biofilm antibiotic resistance through the production of antibiotic-sequestering cyclic glucans, is regulated by RpoS in stationary phase cells and biofilms. One interesting finding of this work was that *ndvB* has an unusually long 5' untranslated region (5'UTR; the median length is 47 nucleotides in *P. aeruginosa* (387)). Therefore, investigating how the 5'UTR influences transcription and translation of *ndvB* will be of interest for future studies. While I primarily examined transcriptional expression in stationary phase cells, it will be interesting to more closely examine *ndvB* expression in biofilms. Gene expression is well known to be heterogeneous in bacterial biofilms (37). Therefore, examining spatial and temporal *ndvB* expression in a variety of different biofilm models (eg. colony biofilms (410) could be done using the transcriptional GFP reporters. It would also be of value to ensure that *ndvB* expression in biofilms colocalizes with areas of *rpoS* expression. While alginate, PEL, and PSL are the major polysaccharide components of *P. aeruginosa* biofilms, the contribution of NdvB-derived glucans to the biofilm matrix probably also warrants further investigation given that these glucans were a major exopolysaccharide identified in PA14 biofilms (388).

Many important questions remain about NdvB and the native function(s) of the β-(1→3)-cyclic glucans that it produces. For instance, Sadovskaya and colleagues showed that NdvB-derived glucans are modified with phosphoglycerol (148) – how are phosphoglycerol moieties added to the cyclic glucans? In *E. coli*, linear periplasmic glucans are substituted with phosphoglycerol moieties by the phosphoglycerol transferase, MdoB (411). I performed a quick BLAST search of the *P. aeruginosa* genome on the *Pseudomonas* Genome Database website (82) with the amino acid sequence of the MdoB polypeptide. This search yielded two genes, PA1115 and PA1689, that encode putative and uncharacterised cytoplasmic membrane proteins from the

MdoB family (COG1368) (83). It would be interesting to determine in the future if one of these candidate phosphoglycerol transferases is responsible for modification of NdvB-derived glucans. A similar search performed with the sequence of CgmB, which adds phosphoglycerol to cyclic glucans in *Sinorhizobium meliloti* (a plant symbiont) (412), did not produce any hits in *P. aeruginosa*. This leads to a second interesting question – what is the source of the phosphoglycerol that decorates NdvB-derived glucans? In *E.coli*, MdoB transfers phosphoglycerol from membrane phosphatidylglycerol lipids onto the glucans to allow for membrane turnover (411). Perhaps the phosphoglycerol moieties on NdvB-dervied glucans are also derived from phosphatidylglycerol. An important finding of **Chapter 3** was that *ndvB* is regulated by RpoS (312), which is active during starvation and growth arrest (24). This suggests that NdvB may somehow be important for adaptation to starvation conditions. As mentioned in **Chapter 1**, it is interesting to note that *rpoS* transcription is induced by PsrA, which responds to fatty acids that can be used for metabolism through β-oxidation (48–52). Perhaps NdvB-derived glucans may be involved in turnover of membrane phosphatidylglycerol that can be used for β-oxidation (413). Maybe phosphatidylglycerol turnover and recycling of the phosphatidylglycerol moiety through NdvB-derived glucans allows for remodeling of the lipid composition and biophysical properties of the membrane as cells enter stationary phase (413). NdvB-derived glucans are also linked to metabolism through ethanol oxidation via an uncharacterized mechanism (149). Ethanol oxidation genes are upregulated in biofilm cells compared to exponential phase cells (149) – are these genes also upregulated in stationary phase cells? Is there a role for ethanol oxidation as a metabolic pathway in stationary phase cells?

It is also interesting to note that another type of periplasmic glucan also exists in *P. aeruginosa*. These glucans, which are synthesized by enzymes encoded by the *opgGH* locus, are

linear and succinylated (414). It is uncommon for bacteria to have both cyclic and linear periplasmic glucans (415), which begs the question: why are two types of glucan produced by *P. aeruginosa*? Do these periplasmic glucans have some functional redundancy or are they functionally divergent?

Chapter 3 also documented a role for RpoS in stationary phase tolerance to tobramycin. Interestingly, this tolerance did not seem to depend on *ndvB*. How might RpoS contribute to stationary phase tolerance? An interesting hypothesis stems from the finding by Martins and colleagues that the superoxide dismutase SodB is important for stationary phase tolerance to antibiotics (181). Expression of *sodB* is dependent on both the stringent response and RpoS in *P. aeruginosa* (181). SodB seems to be important in stationary phase cells for regulating membrane permeability to antibiotics, although the mechanism is not yet clear. Membrane permeability can be approximated using ethidium bromide accumulation assay as was done by Martins *et al* (181). To determine if stationary phase Δ*rpoS* cells might have increased permeability, I performed a pilot experiment where I assessed steady state accumulation of ethidium bromide in the absence or presence of CCCP. CCCP inhibits the activity of RND efflux pumps that can efflux ethidium bromide out of the cell and was used to ensure that differences in steady state accumulation between strains were not due to efflux. Interestingly, the Δ*rpoS* mutant accumulated more ethidium bromide than the wildtype, suggesting that membrane permeability might be increased in Δ*rpoS* cells (**Fig 5-1**). Whether this increased permeability is due to downregulation of *sodB* in the Δ*rpoS* mutant and whether this contributes to tobramycin tolerance are questions that should be explored in the future.

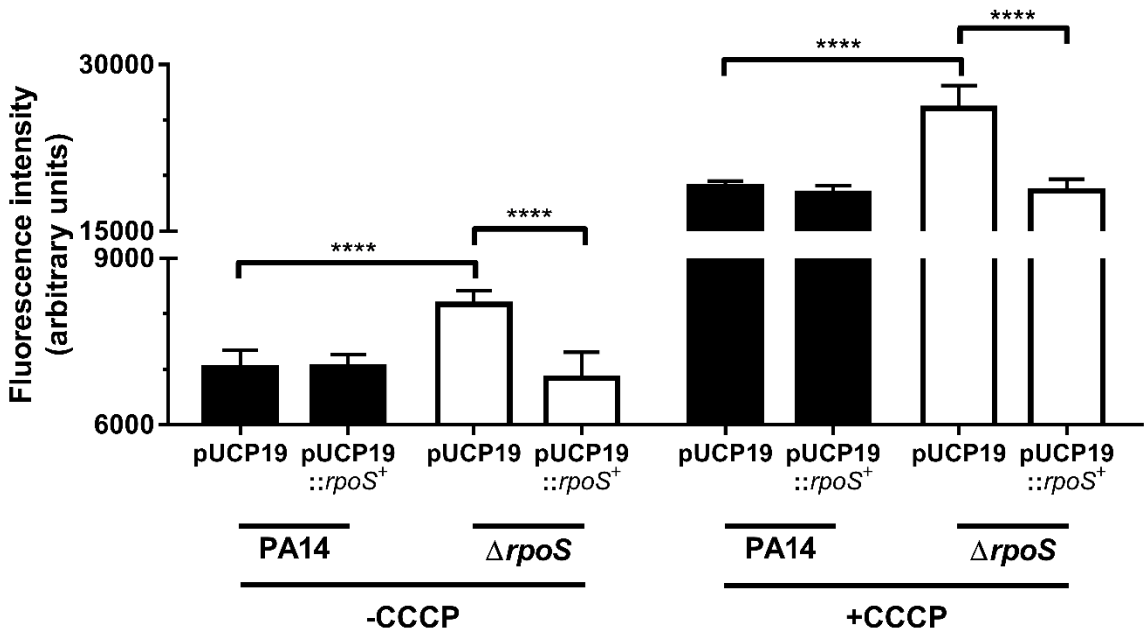

Figure 5-1. Accumulation of ethidium bromide is increased in Δ*rpoS* stationary phase cells. Stationary phase accumulation of ethidium bromide was performed as described by Martins *et al*. Steady state fluorescence was measured in a plate reader (Ex/Em 490/585 nm). Data are shown as mean + SEM for three biological replicates tested in quadruplicate technical repeats.

Chapter 4 provided the first demonstration of a clinically relevant mechanism of bacterial non-susceptibility to potentiation of antibiotic killing by a metabolite. I found that RpoN is required for potentiation of tobramycin killing by fumarate in *P. aeruginosa*. Importantly, RpoN loss-of-function mutations are common in *P. aeruginosa* isolated from the CF lung (288). The potential clinical impact of this finding is quite clear – if tobramycin and fumarate combination treatment is to be used in CF patients to treat chronic *P. aeruginosa* lung infections, it is possible that patients with a high burden of RpoN mutants will not benefit from the combination treatment. That being said, this is still very much a theoretical concern for a variety of reasons. Firstly, I still need to show that actual CF isolates lacking RpoN function are, like the laboratory strain, non-susceptible to the combination treatment. Secondly, the combination of tobramycin and fumarate has actually not yet been shown to have any clinical benefit in CF patients. The company Enbiotix,

which is developing tobramycin and fumarate as a drug called EBX-001, is purportedly beginning the process to test efficacy in clinical trials in CF patients. Thirdly, the true prevalence of RpoN loss-of-function mutants among CF patients as well as the frequency of mutants within a given patient's lung are not known. Frequency of *rpoN* mutant alleles in CF sputum could be done using FREQ-Seq (416) as was done recently for *lasR* mutant alleles (310). This relative frequency of mutant alleles could be used to prospectively or retrospectively stratify CF patients to determine if efficacy of tobramycin and fumarate combination inversely correlates with the burden of RpoN mutants in the lung. If efficacy of tobramycin and fumarate is affected by RpoN mutant burden, then this parameter could be used in a personalized medicine approach to determine which patients would benefit most from the combination treatment. Finally, the actual clinical significance of RpoN mutants is virtually unknown. For instance, do patients have worse clinical prognoses if their lungs are dominated by bacteria lacking RpoN function? All of these questions require answers before we will know if my findings in **Chapter 4** are of true clinical value.

Antibiotics are precious healthcare resources that are the cornerstone of modern medicine. Understanding the mechanisms underpinning antibiotic resistance and tolerance as well how these mechanisms are regulated is critical in order to guide strategies that will help keep our antibiotic arsenal relevant. Taking biofilms as an example, several new and exciting strategies have been developed to disrupt or prevent these antibiotic tolerant populations (146). Understanding transcriptional regulation of antibiotic resistance and tolerance is one strategy that has been taken by us and others (366, 417–422) in the hopes that this understanding may unveil steps in regulatory networks that can be targeted therapeutically to render bacteria susceptible to antibiotics.

References

1. Hall CW, Mah T-F. 2017. Molecular mechanisms of biofilm-based antibiotic resistance and tolerance in pathogenic bacteria. FEMS Microbiol Rev 41:276–301.

2. Döring G, Jansen S, Noll H, Grupp H, Frank F, Botzenhart K, Magdorf K, Wahn U. 1996. Distribution and transmission of Pseudomonas aeruginosa and Burkholderia cepacia in a hospital ward. Pediatr Pulmonol 21:90–100.

3. Bodey GP, Bolivar R, Fainstein V, Jadeja L. Infections caused by Pseudomonas aeruginosa. Rev Infect Dis 5:279–313.

4. Lyczak JB, Cannon CL, Pier GB. 2002. Lung infections associated with cystic fibrosis. Clin Microbiol Rev 15:194–222.

5. Bassetti M, Vena A, Croxatto A, Righi E, Guery B. 2018. How to manage Pseudomonas aeruginosa infections. Drugs Context 7:212527.

6. Elborn JS. 2016. Cystic fibrosis. Lancet 388:2519–2531.

7. Høiby N, Ciofu O, Bjarnsholt T. 2010. *Pseudomonas aeruginosa* biofilms in cystic fibrosis. Future Microbiol 5:1663–1674.

8. Lebeaux D, Ghigo J-M, Beloin C. 2014. Biofilm-related infections: bridging the gap between clinical management and fundamental aspects of recalcitrance toward antibiotics. Microbiol Mol Biol Rev 78:510–43.

9. Poole K. 2011. Pseudomonas Aeruginosa: Resistance to the Max. Front Microbiol 2:65.

10. Li X-Z, Plésiat P, Nikaido H. 2015. The challenge of efflux-mediated antibiotic resistance in Gram-negative bacteria. Clin Microbiol Rev 28:337–418.

11. Mulcahy LR, Isabella VM, Lewis K. 2014. Pseudomonas aeruginosa biofilms in disease. Microb Ecol 68:1–12.

12. Bjarnsholt T, Alhede M, Alhede M, Eickhardt-Sørensen SR, Moser C, Kühl M, Jensen PØ, Høiby N. 2013. The in vivo biofilm. Trends Microbiol 21:466–474.

13. Flemming H-C, Wingender J, Szewzyk U, Steinberg P, Rice SA, Kjelleberg S. 2016. Biofilms: an emergent form of bacterial life. Nat Rev Microbiol 14:563–575.

14. Stover CK, Pham XQ, Erwin AL, Mizoguchi SD, Warrener P, Hickey MJ, Brinkman FS, Hufnagle WO, Kowalik DJ, Lagrou M, Garber RL, Goltry L, Tolentino E, Westbrock-Wadman S, Yuan Y, Brody LL, Coulter SN, Folger KR, Kas A, Larbig K, Lim R, Smith K, Spencer D, Wong GK, Wu Z, Paulsen IT, Reizer J, Saier MH, Hancock RE, Lory S, Olson M V. 2000. Complete genome sequence of Pseudomonas aeruginosa PAO1, an opportunistic pathogen. Nature 406:959–64.

15. Greenberg EP. 2000. Pump up the versatility. Nature 406:947–948.

16. Poulsen BE, Yang R, Clatworthy AE, White T, Osmulski SJ, Li L, Penaranda C, Lander ES, Shoresh N, Hung DT. 2019. Defining the core essential genome of Pseudomonas aeruginosa. Proc Natl Acad Sci 116:10072–10080.

17. Browning DF, Busby SJW. 2016. Local and global regulation of transcription initiation in bacteria. Nat Rev Microbiol advance on.

18. Feklístov A, Sharon BD, Darst SA, Gross CA. 2014. Bacterial Sigma Factors: A Historical, Structural, and Genomic Perspective. Annu Rev Microbiol 68:357–376.

19. Paget MS, Helmann JD. 2003. The σ 70 family of sigma factors. Genome Biol 4:203.

20. BURGESS RR, TRAVERS AA, DUNN JJ, BAUTZ EKF. 1969. Factor Stimulating Transcription by RNA Polymerase. Nature 221:43–46.

21. Binder SC, Eckweiler D, Schulz S, Bielecka A, Nicolai T, Franke R, Häussler S, Meyer-Hermann M. 2016. Functional modules of sigma factor regulons guarantee adaptability and evolvability. Sci Rep 6:22212.

22. Schulz S, Eckweiler D, Bielecka A, Nicolai T, Franke R, Dötsch A, Hornischer K, Bruchmann S, Düvel J, Häussler S. 2015. Elucidation of sigma factor-associated networks in Pseudomonas aeruginosa reveals a modular architecture with limited and function-specific crosstalk. PLoS Pathog 11:e1004744.

23. Lonetto M, Gribskov M, Gross CA. 1992. The sigma 70 family: sequence conservation and evolutionary relationships. J Bacteriol 174:3843–3849.

24. Potvin E, Sanschagrin F, Levesque RC. 2008. Sigma factors in Pseudomonas aeruginosa. FEMS Microbiol Rev 32:38–55.

25. Paget M. 2015. Bacterial Sigma Factors and Anti-Sigma Factors: Structure, Function and Distribution. Biomolecules 5:1245–1265.

26. Gruber TM, Gross CA. 2003. Multiple Sigma Subunits and the Partitioning of Bacterial Transcription Space. Annu Rev Microbiol 57:441–466.

27. Campbell EA, Westblade LF, Darst SA. 2008. Regulation of bacterial RNA polymerase σ factor activity: a structural perspective. Curr Opin Microbiol 11:121–127.

28. Österberg S, Peso-Santos T del, Shingler V. 2011. Regulation of Alternative Sigma Factor Use. Annu Rev Microbiol 65:37–55.

29. Buck M, Gallegos MT, Studholme DJ, Guo Y, Gralla JD. 2000. The bacterial enhancer-dependent sigma(54) (sigma(N)) transcription factor. J Bacteriol 182:4129–36.

30. Wigneshweraraj S, Bose D, Burrows PC, Joly N, Schumacher J, Rappas M, Pape T, Zhang X, Stockley P, Severinov K, Buck M. 2008. Modus operandi of the bacterial RNA polymerase containing the σ^{54} promoter-specificity factor. Mol Microbiol 68:538–546.

31. Bush M, Dixon R. 2012. The role of bacterial enhancer binding proteins as specialized activators of σ54-dependent transcription. Microbiol Mol Biol Rev 76:497–529.

32. Rombel I, North A, Hwang I, Wyman C, Kustu S. 1998. The bacterial enhancer-binding protein NtrC as a molecular machine. Cold Spring Harb Symp Quant Biol 63:157–66.

33. Tanaka K, Takahashi H. 1994. Cloning, analysis and expression of an rpoS homologue gene from Pseudomonas aeruginosa PAO1. Gene 150:81–5.

34. Schuster M, Hawkins AC, Harwood CS, Greenberg EP. 2004. The Pseudomonas aeruginosa RpoS regulon and its relationship to quorum sensing. Mol Microbiol 51:973–985.

35. Xu KD, Franklin MJ, Park C-H, McFeters GA, Stewart PS. 2001. Gene expression and protein levels of the stationary phase sigma factor, RpoS, in continuously-fed Pseudomonas aeruginosa biofilms. FEMS Microbiol Lett 199:67–71.

36. Pérez-Osorio AC, Williamson KS, Franklin MJ. 2010. Heterogeneous rpoS and rhlR mRNA levels and 16S rRNA/rDNA (rRNA gene) ratios within Pseudomonas aeruginosa biofilms, sampled by laser capture microdissection. J Bacteriol 192:2991–3000.

37. Stewart PS, Franklin MJ. 2008. Physiological heterogeneity in biofilms. Nat Rev Microbiol 6:199–210.

38. Fujita M, Tanaka K, Takahashi H, Amemura A. 1994. Transcription of the principal sigma-factor genes, rpoD and rpoS, in Pseudomonas aeruginosa is controlled according to the growth phase. Mol Microbiol 13:1071–7.

39. Schuster M, Greenberg EP. 2007. Early activation of quorum sensing in Pseudomonas aeruginosa reveals the architecture of a complex regulon. BMC Genomics 8:287.

40. Whiteley M, Parsek MR, Greenberg EP. 2000. Regulation of quorum sensing by RpoS in Pseudomonas aeruginosa. J Bacteriol 182:4356–60.

41. Suh SJ, Silo-Suh L, Woods DE, Hassett DJ, West SE, Ohman DE. 1999. Effect of rpoS mutation on the stress response and expression of virulence factors in Pseudomonas aeruginosa. J Bacteriol 181:3890–7.

42. Irie Y, Starkey M, Edwards AN, Wozniak DJ, Romeo T, Parsek MR. 2010. Pseudomonas aeruginosa biofilm matrix polysaccharide Psl is regulated transcriptionally by RpoS and post-transcriptionally by RsmA. Mol Microbiol 78:no-no.

43. Murakami K, Ono T, Viducic D, Kayama S, Mori M, Hirota K, Nemoto K, Miyake Y. 2005. Role for *rpoS* gene of *Pseudomonas aeruginosa* in antibiotic tolerance. FEMS Microbiol Lett 242:161–167.

44. Kayama S, Murakami K, Ono T, Ushimaru M, Yamamoto A, Hirota K, Miyake Y. 2009. The role of *rpoS* gene and quorum-sensing system in ofloxacin tolerance in *Pseudomonas aeruginosa*. FEMS Microbiol Lett 298:184–192.

45. Stewart PS, Franklin MJ, Williamson KS, Folsom JP, Boegli L, James GA. 2015. Contribution of stress responses to antibiotic tolerance in Pseudomonas aeruginosa biofilms. Antimicrob Agents Chemother 59:3838–47.

46. Jorgensen F, Bally M, Chapon-Herve V, Michel G, Lazdunski A, Williams P, Stewart GSAB. 1999. RpoS-dependent stress tolerance in Pseudomonas aeruginosa. Microbiology 145:835–844.

47. Basta DW, Bergkessel M, Newman DK. 2017. Identification of Fitness Determinants during Energy-Limited Growth Arrest in *Pseudomonas aeruginosa*. MBio 8.

48. Kojic M, Venturi V. 2001. Regulation of rpoS gene expression in Pseudomonas: involvement of a TetR family regulator. J Bacteriol 183:3712–20.

49. Kojic M, Aguilar C, Venturi V. 2002. TetR family member psrA directly binds the Pseudomonas rpoS and psrA promoters. J Bacteriol 184:2324–30.

50. Kojic M, Jovcic B, Vindigni A, Odreman F, Venturi V. 2005. Novel target genes of PsrA transcriptional regulator of *Pseudomonas aeruginosa*. FEMS Microbiol Lett 246:175–181.

51. Kang Y, Nguyen DT, Son MS, Hoang TT. 2008. The Pseudomonas aeruginosa PsrA responds to long-chain fatty acid signals to regulate the fadBA5 -oxidation operon. Microbiology 154:1584–1598.

52. Kang Y, Lunin V V., Skarina T, Savchenko A, Schurr MJ, Hoang TT. 2009. The long-chain fatty acid sensor, PsrA, modulates the expression of *rpoS* and the type III secretion *exsCEBA* operon in *Pseudomonas aeruginosa*. Mol Microbiol 73:120–136.

53. Venturi V. 2003. Control of rpoS transcription in Escherichia coli and Pseudomonas: why so different? Mol Microbiol 49:1–9.

54. Bouillet S, Ba M, Houot L, Iobbi-Nivol C, Bordi C. 2019. Connected partner-switches control the life style of Pseudomonas aeruginosa through RpoS regulation. Sci Rep 9:6496.

55. Lu P, Wang Y, Hu Y, Chen S. 2018. RgsA, an RpoS-dependent sRNA, negatively regulates rpoS expression in Pseudomonas aeruginosa. Microbiology 164:716–724.

56. Thi Bach Nguyen H, Romero A. D, Amman F, Sorger-Domenigg T, Tata M, Sonnleitner E, Bläsi U. 2018. Negative Control of RpoS Synthesis by the sRNA ReaL in Pseudomonas aeruginosa. Front Microbiol 9:2488.

57. van Delden C, Comte R, Bally AM. 2001. Stringent response activates quorum sensing and modulates cell density-dependent gene expression in Pseudomonas aeruginosa. J Bacteriol 183:5376–84.

58. Lloyd MG, Lundgren BR, Hall CW, Gagnon LB-P, Mah T-F, Moffat JF, Nomura CT. 2017. Targeting the alternative sigma factor RpoN to combat virulence in Pseudomonas aeruginosa. Sci Rep 7:12615.

59. Hendrickson EL, Plotnikova J, Mahajan-Miklos S, Rahme LG, Ausubel FM. 2001. Differential roles of the Pseudomonas aeruginosa PA14 rpoN gene in pathogenicity in plants, nematodes, insects, and mice. J Bacteriol 183:7126–34.

60. Hagins JM, Scoffield JA, Suh SJ, Silo-Suh L. 2010. Influence of RpoN on isocitrate lyase activity in Pseudomonas aeruginosa. Microbiology 156:1201–1210.

61. Viducic D, Murakami K, Amoh T, Ono T, Miyake Y. 2017. RpoN Promotes Pseudomonas aeruginosa Survival in the Presence of Tobramycin. Front Microbiol 8:839.

62. Hagins JM, Scoffield J, Suh S-J, Silo-Suh L. 2011. Malate synthase expression is deregulated in the Pseudomonas aeruginosa cystic fibrosis isolate FRD1. Can J Microbiol 57:186–195.

63. Behrends V, Bell TJ, Liebeke M, Cordes-Blauert A, Ashraf SN, Nair C, Zlosnik JEA, Williams HD, Bundy JG. 2013. Metabolite profiling to characterize disease-related bacteria: gluconate excretion by Pseudomonas aeruginosa mutants and clinical isolates from cystic fibrosis patients. J Biol Chem 288:15098–109.

64. Totten PA, Lara JC, Lory S. 1990. The rpoN gene product of Pseudomonas aeruginosa is required for expression of diverse genes, including the flagellin gene. J Bacteriol 172:389.

65. Ishimoto KS, Lory S. 1989. Formation of pilin in Pseudomonas aeruginosa requires the alternative sigma factor (RpoN) of RNA polymerase. Proc Natl Acad Sci U S A 86:1954–7.

66. Valentini M, Storelli N, Lapouge K. 2011. Identification of C(4)-dicarboxylate transport systems in Pseudomonas aeruginosa PAO1. J Bacteriol 193:4307–16.

67. Browning DF, Busby SJW. 2004. The regulation of bacterial transcription initiation. Nat Rev Microbiol 2:57–65.

68. Balleza E, López-Bojorquez LN, Martínez-Antonio A, Resendis-Antonio O, Lozada-Chávez I, Balderas-Martínez YI, Encarnación S, Collado-Vides J. 2009. Regulation by transcription factors in bacteria: beyond description. FEMS Microbiol Rev 33:133–51.

69. Mitrophanov AY, Groisman EA. 2008. Signal integration in bacterial two-component regulatory systems. Genes Dev 22:2601–11.

70. Zschiedrich CP, Keidel V, Szurmant H. 2016. Molecular Mechanisms of Two-Component Signal Transduction. J Mol Biol 428:3752–75.

71. Maddocks SE, Oyston PCF. 2008. Structure and function of the LysR-type transcriptional regulator (LTTR) family proteins. Microbiology 154:3609–23.

72. Ulrich LE, Koonin E V, Zhulin IB. 2005. One-component systems dominate signal transduction in prokaryotes. Trends Microbiol 13:52–6.

73. Gao R, Mack TR, Stock AM. 2007. Bacterial Response Regulators: Versatile Regulatory Strategies from Common Domains. Trends Biochem Sci 32:225.

74. Rodrigue A, Quentin Y, Lazdunski A, Méjean V, Foglino M. 2000. Cell signalling by oligosaccharides. Two-component systems in Pseudomonas aeruginosa: why so many? Trends Microbiol 8:498–504.

75. Gooderham WJ, Hancock REW. 2009. Regulation of virulence and antibiotic resistance by two-component regulatory systems in *Pseudomonas aeruginosa*. FEMS Microbiol Rev 33:279–294.

76. Francis VI, Stevenson EC, Porter SL. 2017. Two-component systems required for virulence in Pseudomonas aeruginosa. FEMS Microbiol Lett 364.

77. Rodrigue A, Quentin Y, Lazdunski A, Méjean V, Foglino M. 2000. Two-component systems in Pseudomonas aeruginosa: why so many? Trends Microbiol 8:498–504.

78. Valentini M, Lapouge K. 2013. Catabolite repression in *Pseudomonas aeruginosa* PAO1 regulates the uptake of C_4 -dicarboxylates depending on succinate concentration. Environ

Microbiol 15:1707–1716.

79. Janausch I., Zientz E, Tran Q., Kröger A, Unden G. 2002. C4-dicarboxylate carriers and sensors in bacteria. Biochim Biophys Acta - Bioenerg 1553:39–56.

80. Cheung J, Hendrickson WA. 2008. Crystal structures of C4-dicarboxylate ligand complexes with sensor domains of histidine kinases DcuS and DctB. J Biol Chem 283:30256–65.

81. LIU P. 1952. Utilization of carbohydrates by Pseudomonas aeruginosa. J Bacteriol 64:773–81.

82. Winsor GL, Griffiths EJ, Lo R, Dhillon BK, Shay JA, Brinkman FSL. 2016. Enhanced annotations and features for comparing thousands of *Pseudomonas* genomes in the Pseudomonas genome database. Nucleic Acids Res 44:D646–D653.

83. Marchler-Bauer A, Derbyshire MK, Gonzales NR, Lu S, Chitsaz F, Geer LY, Geer RC, He J, Gwadz M, Hurwitz DI, Lanczycki CJ, Lu F, Marchler GH, Song JS, Thanki N, Wang Z, Yamashita RA, Zhang D, Zheng C, Bryant SH. 2015. CDD: NCBI's conserved domain database. Nucleic Acids Res 43:D222-6.

84. Rojo F. 2010. Carbon catabolite repression in *Pseudomonas* : optimizing metabolic versatility and interactions with the environment. FEMS Microbiol Rev 34:658–684.

85. Sonnleitner E, Valentini M, Wenner N, Haichar F el Z, Haas D, Lapouge K. 2012. Novel Targets of the CbrAB/Crc Carbon Catabolite Control System Revealed by Transcript Abundance in Pseudomonas aeruginosa. PLoS One 7:e44637.

86. Bush K, Courvalin P, Dantas G, Davies J, Eisenstein B, Huovinen P, Jacoby GA, Kishony R, Kreiswirth BN, Kutter E, Lerner SA, Levy S, Lewis K, Lomovskaya O, Miller JH, Mobashery S, Piddock LJ V, Projan S, Thomas CM, Tomasz A, Tulkens PM, Walsh TR, Watson JD, Witkowski J, Witte W, Wright G, Yeh P, Zgurskaya HI. 2011. Tackling antibiotic resistance. Nat Rev Microbiol 9:894–6.

87. Brauner A, Fridman O, Gefen O, Balaban NQ. 2016. Distinguishing between resistance, tolerance and persistence to antibiotic treatment. Nat Rev Microbiol 14:320–330.

88. Cox G, Wright GD. 2013. Intrinsic antibiotic resistance: Mechanisms, origins, challenges and solutions. Int J Med Microbiol 303:287–292.

89. Blair JMA, Webber MA, Baylay AJ, Ogbolu DO, Piddock LJ V. 2015. Molecular mechanisms of antibiotic resistance. Nat Rev Microbiol 13:42–51.

90. Davies J, Davies D. 2010. Origins and evolution of antibiotic resistance. Microbiol Mol Biol Rev 74:417–33.

91. Krahn T, Gilmour C, Tilak J, Fraud S, Kerr N, Lau CH-F, Poole K. 2012. Determinants of Intrinsic Aminoglycoside Resistance in Pseudomonas aeruginosa. Antimicrob Agents Chemother 56:5591–5602.

92. Lewis K. 2008. Multidrug tolerance of biofilms and persister cells. Curr Top Microbiol Immunol 322:107–31.

93. Dever LA, Dermody TS. 1991. Mechanisms of Bacterial Resistance to Antibiotics. Arch Intern Med 151:886.

94. Ramsey BW, Pepe MS, Quan JM, Otto KL, Montgomery AB, Williams-Warren J, Vasiljev-K M, Borowitz D, Bowman CM, Marshall BC, Marshall S, Smith AL. 1999. Intermittent Administration of Inhaled Tobramycin in Patients with Cystic Fibrosis. N Engl J Med 340:23–30.

95. Serio AW, Keepers T, Andrews L, Krause KM. 2018. Aminoglycoside Revival: Review of a Historically Important Class of Antimicrobials Undergoing Rejuvenation. EcoSal Plus 8.

96. Hancock REW. 1984. Alterations in Outer Membrane Permeability. Annu Rev Microbiol 38:237–264.

97. Krause KM, Serio AW, Kane TR, Connolly LE. 2016. Aminoglycosides: An Overview. Cold Spring Harb Perspect Med 6.

98. Bryan LE, O'Hara K, Wong S. 1984. Lipopolysaccharide changes in impermeability-type aminoglycoside resistance in Pseudomonas aeruginosa. Antimicrob Agents Chemother 26:250–5.

99. Bryan LE, Nicas T, Holloway BW, Crowther C. 1980. Aminoglycoside-resistant mutation of Pseudomonas aeruginosa defective in cytochrome c552 and nitrate reductase. Antimicrob Agents Chemother 17:71–9.

100. Schurek KN, Marr AK, Taylor PK, Wiegand I, Semenec L, Khaira BK, Hancock REW. 2008. Novel Genetic Determinants of Low-Level Aminoglycoside Resistance in Pseudomonas aeruginosa. Antimicrob Agents Chemother 52:4213–4219.

101. Dötsch A, Becker T, Pommerenke C, Magnowska Z, Jänsch L, Häussler S. 2009. Genomewide identification of genetic determinants of antimicrobial drug resistance in Pseudomonas aeruginosa. Antimicrob Agents Chemother 53:2522–31.

102. Hay T, Fraud S, Lau CH-F, Gilmour C, Poole K. 2013. Antibiotic Inducibility of the mexXY Multidrug Efflux Operon of Pseudomonas aeruginosa: Involvement of the MexZ Anti-Repressor ArmZ. PLoS One 8:e56858.

103. Guénard S, Muller C, Monlezun L, Benas P, Broutin I, Jeannot K, Plésiat P. 2014. Multiple mutations lead to MexXY-OprM-dependent aminoglycoside resistance in clinical strains of Pseudomonas aeruginosa. Antimicrob Agents Chemother 58:221–8.

104. Morita Y, Sobel ML, Poole K. 2006. Antibiotic inducibility of the MexXY multidrug efflux system of Pseudomonas aeruginosa: involvement of the antibiotic-inducible PA5471 gene product. J Bacteriol 188:1847–55.

105. Muller C, Plésiat P, Jeannot K. 2011. A two-component regulatory system interconnects resistance to polymyxins, aminoglycosides, fluoroquinolones, and β-lactams in Pseudomonas aeruginosa. Antimicrob Agents Chemother 55:1211–21.

106. Poole K. 2005. Aminoglycoside resistance in Pseudomonas aeruginosa. Antimicrob Agents Chemother 49:479–87.

107. Llano-Sotelo B, Azucena EF, Kotra LP, Mobashery S, Chow CS. 2002. Aminoglycosides modified by resistance enzymes display diminished binding to the bacterial ribosomal aminoacyl-tRNA site. Chem Biol 9:455–63.

108. Islam S, Oh H, Jalal S, Karpati F, Ciofu O, Høiby N, Wretlind B. 2009. Chromosomal mechanisms of aminoglycoside resistance in Pseudomonas aeruginosa isolates from cystic fibrosis patients. Clin Microbiol Infect 15:60–66.

109. Bolard A, Plésiat P, Jeannot K. 2017. Mutations in Gene fusA1 as a Novel Mechanism of Aminoglycoside Resistance in Clinical Strains of Pseudomonas aeruginosa. Antimicrob Agents Chemother 62.

110. Lee S, Hinz A, Bauerle E, Angermeyer A, Juhaszova K, Kaneko Y, Singh PK, Manoil C. 2009. Targeting a bacterial stress response to enhance antibiotic action. Proc Natl Acad Sci U S A 106:14570–5.

111. Lau CH-F, Fraud S, Jones M, Peterson SN, Poole K. 2013. Mutational Activation of the AmgRS Two-Component System in Aminoglycoside-Resistant Pseudomonas aeruginosa. Antimicrob Agents Chemother 57:2243–2251.

112. Hinz A, Lee S, Jacoby K, Manoil C. 2011. Membrane proteases and aminoglycoside antibiotic resistance. J Bacteriol 193:4790–7.

113. Levin BR, Rozen DE. 2006. Non-inherited antibiotic resistance. Nat Rev Microbiol 4:556–562.

114. Balaban NQ, Helaine S, Lewis K, Ackermann M, Aldridge B, Andersson DI, Brynildsen MP, Bumann D, Camilli A, Collins JJ, Dehio C, Fortune S, Ghigo J-M, Hardt W-D, Harms A, Heinemann M, Hung DT, Jenal U, Levin BR, Michiels J, Storz G, Tan M-W, Tenson T, Van Melderen L, Zinkernagel A. 2019. Definitions and guidelines for research on antibiotic persistence. Nat Rev Microbiol.

115. Costerton JW, Stewart PS, Greenberg EP. 1999. Bacterial biofilms: a common cause of persistent infections. Science 284:1318–22.

116. Singh PK, Schaefer AL, Parsek MR, Moninger TO, Welsh MJ, Greenberg EP. 2000. Quorum-sensing signals indicate that cystic fibrosis lungs are infected with bacterial biofilms. Nature 407:762–4.

117. O'Toole G, Kaplan HB, Kolter R. 2000. Biofilm formation as microbial development. Annu Rev Microbiol 54:49–79.

118. Sauer K, Camper AK, Ehrlich GD, Costerton JW, Davies DG. 2002. Pseudomonas aeruginosa Displays Multiple Phenotypes during Development as a Biofilm. J Bacteriol 184:1140–1154.

119. Southey-Pillig CJ, Davies DG, Sauer K. 2005. Characterization of temporal protein production in Pseudomonas aeruginosa biofilms. J Bacteriol 187:8114–26.

120. Monds RD, O'Toole GA. 2009. The developmental model of microbial biofilms: ten years of a paradigm up for review. Trends Microbiol 17:73–87.

121. Petrova OE, Sauer K. 2012. Sticky Situations: Key Components That Control Bacterial Surface Attachment. J Bacteriol 194:2413–2425.

122. Hoffman LR, D'Argenio DA, MacCoss MJ, Zhang Z, Jones RA, Miller SI. 2005. Aminoglycoside antibiotics induce bacterial biofilm formation. Nature 436:1171–5.

123. Petrova OE, Sauer K. 2016. Escaping the biofilm in more than one way: desorption, detachment or dispersion. Curr Opin Microbiol 30:67–78.

124. Babin BM, Atangcho L, van Eldijk MB, Sweredoski MJ, Moradian A, Hess S, Tolker-Nielsen T, Newman DK, Tirrell DA. 2017. Selective Proteomic Analysis of Antibiotic-Tolerant Cellular Subpopulations in Pseudomonas aeruginosa Biofilms. MBio 8:e01593-17.

125. Williamson KS, Richards LA, Perez-Osorio AC, Pitts B, McInnerney K, Stewart PS, Franklin MJ. 2012. Heterogeneity in Pseudomonas aeruginosa biofilms includes expression of ribosome hibernation factors in the antibiotic-tolerant subpopulation and hypoxia-induced stress response in the metabolically active population. J Bacteriol 194:2062–73.

126. Chua SL, Yam JKH, Hao P, Adav SS, Salido MM, Liu Y, Givskov M, Sze SK, Tolker-Nielsen T, Yang L. 2016. Selective labelling and eradication of antibiotic-tolerant bacterial populations in Pseudomonas aeruginosa biofilms. Nat Commun 7:10750.

127. Zhang L, Chiang W-C, Gao Q, Givskov M, Tolker-Nielsen T, Yang L, Zhang G. 2012. The catabolite repression control protein Crc plays a role in the development of antimicrobial-tolerant subpopulations in Pseudomonas aeruginosa biofilms. Microbiology 158:3014–9.

128. Heacock-Kang Y, Sun Z, Zarzycki-Siek J, McMillan IA, Norris MH, Bluhm AP, Cabanas D, Fogen D, Vo H, Donachie SP, Borlee BR, Sibley CD, Lewenza S, Schurr MJ, Schweizer HP, Hoang TT. 2017. Spatial transcriptomes within the *Pseudomonas aeruginosa* biofilm architecture. Mol Microbiol 106:976–985.

129. Whiteley M, Bangera MG, Bumgarner RE, Parsek MR, Teitzel GM, Lory S, Greenberg EP. 2001. Gene expression in Pseudomonas aeruginosa biofilms. Nature 413:860–4.

130. Waite RD, Paccanaro A, Papakonstantinopoulou A, Hurst JM, Saqi M, Littler E, Curtis MA. 2006. Clustering of Pseudomonas aeruginosa transcriptomes from planktonic cultures, developing and mature biofilms reveals distinct expression profiles. BMC Genomics 7:162.

131. Waite RD, Papakonstantinopoulou A, Littler E, Curtis MA. 2005. Transcriptome Analysis of Pseudomonas aeruginosa Growth: Comparison of Gene Expression in Planktonic Cultures and Developing and Mature Biofilms. J Bacteriol 187:6571–6576.

132. Dötsch A, Eckweiler D, Schniederjans M, Zimmermann A, Jensen V, Scharfe M, Geffers R, Häussler S. 2012. The Pseudomonas aeruginosa transcriptome in planktonic cultures and static biofilms using RNA sequencing. PLoS One 7:e31092.

133. Park AJ, Surette MD, Khursigara CM. 2014. Antimicrobial targets localize to the extracellular vesicle-associated proteome of Pseudomonas aeruginosa grown in a biofilm.

Front Microbiol 5:464.

134. Stewart PS, Costerton JW. 2001. Antibiotic resistance of bacteria in biofilms. Lancet 358:135–8.

135. Costerton JW, Cheng KJ, Geesey GG, Ladd TI, Nickel JC, Dasgupta M, Marrie TJ. 1987. Bacterial Biofilms in Nature and Disease. Annu Rev Microbiol 41:435–464.

136. Nickel JC, Ruseska I, Wright JB, Costerton JW. 1985. Tobramycin resistance of Pseudomonas aeruginosa cells growing as a biofilm on urinary catheter material. Antimicrob Agents Chemother 27:619–24.

137. Mah T-F. 2012. Biofilm-specific antibiotic resistance. Future Microbiol 7:1061–72.

138. Mah TF, O'Toole GA. 2001. Mechanisms of biofilm resistance to antimicrobial agents. Trends Microbiol 9:34–9.

139. Ito A, Taniuchi A, May T, Kawata K, Okabe S. 2009. Increased antibiotic resistance of Escherichia coli in mature biofilms. Appl Environ Microbiol 75:4093–100.

140. Alhede M, Kragh KN, Qvortrup K, Allesen-Holm M, van Gennip M, Christensen LD, Jensen PØ, Nielsen AK, Parsek M, Wozniak D, Molin S, Tolker-Nielsen T, Høiby N, Givskov M, Bjarnsholt T. 2011. Phenotypes of non-attached Pseudomonas aeruginosa aggregates resemble surface attached biofilm. PLoS One 6:e27943.

141. Bowler LL, Zhanel GG, Ball TB, Saward LL. 2012. Mature Pseudomonas aeruginosa biofilms prevail compared to young biofilms in the presence of ceftazidime. Antimicrob Agents Chemother 56:4976–9.

142. Haaber J, Cohn MT, Frees D, Andersen TJ, Ingmer H. 2012. Planktonic aggregates of Staphylococcus aureus protect against common antibiotics. PLoS One 7:e41075.

143. Stewart PS. 2015. Antimicrobial Tolerance in Biofilms. Microbiol Spectr 3.

144. Ciofu O, Rojo-Molinero E, Macià MD, Oliver A. 2017. Antibiotic treatment of biofilm infections. APMIS 125:304–319.

145. Römling U, Balsalobre C. 2012. Biofilm infections, their resilience to therapy and innovative treatment strategies. J Intern Med 272:541–561.

146. Koo H, Allan RN, Howlin RP, Stoodley P, Hall-Stoodley L. 2017. Targeting microbial biofilms: current and prospective therapeutic strategies. Nat Rev Microbiol 15:740–755.

147. Mah T-F, Pitts B, Pellock B, Walker GC, Stewart PS, O'Toole GA. 2003. A genetic basis for Pseudomonas aeruginosa biofilm antibiotic resistance. Nature 426:306–310.

148. Sadovskaya I, Vinogradov E, Li J, Hachani A, Kowalska K, Filloux A. 2010. High-level antibiotic resistance in Pseudomonas aeruginosa biofilm: the ndvB gene is involved in the production of highly glycerol-phosphorylated beta-(1->3)-glucans, which bind aminoglycosides. Glycobiology 20:895–904.

149. Beaudoin T, Zhang L, Hinz AJ, Parr CJ, Mah T-F. 2012. The biofilm-specific antibiotic resistance gene ndvB is important for expression of ethanol oxidation genes in

Pseudomonas aeruginosa biofilms. J Bacteriol 194:3128–36.

150. Levin-Reisman I, Ronin I, Gefen O, Braniss I, Shoresh N, Balaban NQ. 2017. Antibiotic tolerance facilitates the evolution of resistance. Science (80-) 355:826–830.

151. Gilbert P, Allison DG, McBain AJ. 2002. Biofilms in vitro and in vivo: do singular mechanisms imply cross-resistance? J Appl Microbiol 92 Suppl:98S–110S.

152. Zhang L, Hinz AJ, Nadeau J-P, Mah T-F. 2011. Pseudomonas aeruginosa tssC1 links type VI secretion and biofilm-specific antibiotic resistance. J Bacteriol 193:5510–3.

153. Zhang L, Mah T-F. 2008. Involvement of a novel efflux system in biofilm-specific resistance to antibiotics. J Bacteriol 190:4447–52.

154. Zhang L, Fritsch M, Hammond L, Landreville R, Slatculescu C, Colavita A, Mah T-F. 2013. Identification of genes involved in Pseudomonas aeruginosa biofilm-specific resistance to antibiotics. PLoS One 8:e61625.

155. Breedveld MW, Miller KJ. 1994. Cyclic beta-glucans of members of the family Rhizobiaceae. Microbiol Rev 58:145–61.

156. Mennink-Kersten MASH, Ruegebrink D, Verweij PE. 2008. Pseudomonas aeruginosa as a cause of 1,3-beta-D-glucan assay reactivity. Clin Infect Dis 46:1930–1.

157. Koya J, Nannya Y, Kobayashi H, Okugawa S, Moriya K, Kurokawa M. 2013. Simultaneous increase in 1,3-β-D-glucan and procalcitonin levels in Pseudomonas aeruginosa infection. J Infect 67:164–6.

158. Filloux A, Hachani A, Bleves S. 2008. The bacterial type VI secretion machine: yet another player for protein transport across membranes. Microbiology 154:1570–83.

159. Ho BT, Dong TG, Mekalanos JJ. 2014. A view to a kill: the bacterial type VI secretion system. Cell Host Microbe 15:9–21.

160. Russell AB, Peterson SB, Mougous JD. 2014. Type VI secretion system effectors: poisons with a purpose. Nat Rev Microbiol 12:137–48.

161. Cianfanelli FR, Monlezun L, Coulthurst SJ. 2016. Aim, Load, Fire: The Type VI Secretion System, a Bacterial Nanoweapon. Trends Microbiol 24:51–62.

162. Lossi NS, Manoli E, Förster A, Dajani R, Pape T, Freemont P, Filloux A. 2013. The HsiB1C1 (TssB-TssC) complex of the Pseudomonas aeruginosa type VI secretion system forms a bacteriophage tail sheathlike structure. J Biol Chem 288:7536–48.

163. Bagge N, Hentzer M, Andersen JB, Ciofu O, Givskov M, Høiby N. 2004. Dynamics and spatial distribution of beta-lactamase expression in Pseudomonas aeruginosa biofilms. Antimicrob Agents Chemother 48:1168–74.

164. Borriello G, Werner E, Roe F, Kim AM, Ehrlich GD, Stewart PS. 2004. Oxygen limitation contributes to antibiotic tolerance of Pseudomonas aeruginosa in biofilms. Antimicrob Agents Chemother 48:2659–64.

165. Werner E, Roe F, Bugnicourt A, Franklin MJ, Heydorn A, Molin S, Pitts B, Stewart PS.

2004. Stratified growth in Pseudomonas aeruginosa biofilms. Appl Environ Microbiol 70:6188–96.

166. Lenz AP, Williamson KS, Pitts B, Stewart PS, Franklin MJ. 2008. Localized gene expression in Pseudomonas aeruginosa biofilms. Appl Environ Microbiol 74:4463–71.

167. de Beer D, Stoodley P, Roe F, Lewandowski Z. 1994. Effects of biofilm structures on oxygen distribution and mass transport. Biotechnol Bioeng 43:1131–8.

168. Anderl JN, Franklin MJ, Stewart PS. 2000. Role of antibiotic penetration limitation in Klebsiella pneumoniae biofilm resistance to ampicillin and ciprofloxacin. Antimicrob Agents Chemother 44:1818–24.

169. Walters MC, Roe F, Bugnicourt A, Franklin MJ, Stewart PS. 2003. Contributions of antibiotic penetration, oxygen limitation, and low metabolic activity to tolerance of Pseudomonas aeruginosa biofilms to ciprofloxacin and tobramycin. Antimicrob Agents Chemother 47:317–23.

170. Stewart PS, Zhang T, Xu R, Pitts B, Walters MC, Roe F, Kikhney J, Moter A. 2016. Reaction–diffusion theory explains hypoxia and heterogeneous growth within microbial biofilms associated with chronic infections. npj Biofilms Microbiomes 2:16012.

171. Anderl JN, Zahller J, Roe F, Stewart PS. 2003. Role of nutrient limitation and stationary-phase existence in Klebsiella pneumoniae biofilm resistance to ampicillin and ciprofloxacin. Antimicrob Agents Chemother 47:1251–6.

172. Crabbé A, Jensen PØ, Bjarnsholt T, Coenye T. 2019. Antimicrobial Tolerance and Metabolic Adaptations in Microbial Biofilms. Trends Microbiol.

173. Tuomanen E, Cozens R, Tosch W, Zak O, Tomasz A. 1986. The rate of killing of Escherichia coli by beta-lactam antibiotics is strictly proportional to the rate of bacterial growth. J Gen Microbiol 132:1297–304.

174. BROWN MRW, ALLISON DG, GILBERT P. 1988. Resistance of bacterial biofilms to antibiotics a growth-rate related effect? J Antimicrob Chemother 22:777–780.

175. Eng RH, Padberg FT, Smith SM, Tan EN, Cherubin CE. 1991. Bactericidal effects of antibiotics on slowly growing and nongrowing bacteria. Antimicrob Agents Chemother 35:1824–8.

176. Evans DJ, Allison DG, Brown MR, Gilbert P. 1991. Susceptibility of Pseudomonas aeruginosa and Escherichia coli biofilms towards ciprofloxacin: effect of specific growth rate. J Antimicrob Chemother 27:177–84.

177. Waite RD, Papakonstantinopoulou A, Littler E, Curtis MA. 2005. Transcriptome analysis of Pseudomonas aeruginosa growth: comparison of gene expression in planktonic cultures and developing and mature biofilms. J Bacteriol 187:6571–6.

178. Folsom JP, Richards L, Pitts B, Roe F, Ehrlich GD, Parker A, Mazurie A, Stewart PS. 2010. Physiology of Pseudomonas aeruginosa in biofilms as revealed by transcriptome analysis. BMC Microbiol 10:294.

179. Nguyen D, Joshi-Datar A, Lepine F, Bauerle E, Olakanmi O, Beer K, McKay G, Siehnel R, Schafhauser J, Wang Y, Britigan BE, Singh PK. 2011. Active starvation responses mediate antibiotic tolerance in biofilms and nutrient-limited bacteria. Science 334:982–6.

180. Verstraeten N, Knapen WJ, Kint CI, Liebens V, Van den Bergh B, Dewachter L, Michiels JE, Fu Q, David CC, Fierro AC, Marchal K, Beirlant J, Versées W, Hofkens J, Jansen M, Fauvart M, Michiels J. 2015. Obg and Membrane Depolarization Are Part of a Microbial Bet-Hedging Strategy that Leads to Antibiotic Tolerance. Mol Cell 59:9–21.

181. Martins D, McKay G, Sampathkumar G, Khakimova M, English AM, Nguyen D. 2018. Superoxide dismutase activity confers (p)ppGpp-mediated antibiotic tolerance to stationary-phase *Pseudomonas aeruginosa*. Proc Natl Acad Sci 115:9797–9802.

182. Khakimova M, Ahlgren HG, Harrison JJ, English AM, Nguyen D. 2013. The stringent response controls catalases in Pseudomonas aeruginosa and is required for hydrogen peroxide and antibiotic tolerance. J Bacteriol 195:2011–20.

183. Navarro Llorens JM, Tormo A, Martínez-García E. 2010. Stationary phase in gram-negative bacteria. FEMS Microbiol Rev 34:476–495.

184. Bergkessel M, Basta DW, Newman DK. 2016. The physiology of growth arrest: uniting molecular and environmental microbiology. Nat Rev Microbiol 14:549–562.

185. Meylan S, Porter CBM, Yang JH, Belenky P, Gutierrez A, Lobritz MA, Park J, Kim SH, Moskowitz SM, Collins JJ. 2017. Carbon Sources Tune Antibiotic Susceptibility in Pseudomonas aeruginosa via Tricarboxylic Acid Cycle Control. Cell Chem Biol 24:195–206.

186. Taber HW, Mueller JP, Miller PF, Arrow AS. 1987. Bacterial uptake of aminoglycoside antibiotics. Microbiol Rev 51:439–57.

187. Damper PD, Epstein W. 1981. Role of the membrane potential in bacterial resistance to aminoglycoside antibiotics. Antimicrob Agents Chemother 20:803–8.

188. Meylan S, Andrews IW, Collins JJ. 2018. Targeting Antibiotic Tolerance, Pathogen by Pathogen. Cell 172:1228–1238.

189. Koeva M, Gutu AD, Hebert W, Wager JD, Yonker LM, O'Toole GA, Ausubel FM, Moskowitz SM, Joseph-McCarthy D. 2017. An Antipersister Strategy for Treatment of Chronic Pseudomonas aeruginosa Infections. Antimicrob Agents Chemother 61:e00987-17.

190. O'Sullivan BP, Freedman SD. 2009. Cystic fibrosis. Lancet 373:1891–1904.

191. Davies JC, Alton EWFW, Bush A. 2007. Cystic fibrosis. BMJ 335:1255–9.

192. Ratjen F, Bell SC, Rowe SM, Goss CH, Quittner AL, Bush A. 2015. Cystic fibrosis. Nat Rev Dis Prim 1:15010.

193. Mak DYF, Sykes J, Stephenson AL, Lands LC. 2016. The benefits of newborn screening for cystic fibrosis: The Canadian experience. J Cyst Fibros 15:302–308.

194. Riordan JR, Rommens JM, Kerem B, Alon N, Rozmahel R, Grzelczak Z, Zielenski J, Lok

S, Plavsic N, Chou JL. 1989. Identification of the cystic fibrosis gene: cloning and characterization of complementary DNA. Science 245:1066–73.

195. Rommens JM, Iannuzzi MC, Kerem B, Drumm ML, Melmer G, Dean M, Rozmahel R, Cole JL, Kennedy D, Hidaka N. 1989. Identification of the cystic fibrosis gene: chromosome walking and jumping. Science 245:1059–65.

196. Kerem B, Rommens JM, Buchanan JA, Markiewicz D, Cox TK, Chakravarti A, Buchwald M, Tsui LC. 1989. Identification of the cystic fibrosis gene: genetic analysis. Science 245:1073–80.

197. Tsui L-C, Dorfman R. 2013. The cystic fibrosis gene: a molecular genetic perspective. Cold Spring Harb Perspect Med 3:a009472.

198. Tsui L-C. 1995. The Cystic Fibrosis Transmembrane Conductance Regulator Gene. Am J Respir Crit Care Med 151:S47–S53.

199. Bear CE, Li CH, Kartner N, Bridges RJ, Jensen TJ, Ramjeesingh M, Riordan JR. 1992. Purification and functional reconstitution of the cystic fibrosis transmembrane conductance regulator (CFTR). Cell 68:809–18.

200. Poulsen JH, Fischer H, Illek B, Machen TE. 1994. Bicarbonate conductance and pH regulatory capability of cystic fibrosis transmembrane conductance regulator. Proc Natl Acad Sci 91:5340–5344.

201. Saint-Criq V, Gray MA. 2017. Role of CFTR in epithelial physiology. Cell Mol Life Sci 74:93–115.

202. Crawford I, Maloney PC, Zeitlin PL, Guggino WB, Hyde SC, Turley H, Gatter KC, Harris A, Higgins CF. 1991. Immunocytochemical localization of the cystic fibrosis gene product CFTR. Proc Natl Acad Sci 88:9262–9266.

203. Cheng SH, Gregory RJ, Marshall J, Paul S, Souza DW, White GA, O'Riordan CR, Smith AE. 1990. Defective intracellular transport and processing of CFTR is the molecular basis of most cystic fibrosis. Cell 63:827–34.

204. Lazrak A, Fu L, Bali V, Bartoszewski R, Rab A, Havasi V, Keiles S, Kappes J, Kumar R, Lefkowitz E, Sorscher EJ, Matalon S, Collawn JF, Bebok Z. 2013. The silent codon change I507-ATC→ATT contributes to the severity of the ΔF508 CFTR channel dysfunction. FASEB J 27:4630–4645.

205. Drumm ML, Wilkinson DJ, Smit LS, Worrell RT, Strong T V, Frizzell RA, Dawson DC, Collins FS. 1991. Chloride conductance expressed by delta F508 and other mutant CFTRs in Xenopus oocytes. Science 254:1797–9.

206. Dalemans W, Barbry P, Champigny G, Jallat S, Jallat S, Dott K, Dreyer D, Crystal RG, Pavirani A, Lecocq J-P, Lazdunski M. 1991. Altered chloride ion channel kinetics associated with the ΔF508 cystic fibrosis mutation. Nature 354:526–528.

207. Sosnay PR, Siklosi KR, Van Goor F, Kaniecki K, Yu H, Sharma N, Ramalho AS, Amaral MD, Dorfman R, Zielenski J, Masica DL, Karchin R, Millen L, Thomas PJ, Patrinos GP, Corey M, Lewis MH, Rommens JM, Castellani C, Penland CM, Cutting GR. 2013.

Defining the disease liability of variants in the cystic fibrosis transmembrane conductance regulator gene. Nat Genet 45:1160–1167.

208. Welsh MJ, Smith AE. 1993. Molecular mechanisms of CFTR chloride channel dysfunction in cystic fibrosis. Cell 73:1251–4.

209. Cutting GR. 2015. Cystic fibrosis genetics: from molecular understanding to clinical application. Nat Rev Genet 16:45–56.

210. Slieker MG, Sanders EAM, Rijkers GT, Ruven HJT, van der Ent CK. 2005. Disease modifying genes in cystic fibrosis. J Cyst Fibros 4:7–13.

211. Frizzell RA, Hanrahan JW. 2012. Physiology of epithelial chloride and fluid secretion. Cold Spring Harb Perspect Med 2:a009563.

212. Gadsby DC, Vergani P, Csanády L. 2006. The ABC protein turned chloride channel whose failure causes cystic fibrosis. Nature 440:477–83.

213. Cheng SH, Rich DP, Marshall J, Gregory RJ, Welsh MJ, Smith AE. 1991. Phosphorylation of the R domain by cAMP-dependent protein kinase regulates the CFTR chloride channel. Cell 66:1027–1036.

214. Anderson MP, Berger HA, Rich DP, Gregory RJ, Smith AE, Welsh MJ. 1991. Nucleoside triphosphates are required to open the CFTR chloride channel. Cell 67:775–84.

215. Pier GB. 2002. CFTR mutations and host susceptibility to Pseudomonas aeruginosa lung infection. Curr Opin Microbiol 5:81–6.

216. Kunzelmann K, Kiser GL, Schreiber R, Riordan JR. 1997. Inhibition of epithelial Na+ currents by intracellular domains of the cystic fibrosis transmembrane conductance regulator. FEBS Lett 400:341–4.

217. Schreiber R, Hopf A, Mall M, Greger R, Kunzelmann K. 1999. The first-nucleotide binding domain of the cystic-fibrosis transmembrane conductance regulator is important for inhibition of the epithelial Na+ channel. Proc Natl Acad Sci 96:5310–5315.

218. Mall M, Grubb BR, Harkema JR, O'Neal WK, Boucher RC. 2004. Increased airway epithelial Na+ absorption produces cystic fibrosis-like lung disease in mice. Nat Med 10:487–493.

219. Knowles MR, Boucher RC. 2002. Mucus clearance as a primary innate defense mechanism for mammalian airways. J Clin Invest 109:571–7.

220. Matsui H, Davis CW, Tarran R, Boucher RC. 2000. Osmotic water permeabilities of cultured, well-differentiated normal and cystic fibrosis airway epithelia. J Clin Invest 105:1419–1427.

221. Rogers CS, Stoltz DA, Meyerholz DK, Ostedgaard LS, Rokhlina T, Taft PJ, Rogan MP, Pezzulo AA, Karp PH, Itani OA, Kabel AC, Wohlford-Lenane CL, Davis GJ, Hanfland RA, Smith TL, Samuel M, Wax D, Murphy CN, Rieke A, Whitworth K, Uc A, Starner TD, Brogden KA, Shilyansky J, McCray PB, Zabner J, Prather RS, Welsh MJ. 2008. Disruption of the CFTR Gene Produces a Model of Cystic Fibrosis in Newborn Pigs.

Science (80-) 321:1837–1841.

222. Ostedgaard LS, Meyerholz DK, Chen J-H, Pezzulo AA, Karp PH, Rokhlina T, Ernst SE, Hanfland RA, Reznikov LR, Ludwig PS, Rogan MP, Davis GJ, Dohrn CL, Wohlford-Lenane C, Taft PJ, Rector M V., Hornick E, Nassar BS, Samuel M, Zhang Y, Richter SS, Uc A, Shilyansky J, Prather RS, McCray PB, Zabner J, Welsh MJ, Stoltz DA. 2011. The F508 Mutation Causes CFTR Misprocessing and Cystic Fibrosis-Like Disease in Pigs. Sci Transl Med 3:74ra24-74ra24.

223. Meyerholz DK. 2016. Lessons learned from the cystic fibrosis pig. Theriogenology 86:427–32.

224. Chen J-H, Stoltz DA, Karp PH, Ernst SE, Pezzulo AA, Moninger TO, Rector M V., Reznikov LR, Launspach JL, Chaloner K, Zabner J, Welsh MJ. 2010. Loss of Anion Transport without Increased Sodium Absorption Characterizes Newborn Porcine Cystic Fibrosis Airway Epithelia. Cell 143:911–923.

225. Itani OA, Chen J-H, Karp PH, Ernst S, Keshavjee S, Parekh K, Klesney-Tait J, Zabner J, Welsh MJ. 2011. Human cystic fibrosis airway epithelia have reduced Cl- conductance but not increased Na+ conductance. Proc Natl Acad Sci 108:10260–10265.

226. Stoltz DA, Meyerholz DK, Pezzulo AA, Ramachandran S, Rogan MP, Davis GJ, Hanfland RA, Wohlford-Lenane C, Dohrn CL, Bartlett JA, Nelson GA, Chang EH, Taft PJ, Ludwig PS, Estin M, Hornick EE, Launspach JL, Samuel M, Rokhlina T, Karp PH, Ostedgaard LS, Uc A, Starner TD, Horswill AR, Brogden KA, Prather RS, Richter SS, Shilyansky J, McCray PB, Zabner J, Welsh MJ. 2010. Cystic Fibrosis Pigs Develop Lung Disease and Exhibit Defective Bacterial Eradication at Birth. Sci Transl Med 2:29ra31-29ra31.

227. Pezzulo AA, Tang XX, Hoegger MJ, Abou Alaiwa MH, Ramachandran S, Moninger TO, Karp PH, Wohlford-Lenane CL, Haagsman HP, van Eijk M, Bánfi B, Horswill AR, Stoltz DA, McCray PB, Welsh MJ, Zabner J. 2012. Reduced airway surface pH impairs bacterial killing in the porcine cystic fibrosis lung. Nature 487:109–113.

228. Abou Alaiwa MH, Reznikov LR, Gansemer ND, Sheets KA, Horswill AR, Stoltz DA, Zabner J, Welsh MJ. 2014. pH modulates the activity and synergism of the airway surface liquid antimicrobials β-defensin-3 and LL-37. Proc Natl Acad Sci 111:18703–18708.

229. Garland AL, Walton WG, Coakley RD, Tan CD, Gilmore RC, Hobbs CA, Tripathy A, Clunes LA, Bencharit S, Stutts MJ, Betts L, Redinbo MR, Tarran R. 2013. Molecular basis for pH-dependent mucosal dehydration in cystic fibrosis airways. Proc Natl Acad Sci 110:15973–15978.

230. Kim D, Liao J, Hanrahan JW. 2014. The buffer capacity of airway epithelial secretions. Front Physiol 5.

231. Hoegger MJ, Fischer AJ, McMenimen JD, Ostedgaard LS, Tucker AJ, Awadalla MA, Moninger TO, Michalski AS, Hoffman EA, Zabner J, Stoltz DA, Welsh MJ. 2014. Impaired mucus detachment disrupts mucociliary transport in a piglet model of cystic fibrosis. Science 345:818–22.

232. Joo NS, Cho H-J, Khansaheb M, Wine JJ. 2010. Hyposecretion of fluid from tracheal submucosal glands of CFTR-deficient pigs. J Clin Invest 120:3161–3166.

233. Meyerholz DK, Stoltz DA, Namati E, Ramachandran S, Pezzulo AA, Smith AR, Rector M V., Suter MJ, Kao S, McLennan G, Tearney GJ, Zabner J, McCray PB, Welsh MJ. 2010. Loss of Cystic Fibrosis Transmembrane Conductance Regulator Function Produces Abnormalities in Tracheal Development in Neonatal Pigs and Young Children. Am J Respir Crit Care Med 182:1251–1261.

234. Quinton PM. 2008. Cystic fibrosis: impaired bicarbonate secretion and mucoviscidosis. Lancet 372:415–417.

235. Quinton PM. 2010. Role of epithelial HCO_3^- transport in mucin secretion: lessons from cystic fibrosis. Am J Physiol Physiol 299:C1222–C1233.

236. Ratner D, Mueller C. 2012. Immune Responses in Cystic Fibrosis. Am J Respir Cell Mol Biol 46:715–722.

237. Cohen TS, Prince A. 2012. Cystic fibrosis: a mucosal immunodeficiency syndrome. Nat Med 18:509–519.

238. Lynch JP, Sayah DM, Belperio JA, Weigt SS, Weigt SS. 2015. Lung transplantation for cystic fibrosis: results, indications, complications, and controversies. Semin Respir Crit Care Med 36:299–320.

239. Adler FR, Aurora P, Barker DH, Barr ML, Blackwell LS, Bosma OH, Brown S, Cox DR, Jensen JL, Kurland G, Nossent GD, Quittner AL, Robinson WM, Romero SL, Spencer H, Sweet SC, van der Bij W, Vermeulen J, Verschuuren EAM, Vrijlandt EJLE, Walsh W, Woo MS, Liou TG. 2009. Lung transplantation for cystic fibrosis. Proc Am Thorac Soc 6:619–33.

240. Filkins LM, O'Toole GA. 2015. Cystic Fibrosis Lung Infections: Polymicrobial, Complex, and Hard to Treat. PLOS Pathog 11:e1005258.

241. Langton Hewer SC, Smyth AR. 2017. Antibiotic strategies for eradicating Pseudomonas aeruginosa in people with cystic fibrosis. Cochrane Database Syst Rev 4:CD004197.

242. Lee TWR, Brownlee KG, Conway SP, Denton M, Littlewood JM. 2003. Evaluation of a new definition for chronic Pseudomonas aeruginosa infection in cystic fibrosis patients. J Cyst Fibros 2:29–34.

243. Kerem E, Corey M, Gold R, Levison H. 1990. Pulmonary function and clinical course in patients with cystic fibrosis after pulmonary colonization with Pseudomonas aeruginosa. J Pediatr 116:714–9.

244. Konstan MW, Morgan WJ, Butler SM, Pasta DJ, Craib ML, Silva SJ, Stokes DC, Wohl MEB, Wagener JS, Regelmann WE, Johnson CA, Scientific Advisory Group and the Investigators and Coordinators of the Epidemiologic Study of Cystic Fibrosis. 2007. Risk Factors For Rate of Decline in Forced Expiratory Volume in One Second in Children and Adolescents with Cystic Fibrosis. J Pediatr 151:134–139.e1.

245. Hudson VL, Wielinski CL, Regelmann WE. 1993. Prognostic implications of initial

oropharyngeal bacterial flora in patients with cystic fibrosis diagnosed before the age of two years. J Pediatr 122:854–60.

246. Somayaji R, Lam JC, Surette MG, Waddell B, Rabin HR, Sibley CD, Purighalla S, Parkins MD. 2017. Long-term clinical outcomes of "Prairie Epidemic Strain" Pseudomonas aeruginosa infection in adults with cystic fibrosis. Thorax 72:333–339.

247. Demko CA, Byard PJ, Davis PB. 1995. Gender differences in cystic fibrosis: Pseudomonas aeruginosa infection. J Clin Epidemiol 48:1041–9.

248. Corey M, Farewell V. 1996. Determinants of Mortality from Cystic Fibrosis in Canada, 1970-1989. Am J Epidemiol 143:1007–1017.

249. Pamukcu A, Bush A, Buchdahl R. 1995. Effects of pseudomonas aeruginosa colonization on lung function and anthropometric variables in children with cystic fibrosis. Pediatr Pulmonol 19:10–5.

250. Kosorok MR, Zeng L, West SE, Rock MJ, Splaingard ML, Laxova A, Green CG, Collins J, Farrell PM. 2001. Acceleration of lung disease in children with cystic fibrosis after Pseudomonas aeruginosa acquisition. Pediatr Pulmonol 32:277–87.

251. Nixon GM, Armstrong DS, Carzino R, Carlin JB, Olinsky A, Robertson CF, Grimwood K. 2001. Clinical outcome after early Pseudomonas aeruginosa infection in cystic fibrosis. J Pediatr 138:699–704.

252. Emerson J, Rosenfeld M, McNamara S, Ramsey B, Gibson RL. 2002. Pseudomonas aeruginosa and other predictors of mortality and morbidity in young children with cystic fibrosis. Pediatr Pulmonol 34:91–100.

253. Sawicki GS, Rasouliyan L, McMullen AH, Wagener JS, McColley SA, Pasta DJ, Quittner AL. 2011. Longitudinal assessment of health-related quality of life in an observational cohort of patients with cystic fibrosis. Pediatr Pulmonol 46:36–44.

254. West SEH, Zeng L, Lee BL, Kosorok MR, Laxova A, Rock MJ, Splaingard MJ, Farrell PM. 2002. Respiratory infections with Pseudomonas aeruginosa in children with cystic fibrosis: early detection by serology and assessment of risk factors. JAMA 287:2958–67.

255. Courtney JM, Bradley J, Mccaughan J, O'connor TM, Shortt C, Bredin CP, Bradbury I, Elborn JS. 2007. Predictors of mortality in adults with cystic fibrosis. Pediatr Pulmonol 42:525–532.

256. Navarro J, Rainisio M, Harms HK, Hodson ME, Koch C, Mastella G, Strandvik B, McKenzie SG. 2001. Factors associated with poor pulmonary function: cross-sectional analysis of data from the ERCF. European Epidemiologic Registry of Cystic Fibrosis. Eur Respir J 18:298–305.

257. Ranganathan SC, Skoric B, Ramsay KA, Carzino R, Gibson A-M, Hart E, Harrison J, Bell SC, Kidd TJ, Australian Respiratory Early Surveillance Team for Cystic Fibrosis (AREST-CF) *. 2013. Geographical Differences in First Acquisition of *Pseudomonas aeruginosa* in Cystic Fibrosis. Ann Am Thorac Soc 10:108–114.

258. Kelly NM, Fitzgerald MX, Tempany E, O'Boyle C, Falkiner FR, Keane CT. 1982. Does

pseudomonas cross-infection occur between cystic-fibrosis patients. Lancet (London, England) 2:688–90.

259. Kidd TJ, Ramsay KA, Vidmar S, Carlin JB, Bell SC, Wainwright CE, Grimwood K, Wainwright CE, Grimwood K, Francis PW, Dakin C, Cheney J, George N, Carlin JB, Robertson CF, Vidmar S, Moodie M, Carzino R, Carter R, Armstrong DS, Cooper PJ, McKay K, (James) Martin A, Whitehead B, Hunter J, Byrnes CA, Tiddens HA, Graniel K, Gerbrands K, Mott L. 2015. Pseudomonas aeruginosa genotypes acquired by children with cystic fibrosis by age 5-years. J Cyst Fibros 14:361–369.

260. Grothues D, Koopmann U, von der Hardt H, Tümmler B. 1988. Genome fingerprinting of Pseudomonas aeruginosa indicates colonization of cystic fibrosis siblings with closely related strains. J Clin Microbiol 26:1973–7.

261. Jeukens J, Freschi L, Kukavica-Ibrulj I, Emond-Rheault J-G, Allard C, Barbeau J, Cantin A, Charette SJ, Déziel E, Malouin F, Milot J, Nguyen D, Popa C, Boyle B, Levesque RC. 2019. The Pseudomonas aeruginosa Population among Cystic Fibrosis Patients in Quebec, Canada: a Disease Hot Spot without Known Epidemic Isolates. J Clin Microbiol 57:e02019-18.

262. Parkins MD, Somayaji R, Waters VJ. 2018. Epidemiology, Biology, and Impact of Clonal Pseudomonas aeruginosa Infections in Cystic Fibrosis. Clin Microbiol Rev 31:e00019-18.

263. Aaron SD, Vandemheen KL, Ramotar K, Giesbrecht-Lewis T, Tullis E, Freitag A, Paterson N, Jackson M, Lougheed MD, Dowson C, Kumar V, Ferris W, Chan F, Doucette S, Fergusson D. 2010. Infection With Transmissible Strains of Pseudomonas aeruginosa and Clinical Outcomes in Adults With Cystic Fibrosis. JAMA 304:2145.

264. Beaudoin T, Aaron SD, Giesbrecht-Lewis T, Vandemheen K, Mah T-F. 2010. Characterization of clonal strains of Pseudomonas aeruginosa isolated from cystic fibrosis patients in Ontario, Canada. Can J Microbiol 56:548–57.

265. Taylor RF, Morgan DW, Nicholson PS, Mackay IS, Hodson ME, Pitt TL. 1992. Extrapulmonary sites of Pseudomonas aeruginosa in adults with cystic fibrosis. Thorax 47:426–428.

266. Hansen SK, Rau MH, Johansen HK, Ciofu O, Jelsbak L, Yang L, Folkesson A, Jarmer HØ, Aanæs K, von Buchwald C, Høiby N, Molin S. 2012. Evolution and diversification of Pseudomonas aeruginosa in the paranasal sinuses of cystic fibrosis children have implications for chronic lung infection. ISME J 6:31–45.

267. Mainz JG, Naehrlich L, Schien M, Kading M, Schiller I, Mayr S, Schneider G, Wiedemann B, Wiehlmann L, Cramer N, Pfister W, Kahl BC, Beck JF, Tummler B. 2009. Concordant genotype of upper and lower airways P aeruginosa and S aureus isolates in cystic fibrosis. Thorax 64:535–540.

268. Walter S, Gudowius P, Boßhammer J, Thorax UR-, 1997 undefined. Epidemiology of chronic Pseudomonas aeruginosa infections in the airways of lung transplant recipients with cystic fibrosis. thorax.bmj.com.

269. Aanæs K. 2013. Bacterial sinusitis can be a focus for initial lung colonisation and chronic

lung infection in patients with cystic fibrosis. J Cyst Fibros 12:S1–S20.

270. Muhlebach MS, Miller MB, Moore C, Wedd JP, Drake AF, Leigh MW. 2006. Are lower airway or throat cultures predictive of sinus bacteriology in cystic fibrosis? Pediatr Pulmonol 41:445–451.

271. Whiteson KL, Bailey B, Bergkessel M, Conrad D, Delhaes L, Felts B, Harris JK, Hunter R, Lim YW, Maughan H, Quinn R, Salamon P, Sullivan J, Wagner BD, Rainey PB. 2014. The Upper Respiratory Tract as a Microbial Source for Pulmonary Infections in Cystic Fibrosis. Parallels from Island Biogeography. Am J Respir Crit Care Med 189:1309–1315.

272. Høiby N, Frederiksen B, Pressler T. 2005. Eradication of early Pseudomonas aeruginosa infection. J Cyst Fibros 4:49–54.

273. Mogayzel PJ, Naureckas ET, Robinson KA, Mueller G, Hadjiliadis D, Hoag JB, Lubsch L, Hazle L, Sabadosa K, Marshall B, Committee the PCPG. 2013. Cystic Fibrosis Pulmonary Guidelines. Am J Respir Crit Care Med 187:680–689.

274. Mayer-Hamblett N, Ramsey BW, Kulasekara HD, Wolter DJ, Houston LS, Pope CE, Kulasekara BR, Armbruster CR, Burns JL, Retsch-Bogart G, Rosenfeld M, Gibson RL, Miller SI, Khan U, Hoffman LR. 2014. Pseudomonas aeruginosa Phenotypes Associated With Eradication Failure in Children With Cystic Fibrosis. Clin Infect Dis 59:624–631.

275. Cohen-Cymberknoh M, Gilead N, Gartner S, Rovira S, Blau H, Mussaffi H, Rivlin J, Gur M, Shteinberg M, Bentur L, Livnat G, Aviram M, Picard E, Tenenbaum A, Armoni S, Breuer O, Shoseyov D, Kerem E. 2016. Eradication failure of newly acquired Pseudomonas aeruginosa isolates in cystic fibrosis. J Cyst Fibros 15:776–782.

276. Smith WD, Bardin E, Cameron L, Edmondson CL, Farrant K V., Martin I, Murphy RA, Soren O, Turnbull AR, Wierre-Gore N, Alton EW, Bundy JG, Bush A, Connett GJ, Faust SN, Filloux A, Freemont PS, Jones AL, Takats Z, Webb JS, Williams HD, Davies JC. 2017. Current and future therapies for Pseudomonas aeruginosa infection in patients with cystic fibrosis. FEMS Microbiol Lett 364.

277. Bhatt JM. 2013. Treatment of pulmonary exacerbations in cystic fibrosis. Eur Respir Rev 22:205–16.

278. Smith S, Rowbotham NJ, Charbek E. 2018. Inhaled antibiotics for pulmonary exacerbations in cystic fibrosis. Cochrane Database Syst Rev.

279. Stenbit AE, Flume PA. 2011. Pulmonary exacerbations in cystic fibrosis. Curr Opin Pulm Med 17:1.

280. Bjarnsholt T, Jensen PØ, Fiandaca MJ, Pedersen J, Hansen CR, Andersen CB, Pressler T, Givskov M, Høiby N. 2009. *Pseudomonas aeruginosa* biofilms in the respiratory tract of cystic fibrosis patients. Pediatr Pulmonol 44:547–558.

281. Secor PR, Michaels LA, Ratjen A, Jennings LK, Singh PK. 2018. Entropically driven aggregation of bacteria by host polymers promotes antibiotic tolerance in *Pseudomonas aeruginosa*. Proc Natl Acad Sci 115:10780–10785.

282. Roberts AEL, Kragh KN, Bjarnsholt T, Diggle SP. 2015. The Limitations of In Vitro

Experimentation in Understanding Biofilms and Chronic Infection. J Mol Biol 427:3646–3661.

283. Sønderholm M, Kragh KN, Koren K, Jakobsen TH, Darch SE, Alhede M, Jensen PØ, Whiteley M, Kühl M, Bjarnsholt T. 2017. Pseudomonas aeruginosa Aggregate Formation in an Alginate Bead Model System Exhibits In Vivo-Like Characteristics. Appl Environ Microbiol 83:e00113-17.

284. Staudinger BJ, Muller JF, Halldórsson S, Boles B, Angermeyer A, Nguyen D, Rosen H, Baldursson Ó, Gottfreðsson M, Guðmundsson GH, Singh PK. 2014. Conditions Associated with the Cystic Fibrosis Defect Promote Chronic *Pseudomonas aeruginosa* Infection. Am J Respir Crit Care Med 189:812–824.

285. Palmer KL, Aye LM, Whiteley M. 2007. Nutritional cues control Pseudomonas aeruginosa multicellular behavior in cystic fibrosis sputum. J Bacteriol 189:8079–87.

286. Yan Z, Stewart ZA, Sinn PL, Olsen JC, Hu J, McCray PB, Engelhardt JF, Engelhardt JF. 2015. Ferret and pig models of cystic fibrosis: prospects and promise for gene therapy. Hum Gene Ther Clin Dev 26:38–49.

287. Didelot X, Walker AS, Peto TE, Crook DW, Wilson DJ. 2016. Within-host evolution of bacterial pathogens. Nat Rev Microbiol 14:150–162.

288. Winstanley C, O'Brien S, Brockhurst MA. 2016. Pseudomonas aeruginosa Evolutionary Adaptation and Diversification in Cystic Fibrosis Chronic Lung Infections. Trends Microbiol 24:327–337.

289. Yang L, Jelsbak L, Marvig RL, Damkiær S, Workman CT, Rau MH, Hansen SK, Folkesson A, Johansen HK, Ciofu O, Høiby N, Sommer MOA, Molin S. 2011. Evolutionary dynamics of bacteria in a human host environment. Proc Natl Acad Sci U S A 108:7481–6.

290. Folkesson A, Jelsbak L, Yang L, Johansen HK, Ciofu O, Høiby N, Molin S. 2012. Adaptation of Pseudomonas aeruginosa to the cystic fibrosis airway: an evolutionary perspective. Nat Rev Microbiol 10:841–851.

291. Nguyen D, Singh PK. 2006. Evolving stealth: genetic adaptation of Pseudomonas aeruginosa during cystic fibrosis infections. Proc Natl Acad Sci U S A 103:8305–6.

292. Yang L, Jelsbak L, Molin S. 2011. Microbial ecology and adaptation in cystic fibrosis airways. Environ Microbiol 13:1682–1689.

293. Marvig RL, Sommer LM, Molin S, Johansen HK. 2015. Convergent evolution and adaptation of Pseudomonas aeruginosa within patients with cystic fibrosis. Nat Genet 47:57–64.

294. Damkiær S, Yang L, Molin S, Jelsbak L. 2013. Evolutionary remodeling of global regulatory networks during long-term bacterial adaptation to human hosts. Proc Natl Acad Sci U S A 110:7766–71.

295. Snitkin ES, Segre JA. 2015. Pseudomonas aeruginosa adaptation to human hosts. Nat Genet 47:2–3.

296. Smith EE, Buckley DG, Wu Z, Saenphimmachak C, Hoffman LR, D'Argenio DA, Miller SI, Ramsey BW, Speert DP, Moskowitz SM, Burns JL, Kaul R, Olson M V. 2006. Genetic adaptation by Pseudomonas aeruginosa to the airways of cystic fibrosis patients. Proc Natl Acad Sci 103:8487–8492.

297. Huus KE, Joseph J, Zhang L, Wong A, Aaron SD, Mah T-F, Sad S. 2016. Clinical Isolates of Pseudomonas aeruginosa from Chronically Infected Cystic Fibrosis Patients Fail To Activate the Inflammasome during Both Stable Infection and Pulmonary Exacerbation. J Immunol 196:3097–108.

298. Li Z, Kosorok MR, Farrell PM, Laxova A, West SEH, Green CG, Collins J, Rock MJ, Splaingard ML. 2005. Longitudinal Development of Mucoid <EMPH>Pseudomonas aeruginosa</EMPH> Infection and Lung Disease Progression in Children With Cystic Fibrosis. JAMA 293:581.

299. Pritt B, O'Brien L, Winn W. 2007. Mucoid *Pseudomonas* in Cystic Fibrosis. Am J Clin Pathol 128:32–34.

300. SIMPSON JA, SMITH SE, DEAN RT. 1988. Alginate Inhibition of the Uptake of Pseudomonas aeruginosa by Macrophages. Microbiology 134:29–36.

301. Boucher JC, Yu H, Mudd MH, Deretic V. 1997. Mucoid Pseudomonas aeruginosa in cystic fibrosis: characterization of muc mutations in clinical isolates and analysis of clearance in a mouse model of respiratory infection. Infect Immun 65:3838–46.

302. Martin DW, Holloway BW, Deretic V. 1993. Characterization of a locus determining the mucoid status of Pseudomonas aeruginosa: AlgU shows sequence similarities with a Bacillus sigma factor. J Bacteriol 175:1153–1164.

303. Hershberger CD, Ye RW, Parsek MR, Xie ZD, Chakrabarty AM. 1995. The algT (algU) gene of Pseudomonas aeruginosa, a key regulator involved in alginate biosynthesis, encodes an alternative sigma factor (sigma E). Proc Natl Acad Sci 92:7941–7945.

304. Hamood AN, Griswold J, Colmer J. 1996. Characterization of elastase-deficient clinical isolates of Pseudomonas aeruginosa. Infect Immun 64:3154–60.

305. Venturi V. 2006. Regulation of quorum sensing in *Pseudomonas*. FEMS Microbiol Rev 30:274–291.

306. Hoffman LR, Kulasekara HD, Emerson J, Houston LS, Burns JL, Ramsey BW, Miller SI. 2009. Pseudomonas aeruginosa lasR mutants are associated with cystic fibrosis lung disease progression. J Cyst Fibros 8:66–70.

307. Hoffman LR, Richardson AR, Houston LS, Kulasekara HD, Martens-Habbena W, Klausen M, Burns JL, Stahl DA, Hassett DJ, Fang FC, Miller SI. 2010. Nutrient Availability as a Mechanism for Selection of Antibiotic Tolerant Pseudomonas aeruginosa within the CF Airway. PLoS Pathog 6:e1000712.

308. D'Argenio DA, Wu M, Hoffman LR, Kulasekara HD, Déziel E, Smith EE, Nguyen H, Ernst RK, Larson Freeman TJ, Spencer DH, Brittnacher M, Hayden HS, Selgrade S, Klausen M, Goodlett DR, Burns JL, Ramsey BW, Miller SI. 2007. Growth phenotypes of Pseudomonas aeruginosa lasR mutants adapted to the airways of cystic fibrosis patients.

Mol Microbiol 64:512–533.

309. Zhao K, Zhou X, Li W, Zhang X, Yue B. 2016. Nutrient reduction induced stringent responses promote bacterial quorum-sensing divergence for population fitness. Sci Rep 6:34925.

310. LaFayette SL, Houle D, Beaudoin T, Wojewodka G, Radzioch D, Hoffman LR, Burns JL, Dandekar AA, Smalley NE, Chandler JR, Zlosnik JE, Speert DP, Bernier J, Matouk E, Brochiero E, Rousseau S, Nguyen D. 2015. Cystic fibrosis–adapted *Pseudomonas aeruginosa* quorum sensing *lasR* mutants cause hyperinflammatory responses. Sci Adv 1:e1500199.

311. Hall CW, Zhang L, Mah T-F. 2017. PA3225 Is a Transcriptional Repressor of Antibiotic Resistance Mechanisms in Pseudomonas aeruginosa. Antimicrob Agents Chemother 61:e02114-16.

312. Hall CW, Hinz AJ, Gagnon LB-P, Zhang L, Nadeau J-P, Copeland S, Saha B, Mah T-F. 2018. *Pseudomonas aeruginosa* Biofilm Antibiotic Resistance Gene *ndvB* Expression Requires the RpoS Stationary-Phase Sigma Factor. Appl Environ Microbiol 84.

313. Cascales E, Cambillau C. 2012. Structural biology of type VI secretion systems. Philos Trans R Soc Lond B Biol Sci 367:1102–11.

314. Mougous JD, Cuff ME, Raunser S, Shen A, Zhou M, Gifford CA, Goodman AL, Joachimiak G, Ordoñez CL, Lory S, Walz T, Joachimiak A, Mekalanos JJ. 2006. A virulence locus of Pseudomonas aeruginosa encodes a protein secretion apparatus. Science 312:1526–30.

315. Sana TG, Berni B, Bleves S. 2016. The T6SSs of Pseudomonas aeruginosa Strain PAO1 and Their Effectors: Beyond Bacterial-Cell Targeting. Front Cell Infect Microbiol 6:61.

316. Goodman AL, Kulasekara B, Rietsch A, Boyd D, Smith RS, Lory S. 2004. A signaling network reciprocally regulates genes associated with acute infection and chronic persistence in Pseudomonas aeruginosa. Dev Cell 7:745–54.

317. Moscoso JA, Mikkelsen H, Heeb S, Williams P, Filloux A. 2011. The Pseudomonas aeruginosa sensor RetS switches type III and type VI secretion via c-di-GMP signalling. Environ Microbiol 13:3128–38.

318. Goodman AL, Merighi M, Hyodo M, Ventre I, Filloux A, Lory S. 2009. Direct interaction between sensor kinase proteins mediates acute and chronic disease phenotypes in a bacterial pathogen. Genes Dev 23:249–59.

319. Brencic A, McFarland KA, McManus HR, Castang S, Mogno I, Dove SL, Lory S. 2009. The GacS/GacA signal transduction system of Pseudomonas aeruginosa acts exclusively through its control over the transcription of the RsmY and RsmZ regulatory small RNAs. Mol Microbiol 73:434–45.

320. Brencic A, Lory S. 2009. Determination of the regulon and identification of novel mRNA targets of Pseudomonas aeruginosa RsmA. Mol Microbiol 72:612–32.

321. Lesic B, Starkey M, He J, Hazan R, Rahme LG. 2009. Quorum sensing differentially

regulates Pseudomonas aeruginosa type VI secretion locus I and homologous loci II and III, which are required for pathogenesis. Microbiology 155:2845–55.

322. Winsor GL, Griffiths EJ, Lo R, Dhillon BK, Shay JA, Brinkman FSLSL. 2015. Enhanced annotations and features for comparing thousands of Pseudomonas genomes in the Pseudomonas genome database. Nucleic Acids Res 44:D646-53.

323. Hoang TT, Karkhoff-Schweizer RR, Kutchma AJ, Schweizer HP. 1998. A broad-host-range Flp-FRT recombination system for site-specific excision of chromosomally-located DNA sequences: application for isolation of unmarked Pseudomonas aeruginosa mutants. Gene 212:77–86.

324. Hmelo LR, Borlee BR, Almblad H, Love ME, Randall TE, Tseng BS, Lin C, Irie Y, Storek KM, Yang JJ, Siehnel RJ, Howell PL, Singh PK, Tolker-Nielsen T, Parsek MR, Schweizer HP, Harrison JJ. 2015. Precision-engineering the Pseudomonas aeruginosa genome with two-step allelic exchange. Nat Protoc 10:1820–41.

325. Shanks RMQ, Caiazza NC, Hinsa SM, Toutain CM, O'Toole GA. 2006. Saccharomyces cerevisiae-based molecular tool kit for manipulation of genes from gram-negative bacteria. Appl Environ Microbiol 72:5027–36.

326. Simon R, Priefer U, Pühler A. 1983. A Broad Host Range Mobilization System for In Vivo Genetic Engineering: Transposon Mutagenesis in Gram Negative Bacteria. Bio/Technology 1:784–791.

327. Rahme L, Stevens E, Wolfort S, Shao J, Tompkins R, Ausubel F. 1995. Common virulence factors for bacterial pathogenicity in plants and animals. Science (80-) 268:1899–1902.

328. Sikorski RS, Hieter P. 1989. A system of shuttle vectors and yeast host strains designed for efficient manipulation of DNA in Saccharomyces cerevisiae. Genetics 122.

329. Blatny JM, Brautaset T, Winther-Larsen HC, Karunakaran P, Valla S. 1997. Improved broad-host-range RK2 vectors useful for high and low regulated gene expression levels in gram-negative bacteria. Plasmid 38:35–51.

330. Jutras BL, Verma A, Stevenson B. 2012. Identification of novel DNA-binding proteins using DNA-affinity chromatography/pull down. Curr Protoc Microbiol Chapter 1:Unit1F.1.

331. Bryson V, Szybalski W. 1952. Microbial Selection. Science 116:45–51.

332. Mah T-F. 2014. Establishing the minimal bactericidal concentration of an antimicrobial agent for planktonic cells (MBC-P) and biofilm cells (MBC-B). J Vis Exp e50854.

333. Srikumar R, Kon T, Gotoh N, Poole K. 1998. Expression of Pseudomonas aeruginosa multidrug efflux pumps MexA-MexB-OprM and MexC-MexD-OprJ in a multidrug-sensitive Escherichia coli strain. Antimicrob Agents Chemother 42:65–71.

334. Bolger AM, Lohse M, Usadel B. 2014. Trimmomatic: a flexible trimmer for Illumina sequence data. Bioinformatics 30:2114–20.

335. Trapnell C, Pachter L, Salzberg SL. 2009. TopHat: discovering splice junctions with RNA-Seq. Bioinformatics 25:1105–11.

336. Langmead B, Trapnell C, Pop M, Salzberg SL. 2009. Ultrafast and memory-efficient alignment of short DNA sequences to the human genome. Genome Biol 10:R25.

337. Anders S, Pyl PT, Huber W. 2015. HTSeq--a Python framework to work with high-throughput sequencing data. Bioinformatics 31:166–9.

338. Anders S, Huber W. 2010. Differential expression analysis for sequence count data. Genome Biol 11:R106.

339. Robinson MD, McCarthy DJ, Smyth GK. 2010. edgeR: a Bioconductor package for differential expression analysis of digital gene expression data. Bioinformatics 26:139–40.

340. Edgar R. 2002. Gene Expression Omnibus: NCBI gene expression and hybridization array data repository. Nucleic Acids Res 30:207–210.

341. Barrett T, Wilhite SE, Ledoux P, Evangelista C, Kim IF, Tomashevsky M, Marshall KA, Phillippy KH, Sherman PM, Holko M, Yefanov A, Lee H, Zhang N, Robertson CL, Serova N, Davis S, Soboleva A. 2013. NCBI GEO: archive for functional genomics data sets--update. Nucleic Acids Res 41:D991-5.

342. Schweizer HP. 1991. Escherichia-Pseudomonas shuttle vectors derived from pUC18/19. Gene 97:109–21.

343. O'Toole GA. 2011. Microtiter dish biofilm formation assay. J Vis Exp e2437.

344. Evans K, Adewoye L, Poole K. 2001. MexR repressor of the mexAB-oprM multidrug efflux operon of Pseudomonas aeruginosa: identification of MexR binding sites in the mexA-mexR intergenic region. J Bacteriol 183:807–12.

345. Ünal CM, Steinert M. 2014. Microbial peptidyl-prolyl cis/trans isomerases (PPIases): virulence factors and potential alternative drug targets. Microbiol Mol Biol Rev 78:544–71.

346. Duguay AR, Silhavy TJ. 2004. Quality control in the bacterial periplasm. Biochim Biophys Acta 1694:121–34.

347. Pederick VG, Eijkelkamp BA, Ween MP, Begg SL, Paton JC, McDevitt CA. 2014. Acquisition and role of molybdate in Pseudomonas aeruginosa. Appl Environ Microbiol 80:6843–52.

348. Bailey TL, Boden M, Buske FA, Frith M, Grant CE, Clementi L, Ren J, Li WW, Noble WS. 2009. MEME SUITE: tools for motif discovery and searching. Nucleic Acids Res 37:W202–W208.

349. Li XZ, Nikaido H, Poole K. 1995. Role of mexA-mexB-oprM in antibiotic efflux in Pseudomonas aeruginosa. Antimicrob Agents Chemother 39:1948–53.

350. Masuda N, Sakagawa E, Ohya S, Gotoh N, Tsujimoto H, Nishino T. 2000. Substrate specificities of MexAB-OprM, MexCD-OprJ, and MexXY-oprM efflux pumps in Pseudomonas aeruginosa. Antimicrob Agents Chemother 44:3322–7.

351. Poole K, Tetro K, Zhao Q, Neshat S, Heinrichs D, Bianco N. 1996. Expression of the multidrug resistance operon mexA-mexB-oprM in Pseudomonas aeruginosa: mexR encodes a regulator of operon expression. Antimicrob Agents Chemother 40:2021–2028.

352. Saito K, Eda S, Maseda H, Nakae T. 2001. Molecular mechanism of MexR-mediated regulation of MexABâ□“OprM efflux pump expression in Pseudomonas aeruginosa. FEMS Microbiol Lett 195:23–28.

353. SÃ¡nchez P, Rojo F, MartÄ±Ì• nez JL. 2002. Transcriptional regulation of mexR , the repressor of Pseudomonas aeruginosa mexAB-oprM multidrug efflux pump. FEMS Microbiol Lett 207:63–68.

354. Morita Y, Cao L, Gould VC, Avison MB, Poole K. 2006. nalD encodes a second repressor of the mexAB-oprM multidrug efflux operon of Pseudomonas aeruginosa. J Bacteriol 188:8649–54.

355. Sobel ML, Hocquet D, Cao L, Plesiat P, Poole K. 2005. Mutations in PA3574 (nalD) lead to increased MexAB-OprM expression and multidrug resistance in laboratory and clinical isolates of Pseudomonas aeruginosa. Antimicrob Agents Chemother 49:1782–6.

356. Tian Z-X, Yi X-X, Cho A, O'Gara F, Wang Y-P. 2016. CpxR Activates MexAB-OprM Efflux Pump Expression and Enhances Antibiotic Resistance in Both Laboratory and Clinical nalB-Type Isolates of Pseudomonas aeruginosa. PLOS Pathog 12:e1005932.

357. Breidenstein EBM, Khaira BK, Wiegand I, Overhage J, Hancock REW. 2008. Complex ciprofloxacin resistome revealed by screening a Pseudomonas aeruginosa mutant library for altered susceptibility. Antimicrob Agents Chemother 52:4486–91.

358. Su H-C, Khatun J, Kanavy DM, Giddings MC. 2013. Comparative genome analysis of ciprofloxacin-resistant Pseudomonas aeruginosa reveals genes within newly identified high variability regions associated with drug resistance development. Microb Drug Resist 19:428–36.

359. Chen L, Duan K. 2016. A PhoPQ-Regulated ABC Transporter System Exports Tetracycline in Pseudomonas aeruginosa. Antimicrob Agents Chemother 60:3016–24.

360. Nikaido H. 2009. Multidrug Resistance in Bacteria. Annu Rev Biochem 78:119–146.

361. Fernandez L, Hancock REW. 2012. Adaptive and Mutational Resistance: Role of Porins and Efflux Pumps in Drug Resistance. Clin Microbiol Rev 25:661–681.

362. Breidenstein EBM, de la Fuente-Núñez C, Hancock REW. 2011. Pseudomonas aeruginosa: all roads lead to resistance. Trends Microbiol 19:419–26.

363. Gallagher LA, Shendure J, Manoil C. 2011. Genome-scale identification of resistance functions in Pseudomonas aeruginosa using Tn-seq. MBio 2:e00315-10.

364. Høiby N, Bjarnsholt T, Givskov M, Molin S, Ciofu O. 2010. Antibiotic resistance of bacterial biofilms. Int J Antimicrob Agents 35:322–32.

365. Conlon BP, Rowe SE, Lewis K. 2015. Persister cells in biofilm associated infections. Adv Exp Med Biol 831:1–9.

366. Liao J, Schurr MJ, Sauer K. 2013. The MerR-like regulator BrlR confers biofilm tolerance by activating multidrug efflux pumps in Pseudomonas aeruginosa biofilms. J Bacteriol 195:3352–63.

367. Nilsson M, Rybtke M, Givskov M, Høiby N, Twetman S, Tolker-Nielsen T. 2016. The dlt genes play a role in antimicrobial tolerance of Streptococcus mutans biofilms. Int J Antimicrob Agents.

368. Naylor LH. 1999. Reporter gene technology: the future looks bright. Biochem Pharmacol 58:749–57.

369. Zhang J, Campbell RE, Ting AY, Tsien RY. 2002. Creating new fluorescent probes for cell biology. Nat Rev Mol Cell Biol 3:906–918.

370. Sternberg C, Christensen BB, Johansen T, Toftgaard Nielsen A, Andersen JB, Givskov M, Molin S. 1999. Distribution of bacterial growth activity in flow-chamber biofilms. Appl Environ Microbiol 65:4108–17.

371. De Kievit TR, Gillis R, Marx S, Brown C, Iglewski BH. 2001. Quorum-Sensing Genes in Pseudomonas aeruginosa Biofilms: Their Role and Expression Patterns. Appl Environ Microbiol 67:1865–1873.

372. Southward CM, Surette MG. 2002. The dynamic microbe: green fluorescent protein brings bacteria to light. Mol Microbiol 45:1191–6.

373. Choi K-H, Kumar A, Schweizer HP. 2006. A 10-min method for preparation of highly electrocompetent Pseudomonas aeruginosa cells: Application for DNA fragment transfer between chromosomes and plasmid transformation. J Microbiol Methods 64:391–397.

374. Figurski DH, Helinski DR. 1979. Replication of an origin-containing derivative of plasmid RK2 dependent on a plasmid function provided in trans. Proc Natl Acad Sci 76:1648–1652.

375. Hanahan D. 1983. Studies on transformation of Escherichia coli with plasmids. J Mol Biol 166:557–80.

376. Andersen JB, Sternberg C, Poulsen LK, Bjorn SP, Givskov M, Molin S. 1998. New unstable variants of green fluorescent protein for studies of transient gene expression in bacteria. Appl Environ Microbiol 64:2240–6.

377. Choi K-H, Gaynor JB, White KG, Lopez C, Bosio CM, Karkhoff-Schweizer RR, Schweizer HP. 2005. A Tn7-based broad-range bacterial cloning and expression system. Nat Methods 2:443–448.

378. Yanisch-Perron C, Vieira J, Messing J. 1985. Improved M13 phage cloning vectors and host strains: nucleotide sequences of the M13mp18 and pUC19 vectors. Gene 33:103–19.

379. Shanks RMQ, Kadouri DE, MacEachran DP, O'Toole GA. 2009. New yeast recombineering tools for bacteria. Plasmid 62:88–97.

380. Hoffman CS, Winston F. 1987. A ten-minute DNA preparation from yeast efficiently releases autonomous plasmids for transformation of Escherichia coli. Gene 57:267–72.

381. Merritt JH, Kadouri DE, O'Toole GA. 2005. Current Protocols in MicrobiologyCurrent protocols in microbiology. John Wiley & Sons, Inc., Hoboken, NJ, USA.

382. Choi K-H, Schweizer HP. 2006. mini-Tn7 insertion in bacteria with single attTn7 sites: example Pseudomonas aeruginosa. Nat Protoc 1:153–61.

383. Miller J. 1972. Assay of B-galactosidase In: Experiments in molecular genetics.

384. Spoering AL, Lewis K. 2001. Biofilms and planktonic cells of Pseudomonas aeruginosa have similar resistance to killing by antimicrobials. J Bacteriol 183:6746–51.

385. Cormack BP, Valdivia RH, Falkow S. 1996. FACS-optimized mutants of the green fluorescent protein (GFP). Gene 173:33–8.

386. Keiler KC, Waller PR, Sauer RT. 1996. Role of a peptide tagging system in degradation of proteins synthesized from damaged messenger RNA. Science 271:990–3.

387. Wurtzel O, Yoder-Himes DR, Han K, Dandekar AA, Edelheit S, Greenberg EP, Sorek R, Lory S. 2012. The Single-Nucleotide Resolution Transcriptome of Pseudomonas aeruginosa Grown in Body Temperature. PLoS Pathog 8:e1002945.

388. Coulon C, Vinogradov E, Filloux A, Sadovskaya I. 2010. Chemical analysis of cellular and extracellular carbohydrates of a biofilm-forming strain Pseudomonas aeruginosa PA14. PLoS One 5:e14220.

389. Stoodley P, Sauer K, Davies DG, Costerton JW. 2002. Biofilms as Complex Differentiated Communities. Annu Rev Microbiol 56:187–209.

390. Billings N, Millan M, Caldara M, Rusconi R, Tarasova Y, Stocker R, Ribbeck K. 2013. The extracellular matrix Component Psl provides fast-acting antibiotic defense in Pseudomonas aeruginosa biofilms. PLoS Pathog 9:e1003526.

391. Ingram-Smith C, Miller KJ. 1998. Effects of Ionic and Osmotic Strength on the Glucosyltransferase of Rhizobium meliloti Responsible for Cyclic beta-(1,2)-Glucan Biosynthesis. Appl Environ Microbiol 64:1290–7.

392. Wimpenny J, Manz W, Szewzyk U. 2000. Heterogeneity in biofilms: Table 1. FEMS Microbiol Rev 24:661–671.

393. Givskov M, Ersbøll BK, Parsek MR, Heydorn A, Hentzer M, Molin S. 2000. Experimental reproducibility in flow-chamber biofilms. Microbiology 146:2409–2415.

394. Ciofu O, Hansen CR, Høiby N. 2013. Respiratory bacterial infections in cystic fibrosis. Curr Opin Pulm Med 19:251–258.

395. Gutierrez A, Jain S, Bhargava P, Hamblin M, Lobritz MA, Collins JJ. 2017. Understanding and Sensitizing Density-Dependent Persistence to Quinolone Antibiotics. Mol Cell 68:1147–1154.e3.

396. Bryan LE, Kwan S. 1983. Roles of ribosomal binding, membrane potential, and electron transport in bacterial uptake of streptomycin and gentamicin. Antimicrob Agents Chemother 23:835–45.

397. Borriello G, Richards L, Ehrlich GD, Stewart PS. 2006. Arginine or Nitrate Enhances Antibiotic Susceptibility of Pseudomonas aeruginosa in Biofilms. Antimicrob Agents Chemother 50:382–384.

398. Allison KR, Brynildsen MP, Collins JJ. 2011. Metabolite-enabled eradication of bacterial persisters by aminoglycosides. Nature 473:216–220.

399. Barraud N, Buson A, Jarolimek W, Rice SA. 2013. Mannitol enhances antibiotic sensitivity of persister bacteria in Pseudomonas aeruginosa biofilms. PLoS One 8:e84220.

400. Price KE, Orazi G, Ruoff KL, Hebert WP, O'Toole GA, Mastoridis P. 2015. Mannitol Does Not Enhance Tobramycin Killing of Pseudomonas aeruginosa in a Cystic Fibrosis Model System of Biofilm Formation. PLoS One 10:e0141192.

401. Lebeaux D, Chauhan A, Létoffé S, Fischer F, de Reuse H, Beloin C, Ghigo J-M. 2014. pH-mediated potentiation of aminoglycosides kills bacterial persisters and eradicates in vivo biofilms. J Infect Dis 210:1357–66.

402. Crabbé A, Ostyn L, Staelens S, Rigauts C, Risseeuw M, Dhaenens M, Daled S, Van Acker H, Deforce D, Van Calenbergh S, Coenye T. 2019. Host metabolites stimulate the bacterial proton motive force to enhance the activity of aminoglycoside antibiotics. PLOS Pathog 15:e1007697.

403. Mahenthiralingam E, Campbell ME, Speert DP. 1994. Nonmotility and phagocytic resistance of Pseudomonas aeruginosa isolates from chronically colonized patients with cystic fibrosis. Infect Immun 62:596–605.

404. Wong A, Rodrigue N, Kassen R. 2012. Genomics of Adaptation during Experimental Evolution of the Opportunistic Pathogen Pseudomonas aeruginosa. PLoS Genet 8:e1002928.

405. Payne SR, Pau DI, Whiting AL, Kim YJ, Pharoah BM, Moi C, Boddy CN, Bernal F. 2018. Inhibition of Bacterial Gene Transcription with an RpoN-Based Stapled Peptide. Cell Chem Biol 25:1059–1066.e4.

406. Lloyd MG, Vossler JL, Nomura CT, Moffat JF. 2019. Blocking RpoN reduces virulence of Pseudomonas aeruginosa isolated from cystic fibrosis patients and increases antibiotic sensitivity in a laboratory strain. Sci Rep 9:6677.

407. Yoon SS, Hennigan RF, Hilliard GM, Ochsner UA, Parvatiyar K, Kamani MC, Allen HL, DeKievit TR, Gardner PR, Schwab U, Rowe JJ, Iglewski BH, McDermott TR, Mason RP, Wozniak DJ, Hancock REW, Parsek MR, Noah TL, Boucher RC, Hassett DJ. 2002. Pseudomonas aeruginosa anaerobic respiration in biofilms: relationships to cystic fibrosis pathogenesis. Dev Cell 3:593–603.

408. Allsopp LP, Wood TE, Howard SA, Maggiorelli F, Nolan LM, Wettstadt S, Filloux A. 2017. RsmA and AmrZ orchestrate the assembly of all three type VI secretion systems in *Pseudomonas aeruginosa*. Proc Natl Acad Sci 114:7707–7712.

409. Jones CJ, Newsom D, Kelly B, Irie Y, Jennings LK, Xu B, Limoli DH, Harrison JJ, Parsek MR, White P, Wozniak DJ. 2014. ChIP-Seq and RNA-Seq Reveal an AmrZ-Mediated Mechanism for Cyclic di-GMP Synthesis and Biofilm Development by

Pseudomonas aeruginosa. PLoS Pathog 10:e1003984.

410. Cornell WC, Morgan CJ, Koyama L, Sakhtah H, Mansfield JH, Dietrich LEP. 2018. Paraffin Embedding and Thin Sectioning of Microbial Colony Biofilms for Microscopic Analysis. J Vis Exp.

411. Golde LMG V., Schulman H, Kennedy EP. 1973. Metabolism of Membrane Phospholipids and Its Relation to a Novel Class of Oligosaccharides in Escherichia coli. Proc Natl Acad Sci 70:1368–1372.

412. Wang P, Ingram-Smith C, Hadley JA, Miller KJ. 1999. Cloning, sequencing, and characterization of the cgmB gene of Sinorhizobium meliloti involved in cyclic beta-glucan biosynthesis. J Bacteriol 181:4576–83.

413. Zhang Y-M, Rock CO. 2008. Membrane lipid homeostasis in bacteria. Nat Rev Microbiol 6:222–233.

414. Lequette Y, Rollet E, Delangle A, Greenberg EP, Bohin J-P. 2007. Linear osmoregulated periplasmic glucans are encoded by the opgGH locus of Pseudomonas aeruginosa. Microbiology 153:3255–3263.

415. Bontemps-Gallo S, Lacroix J-M. 2015. New insights into the biological role of the osmoregulated periplasmic glucans in pathogenic and symbiotic bacteria. Environ Microbiol Rep 7:690–7.

416. Chubiz LM, Lee M-C, Delaney NF, Marx CJ. 2012. FREQ-Seq: A Rapid, Cost-Effective, Sequencing-Based Method to Determine Allele Frequencies Directly from Mixed Populations. PLoS One 7:e47959.

417. Chambers JR, Sauer K. 2013. The MerR-like regulator BrlR impairs Pseudomonas aeruginosa biofilm tolerance to colistin by repressing PhoPQ. J Bacteriol 195:4678–88.

418. Poudyal B, Sauer K. 2017. The ABC of Biofilm Drug Tolerance: the MerR-Like Regulator BrlR Is an Activator of ABC Transport Systems, with PA1874-77 Contributing to the Tolerance of *Pseudomonas aeruginosa* Biofilms to Tobramycin. Antimicrob Agents Chemother 62:e01981-17.

419. Chambers JR, Liao J, Schurr MJ, Sauer K. 2014. BrlR from Pseudomonas aeruginosa is a c-di-GMP-responsive transcription factor. Mol Microbiol 92:471–87.

420. Liao J, Sauer K. 2012. The MerR-like transcriptional regulator BrlR contributes to Pseudomonas aeruginosa biofilm tolerance. J Bacteriol 194:4823–36.

421. Gupta K, Marques CNH, Petrova OE, Sauer K. 2013. Antimicrobial tolerance of Pseudomonas aeruginosa biofilms is activated during an early developmental stage and requires the two-component hybrid SagS. J Bacteriol 195:4975–87.

422. Gupta K, Liao J, Petrova OE, Cherny KE, Sauer K. 2014. Elevated levels of the second messenger c-di-GMP contribute to antimicrobial resistance of Pseudomonas aeruginosa. Mol Microbiol 92:488–506.

Rights and permissions

The following excerpt from Oxford Academic Journals, which applies to **Chapter 1**, is taken directly from:

https://academic.oup.com/journals/pages/authors/authors_faqs/online_licensing

What rights do I retain as an Oxford Journal author?

- The right, after publication by Oxford Journals, to use all or part of the Article and abstract, for their own personal use, including their own classroom teaching purposes;
- The right, after publication by Oxford Journals, to use all or part of the Article and abstract, in the preparation of derivative works, extension of the article into book-length or in other works, provided that a full acknowledgement is made to the original publication in the journal;
- **The right to include the article in full or in part in a thesis or dissertation, provided that this not published commercially**;

For the uses specified here, please note that there is no need for you to apply for written permission from Oxford University Press in advance. Please go ahead with the use ensuring that a full acknowledgment is made to the original source of the material including the journal name, volume, issue, page numbers, year of publication, title of article and to Oxford University Press and/or the learned society.

The only exception to this is for the re-use of material for commercial purposes. Permission for this kind of re-use is required and can be obtained by using Rightslink.

The following excerpt of the Statement of Author Rights from the American Society for Microbiology, which applies to **Chapter 2** and **Chapter 3** (and **Chapter 4** if manuscript is accepted**)**, is taken directly from:

https://journals.asm.org/content/statement-author-rights

Authors may republish/adapt portions of their articles

"ASM also grants the author the right to republish discrete portions of his/her article in any other publication (including print, CD-ROM, and other electronic formats) of which he or she is author or editor, provided that proper credit is given to the original ASM publication. **An ASM author also retains the right to reuse the full article in his/her dissertation or thesis.** "Proper credit" means either the copyright lines shown on the top of the first page of the PDF version, or "Copyright © American Society for Microbiology, [insert journal name, volume number, year, page numbers and DOI]" of the HTML version."